STRUCTURAL BEHAVIOR OF RUBBERIZED CONCRETE CONTAINING SYNTHETIC FIBERS

By

© Basem Hassan Abdelbaset AbdelAleem, B.Sc., M.Sc.

A thesis submitted to

The School of Graduate Studies

in partial fulfillment of the requirements for the degree of

Doctor of Philosophy (Civil Engineering)

Faculty of Engineering and Applied Science

Memorial University of Newfoundland

August 2019

St. John’s, Newfoundland, Canada

Abstract

This research program aims to investigate the combining effect of crumb rubber (CR) and synthetic/metal fibers (SFs/MFs) in the development of concrete suitable for structural applications subjected to monotonic and cyclic loading. The research also aims to overcome the challenge of optimizing the strength and stability of self-consolidating concrete (SCC) containing CR and SFs/MFs. Five comprehensive experimental studies were conducted on both small-scale and large-scale concrete samples to meet the research objectives. The first study aimed to develop and optimize a number of successful self-consolidating rubberized concrete (SCRC) and synthetic fiber SCRC (SFSCRC) mixtures with a maximized percentage of CR and minimized reduction in strength. The variables in this study included various supplementary cementing materials (SCMs) specifically metakaolin (MK), silica fume (SLF), fly ash (FA), and ground granulated blast-furnace slag (GGBS), different binder contents (500, 550, and 600 kg/m^3), varying percentages of CR (0% to 30%), different types of SFs specifically micro-synthetic fibers (MISFs), and macro-synthetic fibers (MASFs), different lengths of SFs (19mm, 27mm, 38mm, 50mm, and 54mm), and different SFs volume fractions (0%, 0.2%, and 1%).

The second and third studies evaluated the flexural and shear behavior of large-scale reinforced concrete beams made with SCRC, vibrated rubberized concrete (VRC), SFSCRC, and synthetic fiber VRC (SFVRC).

The fourth study investigated the structural performance of rubberized beam-column joints reinforced with SFs/MFs under reverse cyclic loading. This study consisted of three stages: the first stage contained a total of six SCRC mixtures selected to cast six beam-

column joints with varied percentages of CR (0-25%). The second stage included eight rubberized concrete mixtures with different coarse aggregate sizes and different MFs lengths and volumes selected to pour eight beam-column joints to be tested under cyclic loading. The third stage contained seven rubberized concrete beam-column joints reinforced with different types, lengths, and volumes of SFs to be tested under cyclic loading.

The fifth study evaluated the cyclic behavior of engineering cementitious composite (ECC) beam-column joints made with different percentages of CR, different SCMs, and different sand types. In this study a total of eight beam-column joints were cast and tested under reverse cyclic loading.

The main results drawn from the first study indicated that the addition of SFs reduced the fresh properties, which limited the maximum percentage of CR that could be used in SCRC mixtures to 20%, compared to a 30% maximum percentage of CR used in developing successful SCRC mixtures without SFs. However, using SFs in SCRC mixtures increased the impact resistance and appeared to alleviate the reduction in splitting tensile strength (STS) and flexural strength (FS) that resulted from adding CR.

The main results of the flexural testing conducted in study 2 indicated that using MISFs slightly enhanced the deformability, flexural stiffness, ductility, energy absorption, first cracking moment, and bending moment capacity, while this enhancement significantly increased when MASFs were used. Combining high percentage of MASFs (1%) with high percentage of CR (30%) compensated for the reduction in the bending moment capacity that resulted from using high percentage of CR, and helped to develop semi-lightweight concrete beams.

The inclusion of CR in study 3 negatively affected the ultimate shear load, post-diagonal cracking resistance, and first cracking moment of the tested beams while it improved the deformation capacity, self-weight, and cracking pattern. Combining CR with MISFs or MASFs, further improved the deformation capacity, self-weight, and narrowed the crack widths of the tested beams. The results of this study also indicated that the use of a relatively higher percentage of fibers (1% compared to 0.2%) in VRC beams significantly compensated for the reduction in shear strength resulting from a high CR percentage (30%).

The results of the fourth study revealed that the optimum percentage of CR to be used in beam-column joint mixtures is 15%. Although using this percentage slightly reduced the load carrying capacity, it greatly enhanced the ductility, brittleness index, deformability, and energy dissipation. The results also revealed that using MISFs slightly improved the structural performance of beam-column joints, while using MASFs had a significant effect on enhancing the load carrying capacity, ductility, stiffness, and energy dissipation of tested joints.

The main results of the fifth study reported that increasing the percentage of CR up to 15% significantly increased the deformability, cracking behavior, ductility, and energy dissipation of ECC joints, while the initial stiffness, first crack load, and ultimate load were decreased.

Papers published from this research

The majority of the results and discussions presented in this thesis have been published in the following journals:

1. **Basem H. AbdelAleem**, Mohamed K. Ismail, and Assem A. A. Hassan (2017). Properties of self-consolidating rubberized concrete reinforced with synthetic fibers. *Magazine of Concrete Research*, *69*(10), 526-540. (https://www.icevirtuallibrary.com/doi/abs/10.1680/jmacr.16.00433)
2. **Basem H. AbdelAleem**, Mohamed K. Ismail, and Assem A. A. Hassan (2018). The combined effect of crumb rubber and synthetic fibers on impact resistance of self-consolidating concrete. *Construction and Building Materials*, *162*, 816-829. (https://www.sciencedirect.com/science/article/abs/pii/S0950061817324753)
3. **Basem H. AbdelAleem** and Assem A. A. Hassan (2018). Development of self-consolidating rubberized concrete incorporating silica fume. *Construction and Building Materials*, *161*, 389-397. (https://www.sciencedirect.com/science/article/abs/pii/S0950061817323656)
4. **Basem H. AbdelAleem**, Mohamed K. Ismail, and Assem A. A. Hassan (2018). Effect of Synthetic Fibers on Shear Capacity of Reinforced Rubberized Concrete Beams. *ACI Materials Journal*, *115*(2), 279-288. (https://www.concrete.org/publications/internationalconcreteabstractsportal.aspx?m=results)

5. **Basem H. AbdelAleem** and Assem A. A. Hassan (2018). Influence of rubber content on enhancing the structural behaviour of beam–column joints. *Magazine of Concrete Research, 70*(19), 984-996.

(https://www.icevirtuallibrary.com/doi/abs/10.1680/jmacr.17.00323)

6. **Basem H. AbdelAleem** and Assem A. A. Hassan (2019). Effect of combining steel fibers with crumb rubber on enhancing the behavior of beam-column joints under cyclic loading. *Engineering Structures, 182*, 510-527.

(https://www.sciencedirect.com/science/article/pii/S0141029618309167)

7. **Basem H. AbdelAleem** and Assem A. A. Hassan (2019). Cyclic Behavior of Rubberized Beam-Column Joints Reinforced with Synthetic Fibers. *ACI Materials Journal, 116(2), 105-118.*

(https://www.concrete.org/publications/internationalconcreteabstractsportal.aspx?m=details&ID=51714456)

8. **Basem H. AbdelAleem** and Assem A. A. Hassan. Structural behavior of rubberized ECC beam-column joints under cyclic loading. (under review in ACI Materials Journal)
9. **Basem H. AbdelAleem** and Assem A. A. Hassan. Influence of Synthetic fibers' type, length, and volume on enhancing the structural performance of rubberized concrete. (under review in Construction and Building Materials)

Acknowledgments

First of all, I would like to thank The Almighty ALLAH for giving me the opportunity, strength, knowledge, and ability to complete my research study successfully. Without his blessings, this achievement would not have been possible.

I want to express my sincere thanks and gratitude to my thesis advisor Dr. Assem Hassan for his unlimited guidance, support, encouragement, valuable discussions, and great efforts to accomplish the thesis's objectives. I have been extremely lucky to have a supervisor who cared so much about my academic and personal life. Therefore, a thank you word is not enough to express how much I appreciate his role in my life that will never be forgotten.

I would like to thank my committee members, Dr. John Molgaard and Dr. Samer Nakla for their valuable guidance and recommendations.

I would like to thank Mr. Shawn Organ, Mr. Matt Curtis, and Mr. Jason Murphy for their kind assistance and support during the various stages of my experimental program. I am also very grateful to my friends who spiritually and physically helped me to finish this Ph.D. degree, especially Mohamed Ismail, Md Shahriar Nizam, Madolyn Lundrigan, Owais Kiblawi, Bruce Dragan, Ahmed Taha, and shamim J Munna

I am gratefully acknowledging the financial assistance provided by Dr. Assem Hassan and School of Graduate Studies.

My deepest appreciation and love to my father, mother, sister, and brother who are always behind me for the success. I would not have achieved this work without their help and support.

Above all my deepest appreciation and love to my wife Rowyda Zaki for her infinite love and tender. She was every time beside me supporting and encouraging me to complete this work. Without her in my life the completion of this research would not have been possible to me.

Basem H. AbdelAleem

Table of contents

List of tables

List of figures

List of symbols, nomenclature or abbreviations

ACI = American Concrete Institute

AS= Australian Standard

ASTM = American Society for Testing and Materials

BI= Brittle Index

BS= British Standards

CR= Crumb Rubber

CSA= Canadian Standards Association

C/F= Coarse-to-Fine Aggregate

EC 2= Eurocode 2

Ed= Energy dissipation

EFNARC= European guidelines for Self-Consolidating Concrete

FA= Fly Ash

f_c' = Characteristic Compressive Strength of Concrete (MPa)

FS= Flexural Strength (MPa)

HRWRA= High-Range Water-Reducer Admixture

ITZ= Interfacial Transition Zone

M_{cr}^{exp}= Experimental First Cracking Moment

M_{cr}^{theo}= Theoretical First Cracking Moment Calculated by Design Codes

ME= Modulus of Elasticity

MFs= Metal fibers

MFSCRC= Metal Fiber Self-Consolidating Rubberized Concrete

MFVRC= Metal Fiber Vibrated Rubberized Concrete

MISFs= Micro-synthetic fibers

MASFs= Macro-synthetic fibers

MK= Metakaolin

M_u^{exp}= Experimental Ultimate Moment Capacity

SCC= Self-Consolidating Concrete

SCMs= Supplementary Cementing Materials

SCRC= Self-Consolidating Rubberized Concrete

SFs= Synthetic fibers

SFSCRC= synthetic Fiber Self-Consolidating Rubberized Concrete

SFVRC= Synthetic Fiber Vibrated Rubberized Concrete

SR= Segregation Resistance (%)

STS = Splitting Tensile Strength of Concrete (MPa)

$T_{50=}$ Time to Reach 500mm Slump Flow Diameter (seconds)

$T_{50J=}$ Time to Reach 500mm J-ring Diameter (seconds)

V_C= Vibrated Concrete

v_{exp}= Experimental Shear Strength of Tested Beams

VRC= Vibrated Rubberized Concrete

w/b= Water-to-Binder Ratio

1 Introduction

1.1 Background and research motivation

A large amount of waste solid materials has been generated due to worldwide industrialization and technological innovation. About 1.5 billion tires per year are discarded, as a result of ineffective recycling of waste tires which leads to environmental pollution. Many studies have investigated the reuse of waste tire rubber as a partial replacement for aggregate in concrete. The rubber material itself has high durability and elasticity that can compensate for the limited properties of concrete in the areas of elasticity and capacity to absorb energy (wang et al., 2000). Also, the low density of rubber aggregate compared to conventional aggregate can significantly contribute to the development of semi-lightweight and lightweight concrete (Batayneh et al., 2008), which helps to reach a more economical design (Najim and Hall, 2010). However, using rubber, in general, has a negative effect on the fresh properties of self-consolidating concrete (SCC) mixtures. Previous researchers report that the low density of crumb rubber (CR) encourages CR particles to float towards the concrete surface, thus increasing the risk of segregation (Topcu and Bilir, 2009; Güneyisi, 2010). The addition of rubber also has a significant effect on the mechanical properties of concrete. Many studies report that compressive strength, splitting tensile strength (STS), and flexure strength (FS) decreased as CR content increased. This reduction in the mechanical properties with higher percentages of CR may be attributed to; (i) the lower modulus of elasticity for rubber particles compared to hardened cement paste, which may encourage precocious cracking around the rubber particles under loading (Najim and Hall, 2012; Lijuan et al., 2014), (ii)

the poor strength of the interface between the rubber particles and surrounding mortar, as observed by other researcher (Onuaguluchi, 2015; Najim and Hall, 2013).To alleviate the reduction in the fresh and mechanical properties that resulted from using CR, supplementary cementing materials (SCMs) have been used. Metakaolin (MK) is one of the most effective SCMs at improving the viscosity of SCC mixtures, which in turn improves the aggregates' suspension in the mixture and reduces the risk of segregation. In addition, the high pozzolanic reactivity of MK can compensate for the reduction in the mechanical properties of concrete that results from the use of rubber (Hassan et al., 2010). Further compensations for the weakened tensile and flexural strengths resulting from rubber can be achieved by adding fibers; the bridging mechanism of fibers significantly helps restrict the development of cracks, thus increasing the ability of concrete to endure higher stress. Moreover, including fibers in concrete was found to increase its toughness, ductility, and impact resistance (Grabois et al., 2016; Yap et al., 2014; Hamoush et al., 2010). Among the different types of fibers, metal fibers (MFs) and synthetic fibers (SFs) have received much attention and become widely used. In the studies conducted, the improvement in tensile strength of concrete appeared to be more pronounced when MFs were used. However, the low density of the SFs further decreases the self-weight of concrete. In addition, the SFs have no tendency to corrosion (Jun et al., 2016), which extends their possible applications.

Meanwhile, in large-scale testing, most of the structural elements such as beam-column joints require high ductility and energy absorption capacity to ensure appropriate design of the structure. These joints are considered one of the most important locations in framed structures designed for resisting lateral loads such as earthquakes, which impact the

overall structure integrity (Ganesan et al., 2007). Designers have paid a great deal of attention to providing sufficient ductility in beam-column joints in order to prevent sudden collapse of structures (Bindhu and Jaya, 2010). Using closely spaced stirrups in beam-column joints helps to provide a ductile failure when the joints are subjected to reverse cyclic loading (BIS, 1993). However, using closely spaced stirrups usually forms congested areas and interrupts the flowability and compaction of concrete within the joint. Previous studies also indicated that using rubber particles in concrete appeared to improve the strain capacity, energy dissipation, deformability, and impact resistance (Najim and Hall, 2012; Zheng et al., 2008; Al-Tayeb et al., 2013). The use of rubber particles in concrete can also help to enhance the ductility and reduce brittle failure. This can be attributed to the elastic nature of rubber particles that can tolerate large elastic deformations before failure (Ganesan et al., 2013).

Although using self-consolidating rubberized concrete (SCRC) mixtures in beam-column joints has potential benefits, such as improved ductility, energy absorption, and strain capacity, the development of rubberized concrete mixtures must take into account the possible reductions in the mechanical properties and shear strength of such mixtures. Several studies show that using a high percentage of CR reduced the shear strength of concrete (Ismail and Hassan, 2017; Hall and Najim, 2014). Adding fibers to SCRC mixtures can help to compensate for the reduction in the mechanical properties that result from using rubber particles and combine the beneficial effect of CR with the desired properties of fibers, achieving a better structural performance of concrete elements.

Despite the potential difficulties in optimizing the fresh properties of SCC with CR and fibers, developing such composites is increasingly needed in order to produce new types

of concrete with higher ductility, impact resistance, and energy absorption. For this reason and because of the lack of information regarding the effect of combining CR particles with SFs on the structural performance of large-scale concrete elements, this research aims to develop and optimize a number of SCRC and synthetic fiber self-consolidating rubberized concrete (SFSCRC) mixtures with different types, lengths, and volumes of SFs and maximized percentage of CR. This research focuses on the structural performance of beam-column joints subjected to reverse cyclic loading, in addition to the flexural and shear behavior of full-scale reinforced concrete beams developed with the optimized mixtures.

1.2 Research objectives and significance

Although the literature includes extensive studies that have investigated the effects of using CR as a replacement for fine and coarse aggregate in concrete mixtures, there is a lack of data available regarding the combining effect of SFs with CR on the fresh and mechanical properties of SCRC, especially when different types, lengths, and volumes of SFs are used. On the other hand, most of the conducted research has been carried out on small-scale specimens such as cubes, cylinders, and prisms; however, full-scale testing is significantly lacking.

The research conducted in this thesis aimed to develop a number of successful SCRC and SFSCRC mixtures with maximized percentage of CR and minimized reduction in mechanical properties. Various SCMs, and different types, lengths, and volumes of SFs were used in order to achieve the research objectives. The research also aimed to determine the optimum percentages of CR that can be used to minimize the degradation

in load carrying capacity and maximize the ductility, energy dissipation, crack resistance, and deformation capacity of beam-column joints when subjected to reverse cyclic loading. This study also aimed to investigate the effects of combining different SFs types, lengths, and volumes with maximized percentages of CR on enhancing the structural performance of beam-column joints subjected to reverse cyclic loading. Moreover, the research focuses on enhancing the flexural and shear behavior of rubberized concrete reinforced beams by using different SFs types, lengths, and volumes.

1.3 Scope of research

This research includes five consecutive experimental studies conducted on small and large-scale concrete samples. The first study was conducted on a material level (small-scale samples such as cylinders and prisms) to optimize SCRC mixtures with a maximum percentage of CR and minimum reductions in the fresh and mechanical properties. In addition, the combined effect of CR and different types, lengths, and volumes of fibers on the fresh and mechanical properties were evaluated in this study. In the first study, two stages were investigated. The first stage includes 16 rubberized concrete mixtures with different types of SCMs, and different binder content. The second stage consists of 31 mixtures developed with different percentage of CR, different types, lengths, and volumes of fibers. This stage particularly evaluated the advantages that can be obtained from adding different types of fibers in rubberized concrete mixtures. The addition of fibers not only compensated for the reductions in mechanical properties that resulted from using CR but also contributed to providing further enhancement in the impact resistance and cracking behavior of concrete samples. In both stages, the fresh properties of SCRC/fiber

reinforced SCRC (FRSCRC) were evaluated as per the criteria given by European guidelines for SCC (EFNARC, 2005). In addition, the behavior of mixtures in the hardened state was evaluated by testing the compressive strength, STS, FS, ME, and impact resistance (cylinders and prisms).

The second and third studies were carried out on selected mixtures optimized from study 1. The second study evaluated the flexural behavior of 12 large-scale rubberized concrete beams reinforced with different types, lengths, and volumes of SFs. The behavior of the tested beams was assessed based on the load-deflection response, cracking behavior, first cracking moment, ultimate moment, ductility, and energy absorption. The performance of some design codes was evaluated in predicting the first cracking moment of tested beams. The third study investigated the shear behavior of 12 large-scale rubberized concrete beams reinforced with different types, lengths, and volumes of SFs and without transversal reinforcement. The combined effect of CR with SFs was evaluated based on cracking behavior, shear capacity, post diagonal cracking resistance, and energy absorption of tested beams.

The fourth and fifth studies were conducted to investigate the structural behavior of different types of rubberized concrete beam-column joints (SCRC, vibrated rubberized concrete (VRC), rubberized ECC) and rubberized beam-column joints reinforced with different types of fibers under reversed cyclic loading. The fourth study includes three stages: the first stage investigated six rubberized concrete beam-column joints with different percentage of CR. The optimum percentage of CR was obtained in the first stage. The second stage investigated eight rubberized beam-column joints with different coarse aggregate size and different lengths and volumes of MFs. The combined effect of

CR and MFs on the cyclic behavior of beam-column joints was considered in this stage. The third stage investigated seven rubberized beam-column joints with different types, lengths, and volumes of SFs. The combined effect of CR with SFs on the behavior of beam-column joints was evaluated in this stage. The fifth study investigated the cyclic behavior of eight ECC beam-column joints with different percentage of CR, different SCMs, and different fine aggregate types. In the fourth and fifth studies the structural behavior of beam-column joints under reverse cyclic loading was assessed based on the envelope load-deflection curve, the rate of strength and stiffness degradation, mode of failure, cracking behavior, ductility, brittleness index, energy dissipation, first crack load, and load carrying capacity.

1.4 Thesis outline

The thesis consists of nine chapters described as follows:

Chapter 1 presents the background, motivation, objectives, significance, and scope of the research completed in this thesis.

Chapter 2 presents a review of the literature pertaining to rubber aggregate manufacturing, synthetic fibers types and manufacturing, effect of rubber aggregate on concrete properties, and effect of combining synthetic fibers and rubber on concrete properties.

Chapter 3 describes the experimental program including the material used, significance and scope of each study, studied parameters, mixing and pouring procedures, description of the tested specimens, curing regimes, and test setup.

Chapter 4 presents the results of the first study regarding the use of SFs/MFs to optimize the fresh properties, stability, and strength of SCRC mixtures with different binder content and SCMs.

Chapter 5 discusses the results of the second study evaluating the flexural behavior of large scale rubberized concrete beams reinforced with SFs.

Chapter 6 presents the results and discussions of the finding observed in the third study which investigated the shear performance of large-scale rubberized concrete beams reinforced with SFs.

Chapter 7 discusses the results obtained from the fourth study regarding the structural behavior of rubberized concrete beam-column joints with/without MFs/SFs under reversed cyclic loading.

Chapter 8 presents the discussions of the results obtained from study 5 which evaluated the cyclic performance of ECC beam-column joints with different percentage of CR, various SCMs, and different sand types.

Chapter 9 contains the conclusions drawn from the conducted studies, research contribution, and recommendations for future works.

1.5 Limitations of research

All the results obtained from this research were typically affected by the properties of the used materials. Therefore, changes in the physical and/or chemical properties of any of the coarse aggregate, fine aggregate, cement, SCMs, admixtures, CR, MFs, and SFs can affect the mixtures' properties in the fresh and hardened states. In the structural studies (study 2, 3, 4, and 5), comparative investigations were conducted to evaluate the

combined effect of CR with MFs/SFs on the shear, flexural, and cyclic performance of reinforced concrete beams/beam-column joints neglecting the effect of changing in the specimens' size, longitudinal reinforcement ratio, and shear span-to-effective depth ratio. At materials and structural level, all tests were conducted based on the available facilities in Memorial University's labs. However, in some tests, such as the impact test, using advanced instruments may result in better measurements with further details. Also, in cyclic load test the available testing frame limits the dimensions of concrete specimens that can be tested to one third of full-scale concrete joint.

2 Literature review

2.1 Introduction

The objective of this chapter is to present a review of available literature studies that relate to the scope of the work conducted in this thesis. This chapter also aims to reveal the areas where knowledge about the behavior of rubberized concrete is lacking, especially, when different types, lengths, and volumes of fibers are used. This chapter is divided into five main parts: I) rubber particle types, manufacturing, and usage; II) effect of CR on the fresh, mechanical, and structural performance of SCC and vibrated concrete (VC); III) synthetic fiber types, manufacturing, and usage; IV) effect of SFs on the fresh, mechanical, and structural performance of SCC and VC) engineering cementitious composites.

2.2 Rubber aggregate manufacturing: types and usage

Since rubber materials are not easily biodegradable, the disposal of discarded tires has become a significant environmental problem (Sadek and El-Atttar, 2014). The accumulation of disposed tires which reaches up to more than 303 million tires per year in the US compounds the problem (Pelisser et al., 2011; Thomas et al., 2014). In order to dispose of worn-out tires unacceptable techniques are commonly used. These include burning and stockpiling in landfills. These techniques are responsible for a series of environmental problems including air pollution as well as the contamination of soil and water which result from the toxic fumes that are released when discarded tires are burned (Garrick, 2005; Turer, 2012; Eldin and Senouci, 1994). In addition, storing waste tires in

landfills provides a breeding medium for mosquitoes and other pests, which can spread many diseases (Mohammed et al., 2012; wang et al., 2013; Thomas et al., 2015). One effective technique for using a huge volume of waste tires is the utilization of rubber, derived from scrap tires, in civil engineering applications, such as concrete production. Incorporation of rubber particles in concrete helps to develop eco-friendly buildings and encourages the concept of sustainable production (Su et al., 2015). Moreover, the low density of rubber particles can contribute to the development of semi-lightweight and lightweight concrete, which helps to achieve more economical designs (Najim and Hall, 2010; Batayneh et al., 2008). Manufacturing rubber aggregate from waste tires is usually carried out in one of two ways: the ambient temperature method or the cryogenic processing method. The ambient temperature method is commonly used in the industry. In this method the scrap tire is cut into small pieces using a granulator and cracker mills. In the cryogenic processing method, the scrap tires are frozen in liquid nitrogen up to the temperature of glass transition (-70° C for rubber) in order to change the behavior of rubber from elastic to brittle. After reaching the temperature of glass transition, the rubber tires are crushed using automatic hammers. In both methods, the steel wires in the tires are extracted by applying a magnetic field to separate the rubber particles (Nagdi, 1993; Leyden, 1991).

Sherwood (1995) stated that the texture and shape of the rubber aggregate can affect the properties of the developed concrete. Previous researches also indicated that the rubber particles produced from the cryogenic method are more efficient than those produced from the ambient method. This is because the rubber particles produced by the cryogenic

method have a more acceptable geometric shape and there is no steel fabric blended with the particles (Eldin and senouci, 1993).

Rubber aggregates can be classified into three types based on the aggregate sizes (Figure 2-1):

- Shredded rubber aggregate: the size of this rubber is equivalent to the size of coarse aggregate. This rubber is usually used as a partial replacement of coarse aggregate. Using this type of rubber in concrete has been proven to increase the air content in the mixture. This may be attributed to the rough surface of the particles and their tendency to repel water and entrap air (Siddique and Naik, 2004; Khaloo et al., 2008).
- Crumb rubber: this type of fine rubber aggregate has a size which ranges from 0.425mm to 4.75mm and is usually used as a partial replacement of fine aggregate.
- Ground rubber (powder rubber): The particle size of this aggregate passes through sieve No. 40 (0.425mm). Several previous studies attempted to use this ground rubber in asphalt and polymer modified bitumen. Other studies used this type of rubber as a partial replacement of fine aggregate in SCRC mixtures (Hernandez-Olivares et al., 2002; Ganjian et al., 2009).

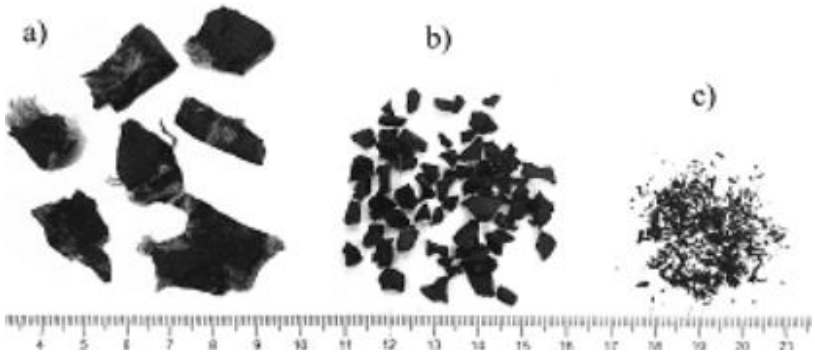

Figure 2-1 Rubber particle classification (a) shredded rubber, (b) crumb rubber, (c) powder rubber (Najim 2012)

2.3 Effect of CR on fresh, mechanical, and structural performance of SCC and VC

2.3.1 Fresh properties

The addition of CR to VC mixtures showed a negative impact on the flowability of the mixture. This may be attributed to the rough texture of the rubber aggregate, which can increase the friction between particles (Reda Taha et al., 2008, Khatib and Bayomy, 1999; Nehdi and Khan, 2001; Batayneh et al., 2008; Fattuhi and Clark, 1996). Youssf et al. (2014) reported that the reduction in the workability that results from using CR can be compensated for by increasing the dosage of HRWRA. Using shredded rubber or combining shredded rubber with CR as partial replacement of aggregate showed a higher reduction in the workability compared to using CR alone (Khaloo et al., 2008; Reda Taha et al., 2008). Adding CR to VC mixtures also showed an increase in the air content of the mixtures as reported by Naito et al., (2014). Reda Taha et al., (2008) also reported that the high compressibility of rubber particles may exhibit an artificial amount of air, which results in a misleading measurement (Naito et al., 2014).

Similarly, using CR in SCC showed negative effects on the fresh properties of the mixtures. Bignozzi and Sandrolini (2006) studied the effect of adding 0%, 22%, and 33% of CR as partial replacements of fine aggregate (by volume). Their study indicated that increasing the percentage of CR in concrete increased the amount of superplasticizer required to develop successful SCC mixtures. Güneyisi (2010) observed that increasing the rubber content caused an increase in T_{50}, V-funnel flow times, and viscosity, but using rubber and fly ash (FA) together reduced the viscosity of the mixture. Topçu and Bilir (2009) reported that the inclusion of rubber in SCC mixtures showed a higher risk of segregation. They also found that the optimum amount of CR (< 4mm) for the fresh and mechanical properties of SCRC was 8% replacement.

2.3.2 Mechanical properties

Based on previous literature utilizing rubber in concrete has a negative effect on the mechanical properties of concrete in areas such as compressive strength, STS, and FS (Gupta et al., 2015; Al-Tayeb et al., 2012; Najim and Hall, 2010; Su et al., 2015; Aiello and Leuzzi, 2010; Karahan et al., 2012). For instance, Batayneh et al. (2008) reported that the compressive strength of the VRC mixture decreased by 90% when 100% of fine aggregate was replaced by CR. Al-Tayeb et al. (2012) also observed that compressive strength, STS, and ME were decreased by 20%, 16.7%, and 22%, respectively, when 20 % CR was used as a partial replacement of fine aggregate. Another study conducted by Onuaguluchi et al. (2014) showed 40%, 35%, and 29.3% reductions in compressive strength, STS, and ME, respectively, when 15% CR was used. With regard to SCRC mixtures, Karahan et al. (2012) stated that using 30% CR as a partial replacement of fine

aggregate decreased the compressive strength, STS, and FS by 53.3%, 22.9%, and 35.6%, respectively. The reductions in the mechanical properties that resulted from using CR may be attributed to: i) the low stiffness of CR compared to the other mixture components, which makes the rubber particles act as large pores and in turn reduces the effective cross-section (Khaloo et al., 2008); ii) the rough texture of CR particles, which entraps air at the surface (Reda Taha et al., 2008), thus reducing the strength of the mixture; iii) the poor strength of rubber-mortar interface (Najim and Hall, 2010), which encourages the initiation and propagation of microcracks.

Several trials have been proposed by researchers to alleviate the reductions in the mechanical properties that resulted from using CR. One of these trials is to use supplementary cementing materials (SCMs). Silica fume (SLF) is considered one of the most effective SCMs to improve the mechanical properties (especially the compressive strength) of the mixture due to its high pozzolanic reactivity (Monteiro et al., 2012; Barluenga et al., 2013). Adding SLF also appears to improve the impact resistance of concrete and increases the adhesion between aggregate and cement paste in concrete mixtures (Massoud et al., 2003; Nili and Afroughsabet, 2010). Sohrabi and Karbalaie (2011) reported that the addition of SLF in VRC fills the nanometric voids in cement mortar, producing a denser structure and in turn, increasing the compressive strength. Guneyisi et al. (2004) observed that using SLF in VRC appeared to increase the modulus of elasticity, but this increase was less than the increase of the compressive strength.

MK is considered one of the best SCMs to improve the viscosity of SCC mixtures. MK improves the aggregates' suspension in the mixture and reduces the risk of segregation (Cyr and Mouret, 2003; Hassan et al., 2010). MK was also proven to increase the

mechanical properties of SCRC. For example, Ismail and Hassan (2016) observed that using 20% MK in SCRC mixtures improved the compressive strength, STS, FS, and modulus of elasticity by an average of 49.2%, 17%, 14.6%, and 24.9% when the CR increased from 20% to 40%. Ganesan et al. (2013) found that pre-treating the rubber particle surface with polyvinyl alcohol enhances the bond between rubber particles and cement mortar which consequently improves the mechanical properties of the mixture. Segre and Joekes (2000) also concluded that treating the rubber particle surface with sodium hydroxide (NaOH) enhances the rubber adhesion with the cement paste. However, other researchers disagree with surface treatment techniques and conclude that the surface treatment of rubber particles does not significantly affect the compressive strength or STS of rubberized concrete when compared to untreated composites (Albano et al., 2005; Khaloo et al., 2008).

2.3.3 The effect of CR in enhancing the impact resistance and structural performance of concrete

Concrete is a brittle material with low strain capacity, energy absorption, and impact resistance (Wang et al., 2000). The inclusion of a elastic material like rubber particles in concrete can help to alleviate the brittleness and contribute to the enhancement of the flexibility and energy absorption of concrete (Zheng et al., 2008; Al-Tayeb et al., 2013; Najim and Hall, 2012; Rahman et al., 2014). Using rubber particles can also provide an eco-friendly alternative to the disposal of worn-out tires in landfills (Pelisser et al., 2011; Thomas et al., 2014). Several studies have investigated the effect of CR on the properties of concrete in small-scale testing (such as cylinders, prisms, and cubes). These studies

indicate that the inclusion of CR particles appears to enhance the strain capacity, damping ratio, and reduce the self-weight (Najim and Hall, 2012; Rahman et al., 2014). The resistance of concrete to abrasion, freezing-thawing action, and acid attack was also found to increase with the inclusion of rubber (Gesoğlu et al., 2014; Thomas et al., 2015; Thomas et al., 2016). Reutilization of CR in concrete mixtures also plays an important role in enhancing the impact resistance of concrete. Gupta et al. (2015) investigated the replacement of fine aggregate with waste rubber up to 25% by volume in mixtures with different water-to-cement ratios. They found that the inclusion of rubber greatly improved the impact absorption energy of VRC by an average of three times compared to concrete without rubber. Reda Taha et al. (2008) reported similar results in small prism VRC samples, in which the CR was used as a replacement for fine aggregate with percentages varied from 0% to 100% in increments of 25% (by volume). This investigation indicated that despite the reduction in the compressive strength, using a 50% CR replacement could achieve the maximum impact energy, while the beams with 75% CR exhibited impact energy mostly equal to the control mixture (CR = 0%). Furthermore, in large scale testing, a limited number of studies have investigated the effect of CR on the structural performance of large-scale reinforced concrete elements. For example, Yousef et al. (2015) studied the effect of using 20% CR on the seismic performance of column-base connections. Their results indicated that using CR enhanced the hysteretic damping ratio and energy dissipation of column-base connections. A similar effect of CR was observed by Sadek and El-Attar (2014), in which the rubber-cement bricks showed high toughness and deformation capacity compared to their counterparts made with conventional concrete. Ismail and Hassan (2015) studied the flexural behavior of reinforced concrete

beams incorporating CR up to a 50% replacement (by fine aggregate volume). They observed that adding up to 20% CR showed an improvement in the ductility and energy absorption capacity of tested beams, while further increasing the CR content led to a general decay in the behavior of tested beams. The use of rubber particles in concrete can also help to enhance the ductility and reduce the brittle failure. This can be attributed to the elastic nature of rubber particles that can present large elastic deformations before failure (Ganesan et al. 2013). Previous research has shown that using crumb or shredded rubbers as partial replacements of fine or coarse aggregate in concrete mixtures appeared to enhance the ductility and deformability of concrete (Zheng et al., 2008; Hall and Najim, 2014). This allows higher energy dissipation in the beam-column joint under cyclic loading and promotes ductile failure.

2.4 Synthetic fibers

SFs are normally made of a number of different polymer materials. SFs can be classified in two types: i) low modulus fibers such as polyethylene, nylon, polyester, polyolefin, and polypropylene; and ii) high modulus fibers such as carbon, PVA, and Kevlar. By reviewing the literature, it can be observed that the fibers with higher modulus of elasticity contribute to increasing the strength of concrete (Bentur, 2007). However, although polypropylene fibers have low modulus of elasticity, they tend to be the most extensive fibers used in comparison to all other types of SFs (Bentur, 2007). Polypropylene fibers have an advantage of being formed into various shapes and sizes and have different surface finishes (Wang et al., 1987), which improves the bond strength between the fibers and cement matrix (Choi et al., 2012). Polypropylene fibers can also

be fabricated at low cost, have a high alkalis resistance, no tendency to corrosion, and remain stable in a cementitious composite over the service life (Wang et al., 1987; Jun et al., 2016; Richardson, 2005; Mu et al., 2002).

Recent studies proposed surface treatment to enhance the bond capacity of polypropylene fibers in fiber reinforced concrete. For example, Zhang et al. (2000) observed that the flexural behavior and toughness of fiber reinforced concrete were enhanced when the surface of polypropylene fibers was treated with temperature cascade arc plasma. Similarly, Tu et al. (1999) reported that using fluorination or oxy-fluorination processes to treat the polypropylene fibers helped to improve the overall behavior of fiber reinforced concrete mixtures.

SFs can be divided into two categories based on the fiber size: micro-synthetic fibers (MISFs) and macro-synthetic fibers (MASFs), as shown in Figure 2-2. MISFs can also be divided into two subcategories based on the fabrication method: monofilament fibers and fibrillated fibers. Monofilament fibers can be described as an individual extruded thin polymer cut to appropriate lengths (Bentur, 2007). Meanwhile, fibrillated fibers can be described as fibers stretched into thin sheets then slit into individual filaments and held together by cross-linking along the length, forming a tape (see Figure 2-2). This tape is twisted into bundles and cut to appropriate lengths (Zheng and Feldman, 1995; Bentur, 2007). Fibrillated fibers showed a better bond strength with concrete matrix compared to monofilament type fibers, as reported by Soroushian et al. (1992). Comparatively, MASFs were fabricated as a stick which consists of two filaments cross-linked along the fiber length (see Figure 2-2). The surface of these fibers is also embossed to create deformations to provide mechanical anchorage between the fibers and the concrete

matrix. The cross-linking, surface deformation, and high modulus of elasticity of MASFs contribute to enhancing the bond strength between fibers and concrete. Choi et al. (2012) reported that the bond strength of MASFs is greatly affected by the mechanical anchorage type and surface area. In their study it was observed that MASFs with crimped surface and modified cross sections can attain bond stress versus bond-slip relationship comparable to that of steel fibers.

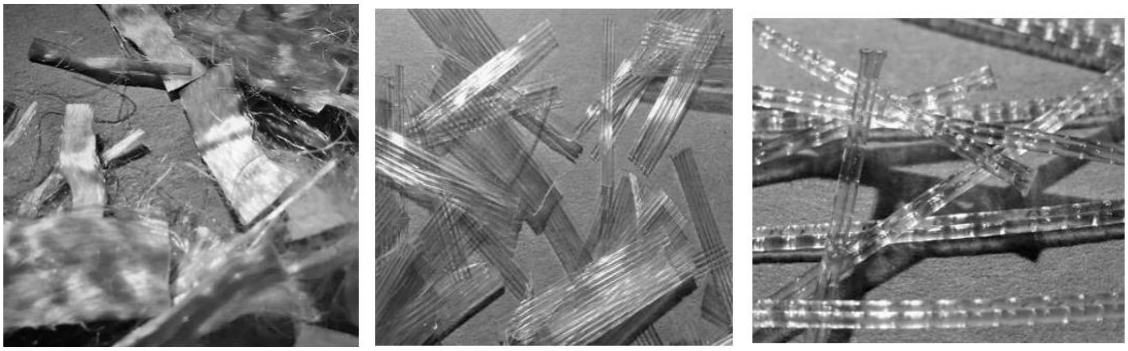

(a) (b) (C)

Figure 2-2 Types of synthetic fibers: (a) Monofilament micro-synthetic fibers, (b) Fibrillated micro-synthetic fibers, (c) macro-synthetic fibers (BASF, 2012)

2.5 Effect of SFs on the fresh, mechanical, and structural performance of concrete

2.5.1 Fresh and mechanical properties of concrete

Adding fibers to concrete mixtures is proven to enhance the mechanical properties of concrete. The bridging mechanism of fibers significantly helps to restrict the development of cracks, thus increasing the ability of concrete to endure higher stress. Using fibers in concrete was also found to increase the toughness, ductility, and impact resistance (Grabois et al., 2016; Yap et al., 2014; Hamoush, 2010). Among the different types of fibers, MFs and SFs have received much attention and become widely used. Previous

studies indicated that the improvement in the tensile strength of concrete appeared to be more pronounced when MFs were used compared to all other types of fibers. For example, Khayat et al. (2014) studied the effects of using 30mm MFs and 40mm SFs on the behavior of SCC. They observed that adding 0.5% MFs or SFs increased the STS by 40.4% and 9.5%, respectively (Corinaldesi and Moriconi, 2015; Grabois et al., 2016; Abadel et al., 2015). On the other hand, the low density of the SFs has an advantage over the other types of fibers in reducing the self-weight of concrete. In addition, SFs have no tendency to corrode (Jun *et al*., 2016), which extends their possible applications.

Adding fibers to SCC mixtures, in general, can significantly reduce the fresh properties of the mixtures. Khaloo *et al*. (2014) reported that it was not possible to develop SCC with higher than 0.5% volume fraction of MFs as the results of L-box test for all mixtures with higher fiber contents did not meet the acceptable limits given by EFNARC (2005) (L-box ratio is less than 0.75). Similar results were reported by Khayat *et al*. (2014) who found that the inclusion of MFs and SFs in SCC generally reduced the flowability and passing ability of the mixture. The inclusion of fibers in concrete mixtures was also found to have positive effects on the impact resistance and energy absorption capacity of concrete (Batayneh et al., 2008; Najim and Hall, 2010, Güneyisi, 2010). Banthia et al. (2003) found that the use of fibers in VC mixtures enhanced the post-fracture stress transfer capability, which in turn improved the resistance to impact loads. They attributed their results to the superior effect of fibers in bridging the matrix cracks. Using fibers also proved to have a positive effect on the tensile strength of concrete. Choi and Yuan (2005) observed that the addition of polypropylene fibers in VC increased the STS by 20% to 50%. Song et al. (2005) found that using 0.1% nylon fibers in VC mixtures increased the

first crack and failure crack by 19% and 30.5%, respectively, while these increases reached up to 11.9% and 17% when polypropylene fibers were used. Hasan et al. (2011) reported that using 0.33-0.5% MASFs in VC mixtures showed an increase in the STS ranging from 10 to 15%. They also observed that the addition of MASFs enhanced the peak strain and post-peak ductility. It should be noted that although the addition of SFs to concrete mixtures exhibited a negligible effect on the compressive strength, using a high volume fraction of SFs may negatively affect the compressive strength due to the poor concrete compaction with such a high volume of fibers (Bentur, 2007).

2.5.2 Structural performance of fiber reinforced concrete elements

Previous research studies have investigated the influence of using fibers on the structural behavior of concrete elements. For example, Hasan et al. (2011) studied the effect of using different volume fractions of MASFs on the mechanical behavior of concrete. Their results indicated that using 0.33%, 0.42%, and 0.51% MASFs enhanced the tensile strength of concrete by 10%, 15%, and 14%, respectively. Their results also indicated that the inclusion of MASFs had a negligible effect on the compressive strength and the failure of the tested specimens appeared to be more ductile when MASFs were used compared to the other tested fibers. Carnovale (2013) studied the shear behavior of small concrete panels reinforced with MASFs and steel fibers under in-plane shear loading. The results of this investigation indicated that using 2% MASFs had a similar structural response to using 1% steel fibers with the same length (50mm). His results also showed that strain hardening and multiple cracking were achieved only when a high percentage of

MASFs was used (2%). Imran et al. (2015) studied the effect of using MASFs on the ductility and strength of reinforced concrete columns subjected to monotonic compressive loading. They reported that the inclusion of MASFs significantly enhanced the ductility of concrete columns, while the strength slightly improved. Their results also revealed that adding MASFs to concrete mixtures helped to delay the brittle degradation of the column strength and provided a ductile failure. Altoubat et al. (2009) studied the effect of MASFs on the performance of slender and short reinforced beams made with conventional concrete. They reported that the inclusion of 40mm MASFs at 0.50%, 0.75%, and 1% volume fractions led to an increase in the ultimate shear strength of slender beams, reaching up to 14%, 23%, and 30%, respectively, compared to beams with no fibers. These increases were more pronounced in short beams, in which adding 0.5% and 0.75% volume fractions of MASF increased the shear capacity of beams by 20% and 28%, respectively. Similar results were observed when Ababneh et al. (2017) studied the influence of SFs on the shear behavior of lightweight concrete beams. Using 7 kg/m^3 of SFs in their study led to considerable improvements in the ultimate shear capacity, deformation capacity, stiffness, and toughness of tested beams, reaching up to 58%, 25%, 21%, and 122%, respectively. Roesler et al. (2006) tested the effect of MASFs on the flexural cracking load and the ultimate flexural load of concrete slabs-on-ground. Their results indicated that using a volume fraction of 0.32% and 0.48% of 40mm MASFs increased the flexural cracking load by 25% and 32%, respectively, while the ultimate flexural load increased by 20% and 34%, respectively, compared to plain concrete without fibers. Altoubat et al. (2009) investigated the use of polypropylene fibers in reinforced concrete beams without stirrups and with variable shear span to depth ratio

(a/d ≥ 2.5, and a/d< 2.5). Their study indicated that the addition of polypropylene fibers contributed to increase the first diagonal cracking load and load carrying capacity. These findings were in agreement with other researchers (Buratti et al., 2011; Bentur, 2007; won et al., 2006; Oh et al., 2002). Moreover, the polypropylene fibers helped to enhance the post-cracking stiffness, which reduced deflections under service loads (Li et al., 1992; Madjzadeh et al., 2006). Altoubat et al. (2009) reported that using polypropylene fibers in concrete beams without stirrups exhibited multiple shear cracks but with controlled crack widths. This, in turn, helped to promote the ductility, deformability, and toughness of concrete beams. Ma et al. (2012) investigated the seismic performance of concrete columns containing MASFs. The use of SFs in their investigation increased the deformation capacity two to three times compared to plain reinforced concrete (without fibers) and delayed the rapid stiffness declination allowing for higher energy absorption.

2.6 Engineering cementitious composites

Engineered cementitious composite (ECC) is considered a special type of high-performance-fiber-reinforced-cement-based composite, which was first developed by Victor Li in the 1990s based on micromechanics theory (Li, 1993). ECC is characterized by adequate strength, high strain capacity, strain hardening, and saturated multiple cracking behavior under tensile loading (Li et al., 2001; Li, 2003; Li and Tailoring, 2012). In addition, ECC proved to have higher impact resistance, fatigue life, and energy dissipation capacity compared to conventional concrete (Zhang and Li, 2002; Suthiwarapirak et al., 2004; Jun and Mechtcherine, 2010). The tensile ductility of ECC was found to be approximately 600 times as much as normal concrete in tension and

tensile strain capacity ranged from 3-5% (Li, 1998; Kong et al., 2003). ECC also characterized by a formation of closely spaced multiple tiny cracks (less than 100- μm) even at large deformation (Sahmaran and Li, 2010).

The performance of ECC is mainly influenced by its mixture composition. ECC is typically developed using cement, different supplementary cementing materials, silica sand, and moderate volume of polymeric fibers. In standard ECC, FA is usually used with high volumes as a replacement for cement, reaching up to 85% by weight of cement (Yang et al., 2007). Although FA helps to improve the workability and decrease the drying shrinkage and crack widths of the mixture (Yang et al., 2007), using high volume of FA in ECC negatively affects its mechanical and durability properties (Sahmaran and Li, 2009). Such negative impacts of high-volume FA can be compensated by using high reactive pozzolanic supplementary cementitious materials (SCMs) such as MK and/or SLF, while the deformation capacity of ECC may be slightly reduced (Özbay et al., 2012; Zhu et al., 2014). The behavior of ECC is also affected by the properties of the silica sand, which is typically used as the fine aggregate in standard ECC (Wang and Li, 2006; Kim et al., 2007; Yang et al., 2012; Zhou and Qian, 2010). However, the low availability, high cost, and environmental problems of the production of silica sand limit the feasibility of employing ECCs in wide construction applications (Huang et al., 2013).

3 Experimental program

3.1 Introduction

This chapter presents the research methodology including the materials properties used in this investigation, mixing procedures, samples type and dimensions, pouring and curing techniques, and tests carried out on the fresh and hardened states of developed mixtures. Furthermore, the details of flexural, shear, and cyclic loading tests of large-scale reinforced concrete elements are provided, including the elements' dimensions, test setup, load application, and measurements.

3.2 Materials

3.2.1 Cement and SCMs

GU Portland cement, MK, FA, ground granulated blast-furnace slag (GGBS), and SLF, conforming to type 1 ASTM C150 (2012), ASTM C618 Class N (2012), ASTM C618 Type F (2012), ASTM C989 (2014), and ASTM C1240 (2000), respectively, were used as binders for developed mixtures. **Figure 3-1** shows cement and SCMs (MK, FA, GGBS, and SLF) used in this study. **Table 3-1** presents the chemical and physical properties of the used cement and other SCMs.

Figure 3-1 The used cement and other SCMs

Table 3-1 The chemical and physical properties of the used cement and other SCMs

Chemical properties (%)	Cement	MK	FA	GGBS	SLF
SiO_2	19.64	51-53	52	40.3	89.1
Al_2O_3	5.48	42-44	23	8.4	0.67
Fe_2O_3	2.38	<2.2	11	0.5	0.49
FeO	-	-	-	-	-
TiO_2	-	<3.0	-	-	-
C	-	-	-	-	-
Cr_2O_3	-	-	-	-	-
MnO	-	-	-	-	-
P_2O_5	-	<0.2	-	-	-
SrO	-	-	-	-	-
BaO	-	-	-	-	-
SO_4	-	<0.5	-	-	-
CaO	62.44	<0.2	5	38.71	6.12
MgO	2.48	<0.1	-	11.06	0.31
Na_2O	-	<0.05	-	-	0.26
C_3S	52.34	-	-	-	-
C_2S	16.83	-	-	-	-
C_3A	10.50	-	-	-	-
C_4AF	7.24	-	-	-	-
K_2O	-	<0.40	-	0.37	0.49

L.O.I	2.05	<0.50	-	0.65	2.81
Physical properties					
Specific gravity	3.15	2.56	2.38	2.9	2.2
Blaine fineness (m^2/kg)	410	19000	420	400	27600

3.2.2 Coarse, fine, and rubber aggregates

Natural crushed stones (with 10mm and 20mm maximum aggregate sizes) and natural sand were used as coarse and fine aggregates, respectively. The fine and coarse aggregates have a specific gravity of 2.6 and water absorption of 1%. CR with a maximum size of 4.75mm, specific gravity of 0.95, and negligible water absorption was used as a partial replacement of fine aggregate. **Figure 3-2** shows the coarse aggregate, fine aggregate, CR used in this study and their gradations.

(a)

Crushed stone
(coarse aggregate)

Natural sand
(fine aggregate)

CR

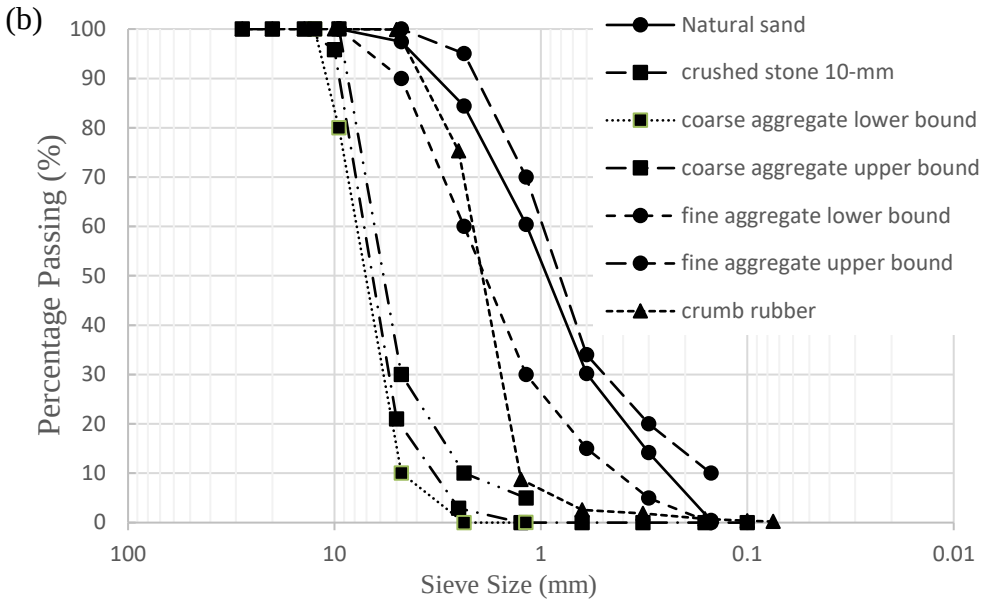

Figure 3-2 Coarse, fine and CR aggregates: (a) shape, (b) gradation curves

3.2.3 Chemical admixtures

A polycarboxylate based HRWRA (Glenium 7700) similar to ASTM C494 Type F with a specific gravity of 1.2, volatile weight of 62%, and pH of 9.5 was used to achieve the required slump flow/workability of the developed mixtures.

3.2.4 Synthetic, metal fibers and steel rebar

Two types of hooked-ends MFs were used in this study. The first type had a length of 35mm, an aspect ratio of 65, and tensile strength of 1150 MPa, while the second type had a length of 60mm, an aspect ratio of 65, and tensile strength of 1150 MPa. Five types of SFs were used: three types of MASFs measuring 38mm, 50mm, and 54mm (MASF38, MASF50, and MASF54) and two types of MISFs measuring 19mm, and 27mm (MISF19 and MISF27). **Table 3-2** presents the physical and mechanical properties of the SFs used,

and **Figure 3-3** shows the configuration and geometry of both MFs and SFs. Steel bars with diameters of 10mm and 25mm were used in the constructed beams as a transversal and longitudinal reinforcement. All steel bars had an average yield stress of 400 MPa and an average tensile strength of 725 MPa.

Table 3-2 Geometrical and mechanical characteristics of SFs used

Fibers used	Type	Length (mm)	Diameter/equivalent diameter (mm)	Specific gravity	Tensile strength (MPa)
MISF19	Micro-synthetic fiber	19	0.66	0.91	300
MISF27	Micro-synthetic fiber	27	0.8	0.91	585
MASF38	Macro-synthetic fiber	38	0.64	0.91	515
MASF50	Macro-synthetic fiber	50	0.66	0.91	415
MASF54	Macro-synthetic fiber	54	0.8	0.91	585

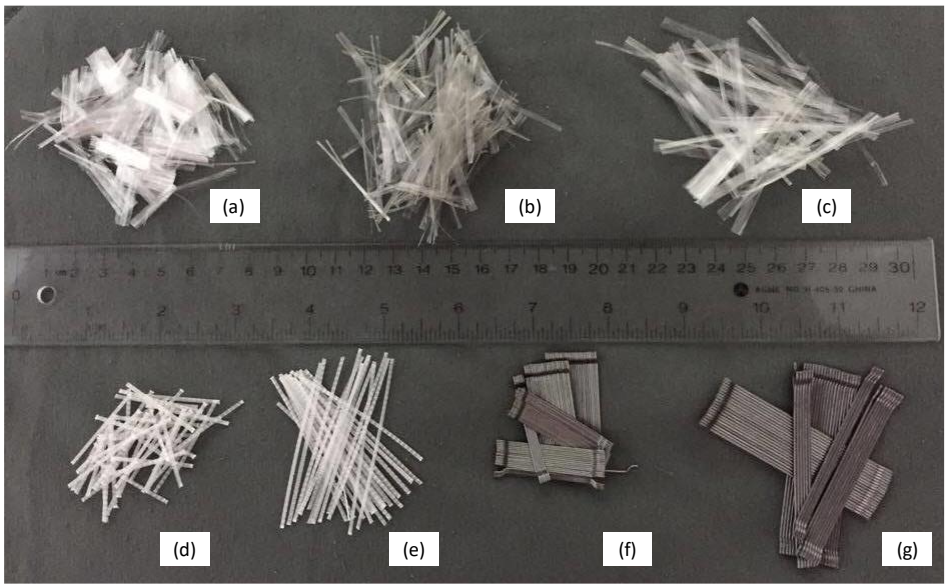

Figure 3-3 The fibers used: (a) MISF19, (b) MASF38, (c) MASF50, (d) MISF27, (e) MASF54, (f) MF35, and (g) MF60

3.3 Experimental study 1: Use of SFs/MFs to optimize the fresh properties, stability, and strength of SCRC mixtures with different binder contents and SCMs

3.3.1 Research significance

This investigation studied the fresh properties, mechanical properties, and impact resistance of SCRC/FRSCRC mixtures developed with different mixture compositions and various SCMs. There are very few studies that have investigated the behavior of VRC incorporating CR and MFs, but there is no data available regarding the impact of combining SFs and CR on the fresh, and mechanical properties of SCC mixtures. In addition, the effect of combining CR with SFs on the impact resistance of SCC concrete mixtures is missing from the literature. This investigation aimed to develop and optimize a number of FRSCRC and fiber reinforced VRC (FRVRC) mixtures with different types, sizes, and volumes of SFs. Using fibers in SCRC can help to alleviate the reduction of STS and FS, which allows a higher percentage of CR to be used in the mixtures. This, in turn, creates eco-friendly mixtures with higher ductility and impact resistance and with an additional reduction of self-weight (especially when SFs are used). This research can contribute to enhancing the performance of FRSCRC and increase the potential use of such concrete in applications that require high impact resistance and energy absorption.

3.3.2 Scope of work (mixtures development)

3.3.2.1 Stage 1- Effect of different SCMs in optimizing SCRC mixtures

In this stage, a total of 16 rubberized concrete mixtures were developed and tested. The experimental investigation aimed to develop a number of SCRC mixtures having maximum percentages of CR (by volume of fine aggregate) and a minimum reduction in strength and stability. The effects of the CR percentage, binder content, and different SCMs (SLF, GGBS, MK, and FA) on the fresh properties, mechanical properties, and stability of SCRC mixtures were investigated and discussed. This study aimed to compare the performance of other SCM (MK, FA, and GGBS) in optimized SCRC mixtures with that of silica fume SCRC (SLFSCRC). The first set of mixtures (mix 1-5) were designed to investigate the effect of increasing the percentage of CR on The SLFSCRC mixtures. The second set of mixtures (mix 6-8) was designed to compare SLFSCRC with the performance of other SCMs (MK, FA, GGBS) in optimized SCRC mixtures with maximum percentages of CR. The third set of mixtures (9-11) investigates the effect of binder content in enhancing and optimizing SLFSCRC mixture with a high percentage of CR. The fourth set of mixtures (12 and 13) investigates the effectiveness of using MK in improving the properties of SLFSCRC in order to allow a higher percentage of CR to be used in SLFSCRC mixture. The fifth set of mixtures (mix 14-16) designed to compare the effect of combining MK with FA on improving the properties of SCRC and allowing a higher percentage of CR with minimum reduction in mechanical properties.

The optimum percentage used of each of SLF, MK, FA, and GGBS were 10%, 20%, 30%, and 30%, respectively. The percentages of SLF, MK, GGBS, and FA were chosen

based on a preliminary trial mixes stage that was carried out on these SCMs to determine their optimal dosage to achieve acceptable fresh properties and a reasonable compressive strength suitable for structural applications. Before selecting the mixture proportions for each mixture, several trial mixtures were done to determine the minimum water-to-binder (w/b) ratio that can be used to develop mixtures meet the accepted fresh properties of SCC without overdosing the HRWRA. The trial mixes indicated that a w/b ratio of at least 0.4 was required to obtain a mixture with a slump flow diameter of 700 ± 50mm and with no visual sign of segregation. All mixtures were developed using 10mm crushed stone aggregate with a constant coarse-to-fine aggregate ratio of 0.7. This percentage was chosen based on previous research the authors conducted on SCC (Hassan et al. 2015). Varied amounts of HRWRA were added to the developed mixtures until the mixtures achieved a slump flow diameter of 700 ± 50mm. The mixture compositions of this stage are shown in **Table 3-3**.

3.3.2.2 Stage 2- Use of different types, lengths, and volumes of SFs to optimize SCRC mixtures (development of FRSCRC mixtures)

This stage aimed to optimize and develop SCRC and FRSCRC mixtures that have superior properties for structural applications requiring high-impact resistance, energy dissipation, and ductility. The development of SCRC and FRSCRC required adequate viscosity to enhance particle suspension and decrease the risk of rubber segregation. In addition, to meet the accepted fresh properties as per EFNARC (2005), the mixtures had to achieve a certain necessary level of flowability. Therefore, as a first step, several trial

mixtures were cast to determine the minimum water-to-binder (w/b) ratio and minimum total binder content that can be used to develop mixtures that meet the accepted fresh properties of SCC without overdosing the HRWRA. The trial mixes showed that a w/b ratio of at least 0.4 and a binder content of 550 kg/m^3 were required to obtain SCC with slump flow diameter of 700 ± 50mm and with no visual sign of segregation. The previous stage (stage 1) showed that the use of FA was necessary to compensate for the reduction in flowability of SCC mixtures resulting from the addition of CR and fibers. Similarly, MK was used to adjust the viscosity of the mixtures in order to improve the suspension of CR particles and reduce their tendency to segregate during mixing. Moreover, MK has a promising potential to increase the mechanical properties and compensate for the reductions that result from using a high percentage of CR (Ismail and Hassan, 2016b; Madandoust and Mousavi, 2012). Based on stage 1, the optimized viscosity/flowability of mixtures was achieved by using 20% MK and 30% FA (by weight of the binder content). Furthermore, all mixtures were developed using 10mm crushed stone aggregate with a constant coarse-to-fine aggregate ratio of 0.7. This percentage was chosen based on previous research conducted on SCC (Hassan et al., 2015). Varied amounts of HRWRA were added to the developed mixtures until the mixtures achieved a slump flow diameter of 700 ± 50mm.

The first set of mixtures evaluated the maximum possible percentage of CR that can be used in SCC mixtures to satisfy the criteria of self-compactibility given by EFNARC (2005) (mixtures 1–7). The second set of mixtures utilized different types of fibers to compensate for the reduction in the tensile and flexural strengths of SCRC mixtures that

resulted from using CR. However, since the fresh properties of SCC mixtures are negatively affected by the inclusion of CR and/or fibers (especially passing ability), limited volumes of CR and fibers could be combined safely to develop mixtures with acceptable properties according to EFNARC (2005). In total, sixteen FRSCRC mixtures were developed in the second set of mixtures. These mixtures were divided into five groups as follows:

a) four mixtures with 5% to 20% CR and 0.2% MISFs (19mm) (mixtures 8–11);

b) three mixtures with 5% to 15% CR and 0.2% MASFs (38mm) (mixtures 12–14);

c) two mixtures with 5% to 10% CR and 0.2% MASFs (50mm) (mixtures 15–16);

d) four mixtures with 5% to 20% CR and 0.2% MISFs (27mm) (mixtures 17–20); and

e) three mixtures with 5% to 15% CR and 0.35% MFs (35mm) (mixtures 21–23).

The author found that further increasing the percentage of CR and/or fiber volume beyond the maximum combinations used in each group led to a significant drop in the L-box value below the acceptable limits given by EFNARC (2005). The mixture compositions of this set are shown in **Table 3-4**.

The last set of mixtures in this work was designed to test VRC mixtures to investigate the possibility of using higher volumes of fibers and CR, since achieving acceptable fresh properties of SCC (especially passing ability) was not a target in these mixtures. Optimizing FRVRC mixtures with higher volumes of fibers and CR in this set of mixtures also aimed to develop mixtures with further reduction of self-weight and higher potentials for structural applications subjected to impact loadings. In addition, utilizing a higher percentage of fibers in VRC mixtures can play an important role in compensating for the reductions in the tensile and flexural strengths resulting from the addition of CR. In total,

seven FRVRC mixtures were developed in this set. Each mixture combined 30% CR and 1% volume fraction from each type of fiber. The selection of the 30% CR and 1% fiber in this set was based on a preliminary trial mixtures stage to obtain acceptable mixture consistency (no visual sign of CR or fiber clumping) and reasonable compressive strengths for the structural application (more than 25 MPa). The detailed mixtures in this stage are shown in **Table 3-4** (mixtures 24–31).

All tested mixtures in the three sets were designated by the percentage of CR, either SCC or VC, type and volume of fiber, and fiber length. For example, an SCC mixture using 15% CR and 0.2% 19mm MISFs would be labeled as 15CR-SCC-0.2MISF19. Also, a VC mixture using 30% CR and 1% 35mm MFs would be labeled as 30CR-VC-1MF35.

Table 3-3 Mix design for rubberized concrete mixtures of stage 1

Mix #	Mixture	Cement (kg/m^3)	SCM (Type)	SCM (kg/m^3)	C. A. (kg/m^3)	F. A. (kg/m^3)	CR (kg/m^3)	HRWRA (L/m^3)
1	550C-0CR-SLF	495	SLF	55	640.65	915.22	0.0	3.6
2	550C-5CR-SLF	495	SLF	55	640.65	869.46	16.72	3.65
3	550C-10CR-SLF	495	SLF	55	640.65	823.69	33.44	3.85
4	550C-15CR-SLF	495	SLF	55	640.65	777.94	50.16	4.00
5	550C-20CR-SLF	495	SLF	55	640.65	732.18	66.88	4.1
6	550C-20CR-MK	440	MK	110	638.4	729.6	66.7	5.26
7	550C-20CR-FA	440	FA	110	636	726.9	66.4	1.84
8	550C-20CR-GGBS	385	GGBS	165	643.3	735.2	67.2	1.84
9	500C-5CR-SLF	450	SLF	50	679.74	922.5	17.74	3.75
10	600C-20CR-SLF	540	SLF	60	601.57	687.51	62.8	3.85
11	600C-25CR-SLF	540	SLF	60	601.57	644.54	78.5	4.00
12	550C-20CR-SLF-MK	385	SLF-MK	55-110	630.93	721.1	65.87	6.10
13	550C-25CR-SLF-MK	385	SLF-MK	55-110	630.93	676	82.33	6.25
14	550C-20CR-MK-FA	275	MK+FA	110+165	620.3	708.9	64.8	3.75
15	550C-25CR-MK-FA	275	MK+FA	110+165	620.3	664.6	80.9	3.75
16	550C-30CR-MK-FA	275	MK+FA	110+165	620.3	620.3	97.1	4.38

Table 3-4 Mix design for SCRC, FRSCRC, VRC, and FRVRC mixtures of stage 2

Mix #	Mixture	Cement (kg/m^3)	SCM (Type)	SCM (kg/m^3)	C. A. (kg/m^3)	F. A. (kg/m^3)	CR (kg/m^3)	HRWRA (L/m^3)	Fiber (V_f%)
SCRC									
1	0CR-SCC	275	MK+FA	110+165	620.3	886.1	0.0	3.43	-
2	5CR-SCC	275	MK+FA	110+165	620.3	841.8	16.2	3.43	-
3	10CR-SCC	275	MK+FA	110+165	620.3	797.5	32.4	3.75	-
4	15CR-SCC	275	MK+FA	110+165	620.3	753.2	48.6	3.75	-
Mix #	Mixture	Cement (kg/m^3)	SCM (Type)	SCM (kg/m^3)	C. A. (kg/m^3)	F. A. (kg/m^3)	CR (kg/m^3)	HRWRA (L/m^3)	Fiber (V_f%)

5	20CR-SCC	275	MK+FA	110+165	620.3	708.9	64.8	3.75	-
6	25CR-SCC	275	MK+FA	110+165	620.3	664.6	80.9	3.75	-
7	30CR-SCC	275	MK+FA	110+165	620.3	620.3	97.1	4.38	-
FRSCRC									
8	5CR-SCC-0.2MISF19	275	MK+FA	110+165	618.13	838.89	16.13	5.75	0.2
9	10CR-SCC-0.2MISF19	275	MK+FA	110+165	618.13	794.73	32.26	6	0.2
10	15CR-SCC-0.2MISF19	275	MK+FA	110+165	618.13	750.58	48.40	6.2	0.2
11	20CR-SCC-0.2MISF19	275	MK+FA	110+165	618.13	706.43	64.53	6.4	0.2
12	5CR-SCC-0.2MASF38	275	MK+FA	110+165	618.13	838.89	16.13	6	0.2
13	10CR-SCC-0.2MASF38	275	MK+FA	110+165	618.13	794.73	32.26	6.23	0.2
14	15CR-SCC-0.2MASF38	275	MK+FA	110+165	618.13	750.58	48.40	6.3	0.2
15	5CR-SCC-0.2SMAF50	275	MK+FA	110+165	618.13	838.89	16.13	6.125	0.2
16	10CR-SCC-0.2MASF50	275	MK+FA	110+165	618.13	794.73	32.26	6.3	0.2
17	5CR-SCC-0.2MISF27	275	MK+FA	110+165	618.13	838.89	16.13	4.75	0.2
18	10CR-SCC-0.2MISF27	275	MK+FA	110+165	618.13	794.73	32.26	5.25	0.2
19	15CR-SCC-0.2MISF27	275	MK+FA	110+165	618.13	750.58	48.40	5.5	0.2
20	20CR-SCC-0.2MISF27	275	MK+FA	110+165	618.13	706.43	64.53	5.5	0.2
21	5CR-SCC-0.35MF35	275	MK+FA	110+165	616.5	836.7	16.1	4.63	0.35
22	10CR-SCC-0.35MF35	275	MK+FA	110+165	616.5	792.7	32.2	4.63	0.35
23	15CR-SCC-0.35MF35	275	MK+FA	110+165	616.5	748.6	48.3	4.63	0.35
VRC/FRVRC									
24	30CR-VC	275	MK+FA	110+165	620.3	620.3	97.1	3.18	-
25	30CR-VC-1MISF19	275	MK+FA	110+165	609.56	609.56	95.45	3.18	1
26	30CR-VC-1MASF38	275	MK+FA	110+165	609.56	609.56	95.45	3.18	1
27	30CR-VC-1MASF50	275	MK+FA	110+165	609.56	609.56	95.45	3.18	1
28	30CR-VC-1MISF27	275	MK+FA	110+165	609.56	609.56	95.45	3.18	1
29	30CR-VC-1MASF54	275	MK+FA	110+165	609.56	609.56	95.45	3.18	1
30	30CR-VC-1MF35	275	MK+FA	110+165	609.56	609.56	95.45	3.18	1
31	30CR-VC-1MF60	275	MK+FA	110+165	609.56	609.56	95.45	3.18	1

3.3.3 Mixing procedures

Prior to mixing, the coarse aggregate, cement, SCMs, CR, and sand were placed in a rotary mixer and then dry-mixed for approximately 1.5 minutes. For fiber mixtures, fibers were gradually added during the dry-mixing process to obtain well-distributed fibers and avoid the formation of fiber balls in the mixture. Next, around 65% of the required amount of water was added to the dry materials and remixed for another 1.5 minutes. The remaining water was first mixed with the required dosage of HRWRA and then added to the mixer and remixed for another 2.5 ± 0.5 minutes.

3.3.4 Casting and curing procedures

For SCRC/FRSCRC mixtures different small-scale specimens including cylinders and prisms were poured without hand compaction or mechanical vibration. On the other hand, the VRC/FRVRC samples were compacted using a mechanical vibrator and trowel-finished for smooth top surfaces (**Figure 3-4a**). All the prepared samples were moist-cured in a curing room with a controlled temperature of 25 ± 1.5° for 7 and 28 days before the mechanical properties were tested (**Figure 3-4b**).

(a)

(b)

Figure 3-4 The developed mixtures (a) the cast- specimens, (b) the moist-curing regime

3.3.5 Fresh properties tests

The fresh properties tests of SCRC and FRSCRC mixtures were conducted as per EFNARC (2005). The fresh properties tests included slump flow, J-ring, V-funnel, L-box, and sieve segregation tests. The time to reach 500mm slump flow diameter, time to reach 500mm J-ring diameter (T_{50} and T_{50J}) and the V-funnel time were used to evaluate the mixture viscosity (**Figure 3-5**). These times were accurately measured for all tested

SCRC and/or SFSCRC mixtures using a videotape recording device connected to a computer to record the time up to 0.01 seconds. Slump flow–J-ring diameter and L-box heights were measured to evaluate the passing ability of SCRC and/or SFSCRC **(Figure 3-5)**. The stability of the mixtures was evaluated using a sieve segregation resistance test to measure segregation resistance of SCRC and/or SFSCRC mixtures. The stability of the mixture was also evaluated by measuring the distribution of the rubber particles in the mixture visually after splitting 100mm diameter x 200mm height concrete cylinder (see **Figure 3-6**). **Figure 3-6** classifies the stability of rubber particles into three cases; namely no segregation (NS), moderate segregation (MS), and heavy segregation (HS). The workability of VRC and FRVRC mixtures was evaluated by slump test, according to ASTM C143 (2015).

(a)  (b)  (c) 

(d) 

Figure 3-5 Fresh properties tests (a) slump flow, (b) J-ring, (c) V-funnel, (d) L-box

(a) (b) (c)

Figure 3-6 Rubber particles stability (a) no segregation (NS), (b) moderate segregation (MS), (c) heavy segregation (HS)

3.3.6 Mechanical properties tests

The mechanical properties tests included compressive strength, STS, FS, and modulus of elasticity (ME). The compressive strength and STS were evaluated using three identical concrete cylinders (100mm diameter x 200mm height), as per ASTM C39 (2011) and C496 (2011), respectively. A concrete prism of 100mm x 100mm cross section and 400mm in length was tested by using a four-point loading test to assess the FS, according to ASTM C78 (2010). The ME was measured by attaching a 25mm strain gauge on a cylinder of 100mm diameter and 200mm length tested under compressive loading. All tested mixtures samples were moist-cured until the age of testing (7 and 28 days).

3.3.7 Impact resistance under drop-weight test

A drop weight test was performed to evaluate the impact resistance of developed mixtures according to ACI 544 (1999). The test was conducted on three specimens 150mm in diameter and 63.5mm thick. These specimens were carefully cut from concrete cylinders measuring 150mm in diameter and 300mm in height after removing the top layer of the

cylinder using a diamond cutter. As per ACI 544 (1999), a 4.45-kg hammer was dropped from a height of 457mm onto a 63.5mm steel ball located at the center of the top surface of the specimen (see Figure 3-7a). The number of blows needed to initiate the first visible crack (N_1) was recorded. The ultimate crack resistance was obtained by recording the number of blows that caused failure (N_2). This number was recorded when the cracked specimen touched the lugs on the baseplate of the device (ACI 544 1999).

3.3.8 Impact resistance under flexural loading

The Flexural Impact test used a three-point flexural loading setup to evaluate the energy absorption of beams made with the developed mixtures (see **Figure 3-7b**). For each of the developed mixtures, three beam samples of 100 x 100mm cross-section and 400mm in length were tested with a loading span of 350mm. A 4.45-kg hammer was dropped from a height of 150mm onto the mid-span of the tested beams. The drop height of 150mm was chosen based on several trials to obtain an acceptable height that helped increase the accuracy of evaluating the impact strength of the tested beams. The SCC/SCRC beams in the second test suddenly broke into two halves. Therefore, only the number of blows that caused failure was recorded to demonstrate the ultimate impact energy. Since the beams reinforced with fibers were difficult to break into two halves, the ultimate failure of FRSCRC and FRVRC beams was identified when the maximum width of the major crack reached 5mm.

For both impact tests, the impact energy (*IE)* was calculated using **Equation (3.1)**:

$$IE = N\,mgh \tag{3.1}$$

Where: N is the number of blows at crack level; m is the mass of the dropped hammer (4.45 kg); g is the gravity acceleration (9.81 m/s^2); and h is the drop height (150 or 457mm).

(a) (b)

Figure 3-7 Impact tests (a) drop-weight test (ACI-544), (b) flexural loading test

3.4 Experimental study 2: Influence of SFs' type, length, and volume on enhancing the structural performance of rubberized concrete

This study aimed to evaluate the flexural performance of 12 beams poured from mixtures that were optimized in study 1.

3.4.1 Research significance

Several structural applications require high ductility and energy absorption in reinforced concrete beams. Using CR in concrete mixtures showed a positive effect on improving the ductility, energy absorption, and impact resistance of concrete. However, adding CR proved to have a negative effect on the mechanical properties of concrete. Using fibers in rubberized concrete can help to compensate for the reductions in the mechanical properties that result from using CR. Using fibers can also further enhance the ductility, energy absorption, and impact resistance when combining fibers with CR in concrete beams. By reviewing the literature, it can be observed that there is a limited number of studies that investigate the effect of using fibers in rubberized concrete beams subjected to four-point loading. Furthermore, there are no available studies that have investigated the effect of using SFs on the structural behavior of rubberized concrete beams, especially when different types, lengths, and volumes of SFs are used. The main objective of this study was to investigate the effect of combining MISFs/MASFs with CR on maximizing the bending moment capacity, ductility, and energy absorption of the tested beams. This study will help to improve understanding of the structural behavior of rubberized concrete beams.

3.4.2 Scope of work

Mixtures optimized from study 1

This study contained a total of twelve mixtures (twelve concrete beams): four SCRC, three SFSCRC, and five synthetic fibers VRC (SFVRC) mixtures. These mixtures were selected based on study 1 that aimed to optimize the fresh and mechanical properties of

SCRC, SFSCRC, and SFVRC mixtures. A total binder content of 550 kg/m^3 and a minimum water-to-binder ratio (w/b) of 0.4 were required to ensure enough flowability and no visual sign of segregation. The binder content included 50% GU Portland cement, 30% FA, and 20% MK. These percentages were found to be optimal to fulfill the requirement of flowability, particle suspension, and strength. For all tested beams in this investigation, the coarse-to-fine aggregate ratio was kept constant at 0.7. **Table 3-5** presents the mixture composition for all tested beams. The selected mixtures are as follows:

- Four SCRC mixtures (beams B1-B4). These mixtures contained different percentages of CR (0%, 10%, 15%, and 20%). The mixtures in these beams were selected to study the effect of increasing the percentage of CR on the flexural and cracking behavior of SCC beams.
- Three SFSCRC mixtures (B5-B7). These mixtures contained 0.2% MASF50+10%CR, 0.2% MASF38+15%CR, and 0.2% MISF19+20%CR, respectively. These mixtures were selected to assess the combined effect of CR and SFs on the structural performance and cracking behavior of SCC beams. These mixtures were developed such that the maximum possible combination of CR and SFs (for each type of SF) was used. Further increase in the percentage of CR and/or SFs in these mixtures resulted in a significant reduction in the flowability and passing ability, as shown in study 1. Moreover, it was not possible to use MASF54 in SFSCRC mixtures due to the longer length, which exhibited high blockage in the L-box device.

- Five VRC and SFVRC mixtures (B8-B12) were developed with 30% CR, 1% MISF19+30%CR, 1% MASF38+30%CR, 1% MASF50+30%CR, and 1% MASF54+30%CR, respectively. These mixtures were designed to investigate the effect of using a maximized percentage of CR and SFs on the structural behavior and cracking of VRC beams. The maximum possible percentage of SFs in these mixtures was found to be 1%. Using a higher percentage of SFs in these mixtures resulted in difficulty mixing and forming fiber balls. Also, the maximum possible percentage of CR in these mixtures was found to be 30%. Using a higher percentage of CR caused a significant drop in the compressive strength of the mixture. It should be noted that it was not possible to develop these mixtures as SCC mixtures. Higher percentages of SFs and CR caused a significant drop in the fresh properties of SCC mixtures.

All tested beams were designated by the concrete type, percentage of CR, and percentage and length of SFs (MISFs or MASFs) (see Table 3-5). For example, the SCC beam with 15% CR and 0.2% MASF38 would be labeled as SCC-15CR-0.2MASF38, and the VC beam with 30% CR and 1% MASF50 would be labeled as VC-30CR-1MASF50. All beams were designed according to CSA standards to fail in flexure.

Table 3-5 Mix design of beams optimized from study 1

beam #	Designation	Cement (kg/m^3)	MK (kg/m^3)	FA (kg/m^3)	C. A. (kg/m^3)	F. A. (kg/m^3)	CR (kg/m^3)	Fibers (kg/m^3)	Density (kg/m^3)
B1	SCC-0CR	275	110	165	620.3	886.1	0.0	-	2276
B2	SCC-10CR	275	110	165	620.3	797.5	32.4	-	2220
B3	SCC-15CR	275	110	165	620.3	753.2	48.6	-	2192
B4	SCC-20CR	275	110	165	620.3	708.9	64.8	-	2164
B5	SCC-20CR-0.2MISF19	275	110	165	618.1	706.4	64.5	1.82	2161
B6	SCC-15CR-0.2MASF38	275	110	165	618.1	750.6	48.4	1.82	2189
B7	SCC-10CR-0.2MASF50	275	110	165	618.1	794.7	32.3	1.82	2217
B8	VC-30CR	275	110	165	620.3	620.3	97.1	9.1	2048
B9	VC-30CR-1MISF19	275	110	165	609.6	609.6	95.5	9.1	2094
B10	VC-30CR-1MASF38	275	110	165	609.6	609.6	95.5	9.1	2094
B11	VC-30CR-1MASF50	275	110	165	609.6	609.6	95.5	9.1	2094
B12	VC-30CR-1MASF54	275	110	165	609.6	609.6	95.5	9.1	2094

Note: All mixtures have a 0.4 w/b ratio, a 0.7 C/F aggregate ratio, and a 10mm maximum aggregate size; C. A. = Coarse aggregates; F. A. = Fine aggregates; CR = Crumb rubber; MK = metakaolin; MISF = micro synthetic fibers; MASF = macro synthetic fibers.

3.4.3 Casting of specimens

After mixing, fresh properties tests were performed. The concrete beams were then cast in preassembled wooden forms. SCRC and SFSCRC beams were poured from one side, allowing concrete to flow under its own weight and reach the other side without any vibration or compaction. On the other hand, the VRC/SFVRC beams were consolidated using electrical vibrators and trowel-finished for smooth top surfaces. The beams were sprayed with water 24 hours after pouring and then covered with plastic sheets for four days and air-cured until the day of testing. **Figure 3-8** shows the reinforcement and formwork details, pouring concrete, and curing regime (first four days) for all tested concrete beams. It should be noted that the specimens which were used to evaluate the compressive strength and STS of beams' mixtures, had been exposed to a condition of curing similar to their tested beams.

a **b** **c**

Figure 3-8 Casting of flexural beams (a) reinforcement and formwork details, (b) pouring concrete, (c) curing regime (first four days)

3.4.4 Dimensions, four-point loading test setup, and loading procedures

Figure 3-9 shows the dimensions, reinforcement details, and test setup for all tested beams. All beams had a similar cross-section of 250mm x 250mm, the total length of 2440 mm, effective span of 2040mm, and an effective depth of 197.5mm. The tension longitudinal reinforcement consisted of two 25M steel bars with a clear concrete cover of 40mm. The compression steel reinforcement (two 10M steel bars) was chosen for the compression reinforcement. The shear reinforcement consisted of 10M steel stirrups spaced at 155mm with a constant clear concrete cover of 30mm.

Figure 3-9 also shows the test setup for tested beams. All tested beams were simply supported subjected to a four-point loading pattern. A hydraulic jack with 500 kN capacity was used to apply a point load on a steel beam, which acted on the concrete surface by distributing the load in two-point loading spaced 680mm. The shear span to effective depth was kept constant of 3.44. A linear variable differential transformer (LVDT) was used to record the vertical displacement at the mid-point of the beam. The developed cracks were detected and then marked on the beam surface. A crack microscope (60X magnification with 0.02mm least count) was used to accurately measure the crack widths at each load stage. The first cracking moment, ultimate moment, deflections, crack patterns/widths, and failure modes were observed and recorded during the test. The ductility and energy absorption were then calculated after the completion of the test.

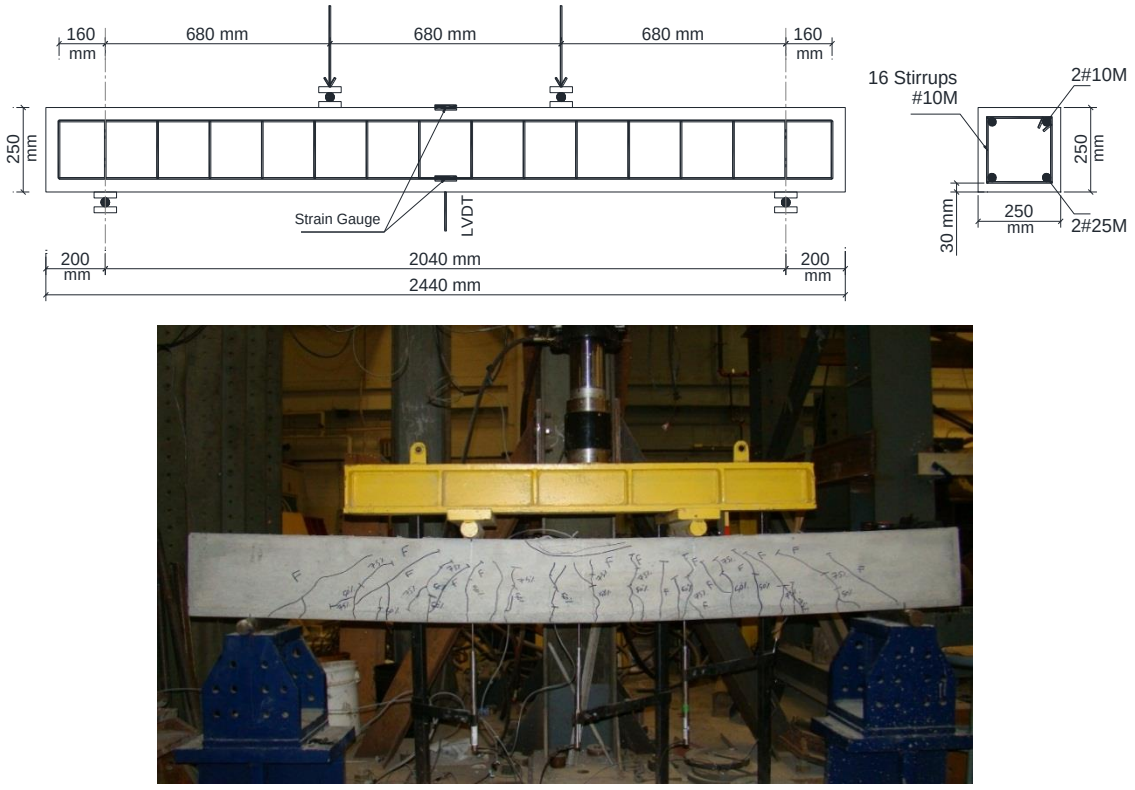

Figure 3-9 Typical test setup, dimensions, reinforcement, and failure mode of tested beams in flexure

3.5 Experimental study 3: Effect of SFs on shear capacity of reinforced rubberized concrete beams

This study aimed to investigate the shear behavior of twelve beams poured from mixtures that were optimized in study 1.

3.5.1 Research significance

The current literature indicates that there is very limited research investigating the performance of full-scale concrete elements made with rubber, and no studies evaluated the combined effect of CR and MISFs/MASFs on the shear capacity of reinforced concrete beams, especially when both VC and SCC are used. Therefore, this study was conducted to cover this knowledge gap by investigating the effect of CR with/without SFs (MISFs and MASFs) on stiffness, ultimate capacity, post-diagonal resistance, energy absorption, and cracking behavior of reinforced concrete beams subjected to shear failure. The results obtained from this study can greatly help to assess the potentials of CR with/without SFs in structural applications.

3.5.2 Scope of work

In this part of the research, twelve beams with mixtures listed in Table 3-5 was studied to evaluate the shear behavior of rubberized concrete reinforced with SFs. The mixtures were selected and designed based on the criteria explained in study 2, clause 3.4.2.

3.5.3 Casting of specimens

All casting and curing procedures in study 3 were carried out as per study 2.

3.5.4 Beams' dimensions, test setup, and loading procedures of the tested beams

Twelve beams with a constant cross-section of 250mm x 250mm, effective depth (*d*) of 197.5mm, and a length of 1500mm were tested, as shown in Figure 3-10. All the beams were constructed without shear reinforcement. The longitudinal reinforcement was kept constant and consisted of two 25M steel bars (25mm diameter) in the tension zone (tension reinforcement ratio (ρ_s) = 2.03%) and two 10M (10mm diameter) steel bars in the compression zone.

As shown in Figure 3-10, all beams were simply supported and subjected to a four-point symmetrical vertical loading condition. The loading pattern shows that the tested beams were typically loaded with a constant shear span (*a*) of 495mm, providing a constant shear span-to-effective depth (*a/d*) ratio of 2.5 that ensures shear failure before bending failure (Kani et al., 1979). A monotonic load was applied gradually using a 500-kN hydraulic jack on a single point and then distributed into two-point loads acting on the beam surface. The vertical midspan deflection of the tested beams was measured and recorded using a linear variable differential transformer (LVDT). The load-midspan deflection of each beam was monitored and recorded continuously until the occurrence of the failure. A crack detection microscope (60x magnification with 0.02mm least count) was used to accurately measure the widths of the developed flexural and shear cracks.

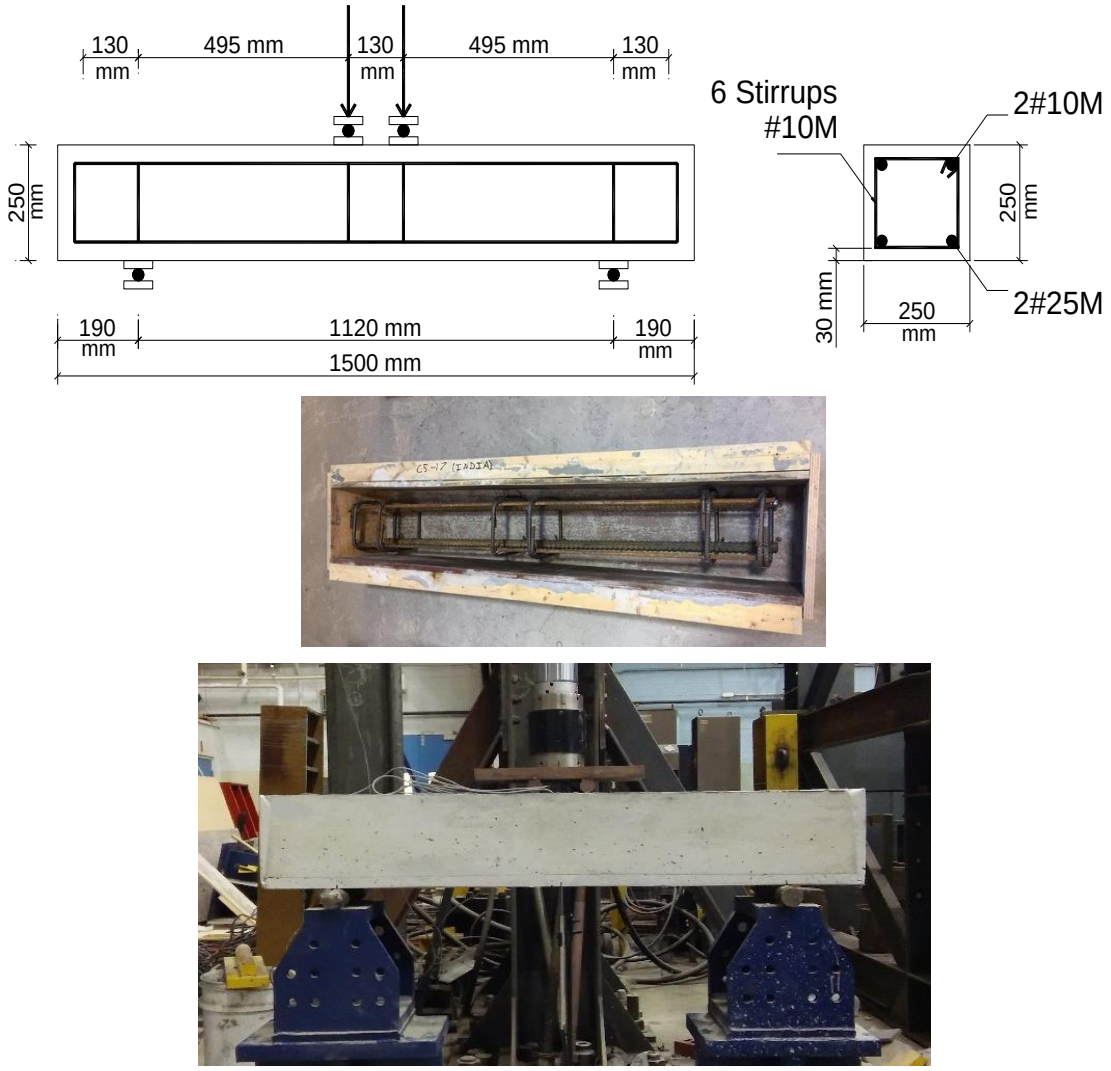

Figure 3-10 Typical test setup, dimensions, and reinforcement of tested beams in shear

3.6 Experimental study 4: Cyclic loading of large-scale rubberized concrete beam-column joints with/without SFs

This study aimed to investigate the structural behavior of rubberized concrete beam-column joints with/without SFs/MFs under cyclic loading. The mixtures used in this study were optimized and developed in study 1.

3.6.1 Research significance

Beam-column joints are considered one of the vulnerable locations in framed structures, which are mainly responsible for resisting lateral cyclic loading such as earthquake loads. These joints require high ductility and energy absorption to ensure appropriate design of the structure. Previous studies have indicated that including CR in concrete mixtures improves the ductility and energy dissipation of concrete structures. Using rubber in SCC mixtures combines the desired properties of SCC, especially in congested areas (like beam-column joints), with the superior properties of CR for structural applications. There is a lack of information, however, regarding the effect of combining CR particles with fibers on the structural performance of beam-column joints. Moreover, there are no available studies that have investigated the effect of using SFs in rubberized concrete on the cyclic behavior of beam-column joints. This investigation was conducted to determine the optimum percentage of CR in SCC to enhance the structural performance of exterior beam-column joints under reverse cyclic loading. The study also aimed to investigate the effect of combining CR with MFs/SFs on maximizing the ductility, energy dissipation, and load carrying capacity of the tested joints, especially when different types, lengths, and volumes of fibers were used. Information regarding first crack load, load carrying

capacity, deformability, ductility, brittleness index, stiffness degradation, cracking behavior, and energy dissipation of beam-column joints under reverse cyclic loading were covered and analyzed in this study.

3.6.2 Scope of work

Stage 1- Determining the optimum percentage of CR

This stage contains six SCRC mixtures selected based on study 1 aimed to develop a number of SCRC mixtures containing a maximum percentage of CR with a minimum reduction in mechanical properties. The percentages of CR in the tested mixtures ranged from 0% to 25% (partial replacement of sand by volume). All tested mixtures/specimens were designated by the concrete type (SCC) and percentage of CR. For example, a specimen containing 10% CR would be labeled as SCC-10CR (see Table 3-6). Six large-scale concrete beam-column joint specimens were prepared using the six different developed mixtures. All specimens were designed according to (CSA, 2004) standards to fail in flexure with ductile behavior.

Stage 2- Effect of using larger coarse aggregate size and MFs in rubberized concrete joints.

This Stage contained a total of eleven mixtures (for eight beam-column joints): four SCRC, one metal fiber SCRC (MFSCRC), and three metal fiber VRC (MFVRC) mixtures (see Table 3-6). These mixtures were selected based on study 1 that aimed to optimize the fresh and mechanical properties of SCRC, VRC, MFSCRC, and MFVRC mixtures. In order to ensure enough flowability and no visual sign of segregation, both SCRC and

MFSCRC mixtures needed a total binder content of at least 550 kg/m^3 and a minimum water-to-binder (w/b) ratio of 0.4. The binder content (550 kg/m^3) included 50% GU portland cement, 30% FA, and 20% MK. This selection was found to be optimal for adjusting the mixtures' flowability. The coarse-to-fine aggregate (c/f) ratio was kept constant at 0.7 in this investigation for all tested mixtures. The maximum percentage of MFs that could be added in SCRC mixtures was found to be 0.35%. Using a higher percentage of MFs in SCRC mixtures resulted in significant reductions in the fresh properties.

The developed mixtures were as follows:

- Joints S4-S5 compared with joints S8-S9. The mixtures in these joints were selected to study the effect of using different coarse aggregate sizes on the performance of the tested joints.
- Joint S11 compared with S4. These two mixtures were selected to study the effect of adding MF to SCRC.
- Joint S12 compared with S11. These two mixtures were selected to study the effect of concrete type (MFVRC compared with MFSCRC).
- Joint S13 compared with S12. These two mixtures were selected to investigate the effect of changing fiber length (MF60 compared with MF35).
- Joint S14 compared with S1. These two mixtures were selected to investigate the effect of maximizing the percentage of CR and MFs on the performance of beam-column joints.

All tested mixtures/joints were designated by the concrete type (SCC/VRC), percentage of CR, and coarse aggregate size or percentage/length of MFs. For example, a specimen containing 15% CR and 0.35% MF35 would be labeled as SCC-15CR-0.35MF35.

All joints were designed according to CSA 2008 standards to fail in flexure with a ductile behavior.

Stage 3 – Effect of combining CR with different types, lengths, and volumes of SFs on the structural behavior of the beam-column joint.

This stage contained a total of ten mixtures (seven beam-column joints): three SFSCRC, and four SFVRC mixtures. These mixtures were selected based on study 1 that aimed to optimize the fresh and mechanical properties of SCRC, SFSCRC, and SFVRC mixtures. In order to ensure enough flowability and no visual sign of segregation, SFSCRC mixtures needed a total binder content of at least 550 kg/m^3 and a minimum water-to-binder (w/b) ratio of 0.4. The binder content (550 kg/m^3) included 50% GU Portland cement, 30% FA, and 20% MK. This selection was found to be optimal for adjusting the mixtures' flowability, particle suspension, and strength. The coarse-to-fine aggregate ratio was kept constant at 0.7 in this investigation for all tested mixtures. The maximum percentage of MISFs and MASFs that could be added in SCRC mixtures was found to be 0.2%. Using a higher percentage of SFs in SCRC mixtures resulted in significant reductions in the fresh properties. An optimum percentage of 15% CR was selected in this investigation. This percentage was chosen based on stage 1 conducted in this study to optimize the percentage of CR in SCRC mixtures. Table 3-6 shows the mixture compositions for all tested joints.

The experimental program was designed based on the following:

- Joints S15-S16 compared to S4. The mixtures in these joints were selected to study the effect of adding different types of MISFs to SCRC.
- Joint S17 compared to S4. These two joints were selected to study the effect of adding MASFs (MASF38) to SCRC.
- Joint S18 compared to S17. The mixtures in these two joints were selected to study the behavior of SFVRC compared to SFSCRC.
- S19-S20 compared to S18. These mixtures were selected to study the effect of using different lengths (MASF50 compared to MASF38) and different types of MASFs (MASF54 compared to MASF38) on the behavior of VRC beam-column joints. It should be noted that it was not possible to develop SCC mixtures with MASF54 and MASF50 due to the significant drop in the L-box value below the acceptable limits given by EFNARC (2005). Therefore, all mixtures in this stage of comparison were developed as VRC.
- S21 compared to S6 and S1. These mixtures were selected to study the effect of using the maximum possible percentage of SFs (1%) to compensate for the reductions in the mechanical properties resulting from a high percentage of CR. Adding higher percentages of SFs (more than 1%) resulted in poor dispersion of the fiber (formation of fiber balls) in the mixture.

All tested mixtures/joints were designated by the concrete type (SCC/VRC), percentage of CR, and percentage/length of SFs. For example, a specimen containing 15% CR, and 0.2% MASF38 would be labeled as SCC-15CR-0.2MASF38.

Table 3-6 mix design of rubberized beam-column joints

Joint #	Mixture ID	Cement (kg/m^3)	SCM (Type)	SCM (kg/m^3)	C. A. (kg/m^3)	F. A. (kg/m^3)	CR (kg/m^3)	HRWRA (L/m^3)	Fibers V_f (%)	Density (kg/m^3)
Stage 1										
S1	SCC-0CR	275	MK+FA	110+165	620.3	886.1	0	3.43	--	2276.4
S2	SCC-5CR	275	MK+FA	110+165	620.3	841.8	16.2	3.43	--	2248.3
S3	SCC-10CR	275	MK+FA	110+165	620.3	797.5	32.4	3.75	--	2220.2
S4	SCC-15CR	275	MK+FA	110+165	620.3	753.2	48.6	3.75	--	2192.1
S5	SCC-20CR	275	MK+FA	110+165	620.3	708.9	64.8	3.75	--	2164
S6	SCC-25CR	275	MK+FA	110+165	620.3	664.6	80.9	3.75	--	2135.8
Stage 2										
S7	SCC-10CR-20	275	MK+FA	110+165	620.3	797.5	32.4	3.75	--	2220.2
S8	SCC-15CR-20	275	MK+FA	110+165	620.3	753.2	48.6	3.75	--	2192.1
S9	SCC-20CR-20	275	MK+FA	110+165	620.3	708.9	64.8	3.75	--	2164
S10	SCC-25CR-20	275	MK+FA	110+165	620.3	664.6	80.9	3.75	--	2135.8
S11	SCC-15CR-0.35MF35	275	MK+FA	110+165	620.3	753.2	48.6	4.63	0.35	2210.88
S12	VRC-15CR-0.35MF35	275	MK+FA	110+165	620.3	753.2	48.6	3.18	0.35	2210.88
S13	VRC-15CR-0.35MF60	275	MK+FA	110+165	620.3	753.2	48.6	3.18	0.35	2210.88
S14	VRC-25CR-1MF35	275	MK+FA	110+165	620.3	664.6	80.9	3.18	1	2163.1
Stage 3										
S15	SCC-15CR-0.2MISF19	275	MK+FA	110+165	620.3	750.6	48.6	3.75	0.2	2192.1
S16	SCC-15CR-0.2MISF27	275	MK+FA	110+165	620.3	750.6	48.6	3.75	0.2	2192.1
S17	SCC-15CR-0.2MASF38	275	MK+FA	110+165	620.3	750.6	48.6	3.75	0.2	2192.1
S18	VRC-15CR-0.2MASF38	275	MK+FA	110+165	620.3	750.6	48.6	3.18	0.2	2192.1

S19	VRC-15CR-0.2MASF50	275	MK+FA	110+165	620.3	750.6	48.6	3.18	0.2	2192.1
S20	VRC-15CR-0.2MASF54	275	MK+FA	110+165	620.3	750.6	48.6	3.18	0.2	2192.1
S21	VRC-25CR-1MASF38	275	MK+FA	110+165	620.3	664.6	80.9	3.18	1	2135.8

3.6.3 Casting of specimens

In the first step of mixing, the coarse aggregate, cement, SCMs, CR, and sand were dry mixed in a rotary mixer for 1.5 minutes. Next, the SFs were added during the dry mixing process to achieve good fiber distribution. Then, the required water was mixed with the HRWRA and then added to the dry material and remixed for another three minutes. Immediately after mixing, fresh properties tests and pouring concrete beam-column joints in wooden forms were carried out. SCRC and FRSCRC joints were cast from one side, allowing the concrete to flow under its own weight and reach the other sides without any vibration or compaction. On the other hand, the VRC/SFVRC beams were consolidated using electrical vibrators and trowel-finished for smooth top surfaces. After 24 hours of casting, the specimens were sprayed with water and covered with plastic sheets for four days and then air-cured until the date of testing. Figure 3-11 shows the specimens' dimensions and reinforcement details.

Figure 3-11 pouring of beam-column joints, formwork and reinforcement details

3.6.4 Test setup, and loading procedures

Figure 3-12a shows the test setup used in this investigation. An axial load of 10% of the capacity of the column was applied to the top of the column using a hydraulic jack in order to simulate the gravity load. An actuator with a capacity of 500 kN was used to apply the vertical load at the beam's tip (90mm from the beam end [Figure 3-12b]). The load was transferred to the beam's tip through the arrangement of two channel sections and two rods. The reversed cyclic quasi-static load was applied with a displacement control according to ACI (2008). The displacement was applied in different load steps until failure. Each load step had three full reversed cycles with a frequency of 0.08 Hz. The applied displacement sequence is presented in Figure 3-13 and Table 3-7. This pattern of loading was assigned to ensure a gradual increase in displacement, neither too large nor too small, until the failure of the specimen. The deflection at the beam's tip and midspan were measured using linear variable differential transformers (LVDTs). Meanwhile, the strains at the section of maximum moment were recorded using two strain gauges attached on each side (the bottom and top of the longitudinal beam's reinforcement). After each displacement load step, the cracks were marked, and their widths were measured using a crack microscope (60X magnification with 0.02mm least count). The first crack load, ultimate load, deformation, crack patterns/widths, and failure modes were observed and recorded during the test. The ductility, energy dissipation, brittleness index, and stiffness degradation were then calculated after the completion of the test.

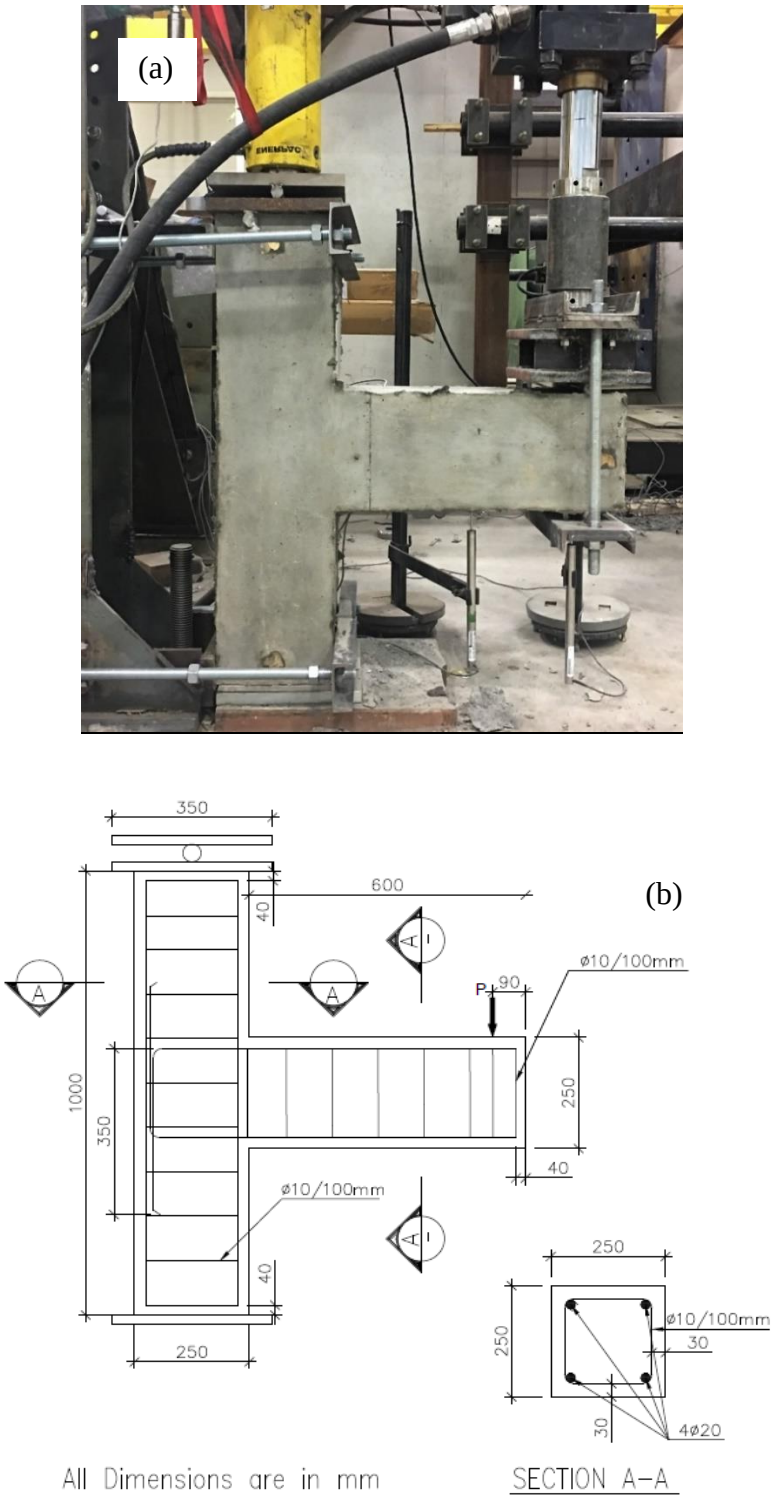

Figure 3-12 **(a) Test setup, (b) specimens' dimensions and reinforcement details**

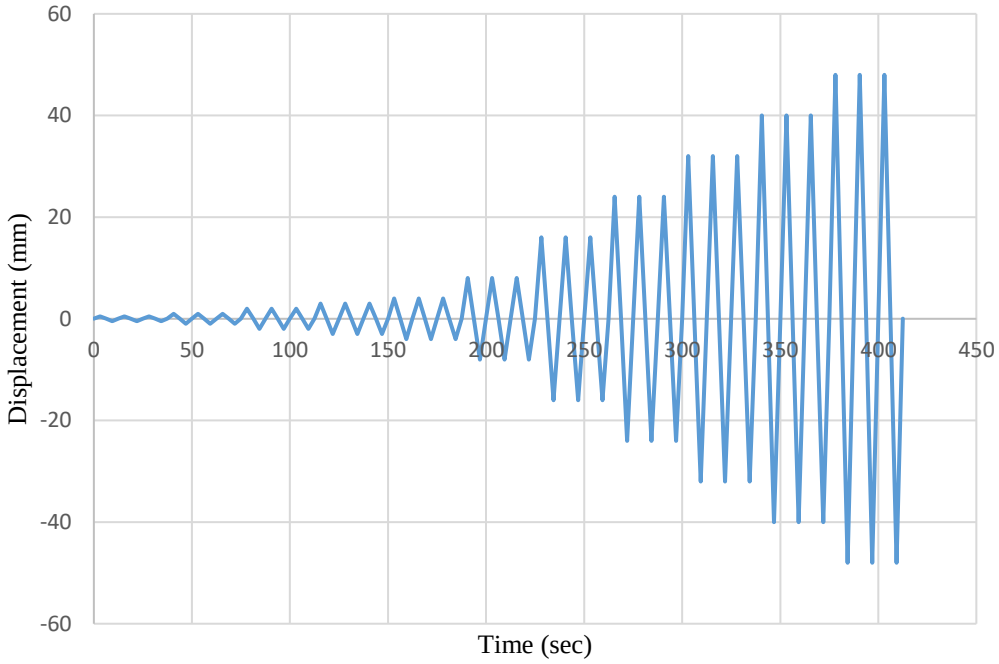

Figure 3-13 Sequence of applied displacement

Table 3-7 Applied displacement sequence

Load step	Number of cycles	Amplitude (mm)
1	3	0.5
2	3	1
3	3	2
4	3	3
5	3	4
6	3	8
7	3	16
8	3	24
9	3	32
10	3	40
11	3	48

3.7 Experimental study 5: Structural behavior of rubberized ECC beam-column joints under cyclic loading

This study aimed to investigate the cyclic behavior of ECC beam-column joints with different percentage of CR, SCMs types, and fine aggregate types.

3.7.1 Research significance

Although there are a sufficient number of studies available in the literature regarding the mechanical and durability properties of ECC, very limited research investigated the behavior of ECC beam-column joints under cyclic loading. Moreover, there are no available studies that have investigated the behavior of rubberized ECC, ECC with different SCMs, and ECC with different sand type in beam-column joints under cyclic loading. Using ECC with an optimized percentage of CR not only can further improve the ductility and energy dissipation of joint but also contributes to developing eco-friendly composites with relatively low environmental impact. The structural performance of tested beam-column joints including the load-deflection envelop response, hysteresis behavior, initial stiffness, deformability, cracking behavior, displacement ductility, brittleness index, energy dissipation, first cracking load, and the ultimate load was covered and analyzed in this study.

3.7.2 Scope of the work

This investigation contained a total of eight mixtures (eight beam-column joints). The experimental program was designed based on the following:

- Joint S1. This joint was selected as a reference. It has a standard ECC mixture (with FA and silica sand).

- Joints S2-S4 compared to S1. The mixtures in these joints were selected to study the effect of using different percentages of CR in ECC on enhancing the structural performance of ECC beam-column joints (compared to the standard ECC joint). The percentages of CR used in this investigation (up to 15%) was chosen based on trial mixes, in which further increase in the CR percentage beyond 15% showed a significant drop in the mechanical properties of ECC mixtures.

- Joints S5-S6 compared to S1. These two joints were selected to study the effect of partially replacing the FA (commonly used in standard ECC) with 20% MK or 10% SLF on enhancing the stiffness and load carrying capacity of beam-column joints. The selection of the 20% and 10% MK and SLF were based on previous investigating conducted by Ismail et al. (2018). In this previous investigation, the authors investigated several mixtures to evaluate the optimum percentages of MK and SLF. They concluded that 20% MK and 10% SLF were the optimum percentages that can develop ECC mixtures with maximized compressive and tensile strengths.

- Joint S7 compared to S1. This joint was selected to evaluate the performance of the beam-column joint made with natural sand instead of silica sand. Such joint was constructed to promote the use of locally available aggregate to develop cost-effective composite with low environmental impact.

- Joint S8 was developed with a strength comparable to the reference ECC Joint (S1) for comparison.

All tested mixtures/joints were designated by the concrete type (ECC), type of SCMs, and percentage of CR or fine aggregate type. For example, ECC joint containing 15% CR, and FA would be labeled as ECC-FA-15CR, while ECC joint containing natural sand and FA would be labeled as ECC-FA-NS (see Table 3-8). All tested joints were designed according to CSA standards to fail in a flexural manner with a ductile behavior. In addition, the tested specimens satisfy the requirement of type 2 connections specified by ACI 352 code. Moreover, in order to avoid bond/slip failure, hocked bars with enough developmental lengths were provided for the beam longitudinal bars.

Table 3-8 mix design of ECC beam-column joints

Joint #	Mixture ID	C	C.A./C	SCM (type)	SCM/C	S/C	PVA (volume %)	CR/silica sand volume replacement (%)
S1	ECC-FA	1	-	FA	1.2	0.8	2	-
S2	ECC-FA-5CR	1	-	FA	1.2	0.76	2	0.05
S3	ECC-FA-10CR	1	-	FA	1.2	0.71	2	0.1
S4	ECC-FA-15CR	1	-	FA	1.2	0.67	2	0.15
S5	ECC-MK	1	-	FA+MK	0.78+0.44	0.8	2	-
S6	ECC-SLF	1	-	FA+SLF	1+0.22	0.8	2	-
S7	ECC-FA-NS	1	-	FA	1.2	0.8	2	-
S8	NC	1	2.26	FA+MK	1	3.22	-	-

3.7.3 Casting of specimens and test setup

All casting and curing procedures and test setup in study 5 were conducted as per study 4.

4 Discussion of results from experimental study 1: use of SFs/MFs to optimize the fresh properties, stability, and strength of SCRC mixtures with different binder content and SCMs

4.1 Introduction

This chapter presents the results and discussion of the concrete mixtures developed in study 1. The main objective was to evaluate the effect of using different SCMs on the development and optimization of SCRC. The study also aimed to develop and optimize SCRC modified by different types and volumes of SFs and MFs. The results of this study help to highlight a number of successful mixtures with high potentials for structural applications requiring high energy absorption, ductility, and impact resistance. The effects of different SCMs (MK, FA, SLF, GGBS), different percentage of CR (0%-30%), binder content (500 kg/m^3, 550 kg/m^3, 600 kg/m^3), SFs types and lengths (MISF19, MISF27, MASF38, MASF50, MASF54), SFs volume (0%, 0.2%, and 1%), MFs lengths (35mm, and 60mm), and MFs volume (0%, 0.35%, 1%) were investigated. The results of fresh properties tests are presented in Table 4-1, and Table 4-2. The results of mechanical properties tests and impact resistance tests are presented in Table 4-3, Table 4-4, and Table 4-5. **Table 4-6** summarizes the ANOVA results for the effect of CR inclusion, and different fibers lengths on the mechanical and impact resistance of tested mixtures. The results and discussions presented in this chapter have been published in the first, second, and third papers mentioned earlier at the beginning of this thesis.

Table 4-1 Fresh properties of tested SCRC mixtures (study 1- stage 1)

Mixture #	Mixture designation	Slump/Slump flow		J-ring		Slump–J-ring (mm)	L-box H2/H *100	V-funnel	SR %	Density (kg/m^3)
		D_s (mm)	T_{50} (sec)	D_J (mm)	T_{50J} (sec)			T_0 (sec)		
1	550C-0CR-SLF	730	1.56	710	2.09	20	88	4.2	2.45	2105.87
2	550C-5CR-SLF	710	1.98	670	2.38	40	83	5.81	3.06	2076.83
3	550C-10CR-SLF	680	2.39	630	3.04	50	79	7.2	3.91	2047.78
4	550C-15CR-SLF	670	2.77	615	3.20	55	77	7.84	4.89	2018.75
5	550C-20CR-SLF	660	3.05	600	3.45	55	76	8.83	4.89	1989.71
6	550C-20CR-MK	680	3.57	650	3.97	30	86	12.01	4.17	1984.7
7	550C-20CR-FA	700	1.99	655	2.32	60	75	5.9	6.67	1979.3
8	550C-20CR-GGBS	705	2.07	675	2.35	40	80	5.9	6.04	1995.7
9	500C-5CR-SLF	690	2.42	630	3.00	60	76	7.62	4.87	2119.98
10	600C-20CR-SLF	690	2.72	640	3.20	50	79	8.01	4.17	1951.88
11	600C-25CR-SLF	670	3.21	615	3.62	55	76	9.5	4.65	1924.61
12	550C-20CR-SLF-MK	690	3.26	645	3.86	45	79	11.89	4.53	1967.9
13	550C-25CR-SLF-MK	660	3.49	590	4.07	65	75	15.48	5.26	1939.26
14	550C-20CR-MK-FA	710	3.14	665	3.51	45	79	9.35	6.50	2164
15	550C-25CR-MK-FA	700	3.35	650	3.88	50	77	14.30	7.50	2135.8
16	550C-30CR-MK-FA	670	3.76	600	4.23	70	75	17.25	8.33	2107.7

Table 4-2 Fresh properties of tested FRSCRC mixtures (study 1- stage 2)

Mixture #	Mixture designation	Slump flow		J-ring		Slump–J-ring (mm)	L-box H2/H1	V-funnel	SR %
		D_s (mm)	T_{50} (sec)	D_J (mm)	T_{50J} (sec)			T_0 (sec)	
Set # 1									
1	0CR-SCC	725	1.95	715	2.34	10	0.91	7.01	2.08
2	5CR-SCC	720	2.39	705	2.77	15	0.88	8.50	2.71
3	10CR-SCC	720	2.74	690	3.17	30	0.84	9.51	3.75
4	15CR-SCC	715	2.96	675	3.40	40	0.82	10.59	5.83
5	20CR-SCC	710	3.14	665	3.51	45	0.77	10.97	6.50
6	25CR-SCC	700	3.35	650	3.88	50	0.77	14.30	7.50
7	30CR-SCC	670	3.76	600	4.23	70	0.75	17.25	8.33
Set # 2									
8	5CR-SCC-0.2SF19	725	2.42	700	2.84	25	0.86	8.9	3.12
9	10CR-SCC-0.2SF19	710	2.78	680	3.23	35	0.82	10.2	3.75
10	15CR-SCC-0.2SF19	715	3.04	670	3.55	45	0.79	11.4	4.37
11	20CR-SCC-0.2SF19	670	3.29	625	3.69	50	0.76	12.12	6.88
12	5CR-SCC-0.2SF38	710	2.68	650	3.56	60	0.81	11.91	3.37
13	10CR-SCC-0.2SF38	670	3.05	600	3.88	60	0.79	14.02	4.55
14	15CR-SCC-0.2SF38	665	3.2	600	4.2	65	0.77	15.3	7.29
15	5CR-SCC-0.2SF50	680	2.95	615	3.82	65	0.79	15.6	4.11
16	10CR-SCC-0.2SF50	710	3.18	645	4.23	85	0.76	16.2	5.51
17	5CR-SCC-0.2SF27	725	2.50	685	2.98	40	0.84	9.5	2.92
18	10CR-SCC-0.2SF27	705	2.84	665	3.43	40	0.81	11.2	3.13
19	15CR-SCC-0.2SF27	690	3.09	640	3.85	50	0.79	12.67	3.96
20	20CR-SCC-0.2SF27	690	3.25	635	3.92	55	0.75	13.50	5.2
21	5CR-SCC-0.35MF35	730	2.62	690	3.25	40	0.80	9.75	2.92
22	10CR-SCC-0.35MF35	715	3.07	650	3.66	65	0.78	10.65	4.13

23	15CR-SCC-0.35MF35	710	3.31	630	4.01	80	0.75	12.05	6.04
Set # 3		Slump (mm)							
24	30CR-VC	190	-	-	-	-	-	-	-
25	30CR-VC-1SF19	175	-	-	-	-	-	-	-
26	30CR-VC-1SF38	150	-	-	-	-	-	-	-
27	30CR-VC-1SF50	130	-	-	-	-	-	-	-
28	30CR-VC-1SF27	165	-	-	-	-	-	-	-
29	30CR-VC-1SF54	125	-	-	-	-	-	-	-
30	30CR-VC-1MF35	160	-	-	-	-	-	-	-
31	30CR-VC-1MF60	110							

Table 4-3 Mechanical properties of tested SCRC mixtures (study 1-stage 1)

Mixture #	Mixture designation	28-day f'_c	28-day STS	28-day FS
		MPa	MPa	MPa
1	550C-0CR-SLF	80.15	4.73	10.46
2	550C-5CR-SLF	62.12	3.92	8.36
3	550C-10CR-SLF	49.11	3.24	6.83
4	550C-15CR-SLF	41.5	3.12	6.10
5	550C-20CR-SLF	33.54	2.78	5.65
6	550C-20CR-MK	34.15	2.84	5.88
7	550C-20CR-FA	26.36	2.18	4.90
8	550C-20CR-GGBS	27.2	2.34	5.21
9	500C-5CR-SLF	58.1	3.66	7.30
10	600C-20CR-SLF	35.12	2.94	5.92
11	600C-20CR-SLF	30.76	2.68	5.36

12	550C-20CR-SLF-MK	34.68	2.88	5.88
13	550C-25CR-SLF-MK	30.16	2.63	5.30
14	550C-20CR-MK-FA	38.79	3.20	5.97
15	550C-25CR-MK-FA	36.1	2.90	4.37
16	550C-30CR-MK-FA	32.86	2.58	3.98

Table 4-4 Mechanical properties of tested FRSCRC mixtures (study 1-stage 2)

Mixture #	Mixture designation	f'_c (MPa)		STS (MPa)		FS (MPa)		ME (GPa)
		7-days	28-days	7-days	28-days	7-days	28-days	28-days
SCRC								
1	0CR-SCC	60.9	75.7	4.0	4.5	5.1	5.7	29.4
2	5CR-SCC	48.9	66.7	3.7	4.1	4.7	5.5	27.5
3	10CR-SCC	40.1	53.5	3.2	3.8	4.2	5.1	25.7
4	15CR-SCC	35.6	44.8	3.0	3.6	4.0	4.8	24.7
5	20CR-SCC	31.5	38.4	2.7	3.3	3.6	4.6	22.0
6	25CR-SCC	27.6	36.8	2.3	3.0	3.3	4.3	20.0
7	30CR-SCC	26.5	31.9	2.2	2.7	3.1	3.9	18.7
FRSCRC								
8	5CR-SCC-0.2SF19	49.0	66.9	3.9	4.4	5.0	5.7	27.7
9	10CR-SCC-0.2SF19	40.4	54.1	3.5	4.1	4.4	5.4	25.9
10	15CR-SCC-0.2SF19	35.7	44.8	3.1	3.9	4.2	5.1	24.9
11	20CR-SCC-0.2SF19	31.8	39.2	3.0	3.6	3.8	4.8	22.1
12	5CR-SCC-0.2SF38	49.2	67.2	4.3	4.7	5.4	6.2	27.9
13	10CR-SCC-0.2SF38	40.8	54.4	3.8	4.4	4.7	5.7	26.3
14	15CR-SCC-0.2SF38	35.8	44.9	3.4	4.2	4.5	5.4	25.4

15	5CR-SCC-0.2SF50	49.1	67.0	4.2	4.6	5.2	6.0	27.8
16	10CR-SCC-0.2SF50	40.7	54.3	3.6	4.3	4.6	5.6	26.1
17	5CR-SCC-0.2SF27	49.1	66.9	4.0	4.5	5.1	5.9	27.8
18	10CR-SCC-0.2SF27	40.6	54.2	3.6	4.2	4.5	5.5	26.0
19	15CR-SCC-0.2SF27	35.8	44.9	3.2	4.0	4.3	5.2	24.9
20	20CR-SCC-0.2SF27	31.9	39.6	3.0	3.6	3.9	4.9	22.2
21	5CR-SCC-0.35MF35	50.5	67.6	4.5	5.3	5.6	6.7	28.0
22	10CR-SCC-0.35MF35	40.5	54.3	4.0	4.7	5.1	6.1	26.7
23	15CR-SCC-0.35MF35	35.6	44.9	3.6	4.3	4.6	5.6	26.0
FRVRC								
24	30CR-VC	28.2	33.5	2.3	2.8	3.3	4.2	19.9
25	30CR-VC-1SF19	23.2	27.2	2.7	3.1	3.8	4.6	20.5
26	30CR-VC-1SF38	24.1	28.3	3.2	3.8	4.1	5.0	21.9
27	30CR-VC-1SF50	22.0	25.6	3.0	3.6	4.0	4.9	21.1
28	30CR-VC-1SF27	24.6	30.5	2.9	3.4	3.9	4.7	21.0
29	30CR-VC-1SF54	27.5	31.8	3.2	3.8	4.2	5.1	22.4
30	30CR-VC-1MF35	28.8	33.6	4.0	4.7	5.6	6.6	22.9
31	30CR-VC-1MF60	30.1	34.7	4.1	4.7	5.7	6.6	23.0

Table 4-5 Impact test results of tested FRSCRC mixtures (study 1-stage 2)

Mixture #	Mixture designation	Drop-weight test					Flexural Impact loading	
		Number of blows			IE (J)		Number of blows	IE (J) Failure
		N_1	N_2	N_2-N_1	Initial	Failure		
SCRC								
1	0CR-SCC	141	143	2	2813	2853	76	498
2	5CR-SCC	153	156	3	3052	3112	92	602
3	10CR-SCC	160	163	3	3192	3252	128	838
4	15CR-SCC	185	190	5	3691	3791	153	1002
5	20CR-SCC	203	209	6	4050	4170	174	1139
6	25CR-SCC	241	248	7	4808	4948	184	1207
7	30CR-SCC	267	273	6	5327	5446	164	1074
FRSCRC								
8	5CR-SCC-0.2SF19	185	203	18	3690	4049	120	786
9	10CR-SCC-0.2SF19	221	244	23	4408	4867	183	1198
10	15CR-SCC-0.2SF19	285	311	26	5686	6204	290	1899
11	20CR-SCC-0.2SF19	354	384	30	7062	7660	328	2148
12	5CR-SCC-0.2SF38	275	315	40	5486	6284	219	1434
13	10CR-SCC-0.2SF38	310	365	55	6184	7281	251	1644
14	15CR-SCC-0.2SF38	420	481	61	8379	9595	305	1997
15	5CR-SCC-0.2SF50	243	273	30	4847	5446	196	1283
16	10CR-SCC-0.2SF50	284	324	40	5665	6463	234	1532
17	5CR-SCC-0.2SF27	201	234	33	4009	4668	150	982
18	10CR-SCC-0.2SF27	253	292	39	5047	5825	210	1375
19	15CR-SCC-0.2SF27	315	358	43	6284	7142	295	1932
20	20CR-SCC-0.2SF27	380	425	45	7581	8478	367	2403

21	5CR-SCC-0.35MF35	337	391	54	6723	7800	252	1650
22	10CR-SCC-0.35MF35	380	440	60	7581	8778	283	1853
23	15CR-SCC-0.35MF35	470	534	64	9377	10653	314	2056
FRVRC								
24	30CR-VC	281	289	8	5606	5766	165	1080
25	30CR-VC-1SF19	453	538	85	9037	10733	314	2056
26	30CR-VC-1SF38	605	715	110	12070	14264	600	3929
27	30CR-VC-1SF50	535	635	100	10673	12668	430	2816
28	30CR-VC-1SF27	497	592	95	9915	11810	350	2292
29	30CR-VC-1SF54	645	770	125	12868	15362	900	5893
30	30CR-VC-1MF35	900	1071	171	17955	21366	1324	8670
31	30CR-VC-1MF60	992	1172	180	19790	23381	1650	10804

Table 4-6 ANOVA results for the effect of CR inclusion and different fibers length on mechanical properties and impact resistance of mixtures.

Property	Factor	Sum of squares	df	Mean square	F value	p-value Prob> F	Significant
Compressive strength							
28-day	CR	3039.19	6.00	506.53	4741.890	< 0.0001	Significant
	SF19	0.32	1.00	0.32	0.002	0.965	Not significant
	SF27	0.61	1.00	0.61	0.004	0.951	Not significant
	SF38	0.38	1.00	0.38	0.003	0.959	Not significant
	SF50	0.30	1.00	0.30	0.004	0.958	Not significant
	SLF35	0.54	1.00	0.54	0.004	0.951	Not significant
STS							

28-day	CR	4.89	6.00	0.81	15.770	< 0.0001	Significant
	SF19	0.18	1.00	0.18	1.588	0.254	Not significant
	SF27	0.28	1.00	0.28	2.199	0.189	Not significant
	SF38	0.54	1.00	0.54	8.526	0.043	significant
	SF50	0.25	1.00	0.25	5.556	0.143	Not significant
	SLF35	1.31	1.00	1.31	8.253	0.045	significant
FS							
28-day	CR	5.77	6.00	0.96	16.930	< 0.0001	Significant
	SF19	0.13	1.00	0.13	0.824	0.399	Not significant
	SF27	0.28	1.00	0.28	1.675	0.243	Not significant
	SF38	0.60	1.00	0.60	4.198	0.110	Not significant
	SF50	0.25	1.00	0.25	3.125	0.219	Not significant
	SLF35	1.57	1.00	1.57	7.762	0.050	significant
ME							
28-day	CR	151.37	6.00	25.23	565.950	< 0.0001	Significant
	SF19	0.06	1.00	0.06	0.011	0.919	Not significant
	SF27	0.13	1.00	0.13	0.023	0.884	Not significant
	SF38	0.48	1.00	0.48	0.266	0.633	Not significant
	SF50	0.12	1.00	0.12	0.080	0.804	Not significant
	SLF35	1.31	1.00	1.31	0.859	0.407	Not significant
Drop-weight test							
28-day	CR	24010000.00	6.00	4002000.00	9.940	0.002	Significant
	SF19	8936000.00	1.00	8936000.00	6.510	0.043	Significant
	SF27	17370000.00	1.00	17370000.00	11.770	0.014	Significant
	SF38	28188000.00	1.00	28188000.00	18.710	0.012	Significant

	SF50	7686800.00	1.00	7686800.00	29.175	0.033	Significant
	SLF35	48598000.00	1.00	48598000.00	43.577	0.003	Significant
Flexural Impact loading							
28-day	CR	2629000.00	6.00	438100.00	11.080	0.001	Significant
	SF19	750300.00	1.00	750300.00	3.360	0.117	Not significant
	SF27	1210000.00	1.00	1210000.00	5.470	0.058	Not Significant
	SF38	1155000.00	1.00	1155000.00	19.039	0.012	Significant
	SF50	472660.00	1.00	472660.00	16.063	0.057	Not Significant
	SLF35	1619000.00	1.00	1619000.00	39.668	0.003	Significant

4.2 Stage 1 - Fresh properties of SCRC mixtures with different SCMs

4.2.1 Effect of increasing the percentage of CR

Mixtures 1 to 5 in Table 4-1 show the effect of increasing CR content on the fresh properties of SLFSCRC mixtures. In general, increasing the percentage of CR had a negative impact on the fresh properties of SLFSCRC mixtures. With 550 kg/m^3 binder content, it was only possible to use up to 20% of CR to develop successful SLFSCRC mixtures. Using more than 20% CR resulted in unsuccessful SCC fresh properties (especially the passing ability) according to EFNARC (2005).

Table 3-3 shows the HRWRA demand to achieve the target slump flow of 700±50mm for SLFSCRC mixtures. It can be seen that the inclusion of CR in SLFSCRC mixtures slightly increased the HRWRA demand. For example, adding 20% CR increased the HRWRA by 13.89% compared to the control mixture (mixture with 0% CR). Table 4-1 also shows the reduction in unit weight of SLFSCRC mixtures resulted from adding CR. It can be observed from the Table that varying the percentage of CR from 0% to 20% reduced the unit weight by 5.5%. This reduction in the unit weight is attributed to the lower density of CR and the ability of CR to entrap more air in the mixture due to the high compressibility of CR particles (Naito et al., 2014).

The viscosity and flowability of the tested mixtures were assessed by using T50, T50J and V-funnel flow times. Table 4-1 and Figure 4-1a show the negative effect of increasing the percentage of CR on the flowability of SLFSCRC mixtures. For example, increasing the percentage of CR from 0% to 20% resulted in an increase in T50 time by

95.5% and similarly, the T50J and V-funnel times were increased by 1.65 and 2.1 times, respectively. According to EFNARC (2005), both of SLFSCRC mixtures with 0% and 5% CR has a T50 less than 2 seconds and V-funnel less than 8 seconds, and therefore, they can be classified as VS1/VF1. On the other hand, the SLFSCRC mixtures with 10%, 15%, and 20% CR meet the limits of VS2/VF2, in which the T50 flow times are more than 2 seconds. As a result, all SLFSCRC mixtures with up to 20% CR have a good potential to be used in structural application such as slabs, columns, piles, and ramps.

The L-box ratio (H2/H1) and the difference between slump flow and J-ring diameters were used to evaluate the passing ability of SLFSCRC mixtures. Table 4-1 and Figure 4-1c illustrate the impact of varying the percentage of CR on the passing ability, in which increasing the percentage of CR generally reduced the passing ability of SLFSCRC mixtures. For example, varying the percentage of CR from 0% to 20% in SLFSCRC mixtures reduced the L-box ratio by 13.6%. Similarly, the difference between slump flow and J-ring diameters increased from 20 to 55mm as the percentage of CR increased from 0% to 20%. The reduction in passing ability may be related to the high friction and blockage between coarse aggregate and CR particles. Despite the reduction in passing ability that resulted from increasing the percentage of CR, all tested SLFSCRC mixtures with up to 20% CR met the minimum requirement of successful L-box test ($H2/H1 \geq 0.75$) recommended by the EFNARC (2005).

The segregation resistance of SLFSCRC is shown in Table 4-1 and Figure 4-1e. As the percentage of CR increased the segregation resistance values (SR) increased indicating a reduction in the stability of mixtures. For example, increasing the percentage of CR from 0% to 20% resulted in increasing the SR values from 2.45% to 4.89%. The low density of

the rubber (0.95) increased the probability of the rubber particles to float towards the concrete surface and therefore, reduced the stability of mixtures. However, all tested SLFSCRC mixtures did not exceed the acceptable limit (SR ≤ 15%) recommended by EFNARC (2005).

4.2.2 Effect of binder content

Table 3-3 indicated that increasing the binder content reduced the required dosage of HRWRA to achieve the target slump flow diameter (700±50mm) of SLFSCRC. For example, by comparing mixture 2 to mixture 9, it can be noticed that increasing the binder content from 500 Kg/m^3 to 550 Kg/m^3 reduced the required amount of HRWRA by 2.6% at the same percentage of CR (5%). Moreover, increasing binder content from 550Kg/m^3 to 600 Kg/m^3 at the same percentage of CR (20%) reduced the HRWRA by 6.1% as shown in mixtures 10 compared to mixture 5.

The effect of increasing the binder content on the flowability of SLFSCRC mixtures is shown in Table 4-1 and Figure 4-1a. Increasing the binder content from 500Kg/m^3 to 550Kg/m^3 (mixture 2 compared to mixture 9) enhanced the flowability of SLFSCRC which resulted in reductions in the T50, T50J, and V-funnel times by 18.18%, 20.67%, and 23.75%, respectively. Same results were observed when the binder content increased from 550Kg/m^3 to 600 kg/m^3 at 20% CR replacement (mixture 5 compared to mixture 10), such that T50, T50J, and V-funnel times decreased by 10.8%, 7.2%, and 9.3%, respectively. These results match with other researchers' results (Gencel et al., 2011), in which increasing the binder content improved the flowability of SCC mixtures with polypropylene fibers.

Increasing the binder content had a significant effect on improving the passing ability and maximizing the percentage of CR that could be used in SLFSCRC (Table 4-1 and Figure 4-1c). For example, using 500 Kg/m^3 binder content (mixture 10) limited the maximum percentage of CR that could be used to obtain successful SLFSCRC mixtures to 5% [higher percentage of CR resulted in an unacceptable H2/H1 ratio (<0.75)]. On the other hand, using 550 kg/m^3 and 600 Kg/m^3 extend that percentage to 20% and 25%, respectively (mixture 5 and mixture 11). It is worth noting that increasing the binder content from 500 kg/m^3 to 550 Kg/m^3 increased the L-box ratio from 76% to 83% at the same level of CR replacement (5%), as shown in mixture 2 compared to mixture 9. Similarly, increasing binder content from 550 Kg/m^3 to 600 Kg/m^3 increased the L-box ratio and decreased the Slump-J-ring diameters by 4% and 9%, respectively, for the same percentage of CR 20% (see mixtures 5 and 10).

The results of SR indicated a lower risk of segregation when the binder content increased. Increasing the binder content from 500 kg/m^3 to 550 Kg/ m^3 in SLFSCRC mixtures reduced the SR value from 4.87% to 3.06% (mixture 9 compared to mixture 2). Similarly, increasing the binder content from 550 Kg/m^3 to 600 Kg/m^3 (mixture 5 compared to mixture 10) reduced the SR value by 14.8%, see Figure 4-1e. These results match with other researchers' results (Ismail and Hassan, 2016b), in which increasing binder content resulted in a reduction in SR values for SCRC mixtures with MK.

4.2.3 Performance of SLF compared to other SCM

Table 4-1 shows the fresh properties of SLFSCRC mixture (mixture 5) compared to some successful SCRC mixtures with other SCMs having maximized percentages of CR. All

SCRC mixtures with other SCMs (MK, FA, and GGBS) had a maximum percentage of CR of 20%, similar to SLF mixture (mixture 5). By looking at Table 3-3, it can be seen that using either FA or GGBS (mixtures 7and 8) required the same amount of HRWRA to achieve the target slump flow diameter. On the other hand, using MK (mixture 6) increased the HRWRA demand by 2.85 times compared to mixtures with FA or GGBS at the same level of CR replacement (20%). However, SLFSCRC mixture (mixture 5) requires 22.1% less than the MK mixture to achieve the target slump flow diameter of 700±50mm.

From Table 4-1 and Figure 4-1b, it can be seen that SLFSCRC mixture (mixture 5) showed less flowability compared to mixtures with FA or GGBS. For example, the T50, T50J, and V-funnel times increased by 53.2%, 48.7%, and 49.7%, respectively, compared to SCRC mixtures with FA (mixture 5 compared to mixture 7). On the other hand, when comparing the flowability of SLFSCRC mixture to the mixture with MK (mixture 5 compared to mixture 6), it can be noticed that the T50, T50J, and V-funnel times were decreased by 14.6%, 13.1%, and 26.5%, respectively, indicating better flowability. This behavior matches other researchers' results (Cyr and Mouret, 2003; Hassan et al., 2010; Güneyisi, 2010), in which adding SLF to SCC mixtures showed less reduction in flowability compared to mixtures with MK.

By examining mixtures 5-8, it can be noticed that adding MK had a noticeable enhancement in the passing ability of SCRC mixture compared to all other SCMs mixtures (see Figure 4-1d). Despite that SLFSCRC mixture showed a slight improvement in passing ability compared to FA mixture, MK and GGBS mixtures showed better passing ability compared to SLFSCRC. However, in general, the addition of MK, SLF,

GGBS, and/or FA allowed the use of up to 20% CR in SCRC mixtures and maintained acceptable fresh properties.

Table 4-1 and Figure 4-1f show the segregation resistance values for SCRC mixtures with different SCMs (mixtures 5-8). It can be noticed that the addition of SLF considerably reduced the segregation resistance value by 26.7% compared to the mixture with FA. Nevertheless, using MK has a more pronounced effect on the stability of mixture, in which adding MK to SCRC mixture reduced the SR value by 37.48% compared to the mixture with FA. The addition of GGBS in SCRC mixture also showed some improvement in mixture stability. However, this improvement was relatively small compared to that achieved with SLF and MK mixtures. In general, all the tested mixtures satisfied the limit given by EFNARC (2005) (SR ≤ 15%), indicating good stability.

4.2.4 Effect of adding MK to SLFSCRC mixtures

The addition of MK to SLFSCRC generally improved the segregation resistance and passing ability of the mixture. By comparing mixture 12 to mixture 5, it can be noticed that the addition of MK to SLFSCRC mixture with 20% CR increased the L-box ratio from 0.76 to 0.79, while the difference between slump flow -j-ring diameters showed a reduction of 18.18%. This improvement is attributed to the enhancement in mixtures viscosity due to the addition of MK which improved the particle suspension and in turn helped to increase the passing ability (Hassan et al., 2010). The improvement in the passing ability of SLFSCRC with the addition of MK allowed to increase the maximum percentage of CR in SLFSCRC mixture from 20% to 25% (mixture 13 compared to mixture 5) while maintaining acceptable H2/H1 ratio (≥ 0.75) as recommended by the

EFNARC (2005). It should be noted that, although the addition of MK to SLFSCRC mixtures negatively affected the flowability and HRWRA demand (Table 3-3, Table 4-1), the development of SLFSCRC mixture with up to 25% CR still gave acceptable values of T50, T50J, and V-funnel times (see Figure 4-1b, d, and f).

4.2.5 Effect of combining MK and FA on SCRC mixtures

Combining MK and FA in SCRC mixtures contributed to enhance the flowability and passing ability compared to mixtures with MK and SLF. By comparing mixture 14 to mixture 12, it can be seen that combining MK and FA in SCRC mixture with 20% CR reduced the T50, T50J, and V-funnel by 3.8%, 9.9%, and 27.8%, respectively, indicated an enhanced flowability (see Figure 4-1b). This enhancement can be attributed to the effect of FA in enhancing the flowability of the mixture, in addition to the balanced viscosity that resulted from combining MK and FA, which improved the particle suspension and helped to enhance the mixture passing ability. By comparing mixture 14 to mixture 5, it can be seen that combining MK and FA in mixture with 20% CR increased L-box ratio from 0.76 to 0.79, while the difference between slump and J-ring diameters reduced from 55 to 45, indicating a better passing ability compared to mixture with SLF (see Figure 4-1d). This improvement in the flowability and passing ability of mixtures with combined MK and FA allowed to increase the maximum percentage of CR to 30% compared to 20% in mixtures with other SCMs (MK, FA, SLF, and GGBS) and 25% of mixtures with a combination of MK and SLF. On the other hand, despite combining MK with FA showed a negative effect on segregation resistance of SCRC

mixtures, the development of SCRC mixtures with up to 30% CR still gave acceptable values of SR (SR< 15%) according to EFNARC (2005) (see Figure 4-1f).

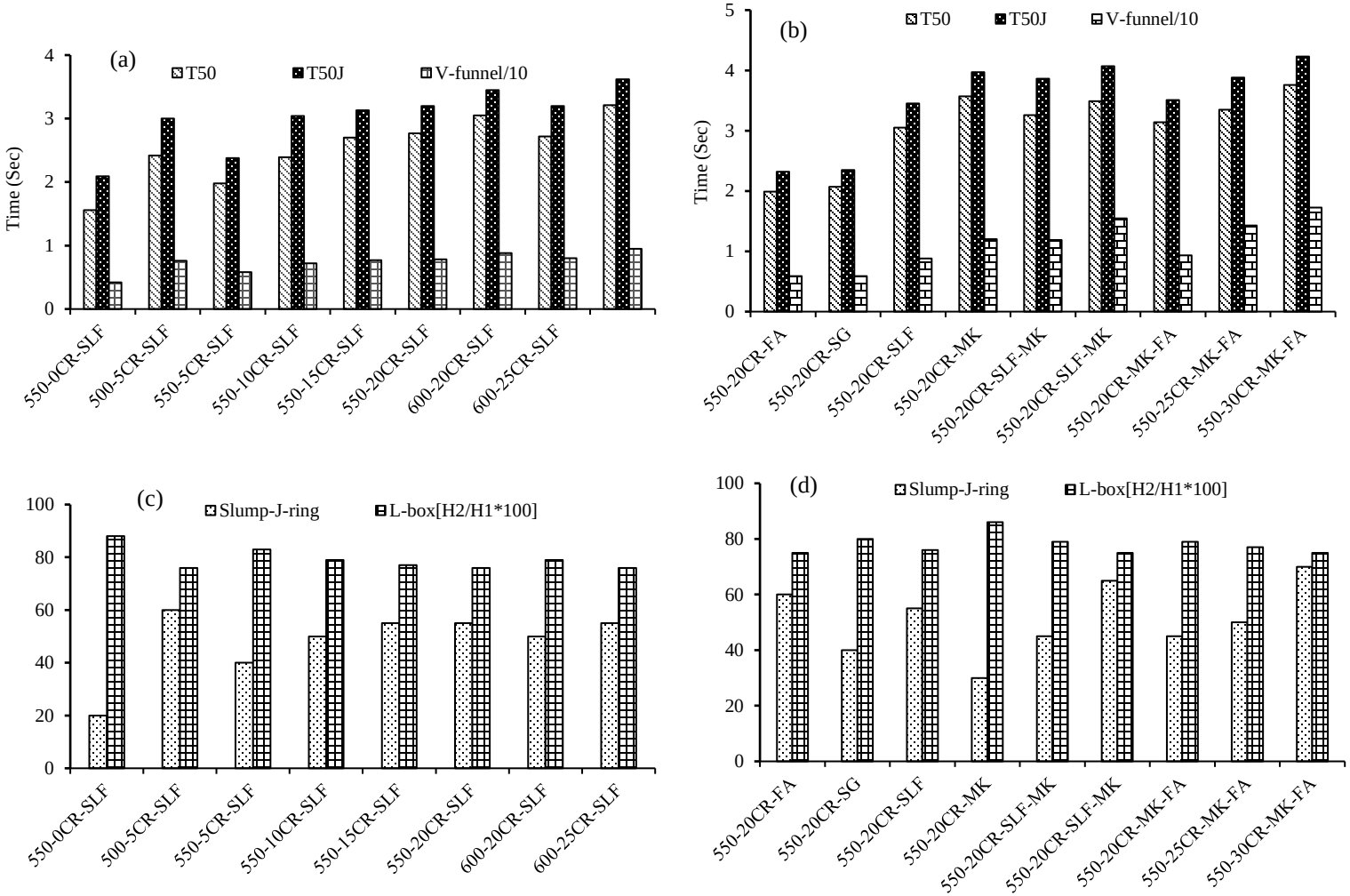
(a)
T50
T50J
V-funnel/10
Time (Sec)
0
1
2
3
4
550-0CR-SLF
500-5CR-SLF
550-5CR-SLF
550-10CR-SLF
550-15CR-SLF
550-20CR-SLF
600-20CR-SLF
600-25CR-SLF
(b)
T50
T50J
V-funnel/10
Time (Sec)
0
1
2
3
4
5
550-20CR-FA
550-20CR-SG
550-20CR-SLF
550-20CR-MK
550-20CR-SLF-MK
550-20CR-SLF-MK
550-20CR-MK-FA
550-25CR-MK-FA
550-30CR-MK-FA
(c)
Slump-J-ring
L-box[H2/H1*100]
0
20
40
60
80
100
550-0CR-SLF
500-5CR-SLF
550-5CR-SLF
550-10CR-SLF
550-15CR-SLF
550-20CR-SLF
600-20CR-SLF
600-25CR-SLF
(d)
Slump-J-ring
L-box[H2/H1*100]
0
20
40
60
80
100
550-20CR-FA
550-20CR-SG
550-20CR-SLF
550-20CR-MK
550-20CR-SLF-MK
550-20CR-SLF-MK
550-20CR-MK-FA
550-25CR-MK-FA
550-30CR-MK-FA

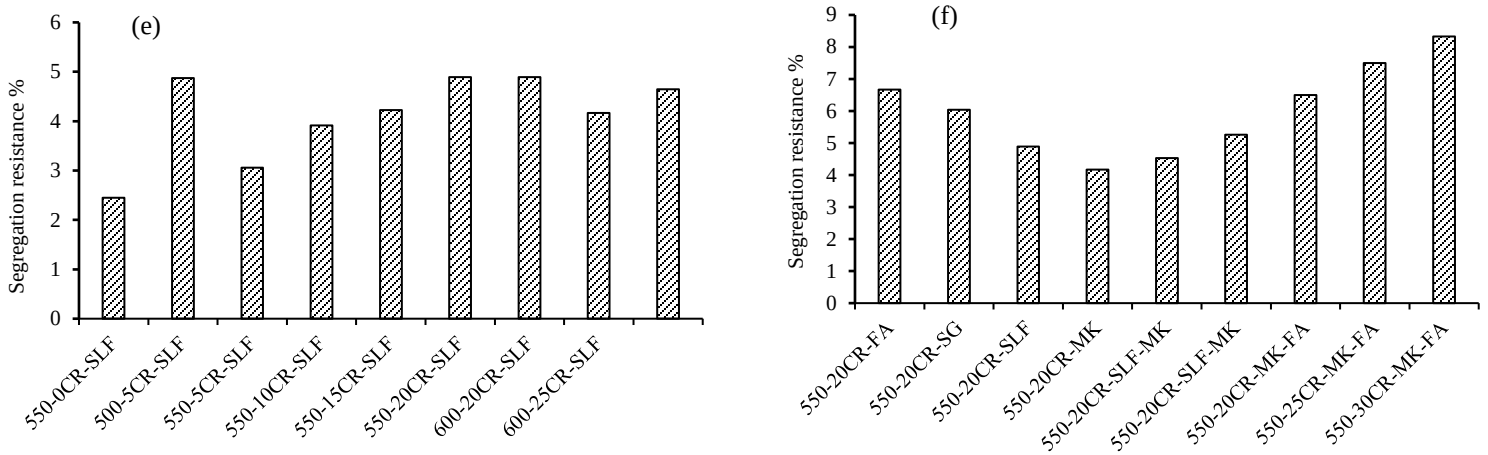

Figure 4-1 Fresh properties of SCRC mixtures with different SCMs (Study 1-stage 1)

4.3 Stage 1- Mechanical properties of SCRC mixtures with different SCMs

4.3.1 Effect of increasing the percentage of CR

Table 4-3 and Figure 4-2a show the 28-day compressive strength, STS, and FS results for tested SLF mixtures. It can be observed that increasing the percentage of CR generally decreased the mechanical properties of the mixtures. By comparing mixture 5 to mixture 1, it can be noted that adding 20% CR to SLFSCRC mixtures decreased 28-day compressive strength, STS, and FS by 58.2%, 41.1%, 45.9%, respectively, compared to control mixtures (without CR mixture 1). These results may be attributed to i) the lower modulus of elasticity for rubber particles compared to mineral aggregates, which simulate the rubber particle as a large pore in the concrete matrix that contributes to decrease the resistance to external loads (Khaloo et al., 2008); ii) the poor strength of the interface between rubber particles and surrounding mortar; iii) the increased entrapped air that resulted from the addition of CR, which has a negative impact on the mechanical properties (Najim and Hall, 2013; Elchalakani, 2015).

4.3.2 Effect of binder content and SCMs

As shown in Table 4-3 and Figure 4-2a increasing the binder content improves the compressive strength, STS, and FS of SLFSCRC mixture. For example, by examining mixture 2 compared to mixture 9, it can be observed that increasing binder content from 500 Kg/m3 to 550 Kg/m3 enhanced the compressive strength, STS, and FS by 6.9%, 7.1%, and 14.4%, respectively. Similar results were noticed when binder content increased from

550 Kg/m3 to 600 Kg/m3 at 20% CR level (see mixtures 5 and 10). This result could be related to the improvement of the adhesion and interfacial transition zone (ITZ) between rubber particles and surrounding mortar with increased binder content.

The results also indicated that the addition of either MK or SLF had a significant effect on the compressive strength, STS, and FS compared to mixtures incorporated with FA. As shown in Table 4-3 and Figure 4-2b, using SLF (mixture 5) increased the 28-day compressive strength, STS, and FS by 27.24%, 27.52%, and 15.3%, respectively, while using MK (mixture 6) showed an increase of 29.55%, 30.27%, and 20%, respectively, compared to mixture with FA (mixture 7). This behavior is related to the higher pozzolanic reactivity of MK and SLF compared to FA. On the other hand, the addition of GGBS to SCRC mixture showed a slight increase in the mechanical properties compared to FA mixture, in which the 28-day compressive strength, STS, and FS increased by 3.2%, 7.3%, and 6.3%, respectively (mixture 8 compared to mixture 7).

4.3.3 Effect of adding MK and FA to SCRC mixtures

Table 4-3 and Figure 4-2b present the mechanical properties results of SLFSCRC mixtures with MK. It can be seen that using MK in SLFSCRC mixture slightly enhanced the mechanical properties. Adding MK to SLFSCRC mixture with 20% CR (mixture 12) increased the 28-day compressive strength, STS, and FS by 3.39%, 3.59%, and 4.07%, respectively, compared to SLFSCRC mixture without MK (mixture 5). Table 4-3 and Figure 4-2b also show the effect of combining MK and FA on the mechanical properties of SCRC mixtures. From the Table, it can be seen that combining MK and FA in the SCRC mixture showed a significant enhancement in the mechanical properties compared to

SLFSCRC and SLFSCRC with MK. The enhancement in the mechanical properties of SCRC mixtures due to the combined effect of MK and FA allowed to use up to 30% CR with a reasonable compressive strength for the structural application (more than 25 MPa).

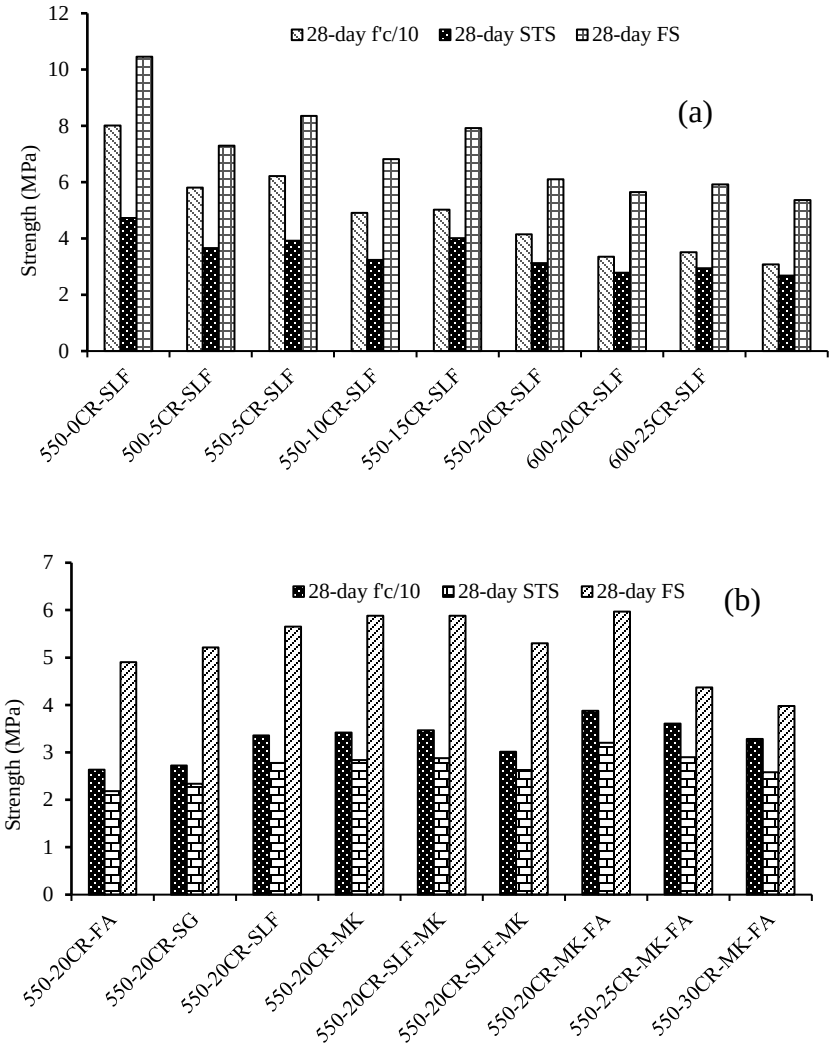

Figure 4-2 Mechanical properties of SCRC mixtures with different SCMs (study 1-stage 1)

4.4 Stage 2 - Fresh properties of SCRC/FRSCRC mixtures

4.4.1 Development of SCRC mixtures without fibers

HRWRA demand

In this study, HRWRA was generally used to achieve a slump flow diameter of 700 ± 50 for the tested SCRC mixtures. Table 3-4 shows the required dosage of HRWRA for different percentages of CR in SCRC mixtures. From the table, it can be seen that adding up to 25% CR in SCRC mixtures increased the HRWRA demand by 9.3% compared to the control mixture (with no CR). Beyond the CR replacement level of 25%, increasing the percentage of CR appeared to have a significant impact on decaying the flowability of mixtures, which required excessive HRWRA to achieve the targeted slump flow diameter. As shown, increasing the percentage of CR up to 30% exhibited an increase in the HRWRA reached up to 27.7% compared to the control mixture. These results are in agreement with those observed by other researchers (Güneyisi, 2010; Topçu and Bilir, 2009).

Viscosity and flowability

T_{50}, T_{50J}, and V-funnel time were measured to evaluate the viscosity and flowability of the developed SCRC mixtures. As shown in Table 4-2 and Figure 4-3a, increasing the percentage of CR from 0% to 30% increased the T_{50}, T_{50j}, and V-funnel time by 92.8%, 80.8%, and 146.1%, respectively. These results may be due to the CR particles having a rough and angular surface, which increased the inter-particle friction and thus contributed to decaying the flowability of mixtures. EFNARC (2005) classified the mixtures into two

categories to assess the viscosity of SCC mixtures based on T_{50} and V-funnel time. The first category, VS1/VF1, includes mixtures with T_{50} of less than 2 seconds and V-funnel time of less than 8 seconds. This category of mixtures has a good filling ability and self-level ability, but on the other hand, it is more likely to suffer from bleeding and segregation. The second category, VS2/VF2, includes mixtures with T_{50} of more than 2 seconds and V-funnel time between 9 and 25 seconds. Unlike VS1/VF1, VS2/VF2 is less likely to suffer from bleeding as it has the ability to limit segregation and bleeding. Based on these categories, and as shown in Table 4-2, only the control mixture can be classified as VS1/VF1, while the other SCRC mixtures with up to 30% CR can be classified as VS2/VF2. As per EFNARC (2005), both VS1/VF1 and VS2/VF2 can be successfully used in multiple structural applications such as slabs, columns, piles, walls, and ramps.

Passing ability

The L-box (H2/H1) ratio and the difference between slump and J-ring diameter were measured to assess the passing ability of the tested mixtures. Table 4-2 and Figure 4-3b indicate that the passing ability of mixtures was negatively affected by the inclusion of CR. Increasing the percentage of CR from 0% to 30% exhibited a reduction in the L-box ratio of up to 18%. Similar behavior was observed when the difference between slump flow and J-ring diameters was calculated: varying the percentage of CR from 0% to 30% increased the difference between slump flow and J-ring diameters from 10mm to 70mm. Such behavior may be attributed to high friction between the angular CR particles and the other components of the mixture, which could increase the possible occurrence of a blockage in both L-box and J-ring devices. This indicates a declined passing ability as the percentage

of CR increases. However, it should be noted that all the tested mixtures in this stage met the acceptable limits given by EFNARC (2005) (H2/H1= 0.75).

Segregation resistance

A sieve segregation resistance test was performed to assess the stability of mixtures. Table 4-2 and Figure 4-3c indicate that the mixture stability decreased as the percentage of CR increased. The segregation resistance factor (SR) increased from 2.08 to 8.33 as the percentage of CR increased from 0% to 30%. These results are in agreement with other researchers' findings (Topçu and Bilir, 2009). In this stage, all the tested mixtures (with CR percentage from 0% to 30%) did not exceed the acceptable limit (SR ≤ 15%) for SCC mixtures, as recommended by EFNARC (2005). Besides the sieve segregation test, a hardened split cylinder was visually inspected for each developed mixture to evaluate the CR distribution along the concrete sample. Since the CR particles have a relatively low density of 0.95, in the case of mixtures with low viscosity, the particles may move upward to float on the concrete surface after concrete pouring. From Figure 4-4, it can be observed that mixtures with up to 30% CR seemed to have a good distribution of CR particles along the splitted samples, which confirms that the developed mixtures have sufficient viscosity to achieve adequate particle suspension.

4.4.2 Development of SCRC mixtures with fibers

HRWRA demand

As shown in all mixtures with fibers (mixtures 8–11, mixtures 12–14, mixtures 15–16, mixtures 17–20, and mixtures 21–23) compared to mixtures without fibers (mixtures 2–5), using fibers regardless of their type, generally increased the amount of HRWRA required

to achieve the target slump flow diameter of 700 ± 50mm (Table 3-4). On the other hand, increasing the length of SFs (from 19mm to 50mm) did not have a significant effect on the amount of HRWRA needed, raising the demand by 5.08%. The results also showed that mixtures with semi-rigid SFs (SF27) and MFs seemed to require a lower dosage of HRWRA compared to mixtures with other SFs to achieve the target slump flow diameter (700 ± 50mm).

Viscosity and flowability

By comparing SFSCRC mixtures (mixtures 8–11, mixtures 12–14, mixtures 15–16, mixtures 17–20, and mixtures 21–23) to mixtures with no fibers (mixtures 2–5), it can be seen that the addition of fibers decreased the flowability of SCRC mixtures (see Table 4-2 and Figure 4-5(a, b, and c)). For example, the inclusion of 0.2% flexible SF19 raised the T_{50}, T_{50j}, and V-funnel time by an average of 2.5%, 3.5%, and 7.5%, respectively, as shown in mixtures 8–11 compared to mixtures 2–5. Such results could be due to the interference and blockage exerted by the fibers, which in turn limited the ability of the fresh mixture to flow freely under its own weight. By examining mixtures with SF19 vs. SF38 vs. SF50, it can be noticed that increasing the fiber length appeared to heighten the interference and blockage in the mixtures, thus leading to higher reductions in flowability. As shown in Table 4-2, using 50mm SFs (SF50) in mixtures 15–16 showed relatively higher increases in the T_{50}, T_{50j}, and V-funnel time up to 7.1%, 8.2%, 23.2% (on average), respectively, compared to mixtures with 38mm SFs (SF38) in mixtures 12–14. Meanwhile, adding 38mm SFs (SF38) in mixtures 12–14 increased the T_{50}, T_{50J}, and V-funnel time by an average of 8.6%, 21.3%, and 35.2%, respectively, compared to mixtures with 19mm SFs (SF19) in mixtures 8–11. It should be noted that although using fibers in SCRC

mixtures resulted in decaying the mixtures' flowability, all the developed mixtures in this stage met the limits of VS2/VF2 class given by EFNARC (2005). This result shows promising potentials for different structural applications such as slabs, floors, piles, walls, and ramps.

Passing ability

The passing ability of SCRC mixtures was negatively affected by the inclusion of SFs, as shown in Table 4-2 and Figure 4-5(d and e). This reduction was attributed to the high friction and blockage from fibers, CR, and coarse aggregates at the vertical steel bars in both L-box and J-ring devices. By comparing mixtures 2–5 to mixtures 8–11, it can be seen that adding SF19 slightly decreased the L-box ratio by 2.7% (on average), while the difference between slump flow and J-ring diameters increased by an average of 1.27 times. The drop in the passing ability increased as the length of SFs increased. This is because the possibility of blockage occurrence through steel rods of both L-box and J-ring devices was increased. For example, using 50mm SFs (SF50) in mixtures 15–16 exhibited a reduction in the L-box ratio reaching up to 8% (on average) and an average increase in the difference between slump flow and J-ring diameters reaching up to 2.5 times as much as mixtures 8–11 that used 19mm SFs (SF19). In the developed mixtures, the passing ability was negatively affected more by the inclusion of SFs than by MFs, and this made it possible for MFs to be used with a volume up to 0.35% compared to 0.2% used with SFs. Such results can be attributed to the fact that for a given volume, the low density of SFs compared to MFs greatly increased the number of single fibers, which increased the blockage and interference. In addition, the flexibility of SFs allows fibers to bend around the mixture's components, especially the coarse aggregate, which heightens the interlocking/interference

between the mixture's components, resulting in a significant reduction in the passing ability of FRSCRC mixtures. The inclusion of fibers also reduced the maximum percentage of CR that can be added to produce acceptable FRSCRC mixtures. For example, a maximum of 20% CR could be used with flexible SF19 mixtures compared to a maximum of 30% CR used in mixtures without fibers. Increasing the length of SFs seemed to reduce the maximum percentage of CR that can be safely used in developing FRSCRC mixtures with acceptable fresh properties. As shown, in mixtures with SF38 the maximum percentage of CR was 15%, while with SF50 the most successful mixtures contained 10% CR. Further increases in the amount of CR and/or fibers showed a higher blockage in the L-box and J-ring tests, which dropped the passing ability below the acceptable limits given by EFNARC (2005) (L-box value ≥ 0.75). In the case of both 0.35% MF35 and 0.2% semi-rigid SF27, the maximum percentage of CR reached 15% and 20%, respectively. It should be noted that it was not possible to develop FRSCRC mixtures with semi-rigid 54mm SFs or 60mm MFs because the distance between the steel bars of the L-box and J-ring devices was relatively narrow (41mm and 58.9mm, respectively), making it difficult for such rigid fibers to pass through.

Segregation resistance

From the results in Table 4-2, mixtures 8–11 compared to mixtures 2–5, it can be observed that the inclusion of 19mm SFs did not show a confirmed effect on the segregation resistance. However, further increase in the fiber length (38mm and 50mm) was found to decrease the stability of mixtures, in which SF38 and SF50 increased the SR value by an average of 23.6% and 49.2%, respectively, compared to mixtures without fibers (mixtures 12–14 and mixtures 15–16 compared to mixtures 2–4). Similarly, the inclusion of MF35 in

FRSCRC mixtures increased the SR value by an average of 7.1% compared to mixtures without fibers (as shown in Figure 4-5f). However, all the tested FRSCRC mixtures satisfied the limit given by EFNARC (2005) (SR ≤ 15%), indicating good stability.

4.4.3 Development of VRC mixtures with higher volumes of CR and fibers

Workability

Table 4-2 shows that increasing the percentage of fibers negatively affected the workability of VC mixtures, similar to the fibers' effects on the flowability of SCRC and FRSCRC mixtures. By comparing mixtures 25–31 to mixture 24, it can be observed that at a constant HRWRA of 3.18 l/m^3 (Table 3-4), increasing the length of SFs or MFs showed a reduction in the slump values. As shown from the slump test, the inclusion of 1% from flexible fibers SF19, SF38, or SF50 decreased the slump by 8.5%, 21.1%, 31.6%, respectively, and for the semi-rigid fibers of SF27 and SF54 these reductions reached up to 15.1% and 34.2%, respectively. A similar trend of results was found in MFs mixtures, in which adding 1% volume fraction from MF35 and MF60 led to a decrease in the slump flow by 15.8% and 42.1%, respectively.

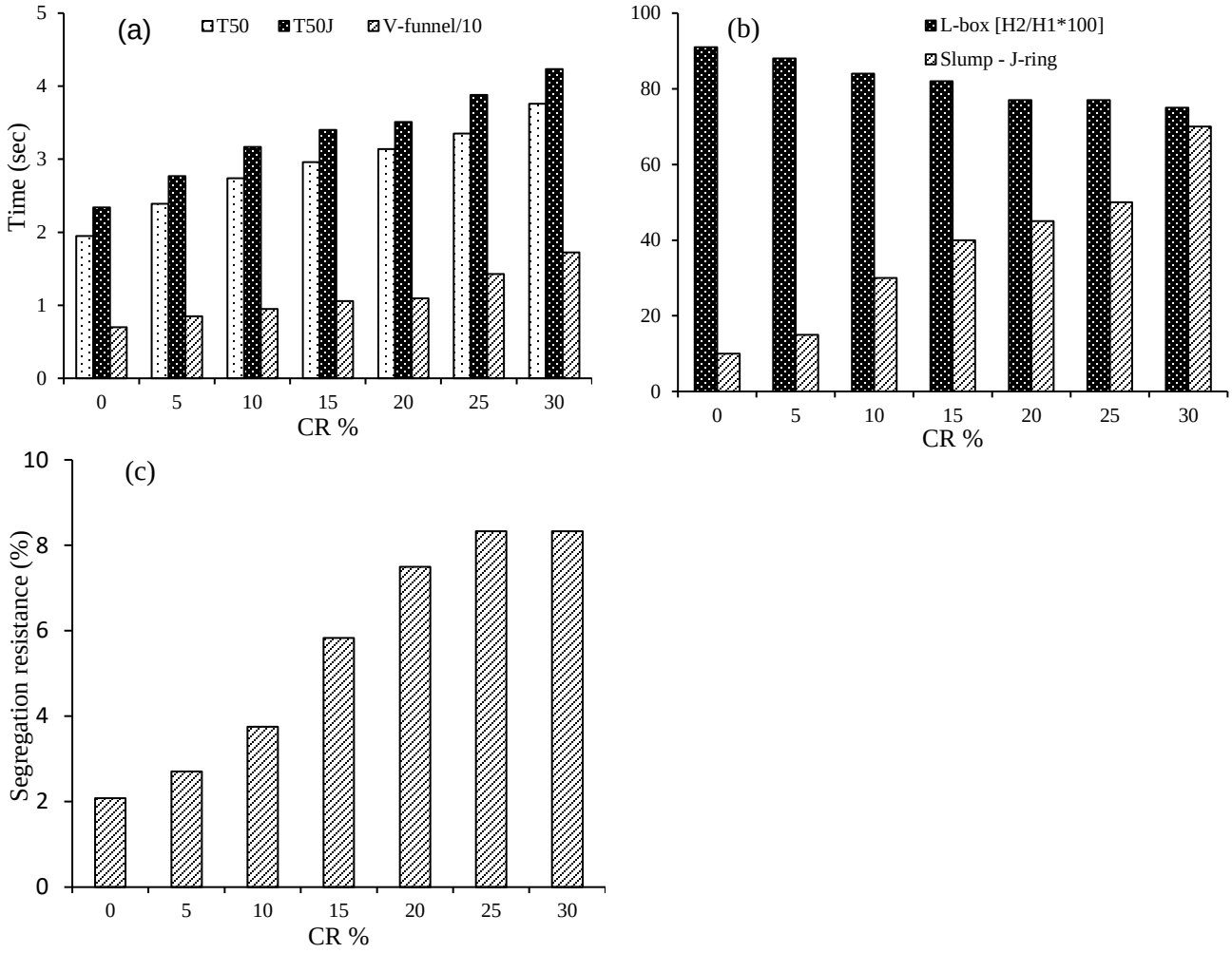

Figure 4-3 Effect of CR replacement on the fresh properties of SCRC (mixtures 1–7): (a) T_{50}, T_{50J}, and V-funnel, (b) passing ability, (c) segregation resistance

(a) (b) (c)

Figure 4-4 Distribution of CR particles: (a) 5% CR, (b) 15% CR, and (c) 30% CR

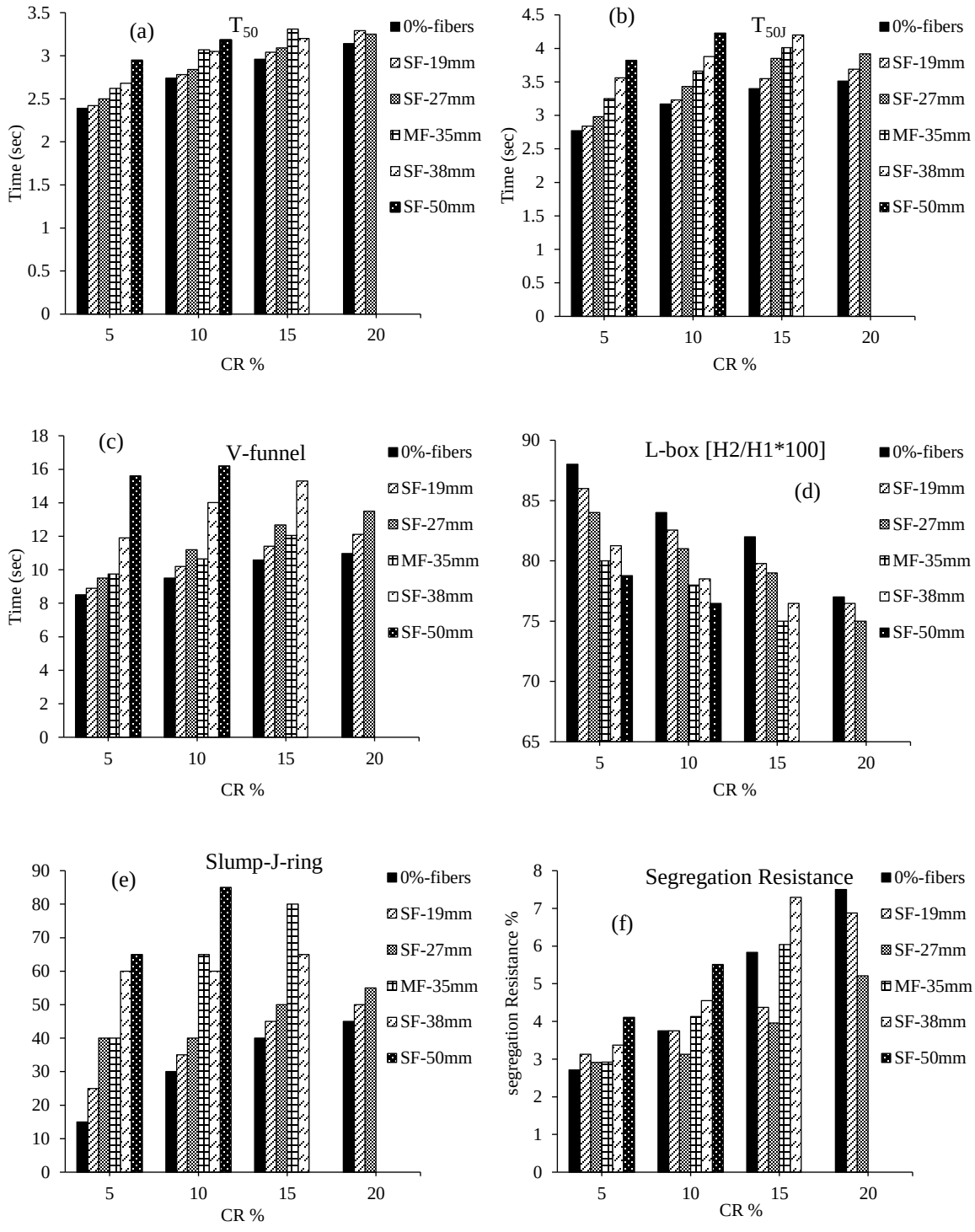

Figure 4-5 Effect of different types and sizes of fibers on the fresh properties of FRSCRC (mixtures 8–23): (a) T_{50}; (b) T_{50J}; (c) V-funnel; (d) L-box; (e) Slump-J-ring; (f) segregation resistance

4.5 Stage 2- Mechanical properties of SCRC/FRSCRC mixtures

4.5.1 Compressive strength

Table 4-4 and Figure 4-6 (a and b) show the 7- and 28-day compressive strengths for different percentages of CR. The addition of CR in SCC mixtures led to a reduction in the compressive strength, in which increasing the percentage of CR from 0% to 30% reduced the 7- and 28-day compressive strengths by 56.5% and 58%, respectively. As stated in previous studies, this behavior may be attributed to (a) the poor strength of rubber-mortar interface (Topcu, 1995), which encourages the initiation and propagation of microcracks; (b) the rough surfaces of CR particles, which entraps air at the surface (Reda Taha et al., 2008), thus increasing the porosity of mixtures; and (c) the low stiffness of CR compared to other mixture compositions, which makes the rubber particles act as large pores and in turn reduces the effective cross-section (Khaloo et al., 2008).

Table 4-4 and Figure 4-6 (c and d) indicate that the addition of fibers to SCRC mixtures appeared to insignificantly affect the compressive strength, in which the maximum increases in the compressive strength reached up to 1.2% and 3.2% due to the inclusion of 0.2% SFs and 0.35% MFs, respectively. The results also indicated that the compressive strengths were not significantly affected by changing the length of SFs (from 19mm to 50mm), as shown in Table 4-4.

Table 4-4 and Figure 4-6 (e and f) also show the 7- and 28-day compressive strengths of VRC and FRVRC mixtures at 30% CR reinforced with different types and lengths of fibers. It can be seen that VRC exhibited a slight increase in the 7- and 28-day compressive strengths, reaching up to 6.65% and 5.05%, respectively, compared to its SCRC

counterpart (mixture 24 compared to mixture 7). The inclusion of high percentage of SFs (1%) appeared to reduce the compressive strength, in which adding 1% SF19 led to a reduction in 7- and 28-day compressive strengths by 17.8% and 18.9%, respectively (mixture 25 compared to mixture 24). The same behavior was noticed when SF38 and SF50 were added. Such results may be attributed to the low stiffness of SFs, which can create weak zones when the fibers accumulate, forming soft fiber balls during mixing. Increasing the rigidity of the fibers helped to reduce the negative effect of adding a high percentage of SFs in VRC mixtures. For example, adding semi-rigid SFs (SF54) slightly decreased the 7- and 28-day compressive strengths by 2.4% and 5.3%, respectively (mixture 29 compared to mixture 24). Moreover, using the same percentage of MFs resulted in a slight increase in compressive strength (mixtures 30 and 31 compared to mixture 24).

The effects of CR and fibers on the compressive strength were further confirmed after performing an analysis of variance (ANOVA). The results of ANOVA are presented in **Table 4-6**. At 5% significant level, the addition of CR had a significant effect on the compressive strength while using fibers showed insignificant effect (see **Table 4-6**).

4.5.2 Tensile and flexural strength

Table 4-4 and Figure 4-7 and Figure 4-8 (a and b) show the 7- and 28-day FS and STS values for SCRC mixtures with different percentages of CR. It can be seen that adding CR to SCC mixtures reduced FS and STS, in which adding 30% CR reduced the 7- and 28-day STS by 45.1% and 40.3%, respectively (mixture 7 compared to mixture 1) (see Figure 4-7

(a and b)). Similarly, varying the CR percentage from 0% to 30% reduced the 7- and 28-day FS by 38.8% and 31.7%, respectively (mixture 7 compared to mixture 1) (see Figure 4-8 (a and b)). These reductions in STS and FS may be related to the same reasons that caused a reduction in the compressive strength (Khaloo et al., 2008; Najim and Hall, 2010; and Reda Taha et al., 2008)

It is also observed from Table 4-4 and Figure 4-7 and Figure 4-8 that the inclusion of SFs in SCRC mixtures increased the 7- and 28-day FS and STS. For example, by comparing mixtures 8–11 to mixtures 2–5, it can be noticed that using SF19 increased the 7- and 28-day STS by an average of 7.7% and 8.2%, respectively, while the 7- and 28-day FS increased by an average of 4.9% and 5.9%, respectively. Similarly, as shown in Table 4-4 and Figure 4-7 (c and d), adding semi-rigid SFs (SF27) appeared to increase the 7- and 28-day STS by an average of 10.05% and 9.9%, respectively, (mixtures 17–20 compared to mixtures 2–5). The 7- and 28-day FS also increased by an average of 7.7% and 7.22%, respectively, when semi-rigid SFs were added (mixtures 17–20 compared to mixtures 2–5) (see Figure 4-8 (c and d)). The increase of STS and FS with the addition of fibers is attributed to the role of fibers in restricting the widening and propagation of cracks, in addition to the fibers' bridging mechanism, which helps transfer the stresses through the cracked section, providing a residual strength for concrete (Jun et al., 2016; Lee et al., 2016; Ganesan et al. 2013).

The 7- and 28-day STS and FS increased as the fiber length increased from 19mm to 38mm. For example, using 38mm SFs (SF38) (mixtures 12–14) increased the 28-day STS and FS by an average of 15.6% and 12.4%, respectively, compared to mixtures without fibers (mixtures 2–3), while these increases were 7.18% and 6.84% (on average) for 19mm

SFs mixtures (mixtures 8–10) (see Figure 4-7d and Figure 4-8d). This increase can be attributed to the fact that longer fibers can develop higher bonding with surrounding mortar, which can contribute to increasing the pullout strength of fibers. Such an increase can effectively promote the role of fibers in arresting the cracks and transferring the tensile stress across the crack's faces (Ghernouti et al., 2015). It should be noted that by visual inspection of the failed samples, 19mm and 27mm SFs appeared to fail under pullout failure while 38mm and 50mm SFs appeared to fail under tensile failure. On the other hand, mixtures with 38mm SFs (SF38) appeared to have better STS and FS strengths compared to mixtures with 50mm SFs (SF50) (mixtures 12–14 compared to mixtures 15–16). This could be attributed to the higher tensile strength of SF38 compared to SF50 (as shown in Table 3-2). This finding indicates that in the case of using fibers long enough to assure adequate pullout strength (pullout failure is not dominant), the tensile strength of fibers can be the key factor controlling how fibers contribute to the STS of concrete. In general, the results indicated that mixtures containing MF35 (mixtures 21–23) showed the highest improvements in STS and FS.

Table 4-4 and Figure 4-7 and Figure 4-8 also showed that at the same level of CR replacement (30%) the VRC showed slightly enhanced STS and FS compared to SCRC mixtures (mixture 24 compared to mixture 7). These increases in the 7- and 28-day STS reached up to 5.4% and 3.4%, respectively, while the increases in the 7- and 28-day FS reached up to 6.4% and 7.4%, respectively. Using a high percentage of SFs (1%) increased the STS and FS of VRC mixtures, as shown in Figure 4-7 (e, f) and Figure 4-8 (e, f). By comparing mixture 25 to mixture 24, it can be seen that adding 1% SF19 increased the 7- and 28-day STS by 17.2% and 12.3%, respectively. These increases reached up to 13.2%

and 10.2% in the 7- and 28-day FS, respectively. Similar to SCRC, the STS and FS of VRC increased as the fiber length/rigidity increased. The inclusion of semi-rigid SFs (SF54) appeared to have the greatest effect on improving the STS and FS in VRC compared to the other SFs, in which the STS and FS increased by 37.9% and 21.6%, respectively, compared to the mixture without fibers (mixture 24). By comparing the results of mixtures with SFs and MFs, it can be clearly observed that the use of MFs exhibited higher improvements in the STS and FS (mixtures 30–31 compared to mixtures 25–29). These results could be related to the higher tensile strength provided by MFs. Generally, adding 1% SFs appeared to significantly compensate for the reductions in the STS and FS resulting from adding 30% CR. For example, adding 30% CR (mixture 24 compared to mixture 1) resulted in a 37.5% average reduction in STS and FS, while when adding 1% SFs (SF54 in mixture 29) this reduction was compensated by 61%. Meanwhile, adding 1% MFs seemed to provide a full recovery from the reduction in STS and FS resulting from adding 30% CR (mixtures 30 and 31 compared to mixture 1). However, using SFs has an advantage over MFs by developing light/semi-lightweight concrete.

The effect of CR and fibers on the STS and FS were also tested using ANOVA (see **Table 4-6**). The results indicated that only CR, SF38, and MF35 had a significant effect on the STS and FS at 5% significant level.

4.5.3 Modulus of elasticity

The ME results for all tested mixtures are presented in Table 4-4. As shown in mixtures 1–7, increasing the percentage of CR decreased the ME of SCRC mixtures. For example, increasing the percentage of CR from 0% to 30% decreased the ME by 36.32%. The reason

for this decrease is due to the low stiffness of CR compared to the replaced sand, which in turn reduced the ME.

By looking at mixtures 8–23 compared to mixtures 2–5 and mixtures 25–31 compared to mixture 24, it can be observed that the ME was insignificantly affected by fiber volume, length, and rigidity. For example, adding SF19 to SCRC mixtures reduced the ME by an average of 6.3% (mixtures 8–11 compared to mixtures 2–5). This may be related to the low ME of SFs, which led to decreases in the stiffness of mortar and in turn reduced the overall ME. Also, by comparing mixtures 8–11 to mixtures 15–16, increasing the fiber length from 19mm to 50mm slightly increased the ME by an average of 5%. However, SF38 showed better improvement in ME compared to SF50. This could be related to the higher tensile strength of SF38 compared to SF50 (as shown in Table 3-2).

The results also showed that the VRC mixture (mixture 24) exhibited a slightly higher ME compared to its counterpart SCRC (mixture 7) by a value of 6.4%. For mixtures 25–31, it can be seen that increasing the fiber volume showed an insignificant increase in the ME, in which increasing the fiber percentage from 0% to 1% increased the ME by an average of 9.6%. Increasing the fiber length also exhibited an insignificant increase in ME, as shown in Table 4-4. The ANOVA results of the effect of CR and different fiber types/lengths on the ME are presented in Table 4-6. From the table, it can be seen that only CR had a significant effect on the ME at 5% significant level.

4.6 Impact resistance of SCRC/FRSCRC mixtures

4.6.1 Impact resistance under drop-weight test

Table 4-5 and Figure 4-9 show the impact resistance results under drop-weight test for all tested mixtures. The results show that the addition of CR generally helped to improve the impact resistance of concrete in terms of a number of blows that were required to cause the first visible crack (N_1) and failure crack (N_2) of the tested specimens. By looking at mixtures 1–7, it can be observed that increasing the percentage of CR from 0% to 30% increased N_1 and N_2 by 89% and 91%, respectively. This behavior is related to the low stiffness of rubber particles, which obviously increased the energy absorption of rubber-cement composites compared to mixtures without CR. It can also be noticed that increasing the percentage of CR resulted in an increase in the difference between a number of blows for ultimate failure and first crack (N_2-N_1), which indicates an increase in the post-cracking resistance and a reduction in the brittleness of SCRC mixtures (Figure 4-9 (a and b)).

By comparing mixtures 8–11, 12–14, 15–16, 17–20, and 21–23 to mixtures 2–5, it can be seen that adding fibers to SCRC mixtures enhanced the impact resistance. For instance, adding SF19 increased N_1 and N_2 by an average of 49.2% and 49%, respectively, as shown in Figure 4-9 (c and d). In addition, the inclusion of fibers significantly increased the difference between N_2 and N_1, indicating higher ductility and post-cracking behavior. These results may be attributed to the beneficial effect of fibers in arresting the cracks and transferring the stress through the bridging action. It is also noted that increasing the fiber length enhanced the impact resistance of SFSCRC mixtures. For example, increasing the length of SFs from 19mm (SF19) to 38mm (SF38) increased N_1 and N_2 by an average of

36.2% and 44.4%, respectively, as shown in Table 4-5 and Figure 4-9 (c and d) (mixtures 8–11 compared to mixtures 12–14). This could be related to the fact that the use of longer fibers helped to develop better bonding between fibers and concrete matrix, which in turn enhanced the role of fibers in arresting the cracks. Using SF50 also showed an improvement in impact resistance. However, this improvement was less than that induced by the inclusion of SF38 (due to similar reasons explained earlier in STS and FS results). It is worth noting that the improvement in impact resistance is more pronounced in mixtures with MFs compared to mixtures with SFs. This may be related to the higher tensile strength and the larger volume of MFs compared to SFs (0.35% compared to 0.2%).

As shown in Table 4-5 and Figure 4-9 (e and f), the results of impact resistance indicated that the VRC mixture with 30% CR (mixture 24) had a slightly increased N_1 and N_2 compared to its SCRC counterpart. The results also showed that combining a high percentage of CR and fibers helped to develop concrete with a promising ability to sustain high-impact loads. In mixtures with 30% CR, increasing the percentage of fibers greatly enhanced the impact resistance, in which adding 1% SF19 increased N_1 and N_2 by 61.2% and 86.12%, respectively, compared to the mixture without fibers (mixture 24) (see Table 4-5 and Figure 4-9 (e and f)). Increasing the fiber length significantly increased the impact energy required to break the specimens. For example, increasing the fiber length from 19mm (SF19) to 50mm (SF50) increased N_1 and N_2 by 1.18 and 1.19 times, respectively (Figure 4-9). However, similar to FRSCRC mixtures, the higher tensile strength of SF38 contributed to achieving greater impact resistance compared to that obtained by SF50 (mixture 26 compared to mixture 27). The SF54 used in VRC had the greatest effect on improving the impact resistance compared to the other SFs. The inclusion of SF54

increased the N_1 and N_2 by 2.29 and 2.66 times, respectively, compared to the mixture without fibers (mixture 24). The addition of MFs appeared to be the most effective type of fiber to enhance the impact energy of concrete. Compared to mixture 24, using MF35 and MF60 (mixtures 30 and 31) increased N_1 by 3.2 and 3.53 times, respectively, and N_2 by 3.7 and 4.1 times, respectively (Figure 4-9 (e and f)).

By comparing the failure patterns shown in Figure 4-10, it can be seen that the inclusion of CR changed the failure pattern from one single big crack (Figure 4-10a) to three intersected small cracks (Figure 4-10b). It can also be observed that combining fibers with rubber in the mixture further increased the cracks number and reduce their widths (Figure 4-10c and Figure 4-10d). The significance of the effects of CR and different fiber types/lengths on the impact resistance (drop weight test) were presented by ANOVA (Table 4-6). The results indicated that the CR and all types of fibers had a significant effect on the impact resistance at 5% significant level.

4.6.2 Impact resistance under flexural loading

The results of the impact resistance under flexural loading for all tested mixtures are presented in Table 4-5. From the table, it can be seen that adding CR to concrete mixtures helped to enhance impact resistance. In mixtures, 1–7, the addition of 25% CR appeared to have the optimal effect on improving the impact energy of SCRC, while further increases in the percentage of CR led to less improvement. Varying the percentage of CR from 0% to 25% increased the ultimate impact energy by 2.42 times while adding 30% CR exhibited an improvement of 2.16 times higher than the control mixture. This result could be

attributed to that at a high percentage of CR, the volume of poor-strength ITZ between rubber and cement increased (Najim and Hall, 2012; Emiroglu et al., 2007). This, in turn, allowed for the initiation and propagation of more cracks between CR particles and the surrounding matrix, which limited the ability of rubber to enhance the energy absorption of concrete. It is worth noting that the optimum percentage of CR in beams subjected to flexural impact loading was 25%, while the results of the drop-weight test showed an increase in the impact resistance as the percentage of CR increased up to 30%. This may be related to the fact that the poor-strength ITZ is more susceptible to the higher tensile stress generated in the flexural loading test compared to the drop-weight test.

Adding fibers to SCRC mixtures generally enhanced the impact resistance and ductility of tested mixtures. For example, adding SF19 increased the ultimate impact energy of tested beams by an average of 68.3% compared to mixtures without fibers (mixtures 8–11 compared to mixtures 2–5). Increasing the fiber length had a significant effect on the ultimate impact energy; using SF38 increased the ultimate impact energy by an average of 88.9% compared to mixtures without fibers (mixtures 2–4). However, adding SF50 showed less of an improvement in the ultimate impact energy than that obtained by adding SF38. This behavior may be related to the same reasons explained earlier for impact resistance under the drop-weight test. Using of MFs in SCRC mixtures showed the highest improvement in ultimate impact energy (mixtures 21–23) compared to mixtures containing SFs.

Table 4-5 also shows that VRC mixture with 30% CR (mixture 24) had similar behavior to its SCRC counterpart (mixture 7), indicating an insignificant effect of concrete type on the ultimate impact energy. Combining high percentage of CR with fibers greatly enhanced the

ultimate impact energy of concrete. For example, using a combination of 1% SF19 and 30% CR in the VRC mixture (mixture 25) increased the ultimate impact energy by 4.13 times compared to the mixture without fibers and/or CR (mixture 1). By examining the investigated SFs, it can be seen that the highest increase in the ultimate impact energy was achieved when SF54 was added. This increase reached up to 5.45 times compared to the mixture without fibers (mixture 24). The results prove that MFs were the most effective type of fiber to improve the impact energy, in which adding MF35 and MF60 increased the ultimate impact energy by 8 and 10 times, respectively, compared to the mixture without fibers (mixture 24).

The ANOVA results of the effects of CR and different fiber types/lengths on the flexural impact resistance are presented in Table 4-6. From the table, it can be seen that only CR, SF38, and SLF35 had a significant effect on the flexural impact resistance at 5% significant level.

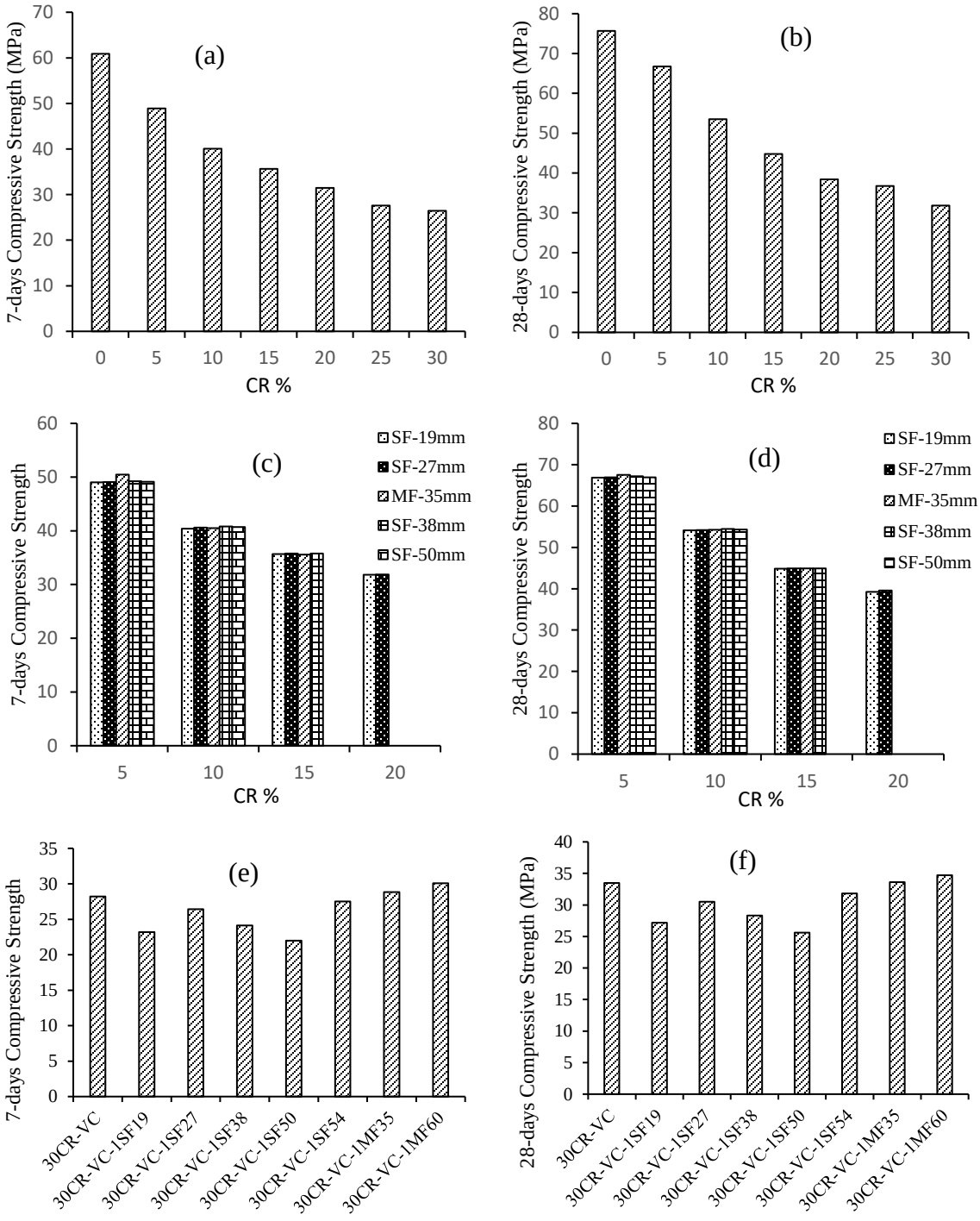

Figure 4-6 7- and 28-day compressive strengths: (a, b) effect of CR on SCRC; (c, d) effect of different types of fiber on SCRC; (e, f) effect of CR and different types of fiber on VRC

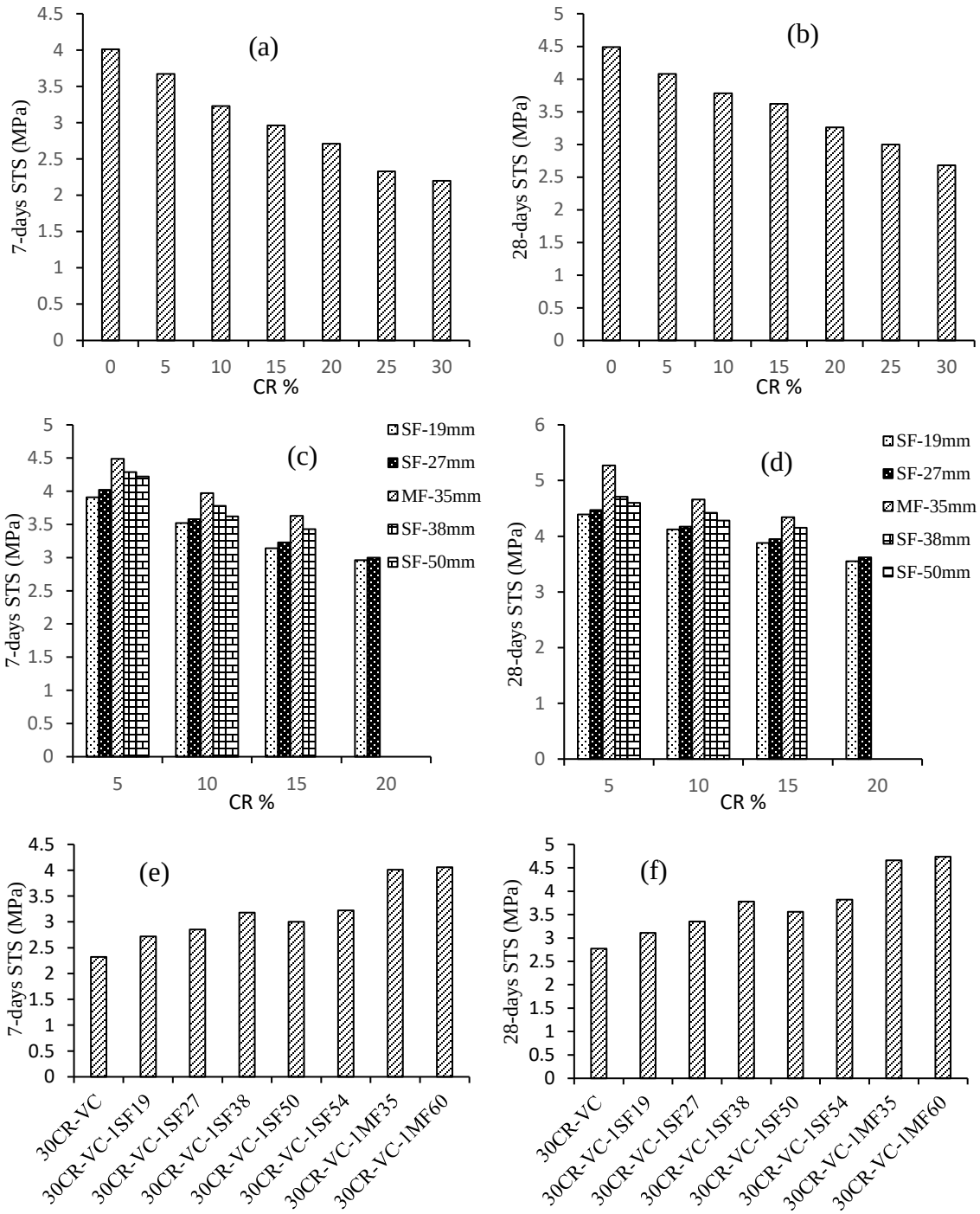

Figure 4-7 7- and 28-day STS: (a, b) effect of CR on SCRC; (c, d) effect of different types of fiber on SCRC; (e, f) effect of CR and different types of fiber on VRC

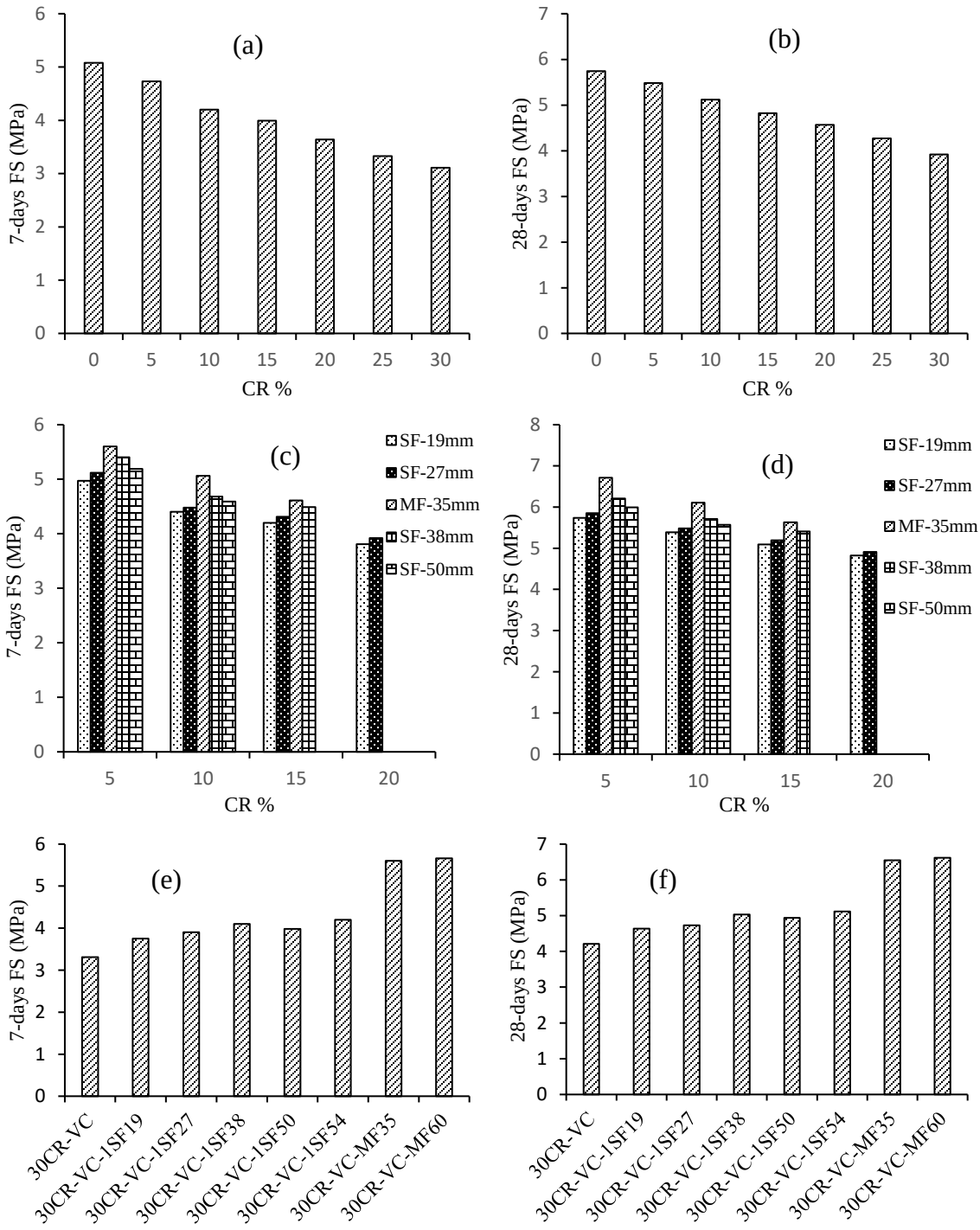

Figure 4-8 7- and 28-day FS: (a, b) effect of CR on SCRC; (c, d) effect of different types of fiber on SCRC; (e, f) effect of CR and different types of fiber on VRC

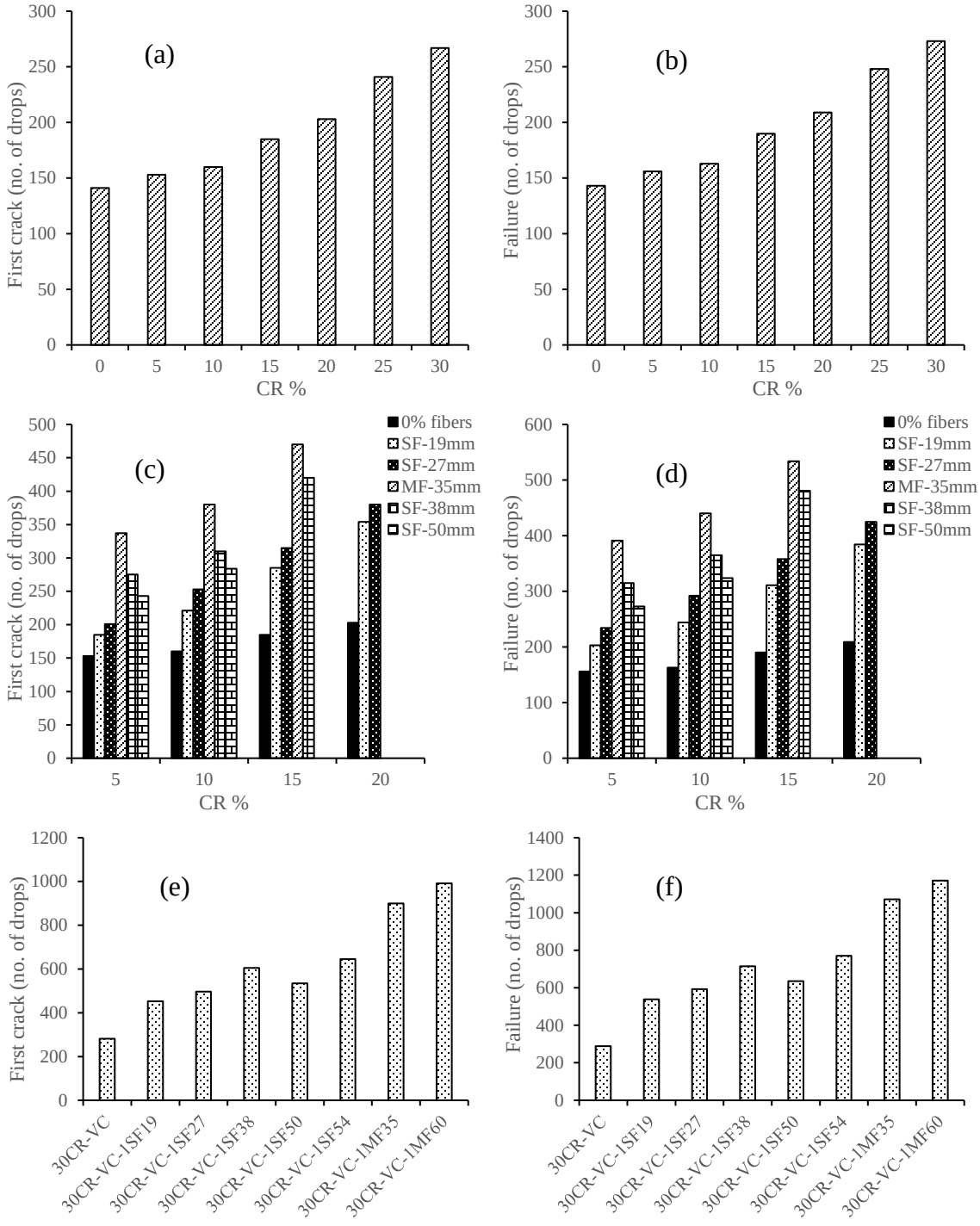

Figure 4-9 Results of impact resistance for the cylindrical specimens under drop-weight test: (a, b) effect of CR on SCRC; (c, d) effect of different types of fiber on SCRC; (e, f) effect of CR and different types of fiber on VRC

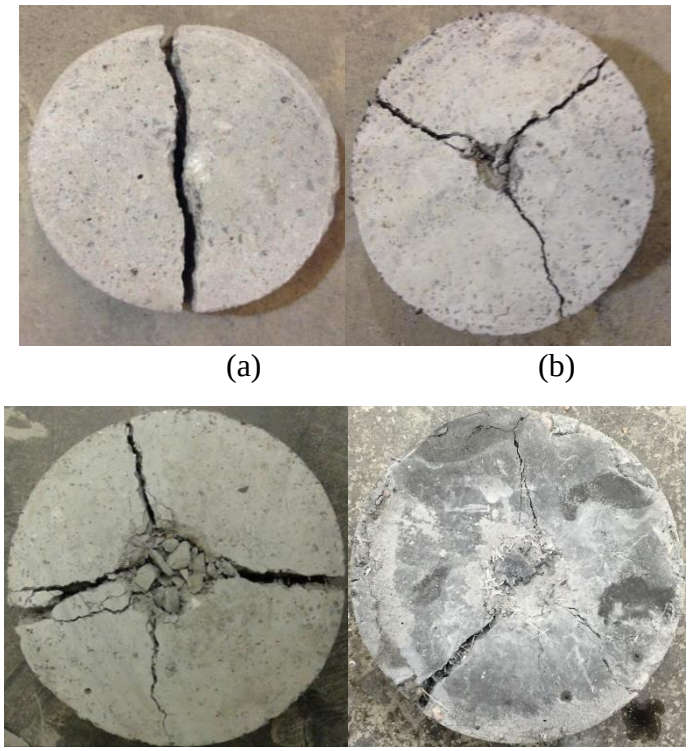

Figure 4-10 Failure patterns: (a) plain specimen, (b) specimen with CR, (c) specimen with CR and MFs, (d) Specimen with CR and SFs

5 Discussion of results from experimental study 2: influence of SFs' type, length, and volume on enhancing the structural performance of rubberized concrete

5.1 Introduction

This chapter highlights the results and discussion of the flexural behavior of rubberized concrete beams reinforced with SFs. The concrete mixtures used in this study were optimized from study 1. The main objective of this study is to investigate the flexural behavior of rubberized concrete beams reinforced with different types, lengths, and volumes of SFs. Different SCRC and VRC with different percentages of CR and SFs were tested. The main parameters were the percentage of CR (0%, 10%, 15%, 20%, and 30% by volume of sand), type of SFs (MISFs and MASFs), length of SFs (19mm, 38mm, 50mm, 54mm), and volume of SFs (0%, 0.2%, and 1%). The flexural performance of the tested beams was assessed based on the characteristics of load-deflection curves, flexural stiffness, cracking behavior, displacement ductility, energy absorption, first cracking moment, and bending moment capacity. Table 5-1 summarizes the fresh properties, compressive strength, and STS of SCRC and SFSCRC tested beams' mixtures. Table 5-2 presents the results obtained from the flexural tests. The results and discussions presented in this chapter have been published in the paper number nine mentioned earlier at the beginning of this thesis.

Table 5-1 Fresh and mechanical properties for tested mixtures

Mix #	Mixtures SCC/SCRC/SFSCRC	T_{50} (sec)	V-funnel (sec)	L-box ratio (H_2/H_1)	HRWRA (kg/m^3)	f'_c (MPa)	STS (MPa)
1	SCC-0CR	1.98	7.21	0.92	3.43	65.6	4.21
2	SCC-10CR	2.71	9.43	0.85	3.75	50.48	3.75
3	SCC-15CR	3.01	10.60	0.81	3.75	45.77	3.59
4	SCC-20CR	3.23	10.89	0.78	3.75	39.2	3.25
5	SCC-20CR-0.2MISF19	3.33	12.0	0.76	6.40	39.5	3.49
6	SCC-15CR-0.2MASF38	3.24	15.25	0.78	6.30	46.91	4.11
7	SCC-10CR-0.2MASF50	3.11	16.16	0.76	6.30	51.32	3.96
	Mixtures VRC/SFVRC	Slump (mm)			HRWRA (kg/m^3)	f'_c (MPa)	STS (MPa)
8	VC-30CR	190			3.18	33.5	2.79
9	VC-30CR-1MISF19	175			3.18	28.6	3.21
10	VC-30CR-1MASF38	145			3.18	28.1	3.42
11	VC-30CR-1MASF50	130			3.18	27.8	3.26
12	VC-30CR-1MASF54	125			3.18	29.6	3.31

Table 5-2 Results of flexure test

Beam #	Designation	Moment Capacity (kN.m)		Deflection (mm)		Ductility	Energy absorption (kN.m)	Failure type	Cracking at the failure stage	
		First Crack	Ultimate	yield	ultimate				Number	Maximum width (mm)
B1	SCC-0CR	10.89	91.28	12.5	35.50	2.84	7.49	flexure	20	3.5
B2	SCC-10CR	8.17	85.78	12.2	37.50	3.07	7.87	flexure	22	3.0
B3	SCC-15CR	7.57	82.15	12.0	38.50	3.20	8.14	flexure	22	2.8
B4	SCC-20CR	6.92	79.00	12.8	36.50	2.85	7.00	flexure	20	2.5
B5	SCC-20CR-0.2MISF19	7.08	80.44	13.0	37.83	2.91	7.27	flexure	22	2.7
B6	SCC-15CR-0.2MASF38	8.34	85.60	12.2	41.50	3.40	9.22	flexure	26	3.2
B7	SCC-10CR-0.2MASF50	8.71	88.44	12.5	39.72	3.18	8.60	flexure	24	3.3
B8	VC-30CR	6.36	68.46	11.5	24.69	2.15	4.80	flexure	18	2.2
B9	VC-30CR-1MISF19	6.75	72.18	11.8	28.61	2.42	5.44	flexure	20	2.6
B10	VC-30CR-1MASF38	8.16	83.10	12.6	35.06	2.78	6.55	flexure	25	3.5
B11	VC-30CR-1MASF50	7.30	74.76	11.8	30.10	2.55	8.85	flexure	21	2.9
B12	VC-30CR-1MASF54	7.68	78.32	12.4	33.04	2.66	7.96	flexure	22	3.1

5.2 Load-deflection curves

Figure 5-1 shows the load-deflection curves for all tested beams. From the figure, it can be seen that for all tested beams the load-deflection curves start with a high slope up to the first cracking load. Beyond the first cracking load, the slope of the curves starts to decrease gradually as the applied load increases. This can be explained by the increased number of developed cracks that resulted from increasing the applied load, which contributed to decreasing the stiffness of the tested beam. By increasing the load application, the longitudinal reinforcement in the tension zone started to yield. After reaching the yield point, the slope of the load-deflection curves significantly decreased, in which high deformation was observed versus a slight increase in the applied load up to the ultimate load. Figure 5-1a shows the load-deflection curves for SCRC beams with varying percentages of CR from 0% to 20%. It can be seen that increasing the percentage of CR generally decreased the flexure stiffness of the tested beam (decrease of the slope of the load-deflection curve). This reduction in the flexure stiffness may be attributed to the low modulus of elasticity of CR particles compared to the replaced fine aggregate, which in turn decreased the overall stiffness of tested beams (Ismail and Hassan, 2017). Table 5-2 shows the ultimate deflections (the deflection corresponding to 90% of the ultimate load in the descending branch of the load-deflection curve) of all tested beams. From the table, it can be observed that increasing the CR percentage from 0% to 15% increased the ultimate deflections by 8.45% (B3 compared to B1). This may be related to the elastic nature of CR particles, which allows for expressing a large elastic deformation

before failure (Ganesan et al., 2013). Increasing the CR percentage from 15% to 20% appeared to decrease the ultimate deflection compared to the beam with 15% CR (B3) but was still slightly higher than the beam without CR (B1). It can also be noted from Figure 5-1a that increasing the CR percentage generally decreased the rate of strength degradation after reaching the ultimate load, indicating more ductile failure.

Figure 5-1b shows the effect of adding MISFs on the structural behavior of SCRC beams. From Figure 5-1b and Table 5-2, it can be seen that adding MISFs to SCRC beams slightly increased the beam stiffness and ultimate deflection. For example, adding MISF19 to the SCRC beam increased the ultimate deflection by 3.6% (B5 compared to B4). On the other hand, using MASFs showed a better enhancement in the beam stiffness and ultimate deflection compared to using MISFs. For example, using MASF38 showed an increase in the beam ultimate deflection up to 7.8% compared to beams without fibers (B6 compared to B3) (see Figure 5-1c). The better results from using MASFs compared to MISFs may be attributed to the better bonding of MASFs with the concrete matrix. The shorter length of MISFs appeared to provide insufficient length to develop adequate bonding between fibers and concrete matrix (pullout failure was noticed). This was confirmed by visual inspection, in which beams reinforced with MISF exhibited a fiber pullout failure, while beams with MASFs showed fiber tensile failure. The results also showed that increasing the MASF length appeared to show less improvement in the beam stiffness and ultimate deflection (see Figure 5-1d and Table 5-2). For instance, using MASF38 and MASF50 increased the ultimate deflection by 7.8% and 5.9%, respectively, compared to beams without fibers (B6 compared to B3 and B7 compared to B2). This may be attributed to the fact that since using MASFs generally provides sufficient length

to achieve adequate bonding stress, using shorter MASFs increases the chance of having a higher number of single fibers at the same fiber volume. Having an increased number of single fibers in the concrete matrix increases the chance of fibers to be oriented across the cracked sections and, in turn, increases the load carrying capacity and beam deformability.

Figure 5-1e shows the load-deflection curve for SFVRC beams. From the figure, it can be seen that although using a high percentage of CR (30%) significantly reduced the load carrying capacity, flexural stiffness, and deformability (B8 compared to B1), adding a high percentage of SFs (1%) compensated for this reduction, achieving higher deformability. Similar to SFSCRC beams, using MISF19 showed the lowest improvement in the bending capacity and deformability of SFVRC beams, while MASF38 showed the highest improvement. The results also showed that increasing the fiber length from MASF50 to MASF54 showed higher flexural stiffness and ultimate deflection compared to beams with MASF50 (but less than MASF38). This may be attributed to the higher rigidity and tensile strength of MASF54 compared to MASF50. The higher tensile strength of MASF54 enhanced the stitching mechanism of fibers and boosted the role of fibers in enhancing load carrying capacity and deformation capacity of tested beams. It is worth noting that using a high percentage of CR (30%) with/without SFs (B8-B12) helped to develop semi-lightweight concrete with a density varied from 2048 kg/m^3 to 2094 kg/m^3 according to CSA (2004).

5.3 Cracking behavior

Table 5-2 and Figure 5-2 show the cracking pattern, number of cracks, and maximum crack width at failure. It can be observed that increasing the CR percentage up to 15% appeared to increase the number of randomly distributed cracks throughout the beam length and showed a reduction in the crack widths. For example, increasing the CR percentage from 0% to 15% increased the number of cracks from 20 to 22 cracks, while the maximum crack width dropped from 3.5mm to 2.8mm. This can be attributed to the reduction in the tensile strength of concrete that resulted from adding CR. This reduction in the tensile strength encouraged the beam to experience a higher number of cracks rather than continuing widening of one crack. Therefore, the number of cracks increased with a reduction in the crack width. Further increase in the CR percentage beyond 15% exhibited a reduction in the number of cracks in addition to the crack widths. This may be attributed to the lower deformation capacity of the tested beams that resulted from using a high percentage of CR.

Table 5-2 and Figure 5-2 also indicated that using SFs in SCRC beams generally increased the number of cracks and maximum crack width compared to counterpart beams without SFs. This may be attributed to the higher deformation capacity that resulted from using SFs, which contributed to the development of a higher number of cracks with larger widths. The results also indicated that using MISFs in SCRC beams slightly increased the number of cracks and maximum crack width, while MASFs showed a significant increase. For example, using MISF19 in SCRC beams increased the number of cracks from 20 to 22 and increased the maximum crack width from 2.5mm to 2.7mm

(B5 compared to B4). On the other hand, the number of cracks increased from 22 to 26, and the maximum crack width increased from 2.8mm to 3.2mm when MASF38 was used (B6 compared to B3).

As mentioned before, using MASFs increased the number of cracks and maximum crack width (compared to SCRC counterpart beams without fiber). However, using longer MASFs (MASF50 compared to MASF38) reduced this increase. This may be attributed to the lower improvement in the deformation capacity that resulted from using MASF50 (compared to MASF38), as discussed before. Using high volume of SFs (1%) in SFVRC beams exhibited a higher increase in the number of cracks and maximum crack width compared to using a lower volume of SFs (0.2%) in SFSCRC beams. For example, using 1% MISF19 and 1% MASF38 in VRC beams increased the number of cracks from 18 to 20 and 25, respectively. In addition, the maximum crack width increased from 2.2 to 2.6 and 3.5 when MISF19 and MASF38 were used (B9 and B10 compared to B8). The higher increase in the maximum crack width and number of cracks that resulted from using MASF38 compared to MISF19 may be attributed to the higher deformation capacity of the concrete beam with MASF38 compared to the beam with MISF19. Using MASF54 in VRC beams showed a higher increase in the number of cracks and maximum crack width compared to MASF50 (but still lower than MASF38). This may be attributed to the higher tensile strength of MASF54 compared to MASF50, which helped the beams to experience higher deformation.

5.4 Displacement ductility

Displacement ductility can be defined as the ratio between the ultimate deflection and the yield deflection. Table 5-2 shows the yield deflection, ultimate deflection, and displacement ductility of all tested beams. From the table, it can be seen that increasing the CR percentage up to 15% resulted in an increase in the displacement ductility of SCRC beams. For example, increasing the CR percentage from 0% to 15% increased the displacement ductility by 12.7% (B3 compared to B1). On the other hand, increasing the CR percentage from 15% to 20% showed a remarkable reduction in the displacement ductility compared to the beam with 15% CR (B4 compared to B3), but still comparable to the beam without CR (B4 compared to B1). This can be attributed to the higher volume of CR, which contributed to limiting the beam from experiencing large deformation beyond the yield point.

The table also shows that using MISFs appeared to have a slight increase in the ductility of SCRC beams. For example, using MISF19 increased the displacement ductility of the SCRC beam with 2.1% compared to the beam without SFs (B5 compared to B4). On the other hand, using MASFs showed an increase in the displacement ductility reaching up to 6.3% and 4.2% when MASF38 and MASF50, respectively, were used. This may be attributed to the larger length of MASFs compared to MISFs. The longer fibers contributed to enhancing the bonding between fibers and concrete matrix, which helped the beams to experience larger deformation and in turn enhanced the displacement ductility.

Using high percentage of CR (30%) significantly decreased the displacement ductility of VRC beams. However, adding high percentage of SFs (1%) to beams with high percentage of CR (30%) compensated for the reduction in the displacement ductility, achieving ductility comparable to the control beam (without CR and fibers). For example, adding 1% MASF38 to the VRC beam with 30% CR increased the beam ductility by 29.3% compared to the beam with 30% CR and no fibers (B10 compared to B8). This increase in the beam ductility reached around 98% of the ductility of the control beam without fiber or CR (B10 compared to B1). Meanwhile, adding 1% MISF19, MASF50, and MASF54 to VRC beams increased the ductility by 12.5%, 18.6%, and 23.7%, respectively, compared to the beam without SFs (B9, B11, and B12 compared to B8). From the results, it can be seen that increasing the fiber length from 38mm in MASF38 to 50mm in MASF50 decreased the improvement in the beam ductility. This can be related to the expected lower number of single fibers oriented perpendicularly to the crack width when longer fibers are used compared to shorter fibers (at similar fiber volume). On the other hand, using MASF54 showed better enhancement in the beam ductility compared to MASF50 (but still less than MASF38). This higher improvement seen with MASF54 compared to MASF50 can be related to the higher tensile strength and rigidity of MASF54 compared to MASF50 (see Table 3-2 and Figure 3-3).

5.5 Energy absorption

The energy absorption capacity of tested beams was calculated by measuring the area under the load-deflection curves up to the failure (a point corresponding to 90% of the

ultimate load at the descending branch of the load-deflection curve). Table 5-2 shows the energy absorption capacity of all tested beams (B1-B12). It should be noted that the ability of beams to absorb energy is a function of their deformation capacity and load carrying capacity. From the results, it can be seen that increasing the CR percentage up to 15% increased the energy absorption by 8.7%. On the other hand, a further increase in the CR percentage showed a significant drop in the energy absorption capacity of tested beams, in which the reduction reached up to 35.9% when 30% CR was used (compared to control beam B1). This may be attributed to the significant reduction in the load carrying capacity and deformation capacity when a high percentage of CR was used.

The results also showed that, in general, incorporating SFs contributed to enhancing the energy absorption capacity of tested beams. This may be attributed to the stitching mechanism of fibers, which helped transfer the stress across the cracked section and in turn, helped the beam to sustain higher load and larger deformation, leading to higher energy absorption. In SFSCRC beams, using MISF19 increased the energy absorption capacity by 3.85% compared to the beam without fibers (B5 compared to B4), while this increase reached up to 13.3% when MASF38 was used. The better enhancement of MASFs compared to MISFs may be related to the same reasons discussed before in the ductility section.

Increasing the volume of SFs resulted in further enhancement of the energy absorption capacity of the tested beams. In SFVRC beams, using 1% MISF19, MASF38, MASF50, and MASF54 increased the energy absorption capacity by 13.3%, 84.4%, 36.5%, and 65.8%, respectively, compared to counterpart beams without fibers (B9, B10, B11, and B12 compared to B8). This enhancement may be attributed to the ability of high-volume

SF beams to sustain higher load carrying capacity and larger deformation, which in turn absorb higher energy. It is worth noting that the greatest improvement in energy absorption was observed when MASF38 was used. Using 1% MASF38 compensated for the reduction in the energy absorption capacity that resulted from adding 30% CR, achieving 1.18 times as much energy absorption as the control beam (without CR and fibers) (B10 compared to B1).

5.6 Theoretical and experimental cracking moment

The first flexural crack was detected with visual inspection and then confirmed by the change of slope in the load-deflection curves. Table 5-2 shows the cracking moment values ($\boldsymbol{M_{cr}^{exp}}$) corresponding to the first crack for all tested beams (B1-B12). The theoretical cracking moment ($\boldsymbol{M_{cr}^{theo}}$) was also calculated based on the ACI (2008), CSA (2004), AS 3600 (2009), and EC2 (2005) (and compared to the experimental one).

As per ACI 318 (2008):

$$\boldsymbol{M_{cr}^{theo}} = f_r \frac{I_g}{y_t} \quad (1)$$

Where $f_r = 0.62\lambda\sqrt{f_c'}$, in which λ =1 for normal weight concrete and 0.85 for lightweight sand; y_t is the distance from the centroid of gross cross-section to the extreme tension fiber; f'_c is the 28-day concrete compressive strength; and I_g is the gross second moment of area.

As per CSA (2004):

$$\boldsymbol{M_{cr}^{theo}} = f_r \frac{I_g}{y_t} \quad (2)$$

Where $f_r = 0.6\lambda\sqrt{f_c'}$, in which λ =1 for normal weight concrete and 0.85 for semi-lightweight concrete (for density ranging from 1850 kg/m^{3}to 2150 kg/m^3); y_t is the distance from the centroid of gross cross-section to the extreme tension fiber; and I_g is the gross second moment of area.

As per AS 3600 (2009):

$$\boldsymbol{M_{cr}^{theo}} = Zf_{cf}' \quad (3)$$

Where f_{cf}' is the characteristic flexural tensile strength of concrete $= 0.6\sqrt{f_c'}$; and Z is the section modulus calculated based on the transformed section referring to extreme tension fiber.

As per EC2 (2005):

$$\boldsymbol{M_{cr}^{theo}} = f_{ctm}\frac{I_e}{(h-x_u)} \quad (4)$$

Where f_{ctm} is the mean value of axial tensile strength of concrete = $0.3f_{ck}^{0.67}$, and f_{ck} is the characteristic compressive strength of concrete at 28 days; I_e is the second moment of area of uncracked transformed section; x_u is the distance from the neutral axis of the concrete cross-section to the extreme top fiber; and h is the height of the beam cross-section.

From Table 5-2, it can be seen that increasing the CR percentage appeared to reduce the experimental first cracking moment. For example, increasing the CR percentage from 0% to 20% decreased the first cracking moment by 36.6%. This may be attributed to the significant reduction in the STS that resulted from increasing the percentage of CR (see Table 5-1). Figure 5-3 shows the theoretical-to-experimental cracking moment ($\boldsymbol{M_{cr}^{theo}}/\boldsymbol{M_{cr}^{exp}}$) for all tested beams. From the figure, it can be observed that all design codes

overestimate the cracking moment for all tested beams. The overestimating of the cracking moment appeared to be more pronounced in beams with CR compared to the control beam. For example, by comparing B4 to B1, it can be seen that the $\boldsymbol{M_{cr}^{theo}/M_{cr}^{exp}}$ ratio ranged from 1.21 to 1.64 in the beam with 20% CR (B4), while the $\boldsymbol{M_{cr}^{theo}/M_{cr}^{exp}}$ ratio ranged from 1.16 to 1.33 in the control beam (B1). This may be attributed to the fact that the $\boldsymbol{M_{cr}^{exp}}$ is more affected by the tensile strength rather than the compressive strength, and the $\boldsymbol{M_{cr}^{theo}}$ in all codes are calculated based on the compressive strength. Also, since the negative effect of CR was more pronounced on the tensile strength, the errors in code predictions were more obvious with the increase in the percentage of CR.

Table 5-2 also shows that adding MISFs to SCRC beams slightly increased the $\boldsymbol{M_{cr}^{exp}}$, while adding MASFs exhibited a considerable increase. For example, adding MISF19 and MASF38 to SCRC beams increased the $\boldsymbol{M_{cr}^{exp}}$ by 2.2% and 10.2%, respectively, compared to their SCRC counterparts without fibers. This may be attributed to the better enhancement of concrete tensile strength when MASF38 was used compared to MISF19, as shown in the STS results in Table 5-1. The results also showed that the increased fiber length in MASF50 compared to MASF38 showed less improvement in the $\boldsymbol{M_{cr}^{exp}}$ (B7 compared to B6). This may be related to the same reasons discussed earlier, in which the better dispersion of MASF38 contributed to enhancing the tensile strength of concrete beams and in turn, showed better improvement in $\boldsymbol{M_{cr}^{exp}}$. The results also showed that increasing the fiber volume significantly increased the $\boldsymbol{M_{cr}^{exp}}$ of SFVRC beams. For example, adding 1% MISF19, 1% MASF38, 1% MASF50, and 1% MASF54 to the VRC beam increased the $\boldsymbol{M_{cr}^{exp}}$ by 6.1%, 28.3%, 14.8%, and 20.7%, respectively, compared to

its VRC counterpart without SFs (B9, B10, B11, and B12 compared to B8). This may be related to the fact that increasing the fiber volume immensely enhanced the tensile strength of concrete beams, and therefore the $\boldsymbol{M_{cr}^{exp}}$ is expected to greatly improve. Increasing the fiber length from MASF50 to MASF54 exhibited higher improvement in the $\boldsymbol{M_{cr}^{exp}}$ (but still less than MASF38). This may be attributed to the higher tensile strength of MASF54 compared to MASF50, which helped to enhance concrete tensile strength and in turn improved the cracking moment. From Figure 5-3, it can be observed that $\boldsymbol{M_{cr}^{theo}/M_{cr}^{exp}}$ ratio appeared to be higher in beams with MISFs compared to beams with MASFs. For example, in the SFSCRC beam with MISF19, $\boldsymbol{M_{cr}^{theo}/M_{cr}^{exp}}$ ranged from 1.19 to 1.61, while in the SFSCRC beam with MASF38 this range was 1.11 to 1.45. This may be attributed to the lower enhancement of $\boldsymbol{M_{cr}^{exp}}$ when MISFs were used compared to MASFs. Meanwhile, the $\boldsymbol{M_{cr}^{theo}}$ was almost the same for MISFs and MASFs as it depends only on the compressive strength, which is not affected by the type of SFs. Figure 5-3 also showed that increasing the fiber volume in SFVRC beams contributed to a further decrease in the $\boldsymbol{M_{cr}^{theo}/M_{cr}^{exp}}$ ratio, in which the $\boldsymbol{M_{cr}^{theo}/M_{cr}^{exp}}$ ranged from 1.05 to 1.35 when 1% SFs was used. This may be explained by the further increase in the $\boldsymbol{M_{cr}^{exp}}$ that resulted from using high percentage of SFs. This is also in addition to the reduction in the $\boldsymbol{M_{cr}^{theo}}$ due to the reduction in the compressive strength that resulted from adding a high percentage of SFs (see Table 5-1).

5.7 Bending moment capacity

Table 5-2 shows the bending moment capacity of all tested beams (B1-B12). From the table, it can be seen that increasing the CR content generally decreased the bending moment capacity. For example, increasing the percentage of CR from 0% to 20% decreased the bending moment capacity by 13.5% compared to the control beam (B4 compared to B1). This may be attributed to the lower compressive strength and weakened rubber-mortar interface that resulted from adding CR and, in turn, decreasing the bending moment capacity of the beams. Further increase in the CR percentage led to a significant drop in the bending moment capacity of the tested beams. For example, adding 30% CR decreased the bending moment capacity by 25% compared to the control beam (B8 compared to B1). This may be related to the increased volume of weakened rubber-mortar interface that resulted from using high percentage of CR, which in turn limited the beams' ability to sustain higher loads.

From the table, it can also be noticed that adding SFs to SCRC beams generally increased the bending moment capacity. For example, adding MISF19 and MASF38 to SCRC beams increased the bending moment capacity by 1.8% and 4.2%, respectively, compared to their counterpart SCRC beams without fibers (B5 compared to B4 and B6 compared to B3). The better improvement seen with MASF38 compared to MISF19 can be related to the larger length of MASF38, which provided adequate bonding to the concrete matrix and in turn, prompted the beam to sustain higher loads. It should also be noted that increasing the MASF length from 38mm to 50mm exhibited less improvement in the bending moment capacity.

Despite the fact that using high percentage of CR (30%) significantly decreased the bending moment capacity, combining high percentage of MASF38 (1%) with high percentage of CR (30%) appeared to compensate for the reduction in the bending moment capacity, reaching to around 91% of the bending capacity of the control beam. In addition, combining high percentage of CR with high percentage of SFs helped to develop semi-lightweight concrete beams with a density of 2094 kg/m^3 according to CSA (2004). Adding 1% MISF19, 1% MASF38, 1% MASF50, and 1% MASF54 to VRC beams increased the bending moment capacity by 5.4%, 21.3%, 9.2%, and 14.4%, respectively, compared to beams without SFs (B9, B10, B11, and B12 compared to B8).

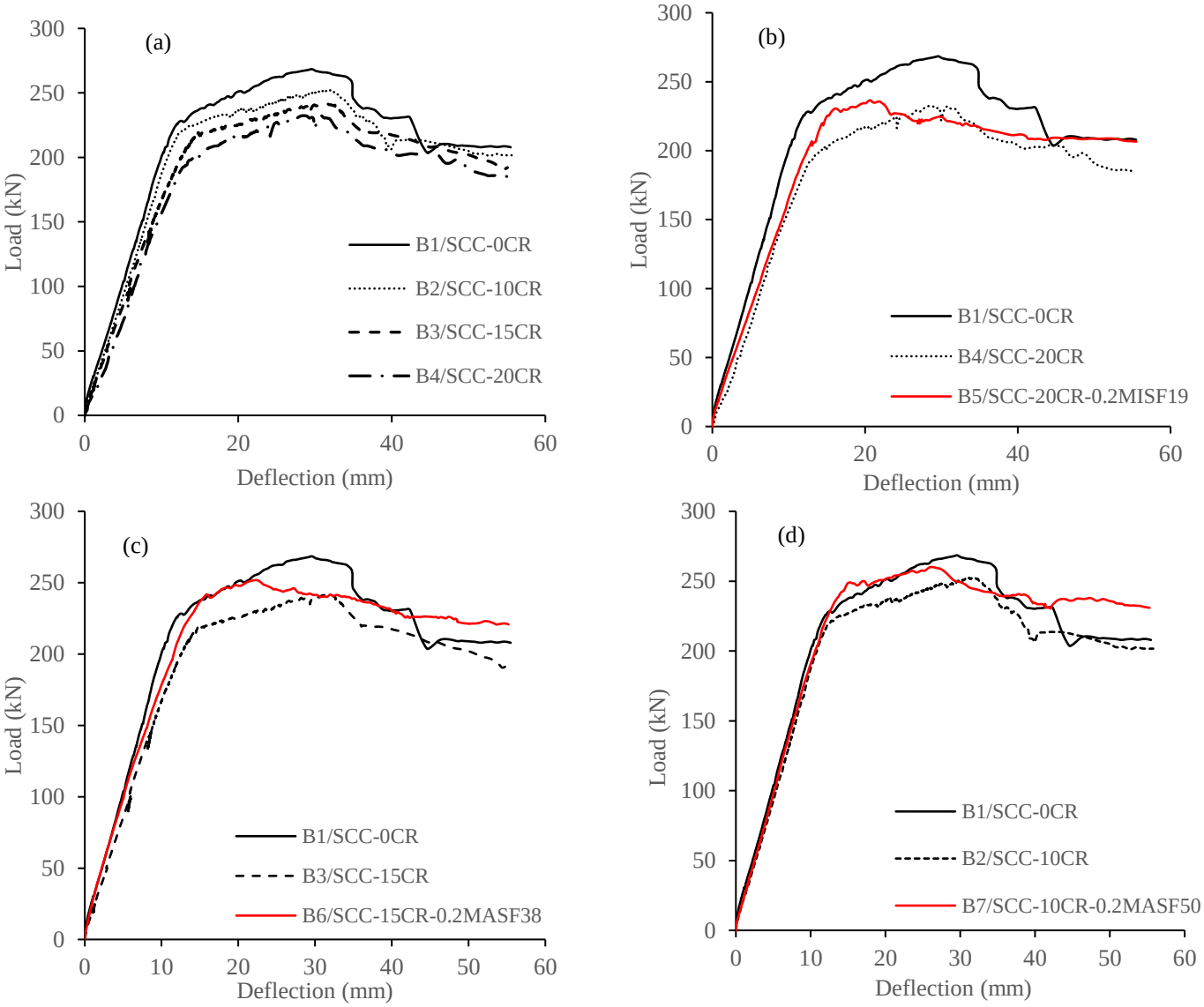
(a)
Load (kN)
Deflection (mm)
B1/SCC-0CR
B2/SCC-10CR
B3/SCC-15CR
B4/SCC-20CR
(b)
Load (kN)
Deflection (mm)
B1/SCC-0CR
B4/SCC-20CR
B5/SCC-20CR-0.2MISF19
(c)
Load (kN)
Deflection (mm)
B1/SCC-0CR
B3/SCC-15CR
B6/SCC-15CR-0.2MASF38
(d)
Load (kN)
Deflection (mm)
B1/SCC-0CR
B2/SCC-10CR
B7/SCC-10CR-0.2MASF50

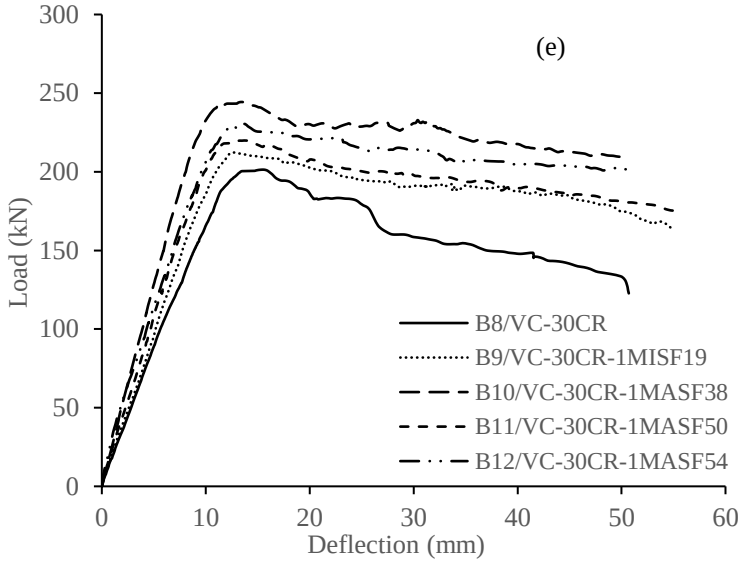

Figure 5-1 Experimental load-midspan deflection responses: (a) SCRC beams with varied percentage of CR; (b) SFSCRC beam with MISF19 versus SCRC counterpart and control beam; (c) SFSCRC beam with MASF38 versus SCRC counterpart and control beam; (d) SFSCRC beam with MASF50 versus SCRC counterpart and control beam; (e) SFVRC beams with different SF types/lengths versus VRC counterpart

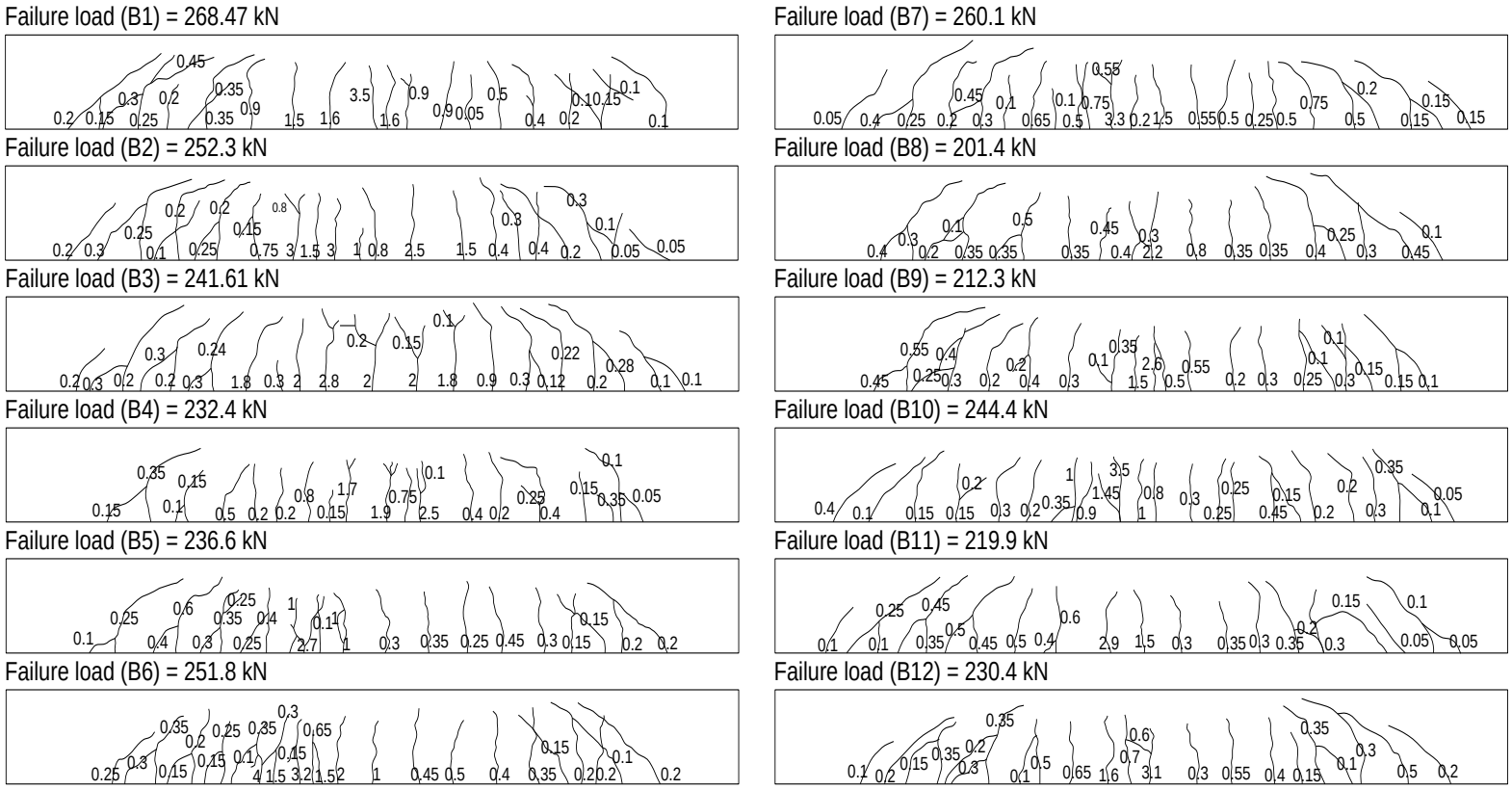

Figure 5-2 Crack patterns of tested beams at failure (crack width in mm)

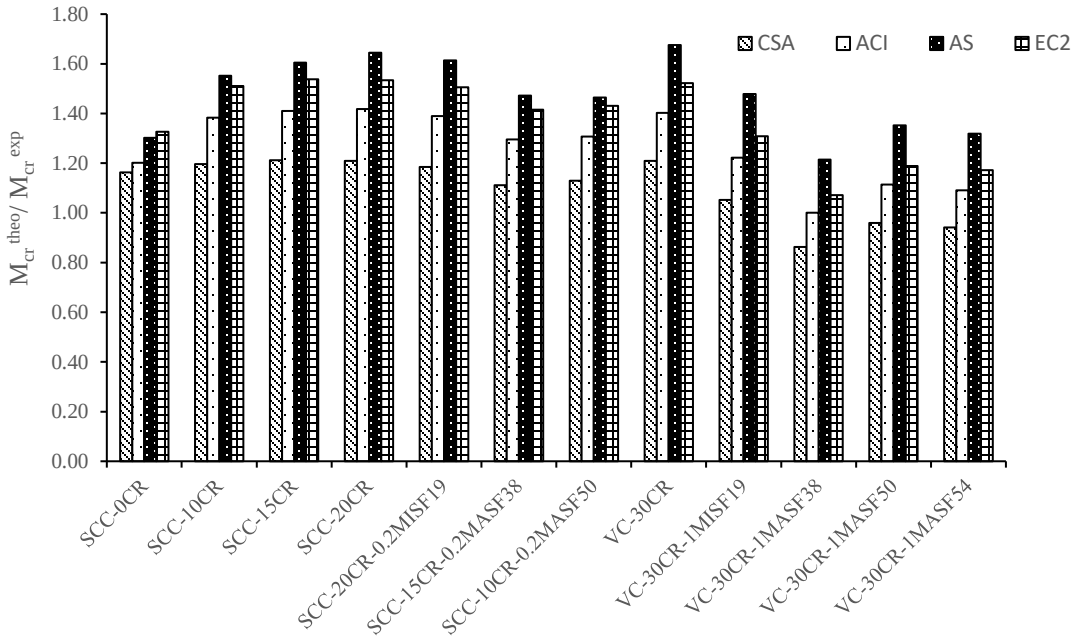

Figure 5-3 The theoretical-to-experimental first cracking moment ratios for all tested beams

6 Discussion of results from experimental study 3: effect of SFs on shear capacity of reinforced rubberized concrete beams

6.1 Introduction

This chapter presents the combined effect of CR and MISFs/MASFs on the shear behavior of reinforced concrete beams. Twelve large-scale SCC and VC beams were constructed with varied percentages of CR (0% to 30%) and different types and volumes (0%, 0.2%, and 1%) of SFs. The shear performance of the tested beams was evaluated based on stiffness, ultimate shear capacity, post-diagonal resistance, energy absorption, and cracking behavior. Table 6-1 summarizes the fresh properties, compressive strength, and STS of all tested beams' mixtures. Table 6-2 shows the results obtained from conducted shear tests. The results and discussions presented in this chapter have been published in the paper number four mentioned earlier at the beginning of this thesis.

Table 6-1 Fresh and mechanical properties for tested mixtures

Mix #	Mixtures SCC/SCRC/FRSCRC	T_{50} (sec)	V-funnel (sec)	L-box ratio (H_2/H_1)	HRWRA (kg/m^3)	f'_c (MPa)	f_{sp} (MPa)
1	SCC-0CR	1.95	7.01	0.91	3.43	64.8	4.30
2	SCC-10CR	2.74	9.50	0.84	3.75	53.5	3.78
3	SCC-15CR	2.96	10.59	0.82	3.75	46.8	3.60
4	SCC-20CR	3.14	10.97	0.77	3.75	38.4	3.26
5	SCC-20CR-0.2MISF19	3.29	12.12	0.76	6.40	39.5	3.47
6	SCC-15CR-0.2MASF38	3.20	15.30	0.77	6.30	48.3	4.01
7	SCC-10CR-0.2MASF50	3.18	16.20	0.76	6.30	53.2	4.11
	Mixtures VRC/FRVRC	Slump (mm)			HRWRA (kg/m^3)	f'_c (MPa)	f_{sp} (MPa)
8	VC-30CR	190			3.18	33.5	2.73
9	VC-30CR-1MISF19	175			3.18	28.7	3.18
10	VC-30CR-1MASF38	150			3.18	28.3	3.38
11	VC-30CR-1MASF50	130			3.18	27.9	3.08
12	VC-30CR-1MASF54	125			3.18	29.7	3.11

Table 6-2 Results of the shear test

Beam #	**Designation**	Cracking moment (kN.m)	First diagonal crack load (kN)	Failure load (kN)	Deflection at failure load (mm)	Ultimate shear load (V_u) (kN)	Post-diagonal cracking %	Energy absorption (kN.mm)	At failure		
									No. of cracks	Max crack width (mm)	Failure angle (deg.)
SCC/SCRC/FRSCRC											
B1	SCC-0CR	11.1	129.2	244.3	3.83	122.1	47.1	626.2	8	6.8	29
B2	SCC-10CR	9.6	116.7	208.4	4.27	104.2	44.0	588.8	8	6.0	29
B3	SCC-15CR	8.6	110.5	194.8	4.52	97.4	43.3	577.9	9	5.5	28
B4	SCC-20CR	7.3	105.5	180.0	4.80	90.0	41.4	556.8	11	4.0	26
B5	SCC-20CR-0.2MISF19	7.5	108.1	190.5	5.04	95.2	43.2	665.9	11	3.5	28
B6	SCC-15CR-0.2MASF38	9.1	118.5	222.5	5.20	111.2	46.7	748.6	10	4.0	26
B7	SCC-10CR-0.2MASF50	10.0	121.6	227.1	4.57	113.6	46.5	719.9	12	4.5	27
VRC/FRVRC											
B8	VC-30CR	6.2	95.0	157.6	4.98	78.8	39.7	505.2	10	4.0	29
B9	VC-30CR-1MISF19	6.7	99.5	180.6	5.72	90.3	44.9	732.9	10	3.8	28
B10	VC-30CR-1MASF38	7.2	118.3	269.3	6.32	134.7	56.1	1139.6	11	3.0	28
B11	VC-30CR-1MASF50	7.0	102.1	209.4	5.83	104.7	51.3	862.3	11	3.5	30
B12	VC-30CR-1MASF54	7.3	110.0	244.0	5.94	122.0	54.9	992.9	12	3.3	30

6.2 Cracking behavior and failure mode

In the early stage of loading, it was observed that the first vertical flexural cracks began at the tension side of the beam at maximum moment zone (between the loading points). As the applied load increased, the existing flexural cracks increased in width and new more vertical cracks appeared within the shear span at both sides of the beam (area between supports and loading points). The cracks in shear span started to propagate diagonally towards the loading zone as the load increased. Additional loading led to more increases in the number and width of both flexural and flexural-shear cracks (diagonal cracks). Then, a shear failure suddenly occurred due to the formation of a major single diagonal crack with angles ranging from 26 to 30 degrees for all tested beams. Figure 6-1 and Table 6-2 show the crack pattern and crack widths/numbers of tested beams at failure stage.

As can be seen in Figure 6-1 and Table 6-2, the SCRC beams appeared to have relatively lower maximum diagonal crack width and higher number of cracks compared to that of the control beam (B1). Increasing the percentage of CR from 0% to 20% (B1 to B4) decreased the maximum crack width from 6.8mm to 4mm, while the number of cracks increased from 8 to 11. This behavior may be attributed to the high strain rate of the CR particles compared to the hardened cement paste, which generates a high tensile stress at the rubber-mortar interface under loading. This allows more fine and significant cracks to propagate instead of continuous widening of one localized crack.

Figure 6-1 also shows that FRSCRC and FRVRC beams generally exhibited similar failure mode as their counterpart beams with no fibers. However, the inclusion of MISFs and/or MASFs helped the beams to sustain higher load accompanying larger deformations, which in turn allowed more flexural cracks to develop prior to the shear failure. The addition of fibers also showed a good ability to stitch the cracks, which contributed to reducing the widths of the cracks. The stitching action of fibers was found to be affected by the length and number of fibers. By examining both FRSCRC and FRVRC beams, it can be observed that the shortest fiber type (MISF19) had the lowest ability to limit the width of cracks, which may be due to its low pull-out strength. Increasing the length of fibers from 19mm to 38mm (MASF38 compared to MISF19) improved the fibers' role in restricting the crack width. Further increase in the length of fibers (higher than 38mm) reduced the effectiveness of fibers (as shown in MASF50 and MASF54). This can be attributed to the fact that for a given fraction volume, increasing the length of fibers higher than that required to achieve adequate pull-out strength decreases the number of single fibers distributed in concrete. This may result in a lower probability of single fibers being oriented perpendicularly to the diagonal cracks, and thus limits the stitching action along cracks.

6.3 Load-deflection behavior

Figure 6-2 shows the effect of CR with/without SFs on the load-midspan deflection of tested beams. From the figure, it can be seen that all tested beams exhibited high stiffness up to the initiation of the first flexural crack. Increasing the applied load beyond the cracking stage led to the initiation and propagation of more cracks, which reduced the

beams' stiffness. With further loading, the beams experienced a higher rate of deformation up to the maximum load, and then the load-carrying capacity declined clearly.

From Figure 6-2a, it can be observed that replacing the fine aggregate with rubber particles appeared to boost the deformability of beams. This can be indicated by decreasing the beams' stiffness (slope of load-midspan deflection curve) and increasing the maximum deflection (δ_u) corresponding to the ultimate failure load as the percentage of CR increased. As shown in SCRC beams (B4 compared to B1), varying the percentage of CR from 0% to 20% increased the δ_u by 25.3%. On the other hand, the addition of CR was found to reduce the ultimate shear load (V_u) of beams, in which the SCRC beam with 20% CR exhibited a reduction in the V_u reached up to 26.3% lower than the control beam (B1). This trend of results was confirmed in the VRC beam (B8), in which the inclusion of 30% CR increased the δ_u by 30% and decreased the V_u by 35.5% compared to the control beam (B1). As reported by Taylor (1974), the shear capacity of beams without stirrups is derived from the contribution of compression shear zone, aggregate interlock mechanism, and dowel action of the longitudinal reinforcement. Hence, the reduction in the ultimate shear load of the tested beams that resulted from adding CR can be attributed to (a) decaying the compressive strength of concrete with CR (as shown in Table 6-1), which limited the contribution of compression shear zone to the shear capacity of beams, and (b) the softness of CR aggregate (compared to conventional aggregate) may decrease the friction forces that are mainly developed across the diagonal shear cracks by aggregate interlock mechanism, resulting in lower resistance against slip (Hassan et al., 2008).

Figure 6-2b to Figure 6-2e show that adding MISFs and MASFs to FRSCRC and FRVRC beams exhibited increases in their V_u and δ_u, which indicates strong potential for SFs to improve the ductility and energy absorption capacity of tested beams. Since the compressive strength of FRSCRC mixtures was not affected by the addition of the fibers (as shown in Table 6-1), the observed increases in the V_u and δ_u in FRSCRC beams could be directly related to the fibers' bridging mechanism, which contributes to transferring stress across the cracks and thus allows the beams to sustain higher load and exhibit larger deformations. The lowest improvements were found in beams with 19mm fibers (MISF19), in which the V_u and δ_u increased by 5.8% and 5%, respectively, as shown in B5 compared to B4. Such limited increases indicated that using short fibers (MISF19) may not have enough length to develop adequate bonding with concrete (pull-out failure mode is dominant), which in turn reduced the ability of fibers to effectively transfer the stress across cracks. This was confirmed by visual inspection of the failed beams, in which 19mm fibers (MISF19) appeared to fail under pull-out failure while longer fibers (38mm (MASF38) and 50mm (MASF50)) appeared to fail under tensile failure. Therefore, using longer fibers (38mm MASF38) exhibited higher increases in the stiffness, shear strength, and ultimate deformation capacity of beams. The addition of MASF38 (38mm fibers as in B6) boosted the V_u and δ_u by 14.2% and 15%, respectively, compared to its counterpart beam without fibers (B2). However, further increase in the fibers' length led to less improvements, in which the beam with MASF50 (50mm fibers as in B7) showed improvements up to 9% and 7%, respectively, in the V_u and δ_u compared to its counterpart beam without fibers (B2). This could be attributed to the fact that at a given fraction volume, as the length of fibers decreased the total number of

single fibers increased. Therefore, in the case of achieving a length long enough to assure an adequate pull-out strength (pull-out failure is not dominant), using shorter fibers (MASF38) provides a higher number of individual fibers (compared to MASF50), which can attain an efficient distribution in concrete and increase the fibers' contribution to the shear strength of concrete beams.

In FRVRC, although the high volume of SFs negatively affected the compressive strength of concrete, the addition of fibers continued to improve the ultimate shear load and deformation capacity of tested beams. Similar to the FRSCRC beams, in FRVRC beams the lowest and highest improvements in both V_u and δ_u were found in beams with 1% MISF19 and 1% MASF38, respectively (Figure 6-2e). Increasing the size (length and diameter) of fibers from MASF50 to MASF54 showed higher increases in both the V_u and δ_u compared to MASF50 (but less than MASF38). This may be attributed to the higher tensile strength and rigidity of MASF54 (as shown in Table 3-2) that requires more stress to cause rupture failure than that required for MASF50. The deformed surface of MASF54 (Figure 3-3 and Table 3-2) may also contribute to improving the interfacial bond properties between fiber and cementitious matrix (Singha et al., 2004, Banthia, 1990).

It is worth noting that combining 30% CR and MASF54 (B12) exhibited comparable V_u to that of the control beam (B1), while the beam with 30% CR and MASF38 (B10) had an increase in the V_u reached up to 10% higher than the control beam (B1). It should be also reported that using 30% CR with/without 1% MISFs and MASFs (B8 to B12) contributed to developing beams with a density varied from 2048 kg/m^3 to 2094 kg/m^3, which are classified as a semi-lightweight concrete according to the CSA (2004).

6.4 Post-diagonal cracking resistance

The post-diagonal cracking resistance indicates the maximum resistance the beam can exhibit beyond the occurrence of the first diagonal crack up to failure. Table 6-2 presents the calculated values of the post-diagonal cracking resistance for each tested beam, which were obtained using a formula of [(Max failure load – first diagonal crack load)/ Max failure load] (Abouhussien et al., 2015; Hassan et al., 2015).

As shown in Table 6-2, increasing the percentage of CR showed a negative impact on the post-diagonal cracking resistance, similar to its effect on the ultimate shear load of tested beams. Varying the percentage of CR from 0% to 20% in SCRC beams (B1 to B4) decreased the post-diagonal cracking resistance by 12.1%. Increasing the percentage of CR to 30% in the VRC beam (B8) led to a reduction in the post-diagonal cracking resistance reaching up to 15.7% compared to the control beam (B1). This can be attributed to the fact that the inclusion of CR increases the weak rubber-mortar interface, which allows cracks to develop at a relatively low level of stress. In addition, the softness of CR decreases the contribution of aggregate interlock (as explained earlier), which expedites the propagation of diagonal cracks and hence reduces the resistance of beams to failure beyond the first diagonal crack.

Table 6-2 also presents the post-diagonal cracking resistance of both FRSCRC and FRVRC beams. The results showed that the addition of fibers generally improved the post-diagonal cracking resistance of tested beams. In FRSCRC beams, the minimum improvement in the post-diagonal cracking reached up to 4.3% when using 0.2% of 19mm fibers (MISF19) (B5 compared to B4) and the maximum improvement reached up

to 7.9% (B6 compared to B3) when using 38mm fibers (MASF38). These results are related to the same reasons explained earlier for the ultimate shear load. Similarly, in FRVRC beams, using 1% of MISF19, MASF38, MASF50, and MASF54 (B9 to B12) increased the post-diagonal cracking resistance by 13.1%, 41.3%, 29.2%, and 38.3%, respectively, compared to beam with no fibers (B8). Also, these beams (B9 to B12) showed post-diagonal cracking resistance values ranged from 0.95 to 1.19 of that obtained by the control beam (B1).

6.5 Energy absorption

In this study, the energy absorption capacity of the tested beams was evaluated by measuring the area under the load-deflection curves (using AutoCAD software) up to the failure/maximum load (shown in Figure 6-2). Hence, the ability of beams is a function of both the deformation capacity and strength of beams. As mentioned earlier, the addition of CR was found to increase the ultimate deformation capacity of beams. However, its effect on decaying the shear strength was more pronounced, which reduced the area enclosed by the load-deflection curve, indicating a reduction in the energy absorption capacity of tested beams. In SCRC beams, varying the percentage of CR from 0% to 20% (B1 to B4) reduced the ability of beams to absorb energy by 11.1%. With a replacement of 30% CR, this reduction reached up to 19.3% compared to B1 (SCC with no CR).

The addition of SFs seemed to increase the energy absorption capacity of the tested beams, as shown in Table 6-2. This can be attributed to the beneficial role of fibers in restricting the widening and propagation of cracks, as explained earlier, which allows the beams to experience higher loads and deformations, and therefore absorb more energy

before failure. In FRSCRC beams, using MISF19, MASF38, and MASF50 (B5 to B7) showed an increase in the energy absorption capacity of tested beams by 19.6%, 29.5%, and 22.3%, respectively, compared to their counterpart beams with no fibers (B2 to B4). Increasing the amount of fibers led to further improvements in the ability of beams to absorb more energy prior to failure. In FRVRC beams (B9 to B12), adding 1% from MISF19, MASF38, MASF50, and MASF54 boosted the energy capacity of tested beams by 45.1%, 125.6%, 70.7%, and 96.6%, respectively, compared to beams with no fibers (B8). It is worth noting that in FRSCRC, beams with 0.2% MISF19 + 20% CR, 0.2% MASF38 + 15% CR, and 0.2% MASF50 + 10% CR absorbed 6.3%, 19.6%, and 15%, respectively, more energy compared to the control beam (B1). In FRVRC beams, combining 30% CR and 1% from MISF19, MASF38, MASF50, or MASF54 exhibited energy absorption of 17%, 82%, 37.7%, and 58.6%, respectively, higher than that of the control beam (B1).

6.6 Cracking moment

Table 6-2 shows the experimental cracking moment (M_{cr}) values corresponding to the first flexural crack. The inclusion of CR generally had a negative impact on the M_{cr} of the tested beams. Varying the percentage of CR from 0% to 20% in SCRC beams (B1 to B4) exhibited a reduction in the M_{cr} reached up to 27.7%. Increasing the percentage of CR to 30% in VRC (B8) decreased the M_{cr} by 43.8% compared to the control beam (B1). This finding could be attributed to the fact that as the percentage of CR increased, the tensile strength of concrete decreased (as shown in the f_{sp} results presented in Table 6-1), which

in turn decreased the load required to develop the first flexural crack within the zone of maximum bending moment.

Table 6-2 also shows that in FRSCRC beams, the M_{cr} slightly increased when 0.2% MISFs and/or MASFs were added. Using 0.2% of MISF19, MASF38, and MASF50 (B5 to B7) increased the M_{cr} by 3.3%, 5.3%, and 4.3%, respectively, compared to their counterpart SCRC beams without fibers (B2 to B4). Increasing the volume of MISF19, MASF38, MASF50, and MASF54 to 1% in FRVRC beams (B9 to B12) raised the M_{cr} up to 8%, 15%, 12.2%, and 16.4%, respectively, higher than the M_{cr} of beams with no fibers (B8). This is due to the fibers' mechanism in controlling the development of micro-cracks and delaying the formation of macro-cracks.

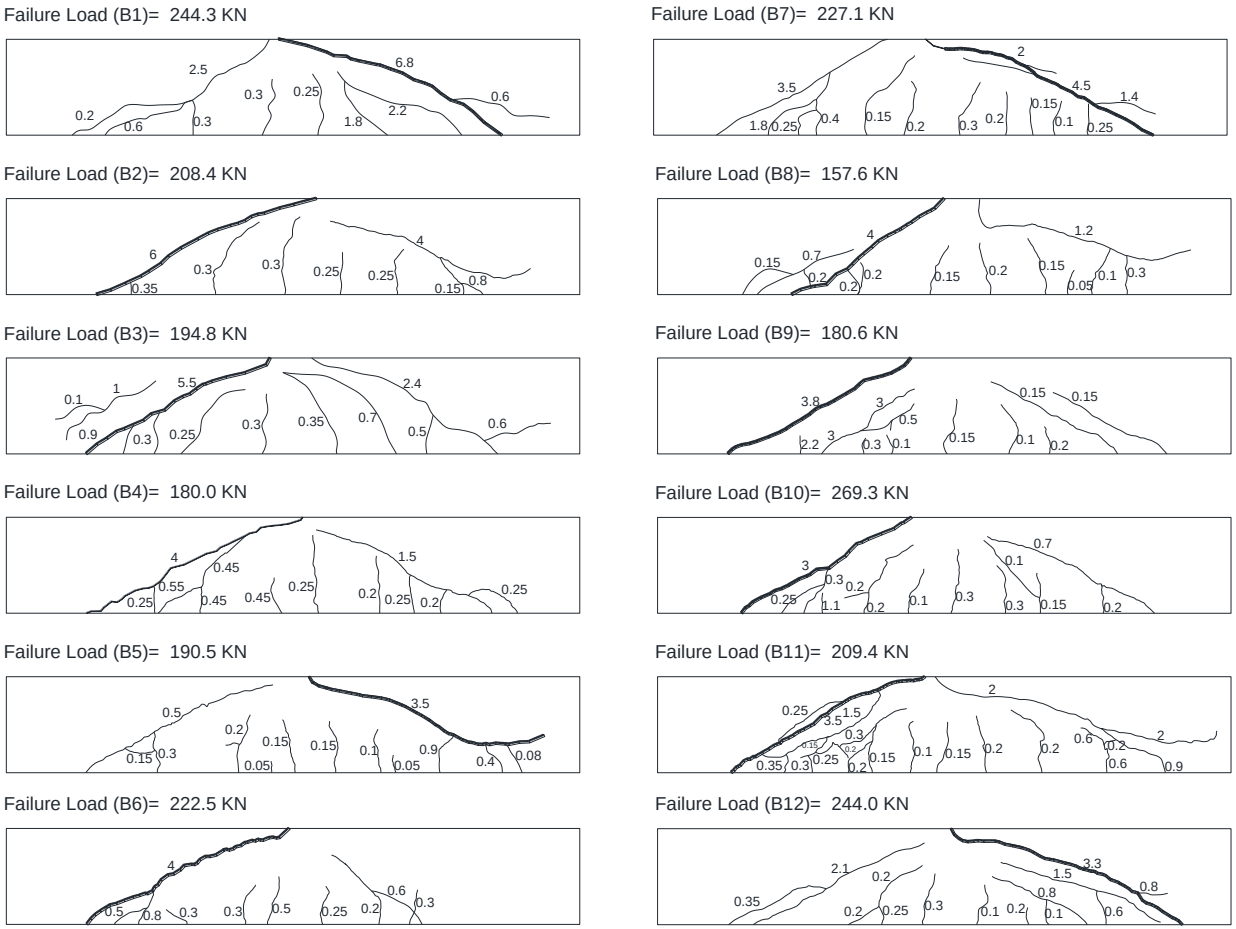

Figure 6-1 Crack patterns of tested beams at failure (crack width in mm)

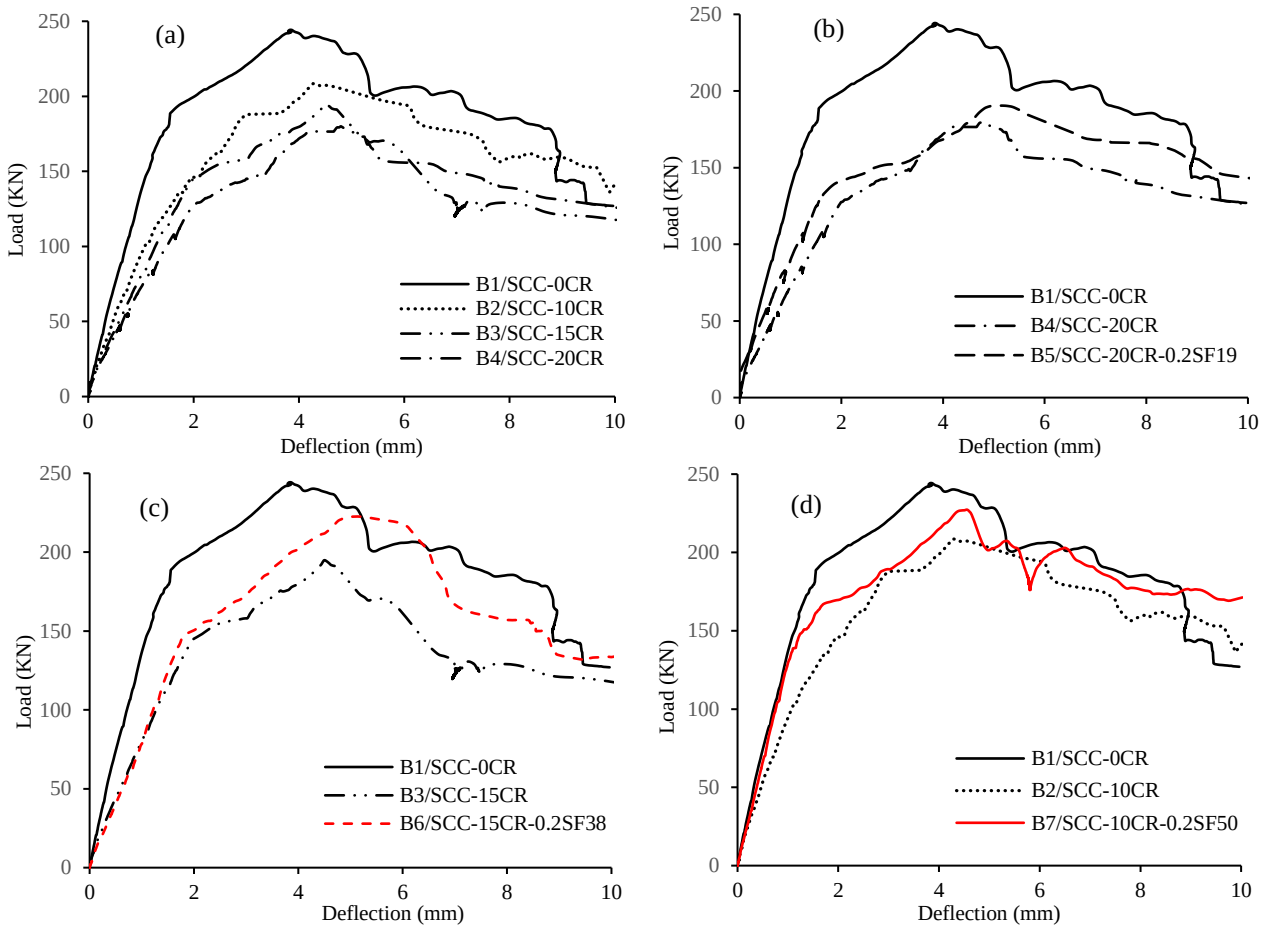
(a)
Load (KN)
Deflection (mm)
B1/SCC-0CR
B2/SCC-10CR
B3/SCC-15CR
B4/SCC-20CR
(b)
Load (KN)
Deflection (mm)
B1/SCC-0CR
B4/SCC-20CR
B5/SCC-20CR-0.2SF19
(c)
Load (KN)
Deflection (mm)
B1/SCC-0CR
B3/SCC-15CR
B6/SCC-15CR-0.2SF38
(d)
Load (KN)
Deflection (mm)
B1/SCC-0CR
B2/SCC-10CR
B7/SCC-10CR-0.2SF50

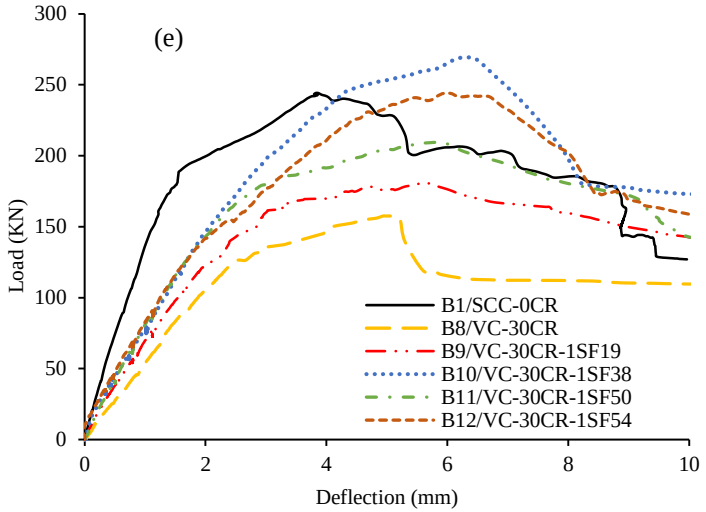

Figure 6-2 Experimental load-midspan deflection responses

7 Discussion of results from experimental study 4: cyclic loading of large-scale rubberized concrete beam-column joints with/without SFs and MFs

7.1 Introduction

This chapter highlights the effect of adding CR on enhancing the structural performance of beam-column joints under cyclic loading. The chapter also presents the effect of combining SFs/MFs with CR on improving the cyclic behavior of beam-column joints. Different types, lengths, and volumes of SFs and MFs were used in this investigation. The main parameters were the percentage of CR (0%-25% by volume of sand), coarse aggregate size (10mm, and 20mm), length of MFs (35mm and 60mm), volume of MFs (0%, 0.35%, 1%), type of SFs (MISFs and MASFs), length of SFs (19mm, 38mm, 50mm, 54mm), and volume of SFs (0%, 0.2%, and 1%). The structural behavior of the tested beam-column joints was evaluated based on load deflection, initial stiffness, rate of stiffness degradation, failure mode, cracking behavior, displacement ductility, brittleness index, energy dissipation, first crack load, and load carrying capacity. A summary of the fresh and mechanical properties of tested joints are presented in Table 7-1. The results obtained from the tested joints are shown in Table 7-2 to Table 7-6. The results and discussions presented in this chapter have been published in the papers number five, six, and seven mentioned earlier at the beginning of this thesis.

Table 7-1 Fresh and mechanical properties of tested joints

Joint #	Mixture ID	T_{50} (sec)	L-box H2/H1	Slump-J-ring diameter	V-funnel	SR %	Air %	28-day f'_c	28-day STS
Stage 1									
S1	0CR-SCC	1.95	0.91	10	7.0	2.1	1.5	75.6	4.5
S2	5CR-SCC	2.39	0.88	15	8.5	2.7	2.0	66.7	4.1
S3	10CR-SCC	2.74	0.84	30	9.5	3.8	2.7	53.4	3.8
S4	15CR-SCC	2.96	0.82	40	10.6	5.8	3.1	44.8	3.6
S5	20CR-SCC	3.14	0.77	45	10.9	7.5	3.4	38.4	3.3
S6	25CR-SCC	3.35	0.77	50	14.3	8.3	4.6	36.8	3.0
Stage 2									
S7	SCC-10CR-20	1.58	0.8	40	6.6	5.4	3.9	47.2	3.5
S8	SCC-15CR-20	1.66	0.78	45	6.9	6.6	4.3	41	3.1
S9	SCC-20CR-20	1.76	0.77	45	7.1	7.6	4.9	35.1	2.9
S10	SCC-25CR-20	1.89	0.75	50	7.4	8.9	5.1	32.9	2.7
S11	SCC-15CR-0.35MF35	3.31	0.75	80	12.05	6.04	3.5	44.94	4.3
S12	VRC-15CR-0.35MF35	-	-	-	-	-	2.5	47.2	4.7
S13	VRC-15CR-0.35MF60	-	-	-	-	-	3.2	48.9	4.8
S14	VRC-25CR-1MF35	-	-	-	-	-	3.7	36.9	5
Stage 3									
S15	SCC-15CR-0.2MISF19	3.04	0.79	45	11.4	4.4	3.3	44.8	3.9
S16	SCC-15CR-0.2MISF27	3.09	0.79	50	12.67	3.9	3.4	44.9	4.0
S17	SCC-15CR-0.2MASF38	3.2	0.77	65	15.3	7.3	3.8	44.9	4.2
S18	VRC-15CR-0.2MASF38	-	-	-	-	-	3.5	47.1	4.5
S19	VRC-15CR-0.2MASF50	-	-	-	-	-	2.5	42.1	4.1
S20	VRC-15CR-0.2MASF54	-	-	-	-	-	3.2	43.2	4.3

S21	VRC-25CR-1MASF38	-	-	-	-	-	3.7	33.7	4.1

Table 7-2 . Results of reverse cyclic loading

Joint #	Mixture ID	First crack load (KN)	Ultimate load (KN)	Failure mode	Initial stiffness (KN/mm)	Crack width	
						At beam-column interface (mm)	Within joint panel (mm)
Stage 1							
S1	0CR-SCC	30.9	102.4	B-mode	13.9	7	-
S2	5CR-SCC	27.7	97.2	B-mode	12.8	6	-
S3	10CR-SCC	24.4	93.7	B-mode	12	5.5	-
S4	15CR-SCC	22.2	91.6	B-mode	11.2	5	-
S5	20CR-SCC	19.9	86.3	BJ-mode	9.5	4	0.95
S6	25CR-SCC	18.8	82.7	BJ-mode	8.7	3.2	0.8
Stage 2							
S7	SCC-10CR-20	23.29	91.7	B-mode	11.43	6.2	-
S8	SCC-15CR-20	21.4	89.4	B-mode	10.41	5.7	-
S9	SCC-20CR-20	20.98	87.3	B-mode	9.14	5.1	-
S10	SCC-25CR-20	19.2	83.2	BJ-mode	8.26	4.5	0.7
S11	SCC-15CR-0.35MF35	31.56	105.9	B-mode	12.45	4	-
S12	VRC-15CR-0.35MF35	32.83	110.6	B-mode	13	3.8	-
S13	VRC-15CR-0.35MF60	30.95	101.9	B-mode	12.15	3.5	-
S14	VRC-25CR-1MF35	31.06	103.2	B-mode	16.98	3	-
Stage 3							
S15	SCC-15CR-0.2MISF19	23.3	92.7	B-mode	11.5	4.7	-
S16	SCC-15CR-0.2MISF27	25.2	94.4	B-mode	11.7	4.5	-

S17	SCC-15CR-0.2MASF38	30.6	101.2	B-mode	12.2	4.2	-
S18	VRC-15CR-0.2MASF38	31.9	102.1	B-mode	12.9	4	-
S19	VRC-15CR-0.2MASF50	26.2	94.6	B-mode	11.8	4.5	-
S20	VRC-15CR-0.2MASF54	27.3	98.3	B-mode	12.1	4.3	-
S21	VRC-25CR-1MASF38	29.9	100.2	B-mode	16.1	4	-

Table 7-3 Yield deflection, ultimate deflection, ductility, and brittleness index

Joint #	Mixture ID	Deflection at yield Δy (mm)	Deflection at ultimate load (mm)	Ultimate deflection Δu (mm)	Ductility (Δu / Δy)	Brittleness index
Stage 1						
S1	0CR-SCC	6.48	22.33	29	4.48	0.29
S2	5CR-SCC	6.69	23.56	32.75	4.89	0.26
S3	10CR-SCC	6.84	24.23	35	5.12	0.24
S4	15CR-SCC	7.29	25.12	38.75	5.32	0.23
S5	20CR-SCC	8.27	22.53	38	4.59	0.28
S6	25CR-SCC	8.55	21.75	36.5	4.27	0.3
Stage 2						
S7	SCC-10CR-20	6.75	23.13	32	4.65	0.27
S8	SCC-15CR-20	7.7	23.85	37.5	4.83	0.25
S9	SCC-20CR-20	8.05	24.76	40	4.97	0.24
S10	SCC-25CR-20	8.3	22.23	37.5	4.52	0.28
S11	SCC-15CR-0.35MF35	6.3	27.33	41	6.51	0.18
S12	VRC-15CR-0.35MF35	6.3	27.77	42.5	6.75	0.15
S13	VRC-15CR-0.35MF60	7.2	27.02	40.5	5.63	0.21
S14	VRC-25CR-1MF35	5.58	27.98	37.5	6.72	0.17
Stage 3						

S15	SCC-15CR-0.2MISF19	7.2	25.3	39	5.39	0.22
S16	SCC-15CR-0.2MISF27	6.8	25.89	39.5	5.74	0.21
S17	SCC-15CR-0.2MASF38	6.3	27.15	40.5	6.43	0.18
S18	VRC-15CR-0.2MASF38	6.25	27.21	41.5	6.64	0.16
S19	VRC-15CR-0.2MASF50	6.75	26.31	40	5.95	0.2
S20	VRC-15CR-0.2MASF54	6.39	26.82	40.5	6.34	0.19
S21	VRC-25CR-1MASF38	5.67	26.53	38.5	6.79	0.15

Table 7-4 Cumulative energy dissipation (stage 1)

Step #	S1	S2	S3	S4	S5	S6
	E_d (KN.mm)	E_d (KN.mm)	E_d (KN.mm)	E_d (KN.mm)	E_d (KN.mm)	E_d (KN.mm)
1	0.27	0.25	0.62	0.58	1.95	0.61
2	1.24	1.16	2.73	3.09	4.9	3.55
3	5.64	5.83	15.83	18.77	11.86	16.51
4	25.1	22.61	51.38	47.06	26.96	41.8
5	49.35	49.41	94.21	87.48	59.65	81.44
6	210.45	212.84	275.48	309.35	279.7	314.1
7	1576.51	1020.36	1667.27	1321.23	1337.32	1316.65
8	4134.18	3456.03	4640.64	3907.89	3641.75	3510.49
9	7377.2	6775.39	7590.37	7581.15	6505.57	6534.28
10	11470.3	11829.65	12602.55	13874.77	9842.17	8996.03
11	-	-	-	-	12978.51	11397.55

Table 7-5 Cumulative energy dissipation (stage 2)

Step #	S7	S8	S9	S10	S11	S12	S13	S14
	E_d (kN.mm)	E_d (kN.mm)	E_d (kN.mm)	E_d (kN.mm)	E_d (kN.mm)	E_d (kN.mm)	E_d (kN.mm)	E_d (kN.mm)
1	0.9	1.18	0.97	0.63	0.66	0.53	1.02	0.9
2	5.35	5.91	3.87	4.15	16.91	12.73	11.34	4.17
3	24.04	24.65	19.69	16.05	47.95	55.57	45.65	22.44
4	56.81	54.19	49.26	40.88	88.77	112.62	96.65	51.58
5	102.17	98.23	92.98	82	328.28	242.86	215.83	96.69
6	390.91	348.21	329.18	288.32	2064.13	1080.77	975.12	336.88
7	2025.07	1909.28	2104.17	1710.26	5816.58	5291.92	4199.86	1861.35
8	4851.18	4952.23	4826.97	4105.2	10125.4	10735	8916.9	5263.9
9	8337.08	8756.49	8412.27	7284.54	15395.7	17418.8	14564.8	10100.6
10	11590.6	12175.4	12793.6	11125.1	20879.3	22244.7	20269.4	17620.4

Table 7-6 Cumulative energy dissipation (stage 3)

Step #	S15	S16	S17	S18	S19	S20	S21
	E_d (KN.mm)	E_d (KN.mm)	E_d (KN.mm)	E_d (KN.mm)	E_d (KN.mm)	E_d (KN.mm)	E_d (KN.mm)
1	1.7	1.8	2.1	2.5	1.8	2.2	0.927
2	6.34	6.54	6.906	7.05	6.74	6.86	4.157
3	24.54	27.51	31.7829	32.34	28.86	30.98	22.007
4	56.06	57.46	69.5419	71.86	61.32	67.23	49.549
5	106.23	108.74	123.242	132.22	114.21	119.59	93.918
6	406.33	420.86	481.962	503.08	461.84	472.28	417.458

7	2191.73	2277.96	2339.13	2576.08	2326.16	2336.94	2237.8
8	5603.64	6320.49	7917.95	8562.08	6412.84	7460.26	6364.4
9	9892.99	10340.5	12289.6	14294.1	11244.84	12183.8	11396.7
10	14442.0	15096.5	18979.3	19494.1	16977.49	17575.5	16572.6

7.2 Load deflection curves

7.2.1 Stage 1- Determining optimum percentage of CR

Figure 7-1 shows the envelop load-tip deflection curves of the joints' hysteretic behavior. These curves were drawn using the points of maximum load with their associated deflections from each first cycle of each load step in the hysteresis loop. The shape of the curves is similar in push and pull direction. It should be noted that there is a slight difference in the value of the ultimate load between the positive and negative direction. This may be related to the geometrical imperfections and steel reinforcement disposition. Table 7-2 and Table 7-3 show the ultimate load, tip deflection at ultimate load, and ultimate deflection (Δu) (the displacement corresponding to 90% of the ultimate load in the descending branch of the envelop load deflection curve). The results indicated that increasing the CR percentage from 0% to 15% increased the tip deflection at ultimate load by 12.5%. This behavior may be attributed to the elastic nature of CR and the ability of CR to present large elastic deformation before failure (Ganesan et al., 2013). Increasing the CR percentage from 15% to 20% also increased the tip deflection compared to the mixture without CR (S1) but with a slight reduction compared to the 15% CR mixture. Further increasing the percentage of CR from 20% to 25% reduced the tip deflection at ultimate load compared to the mixture without CR (S1). It can also be noted from Figure 7-1 that adding CR generally decreased the rate of strength degradation after reaching the ultimate load, indicating a more ductile failure.

7.2.2 Stage 2- Effect of using larger coarse aggregate size and MFs in rubberized concrete joints.

Figure 7-2 shows the envelop load-tip deflection curves for joints with different percentages of CR (Figure 7-2a) and joints with different coarse aggregate sizes (Figure 7-2b). By looking at mixtures with 20mm coarse aggregates (S7-S9), increasing the percentage of CR from 10% to 20% increased the deflection at ultimate load and ultimate deflection by 7.1% and 25%, respectively. Further increase in the percentage of CR above 20% (S10 compared with S9) slightly reduced the deflection at ultimate load and ultimate deflection compared with the 20% CR mixture (S10 compared with S9). On the other hand, the optimal percentage of CR to obtain maximum deflection at ultimate load and ultimate deflection in the 10mm coarse aggregate mixtures was shown to be 15% (see Table 7-3). It should be noted that the elastic nature of CR increases the deformability of the concrete matrix (Ganesan et al., 2013), which can increase the joint deflection. However, the further reduction in the compressive strength and load carrying capacity at relatively high percentage of CR may be the reason for limiting the increase in the joint deflection.

By looking at mixtures with small percentages of CR (up to 15%), increasing the coarse aggregate size from 10mm to 20mm in joints with similar percentage of CR and similar mode of failure (S8 compared with S4) resulted in a slight reduction in the deflection at ultimate load and ultimate deflection (Table 7-3). This may be attributed to the larger volume of the interfacial zone between cement mortar and larger coarse aggregate, which can lead to a reduction in the mixtures' mechanical properties (Table 7-1) (Koehler and Fowler, 2007; Ismail and Hassan 2016b).

Figure 7-3a shows the envelop load-tip deflection curves of joints with different MF lengths and different concrete types. Table 7-2 and Table 7-3 also present the ultimate load, tip deflection corresponding to ultimate load, and ultimate deflection for joints S8-S11. From Figure 7-3a and Table 7-3, it can be seen that adding MFs (35mm) to SCRC mixtures resulted in an increase in the tip deflection at ultimate load and ultimate deflection. For example, using MF35 in SCRC mixture with 15% CR increased the tip deflection at ultimate load and ultimate deflection by 8.8% and 5.8%, respectively (S11 compared with S4). The results show that changing the concrete type from MFSCRC to MFVRC slightly increased the ultimate deflection and deflection at ultimate load (S12 compared with S11). The increased deflection in MFVRC compared with MFSCRC may be related to the higher ultimate load of MFVRC, which resulted in a higher deflection (Table 7-2). Figure 7-3a and Table 7-3 also indicate that using longer MFs (60mm) showed comparable results to those of shorter MFs (35mm) in terms of ultimate deflection and deflection at ultimate load (S13 compared with S12). Figure 7-3b presents the envelop load-tip deflection curve for joints with maximized percentage of MFs and CR. Figure 7-3b and Table 7-3 show that in the VRC mixture (S14), where it was possible to combine 25% CR with 1% SF (it was not possible to develop SCC mixtures with those high percentages of CR and MFs), using these maximized percentages of CR and MFs helped the joint to experience significantly larger ultimate deflection and deflection at ultimate load compared with the control joint (without CR and MFs) (joint S14 compared with joint S1).

7.2.3 Stage 3 – Effect of combining CR with different types, lengths, and volumes of SFs on structural behavior of beam-column joint.

Figure 7-4a shows the envelop load-tip deflection curves for SFSCRC joints with different lengths and types of SFs. Table 7-3 shows the results of deflection corresponding to ultimate load and ultimate deflection (which represent the deflection corresponding to 90% of ultimate load in the descending branch of load-deflection envelop curve). From Figure 7-4a and Table 7-3, it can be observed that using MISFs, in general, showed insignificant increase in the deflection corresponding to ultimate load and ultimate deflection. For example, adding MISF19 to the SCRC joint showed inconsiderable increase in the deflection corresponding to ultimate load and ultimate deflection (not more than 1%) compared to the joint without fibers (S15 compared to S4). Moreover, adding MISF27 only increased the deflection at ultimate load and ultimate deflection by 3% and 2%, respectively, compared to the joint without fibers (S16 compared to S4). The slight improvement of MISF27 compared to MISF19 may be attributed to the increased length and rough texture of MISF27 (see **Figure 3-3**), which exhibited a better bond with concrete compared to MISF19 (S16 compared to S15). On the other hand, using MASFs showed a significant increase in the deflection corresponding to ultimate load and ultimate deflection. For example, the increases in the ultimate deflection and deflection at ultimate load reached up to 4.5% and 8.1%, respectively, when MASF38 was used (S17 compared to S4). The better results of MASFs compared to MISFs could be attributed to the fact that using short fibers (MISFs) did not appear to provide sufficient length to develop adequate bonding with concrete (pullout failure). This was confirmed after a visual inspection of the failed joints, which

showed that all MISFs (19mm) and (27mm) appeared to fail under pullout failure while all MASFs failed under tensile failure.

Figure 7-4b shows the load-deflection envelop curves for joints with different concrete types and different MASF lengths. Table 7-3 also presents the ultimate deflection and deflection corresponding to ultimate load for the same joints. It can be seen that changing the concrete type from SFSCRC to SFVRC showed comparable ultimate deflection and deflection at ultimate load (S18 compared to S17). The results also showed that by comparing joints with similar fiber type (MASFs) but with different fiber lengths, using shorter fibers appeared to have better results compared to longer fibers. For example, using MASF50 (S19) showed a slight reduction of 3.3% and 3.6%, respectively, in the deflection at ultimate load and ultimate deflection compared to the joint with MASF38 (S18). However, this joint (S19) still showed higher deflections compared to the joint without fibers (S19 compared to S4). This behavior may be attributed to the fact that at a given percentage of fibers, using shorter fibers ensures a higher number of individual fibers dispersed in the mixture. The higher number of fibers in the mixture increases the likelihood of single fibers to be oriented across the cracks, and this contributes to increasing the load carrying capacity and, in turn, enhancing the deformability of the mixture (Ismail and Hassan, 2017). However, by comparing joints S20 to joint S19, it can be seen that increasing the size (length and diameter) of fibers from MASF50 to MASF54 showed higher ultimate deflection and deflection at ultimate load compared to MASF50 (but less than MASF38). This may be attributed to the higher tensile strength and rigidity of MASF54 (see Table 3-2), which requires higher stress to cause failure than that required by MASF50.

Figure 7-4c shows the envelop load-deflection curve for joints with maximized percentage of fibers (1%) and CR (25%). From Figure 7-4c and Table 7-3, it can be noticed that although using high percentage of CR (25%) resulted in a significant reduction in the load carrying capacity (S6 compared to S1), adding high percentage of SFs (1% in S21) compensated for this reduction and helped to achieve joint with higher deformability.

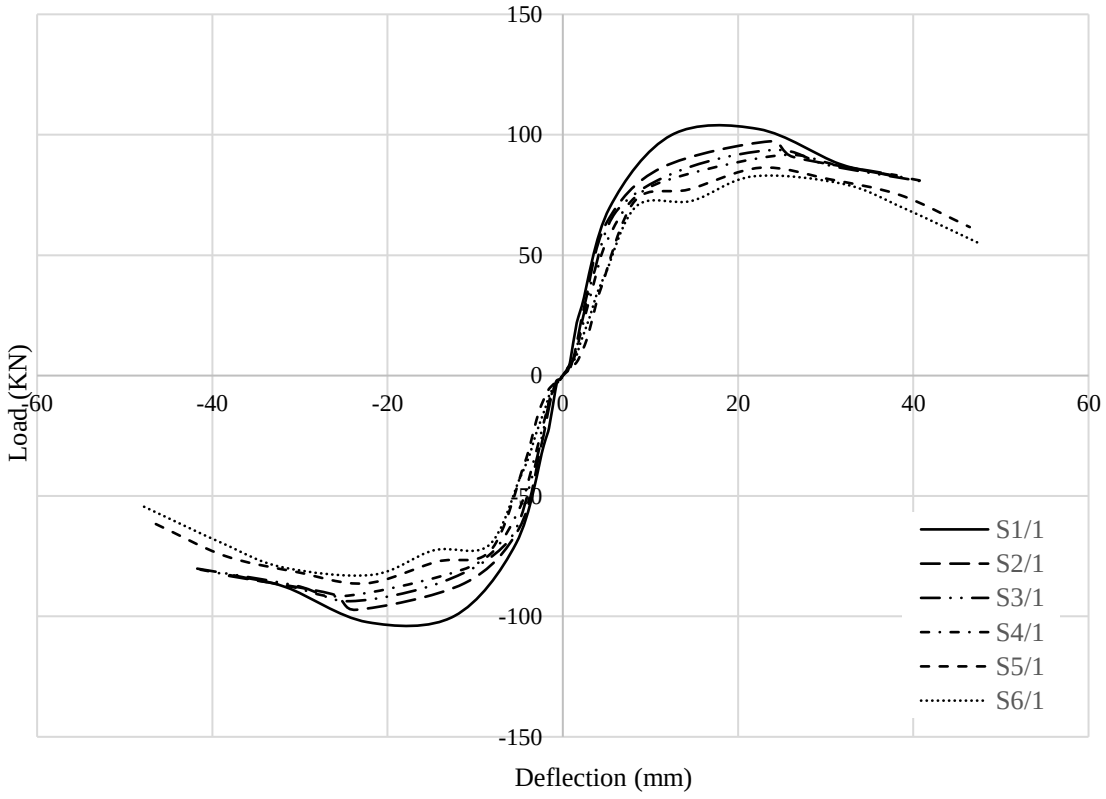

Figure 7-1 Load deflection envelop curves for SCRC joints

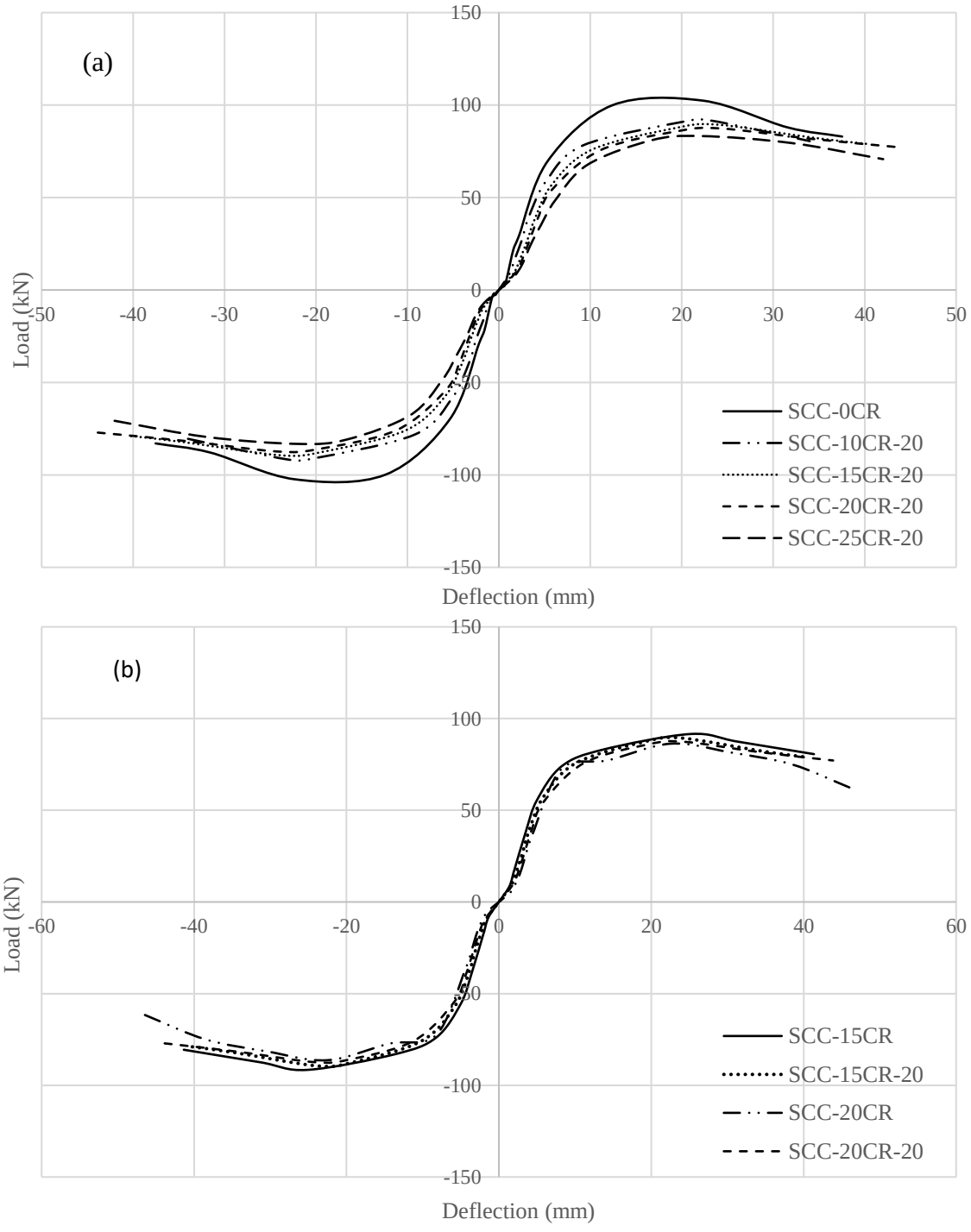

Figure 7-2 Load deflection envelop curves a) joints with different percentages of CR in 20 mm coarse aggregate mixtures b) joints with different coarse aggregate sizes

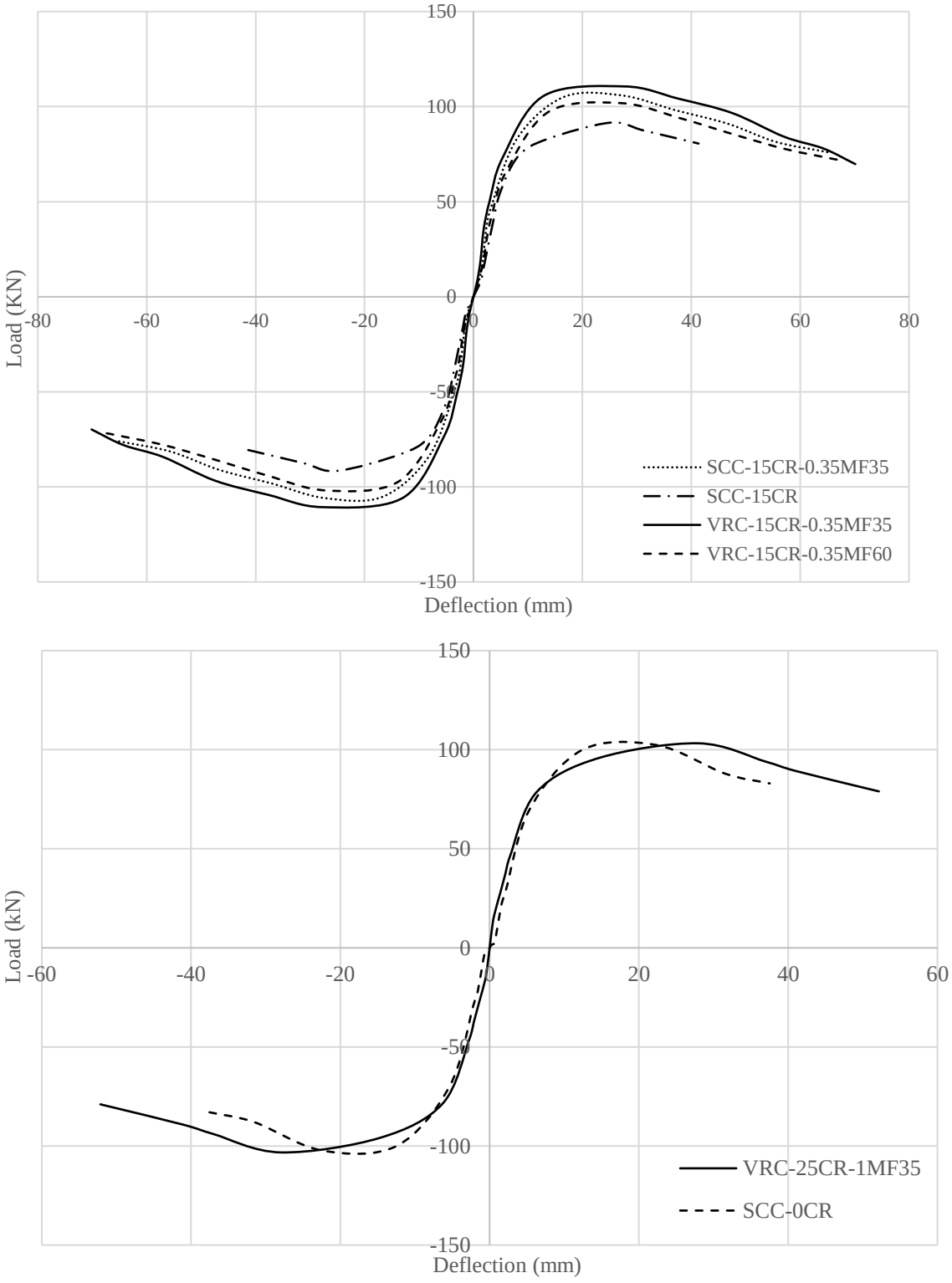

Figure 7-3 Load deflection envelop curves a) joints with different MF lengths and different concrete types b) maximized percentage of SFs and CR

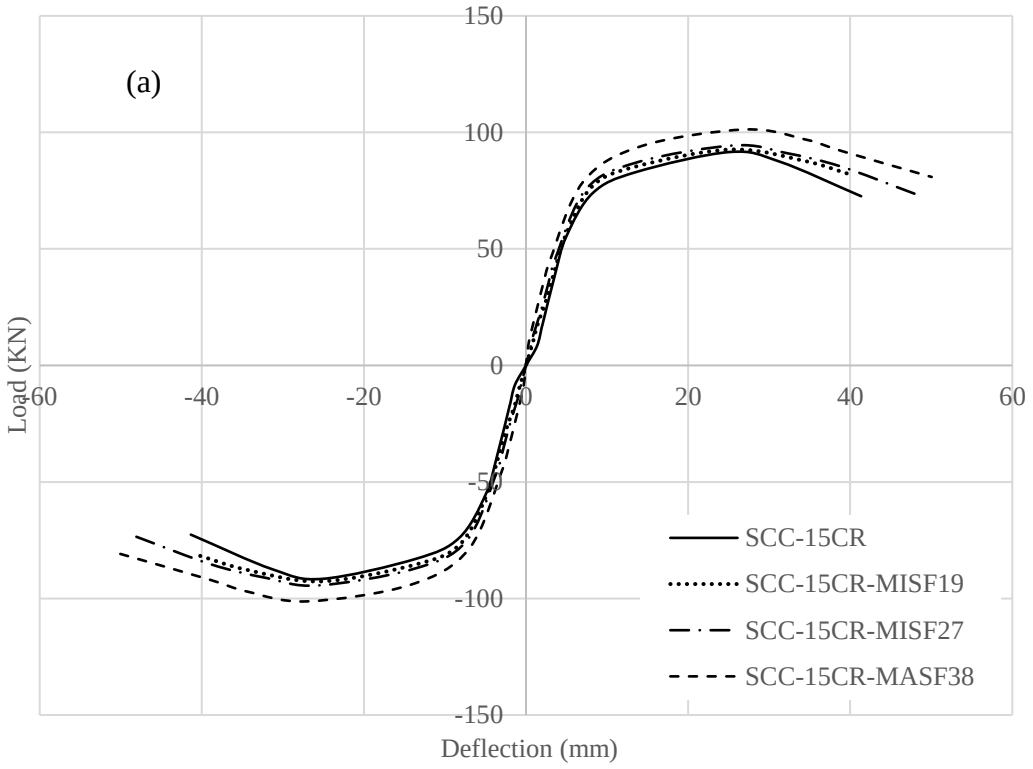
(a)
150
100
50
0
-50
-100
-150
-60
-40
-20
0
20
40
60
Load (KN)
Deflection (mm)
SCC-15CR
SCC-15CR-MISF19
SCC-15CR-MISF27
SCC-15CR-MASF38

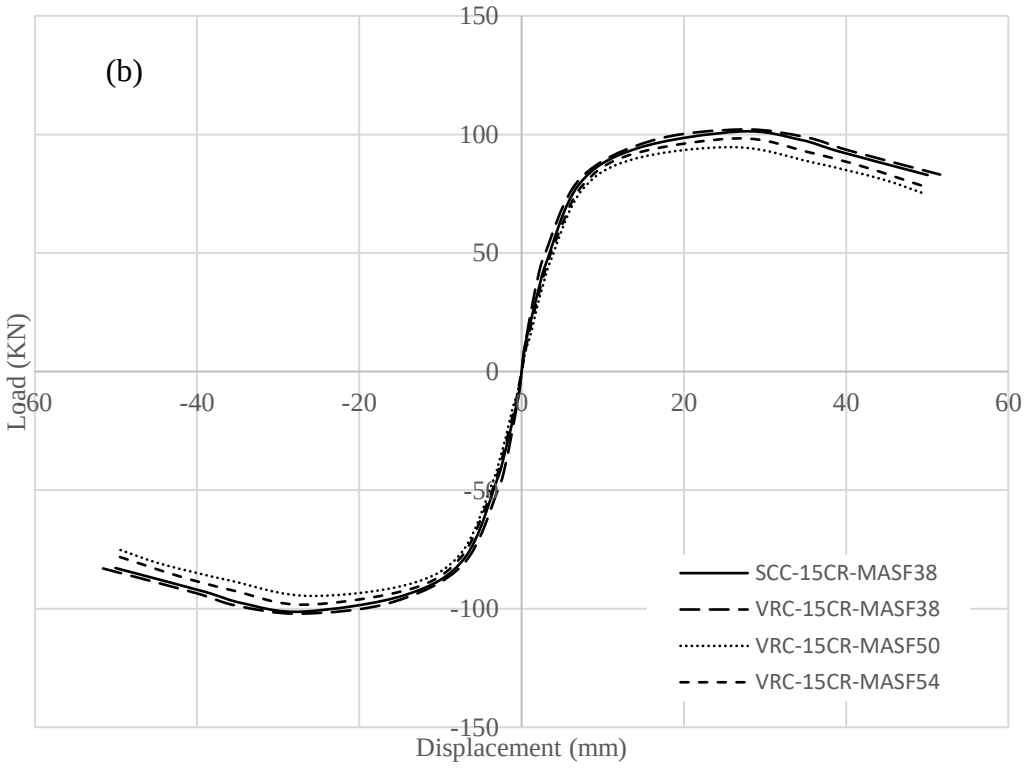
(b)
150
100
50
0
-50
-100
-150
-60
-40
-20
0
20
40
60
Load (KN)
Displacement (mm)
SCC-15CR-MASF38
VRC-15CR-MASF38
VRC-15CR-MASF50
VRC-15CR-MASF54

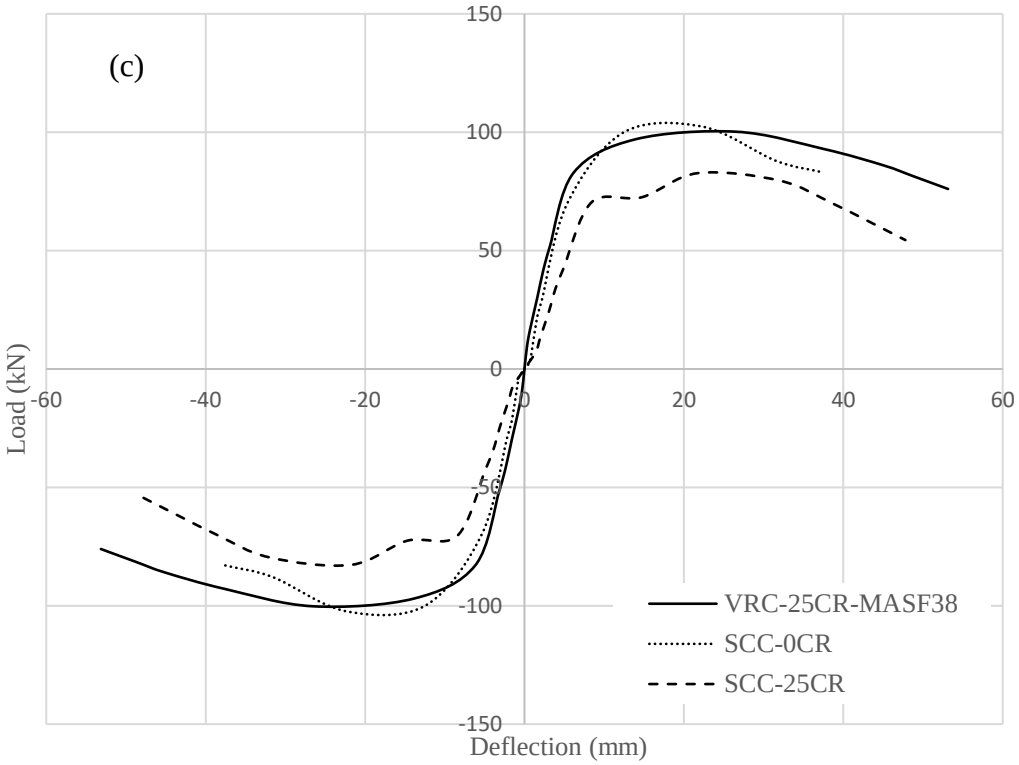

Figure 7-4 Load-deflection envelop curves a) SFSCRC joints with different SF lengths/types, b) SFVRC joints with different SF lengths/types, c) maximized percentage of SFs and CR

7.3 Initial stiffness and stiffness degradation

7.3.1 Stage 1- Determining optimum percentage of CR

Figure 7-5 shows the stiffness versus the number of cycles for all tested beam-column joints. It can be seen from the figure that the initial stiffness continued to decrease as the percentage of CR increased. For example, increasing the percentage of CR from 0% to 25% resulted in a 37% reduction in the initial stiffness. This can be attributed to the decreased modulus of elasticity of CR compared to fine aggregate (Ismail and Hassan, 2016). Figure 7-5 also shows that increasing the number of load cycles reduced the beam-column joint stiffness. It should be noted that at low number of cycles no micro cracks

initiate and hence the stiffness of beam-column joints is not affected. The micro cracks tended to initiate and largely propagate as the number of cycles increased, which in turn decreased the overall stiffness of beam-column joints. By looking at Figure 7-5, it can be noted that for up to 30 cycles, the mixture without CR (S1) showed a stiffness reduction from 13.8 to 2.2 kN/mm while the mixture with 25% CR (S6) showed a stiffness reduction from 8.7 to 1.7, indicating that the rate of stiffness degradation decreased as the percentage of CR increased.

7.3.2 Stage 2- Effect of using larger coarse aggregate size and MFs in rubberized concrete joints.

Figure 7-6 shows the effect of increasing the percentage of CR (Figure 7-6a) and the effect of different coarse aggregate sizes (Figure 7-6b) on the beam-column joint's stiffness throughout 30 cycles of loading. The initial stiffness was calculated in the elastic region by dividing the maximum load of first cycle in first load step by its corresponding displacement. From the figure, it can be seen that the beam-column joint stiffness was not affected up to almost 15 cycles and then started to decrease as the number of load cycles increased.

The results presented in Figure 7-6b and Table 7-2 indicate that increasing the coarse aggregate size slightly reduced the initial stiffness of beam-column joints. For example, increasing the coarse aggregate size from 10mm to 20mm reduced the beam-column joint's initial stiffness by 7.2% (S4 compared with S8). This may be attributed to the larger volume of the interfacial zone between cement mortar and coarse aggregate, which may lead to the initiation of earlier cracks, and hence reduction in the initial stiffness.

Figure 7-7a shows the initial stiffness and stiffness degradation of beam-column joints with different lengths of MFs and different concrete types throughout 30 cycles of loading. From Figure 7-7a and Table 7-2, it can be noticed that adding MFs (35mm) to the SCRC mixture with 15% CR increased the initial stiffness by 11.6% compared with the mixture without SFs (S11 compared with S4). This can be attributed to the higher load (at a given displacement) the joint with MFs sustained compared with joint without MFs (see Figure 7-3a). The results also indicated that changing the concrete type (S12 compared with S11) or the MFs length (S13 compared with S12) did not show a significant effect on the initial stiffness of the beam-column joints. Figure 7-7b shows the effect of maximizing the percentage of CR and MFs on the initial stiffness and stiffness degradation of beam-column joints (S14 compared with S1). From Figure 7-7b, it can be noticed that maximizing the percentage of CR and MFs helped to significantly increase the initial stiffness of beam-column joints and decreased the rate of stiffness degradation. For example, using up to 25% CR and 1% MFs (35mm) increased the initial stiffness by 22.4% compared with the control joint without CR and MFs (S1).

7.3.3 Stage 3 – Effect of combining CR with different types, lengths, and volumes of SFs on structural behavior of beam-column joint.

Figure 7-8a shows the stiffness degradation curves for SFSCRC joints with different SF types throughout 30 cycles of loading. From Figure 7-8a and Table 7-2, it can be seen that adding MISFs (MISF19 or MISF27) to SCRC mixtures insignificantly affected the initial stiffness of beam-column joints. However, using MISF27 appeared to have a better effect compared to the joint with MISF19. This is because of the rough texture of MISF27 (see **Figure 3-3**), which contributed to enhancing the bond between fibers and cement matrix

and, in turn, improving the initial stiffness. On the other hand, using MASFs appeared to have a significant effect on enhancing the initial stiffness of the beam-column joint, in which using MASF38 increased the initial stiffness by 9.3% compared to the joint without fibers (S17 compared to S4). The significant increase in the initial stiffness of MASFs compared to joints without fibers can be attributed to the bridging mechanism of the SFs that helped to restrict the cracks and limited their propagation.

By looking at Figure 7-8a, it can be seen that in the joint without SFs (S4), the stiffness was almost constant up to approximately 9 cycles and then started to decrease. On the other hand, in joints with SFs, the stiffness was almost constant up to 12 cycles (MISF19 or MISF27) or 15 cycles (MASF38) before it started to drop. At early stages of loading (up to 9 cycles), not more than 0.1mm crack widths were recorded in any of the tested joints. As the number of cycles increased, the cracks in the joint without fibers (S4) started to open wider, reducing the overall stiffness of the joint. On the other hand, in joints with SFs (S15, S16, and S17) at a higher number of cycles, the bridging mechanism of the fibers appeared to limit the crack widths and delayed the degradation of the joint's stiffness (see Figure 7-9).

Figure 7-8b shows the stiffness degradation curves for joints with different lengths and types of MASFs and different concrete types. From Figure 7-8b and Table 7-2, it can be noticed that changing the concrete type from SFSCRC to SFVRC had an insignificant effect on the initial stiffness of the beam-column joint (S18 compared to S17). The results also showed that changing the lengths/types of MASFs did not have a noticeable effect on the initial stiffness of beam-column joints (S18 compared to S19, S20).

Figure 7-8c and Table 7-2 show how adding high percentage of SFs to mixtures with high percentage of CR affects the initial stiffness and stiffness degradation. Although using high percentage of CR (25%) significantly reduced the initial stiffness (37.5% compared to the control joint without rubber, S6 compared to S1), adding high volume of MASFs (1%) alleviated this reduction. For example, adding 1% MASF38 increased the initial stiffness by 85% compared to the joint with 25% CR and no fibers (S21 compared to S6). Moreover, adding high percentage of MASFs contributed to delaying the degradation in the stiffness and helped to maintain the initial stiffness almost constant for a higher number of loading cycles. For instance, Figure 7-8c shows that in the joint with high percentage of MASFs (S21), the stiffness started to drop after 15 cycles, while in the joint without fibers (S6) the stiffness started to drop after 9 cycles. This may be attributed to the ability of fibers to restrict the crack propagation, which in turn delayed the deterioration of beam-column joint stiffness

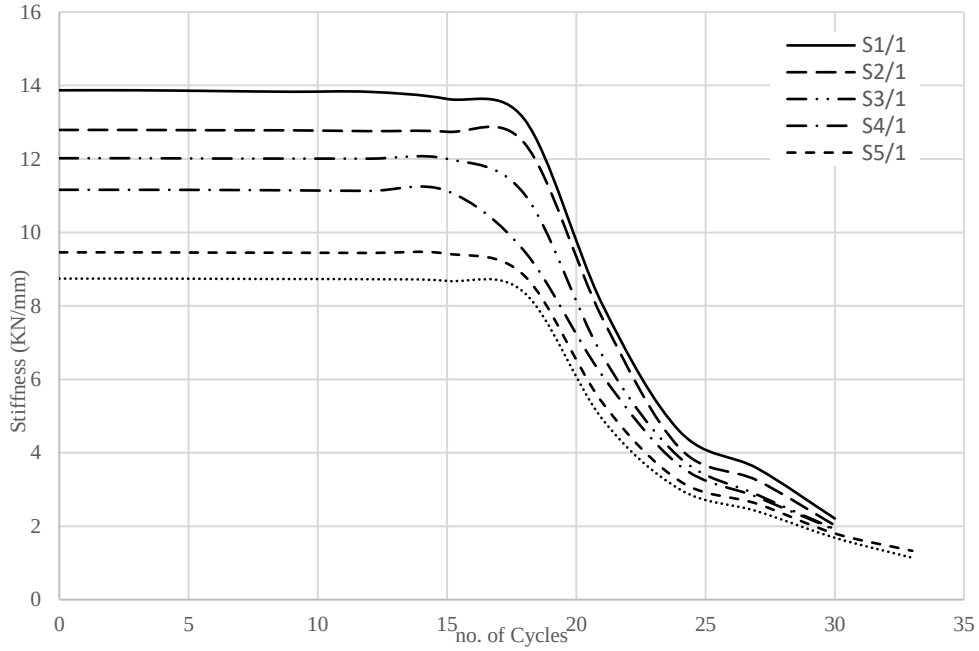

Figure 7-5 Stiffness degradation of SCRC joints

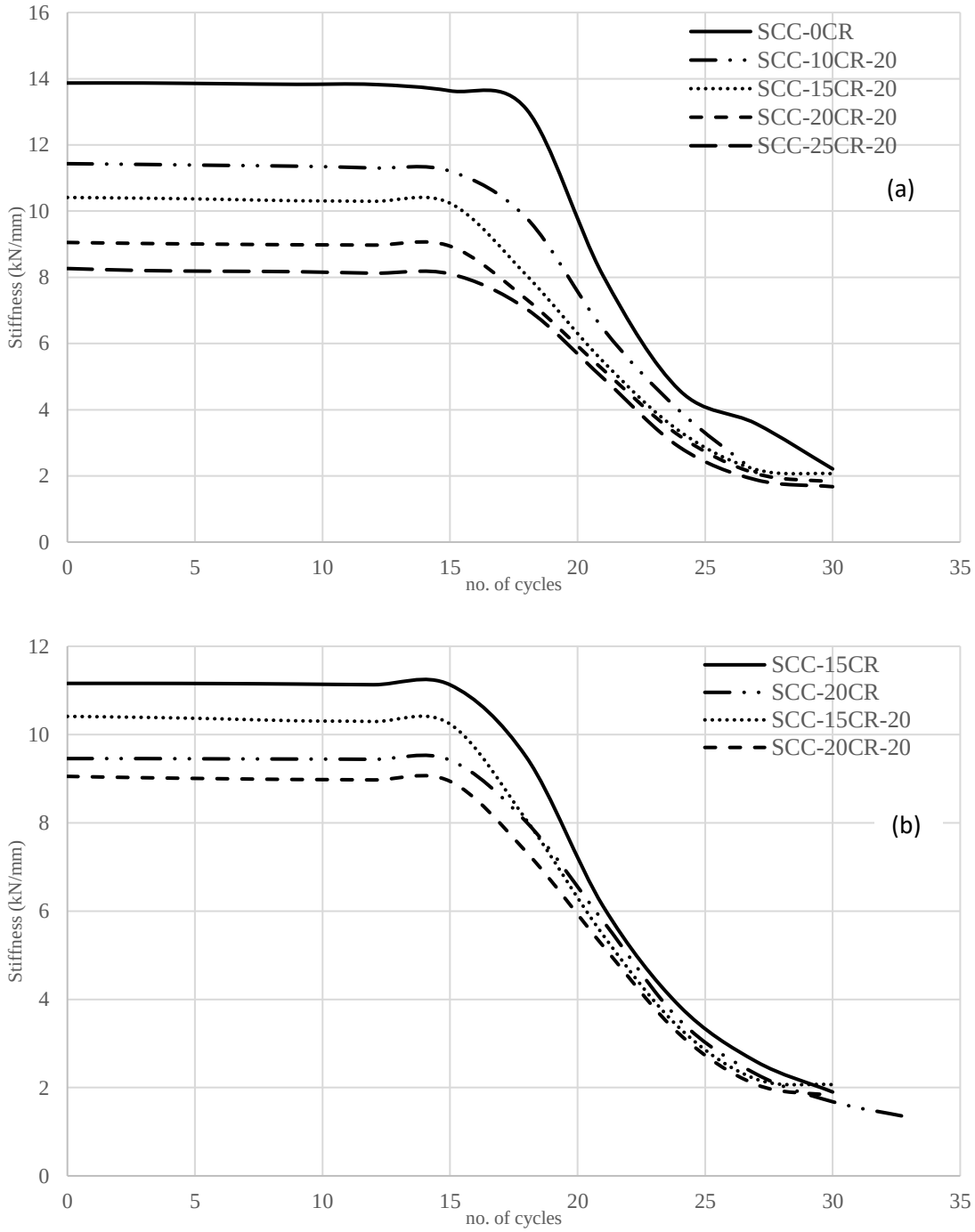

Figure 7-6 Stiffness degradation of tested specimens a) joints with different percentages of CR in 20 mm coarse aggregate mixtures b) joints with different coarse aggregate sizes

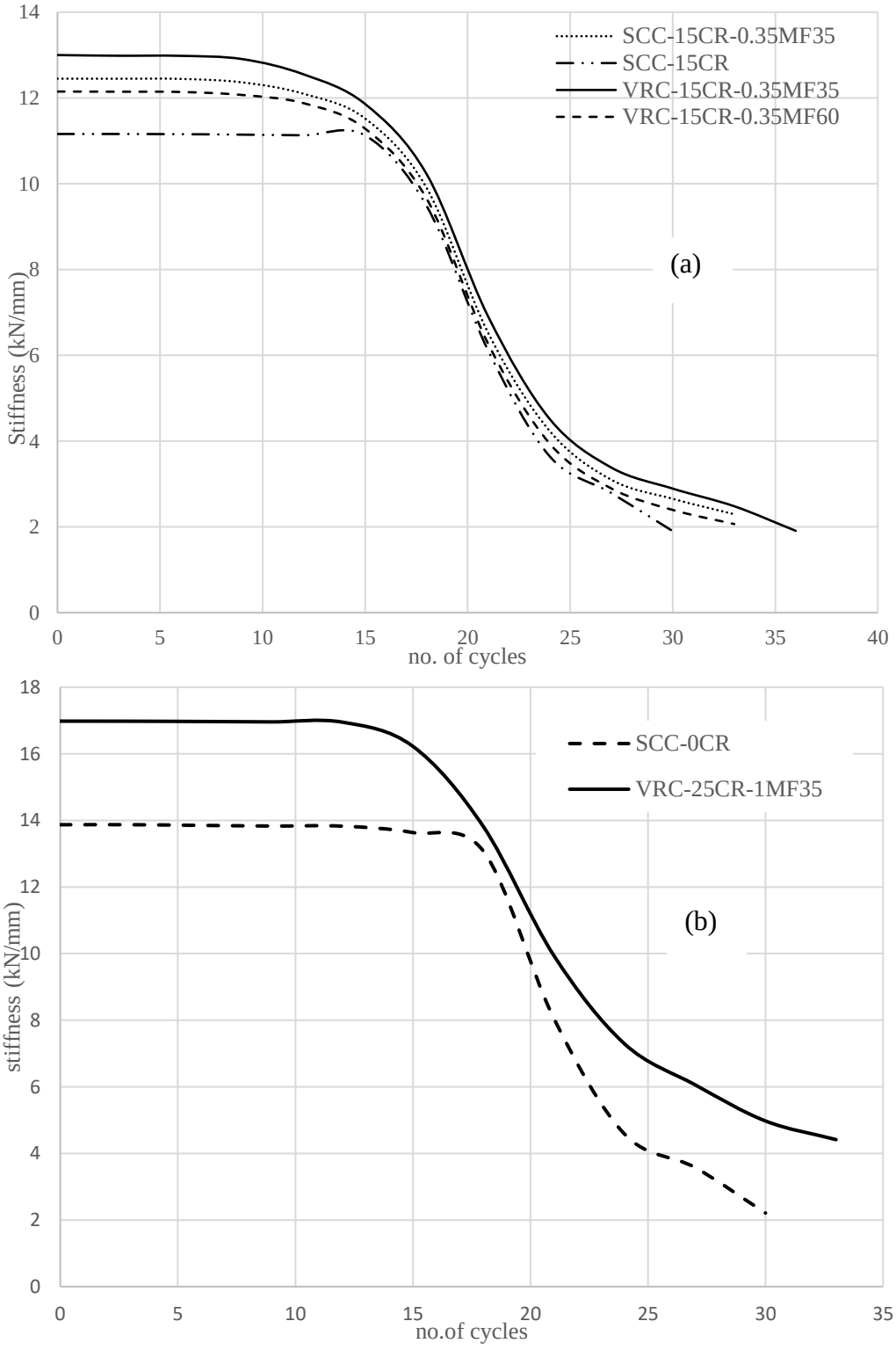

Figure 7-7 Stiffness degradation of tested specimens a) joints with different MF lengths and different concrete types b) maximized percentage of MFs and CR

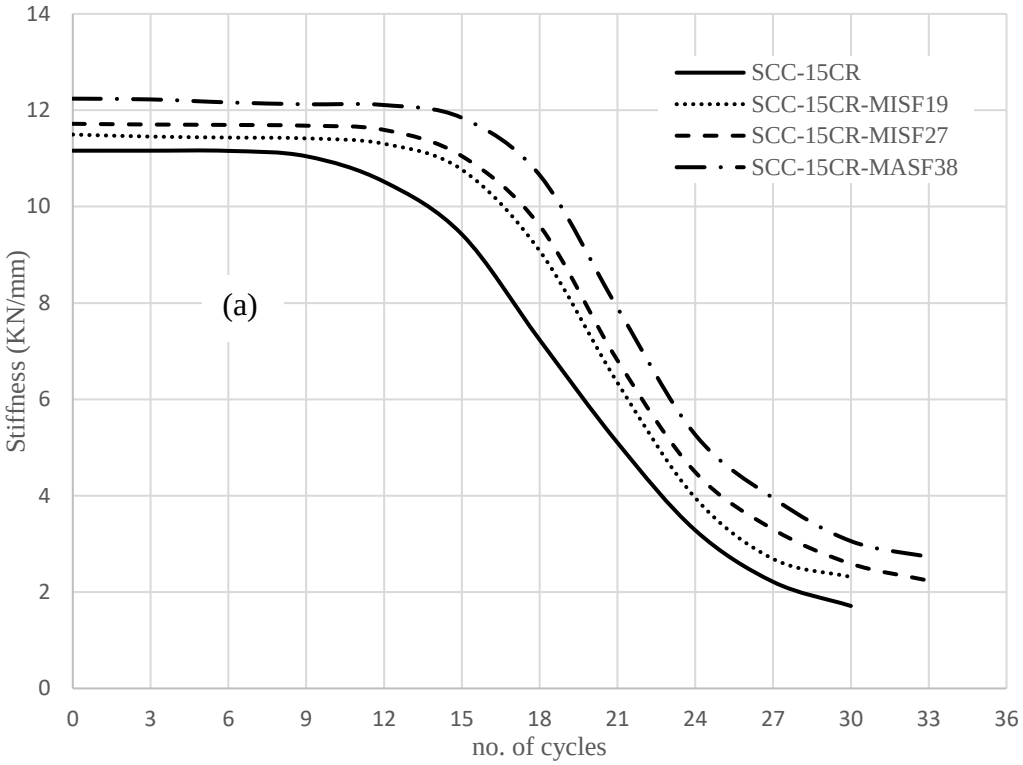
SCC-15CR
SCC-15CR-MISF19
SCC-15CR-MISF27
SCC-15CR-MASF38
(a)
Stiffness (KN/mm)
no. of cycles
0
2
4
6
8
10
12
14
0
3
6
9
12
15
18
21
24
27
30
33
36

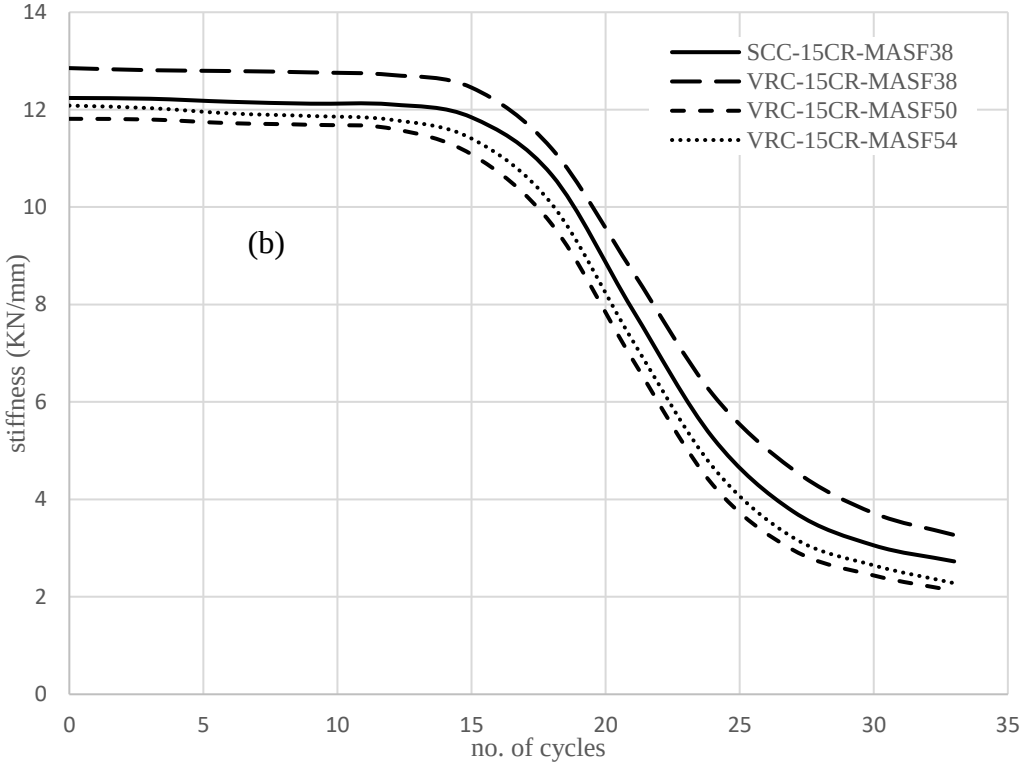
SCC-15CR-MASF38
VRC-15CR-MASF38
VRC-15CR-MASF50
VRC-15CR-MASF54
(b)
stiffness (KN/mm)
no. of cycles
0
2
4
6
8
10
12
14
0
5
10
15
20
25
30
35

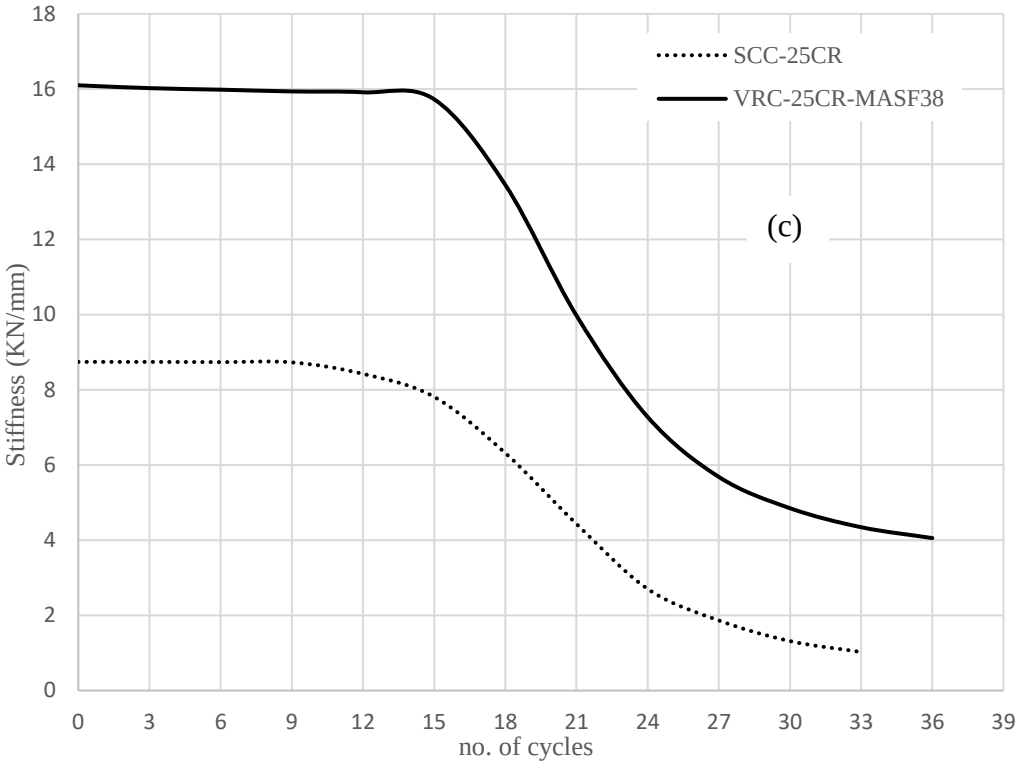

Figure 7-8 Stiffness degradation of tested specimens a) SFSCRC joints with different SF lengths/types, b) SFVRC joints with different SF lengths/types, c) maximized percentage of SFs

7.4 Failure modes and cracking patterns

7.4.1 Stage 1- Determining optimum percentage of CR

The failure modes of beam-column joints subjected to reverse cyclic loading can be classified into four modes of failure: (i) beam yielding failure, “B-mode” (which occurs when the longitudinal beam reinforcement reaches yield and the joint shear strength is higher than the joint shear stress resulting from applied load); (ii) joint shear failure after beam yields, “BJ-mode” (which occurs when the joint shear stress exceeds the joint shear strength after the longitudinal reinforcement reaches yield); (iii) joint shear failure without beam yields, “J-mode” (which occurs when the joint shear stress exceeds the joint shear strength before the longitudinal reinforcement reaches yield); and (iv) compressive

flexural failure at beam end, “CB-mode” (which occurs when concrete crushes under load before beam reinforcement yield and the joint shear strength is higher than the joint shear stress). The results of this investigation indicated that for up to 15% CR the B-mode of failure was the dominant mode, in which the beam longitudinal reinforcement reached yield strength and there was no visual sign of joint shear failure in the cracking pattern (Figure 7-9). Beyond 15% CR, BJ-mode of failure occurred, in which beam longitudinal reinforcement reached yield strength first and then diagonal cracks were formed (see Figure 7-9). As mentioned above, when the joint shear stress exceeds the joint shear strength, the joint is more likely to fail in BJ-mode. At high percentages of CR, the compressive strength of concrete was significantly reduced, which greatly reduced the joint shear strength. Therefore, the mode of failure changed from B-mode to BJ-mode at high percentages of CR.

Figure 7-9 and Table 7-2 show the cracking pattern, maximum crack width at beam-column interface, and maximum crack width within the beam-column joint. From the figure, it can be seen that the number of randomly distributed cracks continued to increase as the percentage of CR increased up to 25%. This can be related to the reduction in STS that resulted from increasing the percentage of CR. Table 7-2 also shows that increasing the percentage of CR from 0% to 25% decreased the maximum crack width at the beam-column interface. Cracks are more likely to interfere with rubber particles during propagation when the percentage of CR is increased. These rubber particles act as a crack arrester due to the deformability and ability of rubber to resist large tensile deformation. Therefore, the maximum crack width at beam-column interface decreased as the percentage of CR increased. On the other hand, within the beam-column joint, the cracks

started to initiate and propagate only at higher percentages of CR (higher than 15%) due to the reduction in joint shear strength (see Figure 7-9). Similar behavior of crack number and width in beam-column interface were observed in beam-column joints containing high percentages of CR (20% and 25% CR).

7.4.2 Stage 2- Effect of using larger coarse aggregate size and MFs in rubberized concrete joints.

Table 7-2 shows the failure mode for all tested joints (S1-S21). It can be seen that the dominant failure mode of joints with 10% to 20% CR in mixtures with 20mm coarse aggregate (S7-S9) was the B-mode failure, in which the longitudinal reinforcement of the beam reached yield with no visual sign of joint shear failure in the cracking pattern (Figure 7-9). Further increase in the percentage of CR beyond 20% appeared to change the failure mode from B-mode to BJ-mode (joint S10), in which beam longitudinal reinforcement reached yield first and then diagonal cracks were formed (see Figure 7-9). Similar behavior was also noted in mixtures with 10mm coarse aggregate (S1-S6), in which the mode of failure changed from B-mode to BJ-mode when the percentage of CR exceeded 15%. The change in failure mode, from B-mode to BJ-mode, may be attributed to the excessive reduction of the compressive strength (resulting from using relatively high percentage of CR), which negatively affects the joint shear strength.

The results also indicated that at higher percentages of CR (20%) using a larger aggregate helped to change the mode of failure from BJ-mode (in 10mm coarse aggregate joint) to B-mode (in 20mm coarse aggregate joint). This may be related the improved aggregate interlock of larger coarse aggregate compared with smaller coarse aggregate, which contributed to enhancing the shear capacity of the joint (S5 compared with S9).

Table 7-2 also indicates that all joints with MFs (whether SCRC or SFVRC) (S11-S14) showed B-mode failure. The results also showed that combining 25% CR and 1% MFs (35mm) resulted in B-mode failure. It is worth noting that although S14 contains high percentage of CR (25%), which typically causes BJ-mode failure, adding the 1% MFs in this joint helped to arrest the cracks, improved the joint shear strength, and in turn changed the failure mode to B-mode failure.

Figure 7-9 also indicates that joints with a larger coarse aggregate (20mm) had different cracking patterns. For example, by comparing S9 to S5 (similar percentage of CR but different coarse aggregate size), S9 with a larger coarse aggregate did not have cracks initiated within the beam-column joint (only at the beam-column interface). This can be attributed to the improvement of the aggregate interlock, which in turn improved the joint shear strength.

Figure 7-9 and Table 7-2 show the cracking pattern, maximum crack width at beam-column interface, and maximum crack width within the beam-column joint for MFSCRC and MFVRC joints. From the figure, it can be seen that using MFs (35mm) (joint S11) appeared to reduce the number of cracks at beam-column interface due to the improved STS. Also, the maximum crack width increased in the joint with MFs compared with the joint without MFs (S11 compared with S4). This can be attributed to the fact that using MFs allows the beam-column joint to experience larger deformation prior to failure, which contributed to developing wider cracks. A similar effect for MFs was also noticed in the MFVRC beam-column joint (S12 compared with S11). Figure 7-9 also shows that using longer MFs (60mm) in VRC joints exhibited similar cracking behavior to those with shorter MFs (35mm) (S13 compared with S12). Combining high percentage of MFs

(1%) with high percentage of CR (25%) compensated for the reduction in the joint's shear strength as a result of using high percentage of CR, showing no cracks within the beam-column joint and minimum crack width at beam-column interface, which indicates a better performance of beam-column joints (see joint S14 in Figure 7-9).

7.4.3 Stage 3 – Effect of combining CR with different types, lengths, and volumes of SFs on structural behavior of beam-column joint.

Table 7-2 also indicates that all joints with SFs (whether SFSCRC or SFVRC) (S15-S21) showed B-mode failure. The results also showed that using high percentage of CR (25%) exhibited BJ-mode failure. And adding 1% SFs (MASF38) (S21) changed this failure mode to B-mode, in which the beam longitudinal reinforcement reached yield without any visual sign of shear failure in the cracking pattern (see Figure 7-9). This can be attributed to the role of fibers in stitching the cracks, which improved the joint shear strength and in turn changed the failure mode to B-mode. The results also indicated that the upper and lower longitudinal reinforcement of the beam reached yield before failure. This was confirmed by the results of strain gauges attached to the upper and lower reinforcement at the beam-column interface section (section of maximum moment).

Figure 7-9 and Table 7-2 show the cracking pattern and maximum crack width at beam-column interface. From the Table and Figure, it can be seen that using MISFs slightly reduced the maximum crack width at failure. For instance, using MISF19 reduced the maximum crack width by 6% compared to the joint without fibers (S15 compared to S4). It should be noted that using MISF27 exhibited a better performance in restricting the cracks and limiting the crack width compared to the joint with MISF19 (S16 compared to S15). This may be attributed to the rough surface of MISF27, which enhanced the role of

fibers in stitching the cracks and limited the crack width, as mentioned earlier. The results also showed that using MASFs in SCRC joints exhibited a higher reduction in the maximum crack width at beam-column interface compared to joints with MISFs. For example, by comparing joint S17 to S15, it can be seen that using MASF38 reduced the maximum crack width by 11% compared to the joint with MISF19. This may be related to the improved bonding between MASF38 and concrete matrix compared to MISF19; the cracked joints showed a fiber pullout failure for MISF19 and a fiber tension failure for MASF38.

Figure 7-9 and Table 7-2 show the cracking pattern, maximum crack width at beam-column interface, and maximum crack width within the beam-column joint for SFVRC joints that have different lengths and types of SFs. By comparing joint S19 to S18, it can be noticed that using shorter MASFs showed higher improvement in the role of fibers in restricting the crack width. This may be attributed to the increased number of single fibers (for a given volume of fibers) in the mixture when shorter fibers are used, as explained before. It should also be noted that a similar effect for MASF38 in SCRC joints was also noticed in VRC joints (S18 compared to S17). Of all types/lengths of SFs, MASF38 showed the highest improvement in the cracking behavior of beam-column joints. The results also showed that adding high volume of MASFs (1%) to high percentage of CR (25%) helped to compensate for the reduction in the joint shear strength resulting from the high percentage of CR. Using a high percentage of MASFs also appeared to restrict the initiation of cracks within the beam-column joint and reduce the number of cracks at the beam-column interface (S21 compared to S6 in Figure 7-9).

Failure Load = 102.4 KN
0% CR

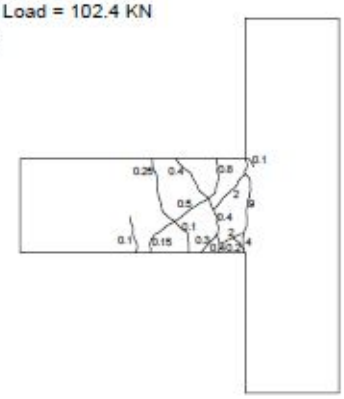

Failure Load = 97.2 KN
5% CR

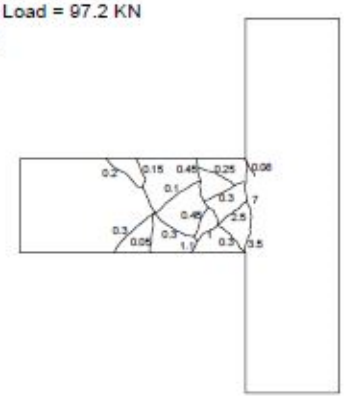

Failure Load = 93.7 KN
10% CR

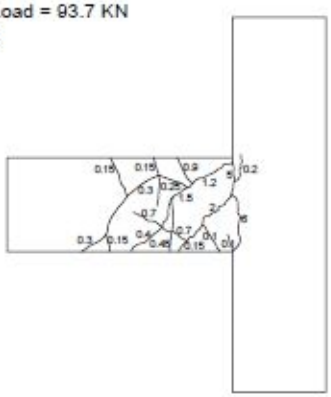

Failure Load = 91.6 KN
15% CR

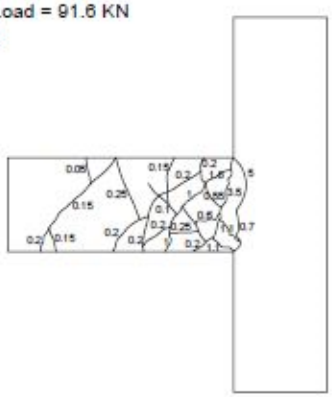

Failure Load = 86.3 KN
20% CR

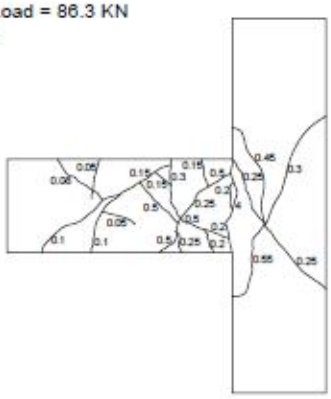

Failure Load = 82.7 KN
25% CR

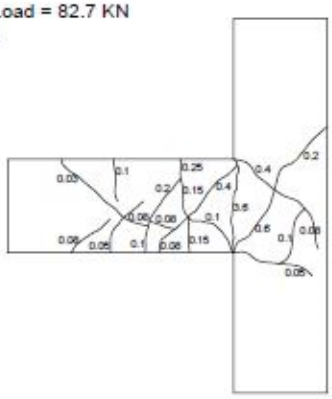

Failure Load = 91.65 KN
SCC-10CR-20

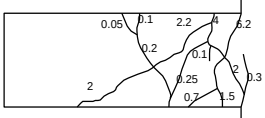

Failure Load = 89.42 KN
SCC-15CR-20

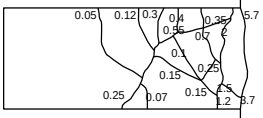

Failure Load = 87.34 KN
SCC-20CR-20

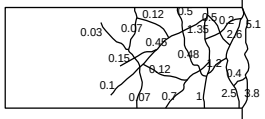

Failure Load = 83.24 KN
SCC-25CR-20

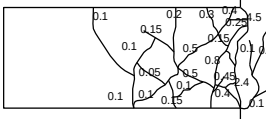

Failure Load = 105.9 KN
SCC-15CR-0.35MF35

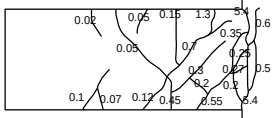

Failure Load = 110.6 KN
VRC-15CR-0.35MF35

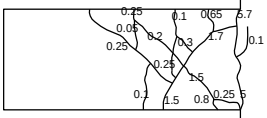

Failure Load = 101.9 KN
VRC-15CR-0.35MF60

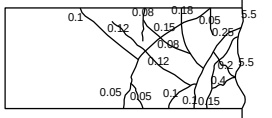

Failure Load = 103.2 KN
VRC-25CR-1MF35

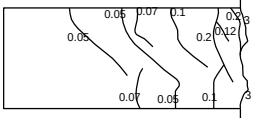

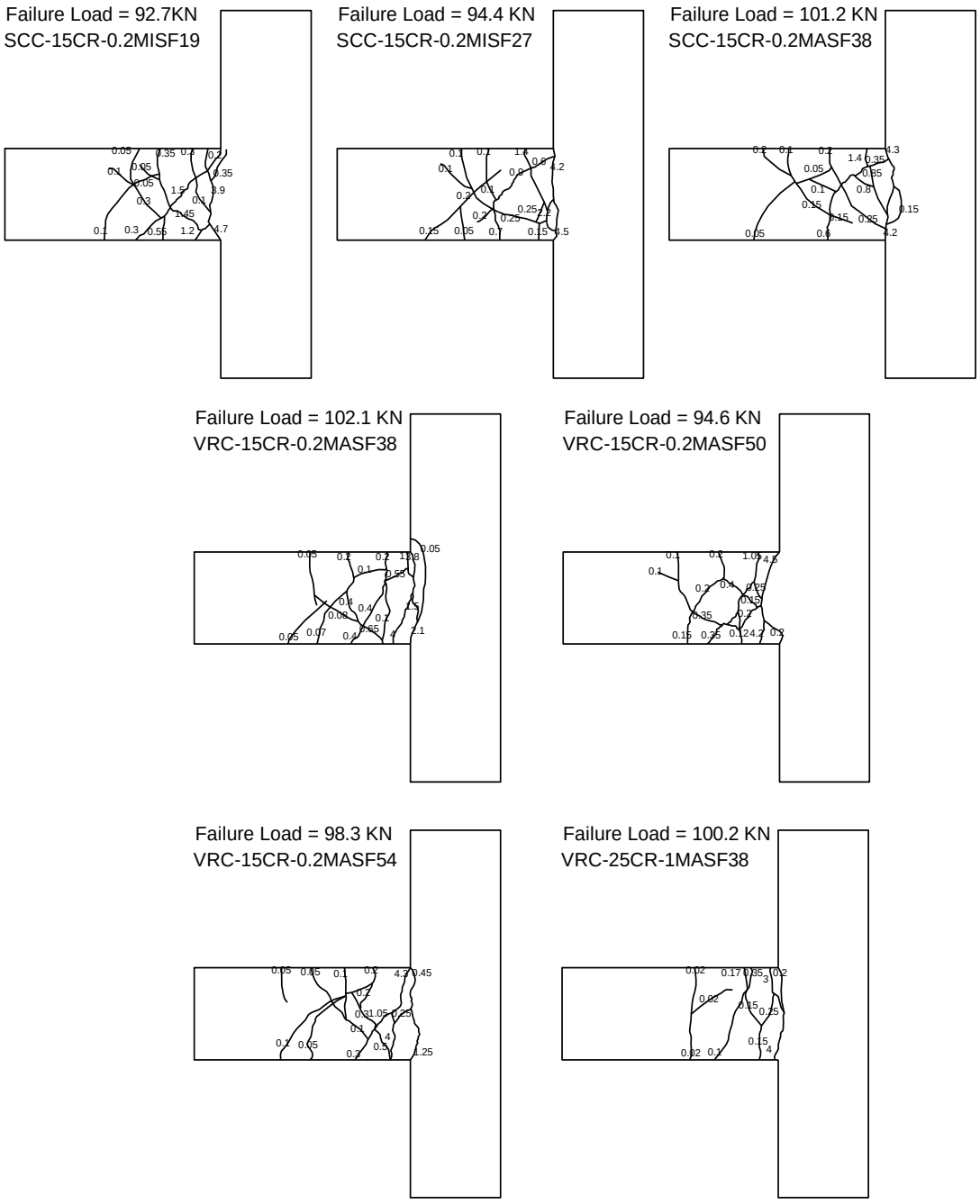

Figure 7-9 Cracking patterns for tested Beam-column joints

7.5 Ductility and brittleness index

7.5.1 Stage 1- Determining optimum percentage of CR

The displacement ductility is defined as the ratio between the ultimate deflection (Δu) and the yield displacement (Δy). Previous studies indicated that proper reinforcement anchorage and bonding capacity is essential to enhance beam-column joint ductility (Rajagopal and Prabavathy, 2014; Shiohara, 2004). Furthermore, bonding capacity and anchorage strength are directly proportioned to square root of compressive strength, in which increasing compressive strength resulted in an enhancement in the bonding capacity and hence enhancing the beam-column joint ductility. The load-tip deflection envelop curve was used to determine the ultimate and yield displacements. The intersection between the horizontal line at 90% of ultimate load and the extension of the line that passes through the origin and 50% of the ultimate load (Shannag et al., 2002) was taken as the yield displacement (Figure 7-10a). Meanwhile, the ultimate deflection (Δu) was taken as the intersection between the horizontal line at 90% of the ultimate load and the descending branch of the load-tip deflection envelop curve. Table 7-3 and Figure 7-11a present the displacement ductility values for all SCRC tested specimens. From the table, it can be seen that increasing the percentage of CR from 0% to 15% exhibited an increase in the displacement ductility reaching up to 18.8%. This can be related to the low stiffness of CR, which enhanced the deformability and strain capacity of the tested specimen. On the other hand, the specimen with 20% CR (S5) showed a noticeable reduction in the displacement ductility compared to the 15% CR specimen (S4), but with a slight improvement in the displacement ductility compared to the control mixture (S1). Further increase in the CR replacement level beyond 20% resulted in a reduction in the

displacement ductility 5% less than the control sample (S1) (see Figure 7-11a). This reduction in the displacement ductility could be attributed to the change in the failure mode from B-mode to BJ-mode when the CR percentage increased above 15%. This change in failure mode induced a limited deformation capacity due to the strength reduction resulting from panel joint cracking.

The brittleness index (BI) was also investigated in this study to evaluate the ductility and deformability of the tested specimens. BI of concrete joints in compression can be defined as (Topçu, 1997) the recovered deformation energy obtained before fracture (elastic energy capacity) divided by the irreversible plastic energy consumed during the failure (plastic energy capacity) (A2/A1 in Figure 7-10b). It is worth noting that unlike ductile materials, concrete as a brittle material should have a high BI value. Table 7-3 and Figure 7-11a show the BI values for all tested specimens. It can be observed that increasing the percentage of CR from 0% to 15% decreased the BI value by 20.9%. The reduced BI values clearly highlight the improved ductility that resulted from increasing the percentage of CR. However, further increase in the percentage of CR appeared to increase the BI value, which negatively affected the concrete's ductility. This behavior can be attributed to the same reasons explained before that caused a reduction in the displacement ductility.

7.5.2 Stage 2- Effect of using larger coarse aggregate size and MFs in rubberized concrete joints.

Table 7-3 and Figure 7-12a show the displacement ductility values for tested joints with different percentages of CR and different coarse aggregate sizes (S7-S10). From the table, it can be seen that increasing the percentage of CR up to optimum limit (20% in mixtures

with 20mm coarse aggregate) increased the displacement ductility. For example, in 20mm coarse aggregate mixtures (S7-S9), increasing the percentage of CR from 10% to 20% increased the displacement ductility by 6.8%. This can be attributed to the high deformability and low stiffness of CR that helped to improve the strain capacity and deformability of beam-column joints. Further increase in the CR percentage beyond 20% (S9) resulted in a reduction in the displacement ductility compared with mixture with 20% CR. This can be related to the reduction in the joints' shear strength, which limited the deformability and changed the failure mode from B-mode to BJ-mode (as discussed above).

The results also indicated that in mixtures with low percentage of CR (up to 15%) increasing the coarse aggregate size from 10mm to 20mm slightly decreased the displacement ductility. For example, by looking at S4 compared with S8 (which have a similar percentage of CR (15%) and failure mode (B-mode)), increasing the coarse aggregate size from 10mm to 20mm reduced the displacement ductility by 9.2%. This can be related to the reduction in the compressive strength (see Table 7-1), which affected the displacement ductility, as mentioned above.

Table 7-3 and Figure 7-12b present the displacement ductility for tested joints with different lengths/volumes of MFs and different types of concrete (S11-S14). From the table and the figure, it can be noticed that adding MFs (35mm) to SCRC mixture with 15% CR significantly increased the displacement ductility, reaching up to 22.4%, compared with joint without MFs (S11 compared with S4). This can be related to the bridging mechanism of MFs, which allowed the joint to exhibit higher ultimate load and large deformation beyond the yield point. The results also indicated that changing the

concrete type from MFSCRC to MFVRC slightly increased the displacement ductility. This may be attributed to the higher ultimate load of MFVRC compared with MFSCRC, which resulted in higher ultimate deformation and in turn increased ductility. Moreover, increasing the fiber length (60mm) also enhanced the ductility compared with the control joint (S1) but with slightly less values compared with the 35mm MFs joint (S13 compared with S12). Figure 7-12b also showed that maximizing the percentage of CR up to 25% and MFs up to 1% significantly improved the displacement ductility reaching up to 50% compared with the control joint without MFs and CR (S14 compared with S1).

The brittleness index (BI) of tested joints was also investigated in this study. It should be noted that since concrete is a brittle material, it should have a higher BI value compared with other ductile materials. Table 7-3 and Figure 7-12a show the BI values for tested joints with different percentages of CR and different coarse aggregate sizes (S7-S10). From the results, it can be seen that the BI decreased as the percentage of CR increased up to optimum limit of 20% in mixtures with 20mm coarse aggregates. For example, increasing the percentage of CR in mixtures with 20mm coarse aggregate from 10% to 20% decreased the BI by 11.1% (S7-S9). The reduced BI values clearly highlight the improved ductility that resulted from increasing the CR percentage. However, further increase in the percentage of CR (more than 20%) appeared to increase the BI value (compared with 20% CR joint). This behavior can be related to the same reason explained before in the ductility section. The results also indicated that increasing the coarse aggregate size in small percentage of CR mixtures (up to 15%) slightly increased the BI of tested joints, which emphasized the slight reduction in the ductility resulted from increasing coarse aggregate size.

Table 7-3 and Figure 7-12b present the BI values for tested joints with different MF lengths/volumes and different concrete types (S11-S14). From the table, it can be seen that combining MFs (35mm) with 15% CR decreased the BI value by 21.7% compared with the mixture without MFs (S11 compared with S4). This reduction in BI value highlights the enhanced ductility of the beam-column joints. The results also showed that changing the concrete type from MFSCRC to MFVRC at the same percentage of MFs and CR slightly decreased the BI value (S12 compared with S11). This can be attributed to the same reason discussed in the ductility section. Also, using longer MFs (60mm) increased the BI value compared with using shorter MFs (35mm) (S13 compared with S12), but still with less BI value (improved ductility) compared with the joint without MFs (S13 compared with S4). Figure 7-12b also shows that combining maximum percentage of CR (25%) with maximum percentage of MFs (1%) significantly reduced the BI value compared with the control joint (S14 compared with S1), in which the reduction in BI value reached up to 41.4%.

7.5.3 Stage 3 – Effect of combining CR with different types, lengths, and volumes of SFs on structural behavior of beam-column joint.

Table 7-3 shows the displacement ductility for SFSCRC tested joints with different SF types (S15-S21). It can be seen that using MISFs appeared to have an inconsiderable effect on the ductility of the beam-column joint. For example, adding MISF19 exhibited an increase in the ductility that did not exceed 1% compared to the joint without fibers (S15 compared to S4). On the other hand, using MASFs appeared to have a significant increase in the displacement ductility, in which adding MASF38 to the SCRC joint

increased the displacement ductility by 20.8% compared to the joint without fibers (S17 compared to S4). This may be attributed to the same reasons discussed in earlier sections.

Table 7-3 and **Figure 7-13** present the displacement ductility for SFVRC tested joints with different lengths/types and volumes of MASFs. Increasing the fiber length generally showed a lower enhancement in the displacement ductility of beam-column joints. For example, using MASF38 in joint S18 and MASF50 in joint S19 increased the displacement ductility by 24.8% and 11.8%, respectively, compared to the joint without fibers (S4). As mentioned before, a higher number of single fibers oriented perpendicularly to the crack width is expected when shorter fibers are used. These fibers can better transfer the stress across the crack width and in turn help the joint to sustain higher load and larger deflection. The results also showed that using MASF54 showed better results in terms of displacement ductility than the joint with MASF50 (S20 compared to S19) but with lower enhancement than that achieved with MASF38 (S20 compared to S18). This may be related to the rough texture and higher tensile strength of MASF54 compared to MASF50 (see Table 3-2 and **Figure 3-3**). The highest improvement in the beam-column joints' ductility was noticed when MASF38 was used.

Table 7-3 and **Figure 7-13** also showed that increasing the CR percentage up to 15% helped to improve the joint ductility. However, further increase in the CR percentage above 15% showed a drop in the joint ductility, in which using 25% CR decreased the ductility by 19.7% compared to the joint with 15% CR (S6 compared to S4). Adding high percentage of MASFs (1%) to the joint with high percentage of CR (25%) compensated for the reduction in the joint ductility; achieving ductility reached up to 59% higher than the joint without fibers (S21 compared to S6). This may be attributed to the significant

contribution of the MASFs in transferring the stress across the cracked section, which helped the joint to sustain higher load/deformation at failure and, in turn, higher displacement ductility.

Table 7-3 and **Figure 7-13** show the BI values for SFSCRC tested joints with different SF types and different coarse aggregate sizes (S15-S21). Similar behavior found in the deformability, initial stiffness, and ductility was also noticed in the BI. Adding MISFs to SCRC joints exhibited a slight effect on the BI value, while adding MASFs appeared to have a significant effect (compared to the joint without fibers). For example, adding MISF19 and MASF38 to SCRC joints showed a reduction in the BI value reaching up to 4.3% and 21.7%, respectively.

Table 7-3 presents the BI values for SFVRC joints with different MASF lengths/types and different concrete types. The table also indicates that increasing the length of the MASFs showed lower reduction in the BI value. This behavior clearly confirmed the better enhancement in the joint ductility when shorter MASFs (38mm) were used compared to longer ones (50mm), as discussed earlier. The results also showed that MASF54 appeared to have a better impact on the joint ductility compared to MASF50. For example, using MASF54 in joint S20 and MASF50 in joint S19 showed a reduction in the BI reaching up to 17.4% and 13%, respectively, compared to the joint without fibers (S4).

The BI value also showed similar results concerning the effect of using high percentage of MASFs (1%) to compensate for the reductions in the joint ductility (resulting from using high percentage of CR). For example, adding high percentage of MASFs (1%) to the joint with high percentage of CR (25%) reduced the BI value by 50% compared to the

joint without fibers (S21 compared to S6). This result clearly emphasizes the significant enhancement in the joint ductility.

7.6 Energy dissipation

7.6.1 Stage 1- Determining optimum percentage of CR

The energy dissipation (Ed) from the structure can be classified into two types: “viscous damping,” which represents the energy dissipation in elastic range; and “hysteretic damping,” which represents the energy dissipation in post-elastic range. The hysteretic energy dissipation capacity is used to evaluate the nonlinear behavior of the structure under lateral loading. The hysteretic energy dissipated capacity for beam-column joints can be calculated by summing up the energy dissipated in successive load-tip displacement loops during the test. The energy dissipated for a cycle can be estimated as the area enclosed by a hysteretic loop in the load-tip deflection curve. Table 7-4 and Figure 7-11c present the energy dissipated for each step and the cumulative energy dissipated for SCRC tested specimens. From Table 7-4 and Figure 7-11, it can be observed that the energy dissipation increased by 21% by increasing the percentage of CR from 0% to 15%. This can be related to the low stiffness of CR particles, which exhibited a higher flexibility and hence dissipated a large amount of energy. On the other hand, further increase in the percentage of CR beyond 15% resulted in a reduction in the energy dissipated. This behavior can be attributed to the fact that higher percentages of CR (20% and 25%) significantly reduced the compressive strength and correspondingly decreased the joint shear strength. Decreasing the joint shear strength appeared to have an undesirable pinching effect, which limited the load carrying capacity/deformability and reduced the energy dissipation.

7.6.2 Stage 2- Effect of using larger coarse aggregate size and MFs in rubberized concrete joints.

Figure 7-14 shows the hysteretic cycles for all tested joints (S1-S21). Table 7-5 and Figure 7-12c show the energy dissipated for each load step and the cumulative energy dissipated for tested joints with different percentages of CR and different coarse aggregate sizes (S7-S10). From the table it can be seen that the hysteretic energy dissipation capacity increased as the percentage of CR increased up to 20% in mixtures with 20mm coarse aggregate. For example, increasing the percentage of CR from 10% to 20% in mixtures with 20mm coarse aggregate increased the energy dissipation capacity by 10.3% (S7 compared with S9). This can be related to the low stiffness of CR particles, which exhibited a higher flexibility and hence dissipated a large amount of energy. However, further increase in the percentage of CR beyond 20% resulted in a reduction in the energy dissipated (compared with mixture with 20% CR). This behavior can be attributed to the reduction in the shear strength from using high percentage of CR (more than 20%), which changed the failure mode from B-mode to BJ-mode. This decrease in the shear strength had an undesirable pinching effect, which limited the load carrying capacity/deformability and reduced energy dissipation. The results also indicated that increasing coarse aggregate size from 10mm to 20mm in mixtures with smaller percentages of CR (up to 15%) decreased the energy dissipation capacity. For example, when comparing S8 to S4, at the same percentage of CR (15%) and failure mode (B-mode), it can be seen that the energy dissipation capacity decreased by 12.2% when the coarse aggregate size increased from 10mm to 20mm. This can be attributed to the reduction in load carrying capacity and deformability that resulted from increasing coarse aggregate size, as mentioned before.

Table 7-5 and Figure 7-12d show the energy dissipation capacity for tested joints with different MF lengths/volumes and different concrete types (S11-S14). From the table, it can be seen that using MFs (35mm) considerably enhanced energy dissipation capacity, in which adding 0.35% MFs (35mm) to SCRC mixture with 15% CR increased the energy dissipation capacity by 50.5% compared with mixture without MFs (S11 compared with S4). This can be attributed to the same reason explained before regarding the effect of MFs in enhancing the ductility and BI. The results also indicated that changing the concrete type from MFSCRC to MFVRC slightly enhanced the energy dissipation by 6.5% (S12 compared with S11). This may be related to the higher ultimate load and ultimate deflection of MFVRC compared with MFSCRC joints. Adding longer MFs (60mm) increased the energy dissipation capacity compared with mixture without MFs but showed reduced energy dissipation compared with mixture with shorter MFs (35mm). For example, adding 60mm MFs to VRC mixture with 15% CR increased the energy dissipation capacity by 46% compared with mixture without MFs (S13 compared with S4) and this increase was less than that obtained when shorter MFs (35mm) was used (S13 compared with S12). At the same volume of MFs, shorter fiber mixtures will have a higher number of fibers disperse in the mixture, which in turn increases the probability of fibers oriented perpendicular to cracks. This can efficiently contribute to transferring the stress across the cracks and allowing higher energy dissipation. It can also be noted that combining high percentage of MFs (1%) with high percentage of CR (25%) appeared to significantly enhance the energy dissipation capacity of beam-column joints. By comparing the energy dissipation capacity of joint S14 to the control joint S1, it can

be noticed that the energy dissipation capacity increased by 53.6% when using high percentage of MFs and CR.

7.6.3 Stage 3 – Effect of combining CR with different types, lengths, and volumes of SFs on structural behavior of beam-column joint.

Table 7-6 shows the energy dissipated for SFSCRC joints with different SF types. It can be seen that adding SFs generally helped to increase the energy dissipation for beam-column joints. This can be attributed to the role of fibers in stitching the cracks and restricting the widening and propagation of the cracks, which helped the joints to sustain higher loads and experience larger deformation, and therefore dissipate more energy before failure. In SFSCRC joints, using MISF19 and MISF27 (S15-S16) increased the energy dissipation capacity by 4.1% and 8.8%, respectively, compared to the joint without fibers (S4), while this increase reached up to 36.8% when MASF38 was used.

Table 7-6 and **Figure 7-13** also show the energy dissipated capacity for SFVRC tested joints with different MASF lengths/types and different concrete types (S18-S21). Changing the concrete type from SFSCRC to SFVRC did not show a significant effect on the energy dissipation capacity of tested joints. The results also showed that increasing the MASF from 38mm to 50mm showed less improvement in the energy dissipation capacity of the beam-column joint compared to the joint without fibers (S4). It should be noted that MASF38 showed the highest increase in energy dissipation among all types/lengths of SFs used in this study. Adding high percentage of MASFs (1%) to the joint that had a high percentage of CR (25%) helped to significantly compensate for the reduction in the energy dissipation capacity that resulted from using high percentage of CR. For example, adding 1% MASFs to the joint with 25% CR (S21) compensated for

the reduction in the energy dissipation capacity up to 45.4% compared to the joint without SFs. (S6). This may be attributed to the stitching mechanism of fibers, which contributed to enhancing the joint shear strength and hence helped the joint to sustain higher ultimate load and larger deformation, leading to higher energy dissipation capacity.

7.7 First crack load and ultimate load

7.7.1 Stage 1- Determining optimum percentage of CR

The first crack load was observed visually and then confirmed with the value associated with the change in slope of the load-tip deflection envelop curve for SCRC tested specimens. Table 7-2 and Figure 7-11b show the first crack load and ultimate load for SCRC tested specimens. It can be observed that increasing the percentage of CR generally reduced the first crack load and ultimate load for beam-column joints subjected to reverse cyclic loading. It can also be noticed that the first crack load was more affected by increasing the percentage of CR compared to the ultimate load. Increasing the percentage of CR from 0% to 25% reduced the first crack load by 39% while the ultimate load was reduced by 19%. It should be noted that the first crack load is more affected by the tensile strength of concrete compared to the ultimate load. Since increasing the percentage of CR in the mixture greatly reduced the tensile strength of concrete (Table 7-1), the reduction in the first crack load was more pronounced than the reduction in the ultimate load.

7.7.2 Stage 2- Effect of using larger coarse aggregate size and MFs in rubberized concrete joints.

Table 7-2 and Figure 7-12e show the first crack load and ultimate load for tested joints with different percentages of CR and different coarse aggregate sizes (S7-S10). From the table, it can be seen that increasing the percentage of CR generally decreased the first crack load and ultimate load for beam-column joints subjected to reverse cyclic loading. It can also be noted that the first crack load was more affected by increasing the percentage of CR compared with the ultimate load. For example, increasing the percentage of CR from 10% to 25% in mixtures with 20mm coarse aggregate (S7-S10) decreased the first crack load by 17.6% while the ultimate load was reduced by 9.3%. It is worth noting that the first crack load is more affected by the tensile strength of concrete compared with the ultimate load. Therefore, reducing tensile strength of concrete due to increasing the percentage of CR (see Table 7-1) significantly reduced the first crack load compared with ultimate load. Table 7-2 also shows that using larger coarse aggregate (20mm) in mixtures with smaller percentages of CR (up to 15%) resulted in a slight reduction in the first crack load and ultimate load compared with joints with smaller aggregate size (S8 compared with S4). However, in beam-column joints with higher percentage of CR (20%), using larger coarse aggregate (20mm) helped to enhance joint shear strength and change failure mode (see Figure 7-9), which in turn increased the ultimate load (S9 compared with S5).

Figure 7-12f and Table 7-2 show the first crack load and ultimate load for MFSCRC and MFVRC tested joints. From the table, it can be seen that using MFs (35mm) appeared to significantly increase the first crack load and load carrying capacity compared with joints without MFs (S11 compared with S4). This behavior may be attributed to the mechanism

of MFs in delaying the initiation of internal micro cracks and forcing the cracks to take a meandering path, demanding more energy for further propagation and in turn increasing the load carrying capacity. Similar behavior for first crack load and ultimate load of MFSCRC joints was also noticed in MFVRC joints (S12 compared with S11). The results also showed that using longer MFs (60mm) slightly decreased the first crack load and load carrying capacity compared with shorter ones (35mm). As mentioned before, beam-column joints with high percentage of CR (25%) exhibited a different failure mode (BJ-mode) with decreased load carrying capacity. Combining high percentage of MFs (1%) with high percentage of CR (25%) (S14) appeared to immensely enhance the beam-column joint behavior. Although S14 contains high percentage of CR (25%), which reduces the load carrying capacity of the joint, adding 1% MFs in this joint enhanced the ductility, BI, deformability, and energy dissipation and also compensated for the reduction in the load carrying capacity, achieving strength comparable to the control joint (S1).

7.7.3 Stage 3 – Effect of combining CR with different types, lengths, and volumes of SFs on structural behavior of beam-column joint.

Table 7-2 presents the first crack load and load carrying capacity of SFSCRC joints with different SF types and different coarse aggregate sizes (S15-S21). It can be seen that adding SFs to SCRC joints generally increased the first crack load and load carrying capacity of beam-column joints. For example, adding MASF38 to the SCRC joint increased the first crack load and ultimate load by 37.8% and 10.4%, respectively, compared to the joint without fibers (S17 compared to S4). This may be attributed to the role of SFs in delaying the initiation of internal micro-cracks and pushing the cracks to

take a meandering path, which requires more energy for further propagation. Table 7-2 also shows that the effect of using fibers was more pronounced on the first crack load compared to the ultimate load. This may be related to the fact that the first crack load is more affected by the tensile strength compared to the ultimate load. Therefore, the increased tensile strength of concrete mixtures that resulted from using SFs significantly increased the first crack load compared to the ultimate load.

Using MASFs in SCRC joints exhibited a higher first crack load and ultimate load compared to using MISFs. For example, using MASF38 increased the first crack load and ultimate load by 31.3% and 9.16%, respectively, compared to the joint with MISF19 (S17 compared to S15).

Table 7-2 shows the first crack load and ultimate load for SFVRC joints with different MASF lengths/types and different concrete types. Shorter MASFs (MASF38) showed better results compared to longer MASFs (MASF50). The highest increase in the first crack load and ultimate load in all tested fibers was noticed with MASF38. Table 7-2 also shows that adding 1% MASF38 to joint with 25% CR contributed to recovering the reductions in the first crack load and ultimate load as a result of using high percentage of CR and achieved strength comparable to the control joint (S21 compared to S1).

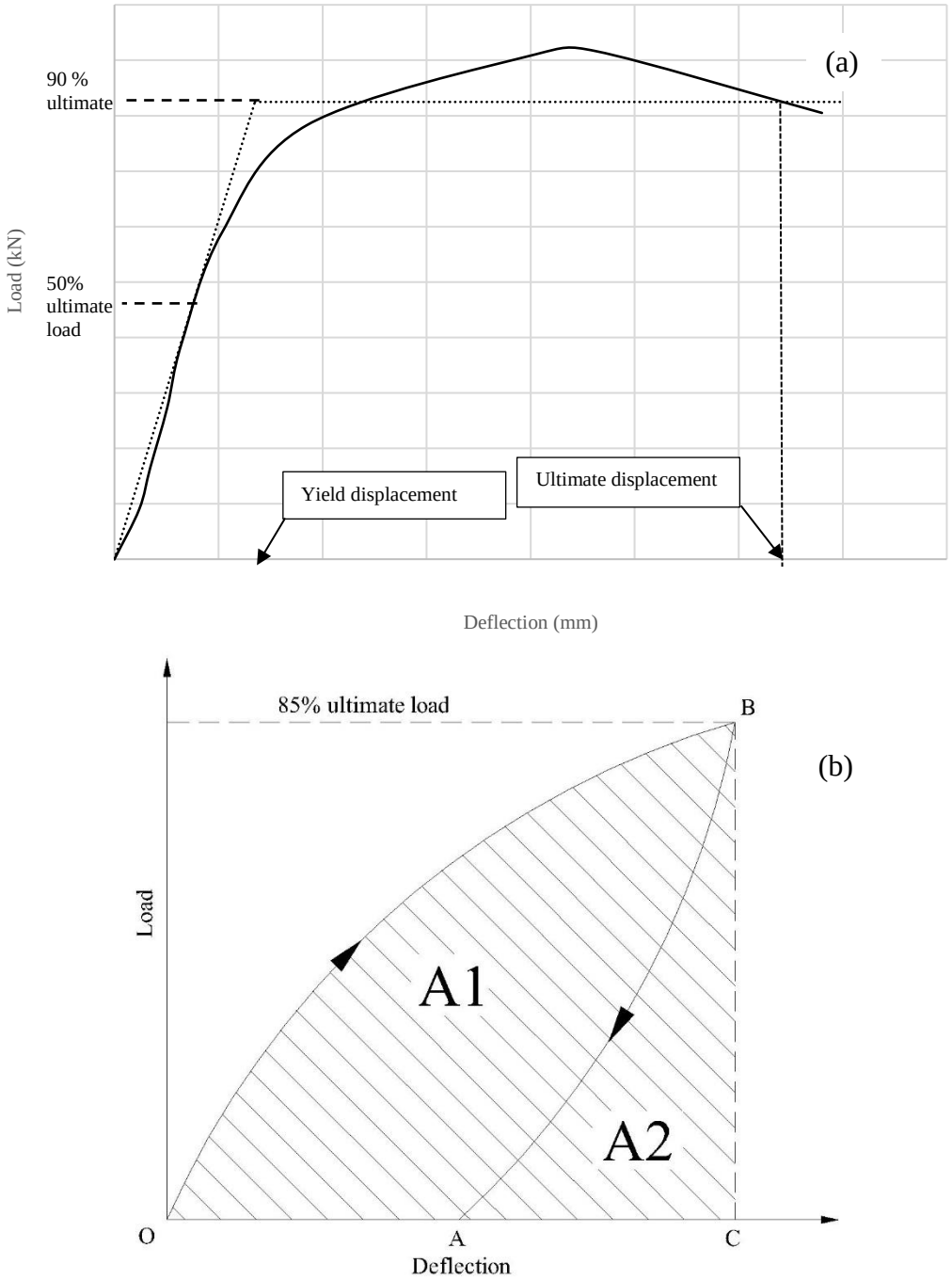

Figure 7-10 (a) Definition of ductility, (b) Definition of brittleness index

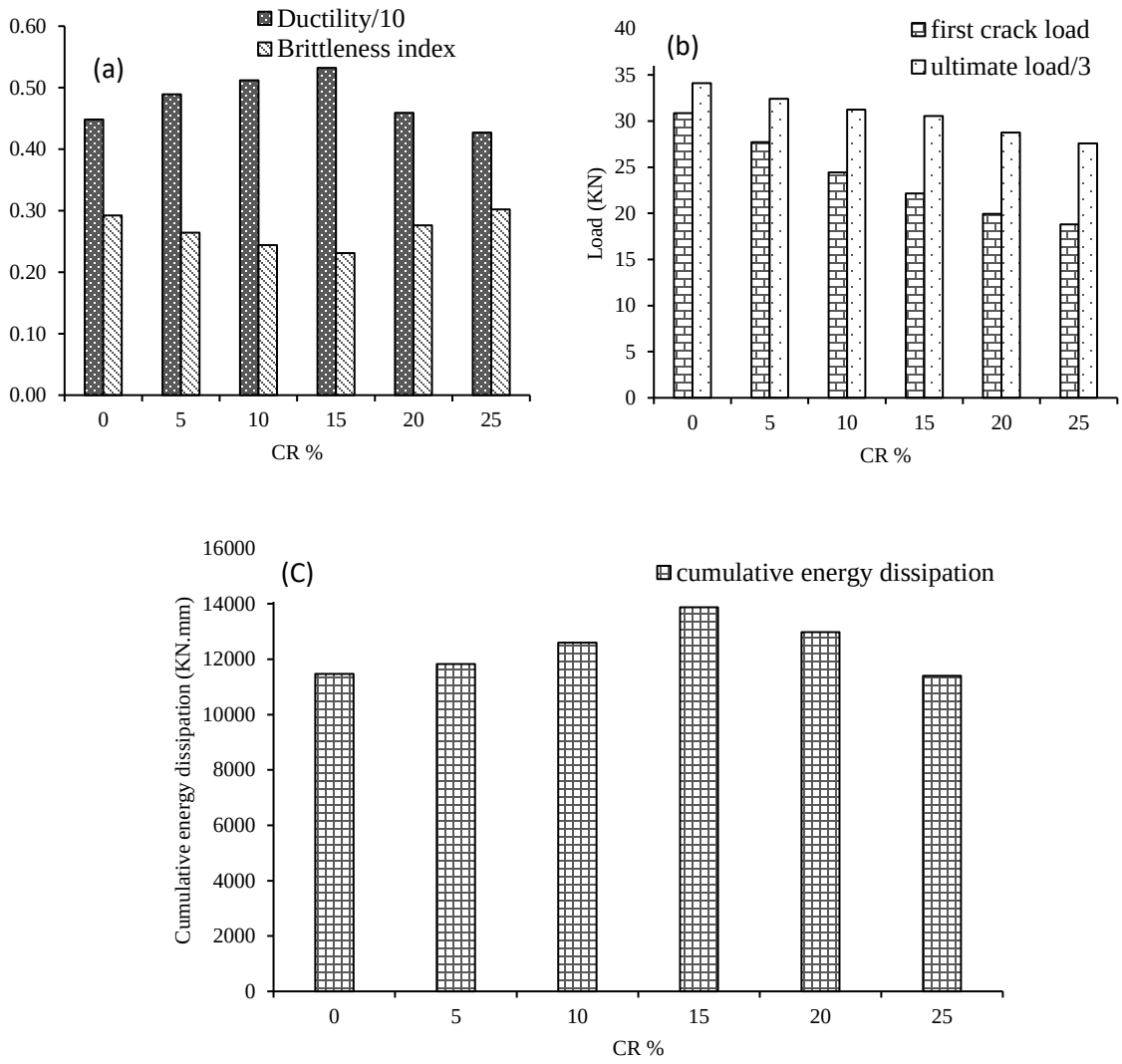

Figure 7-11 Influence of CR % on the first crack load, ultimate load, ductility, brittleness, and energy dissipation

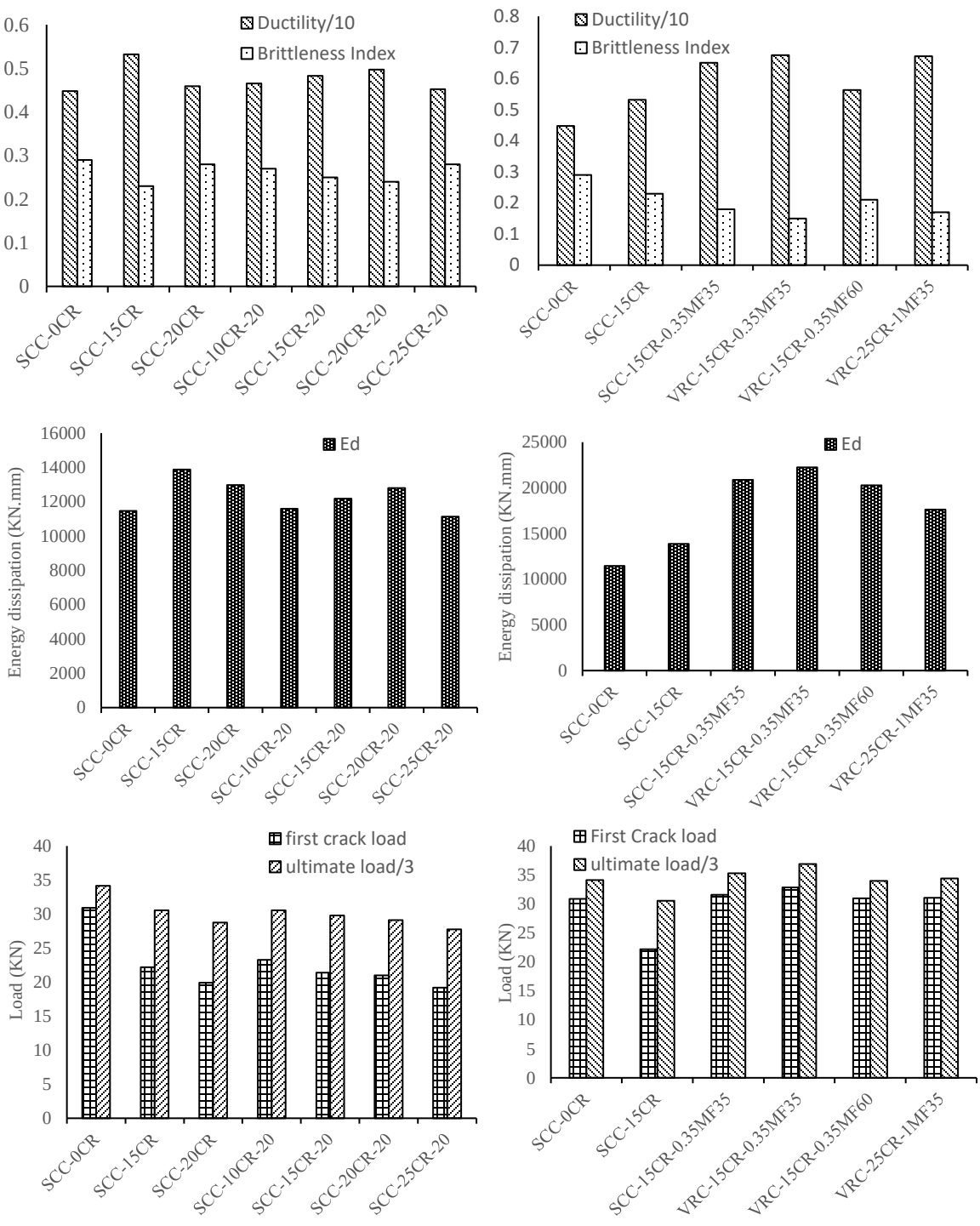

Figure 7-12 Influence of CR %, coarse aggregate size, MFs volumes/lengths on the first crack load, ultimate load, ductility, brittleness, and energy dissipation

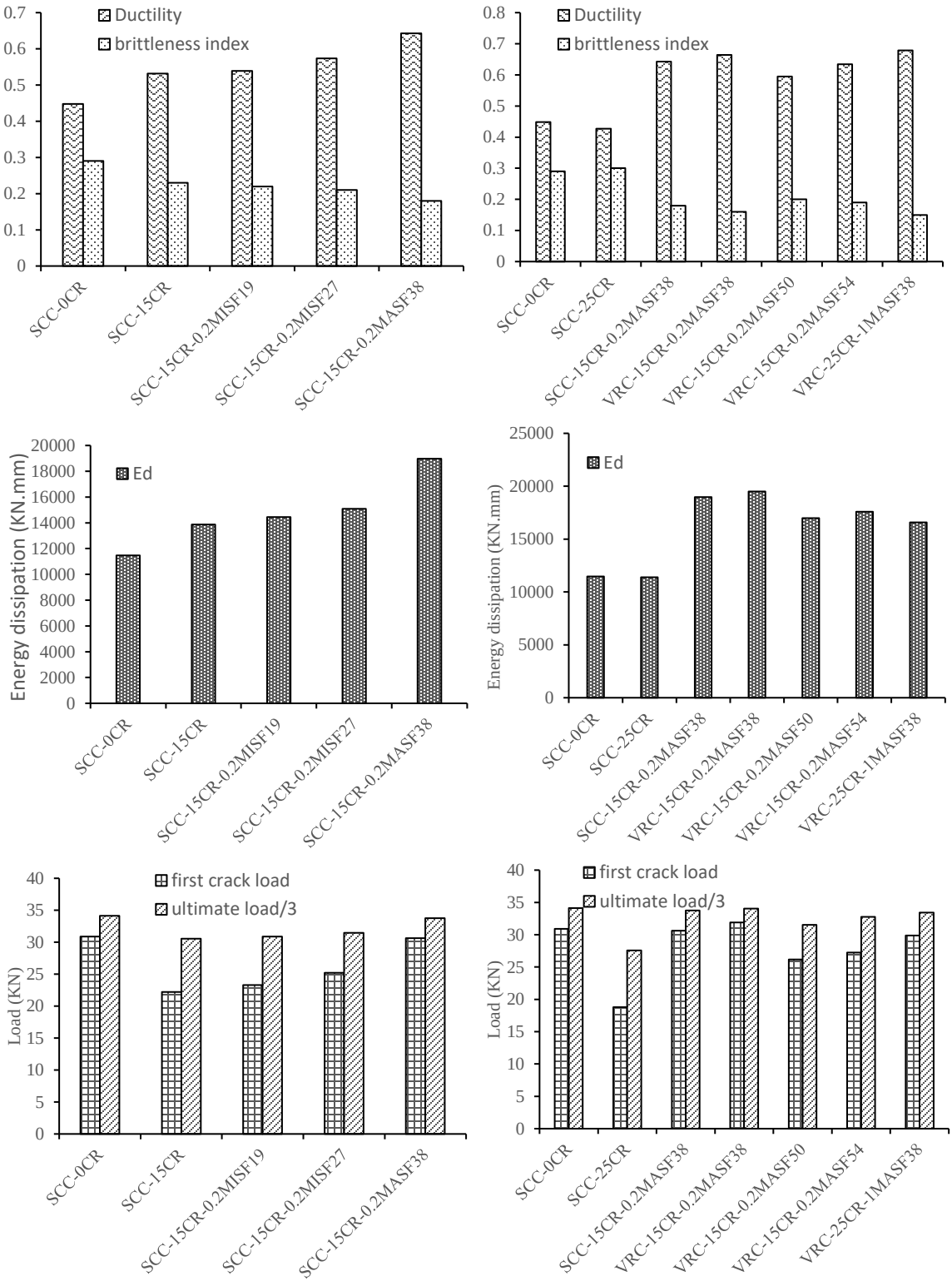

Figure 7-13 Influence of SFs types, lengths, and volumes on the first crack load, ultimate load, ductility, brittleness, and energy dissipation

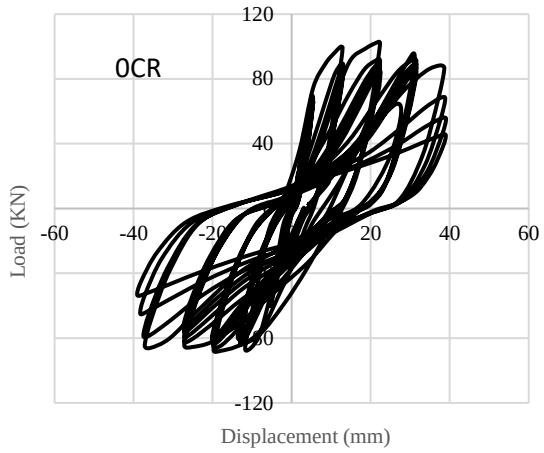
0CR
120
80
40
-120
-60
-40
20
40
60
Load (KN)
Displacement (mm)

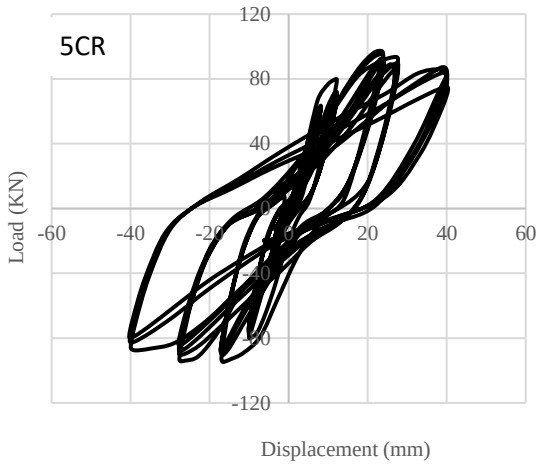
5CR
120
80
40
-120
-60
-40
20
40
60
Load (KN)
Displacement (mm)

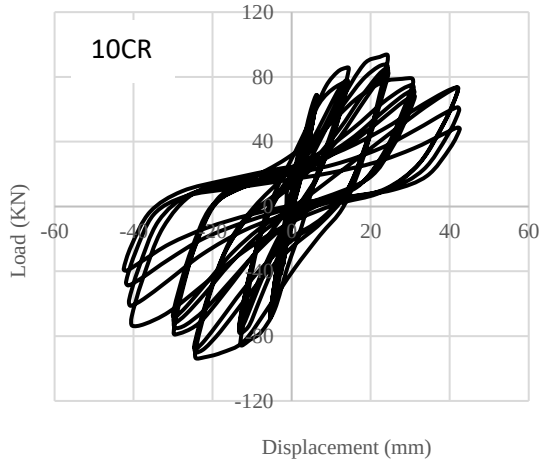
10CR
120
80
40
-120
-60
20
40
60
Load (KN)
Displacement (mm)

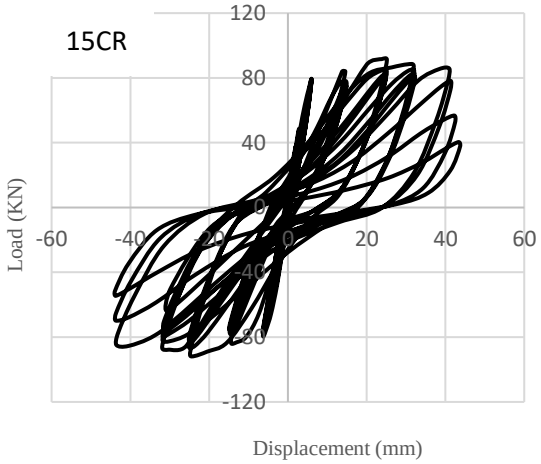
15CR
120
80
40
-120
-60
-40
20
40
60
Load (KN)
Displacement (mm)

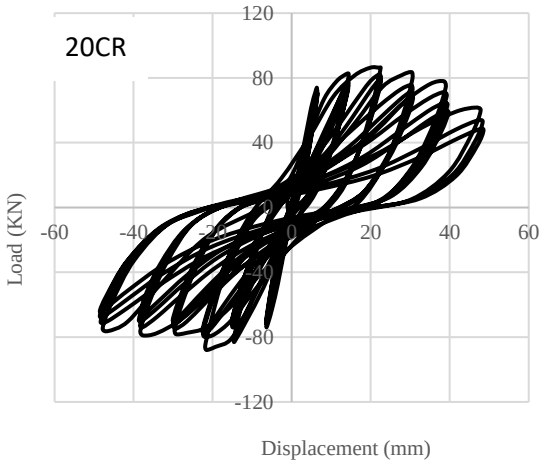
20CR
120
80
40
-80
-120
-60
-40
20
40
60
Load (KN)
Displacement (mm)

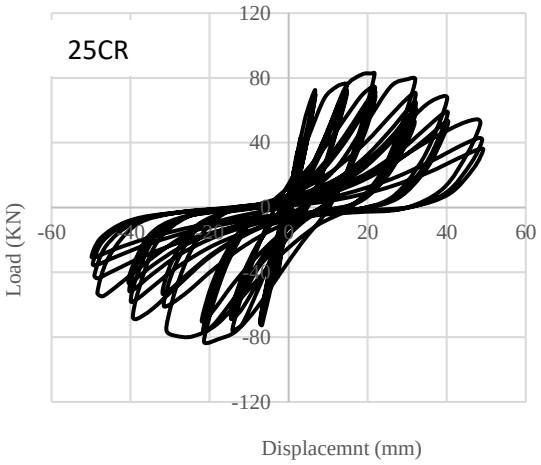
25CR
120
80
40
-80
-120
-60
-40
20
40
60
Load (KN)
Displacemnt (mm)

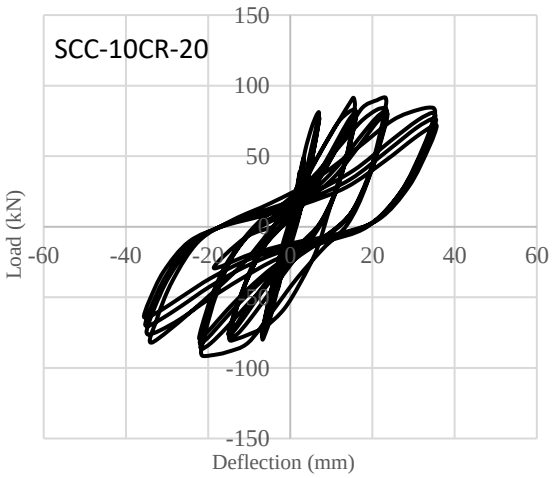
SCC-10CR-20
Load (kN)
Deflection (mm)

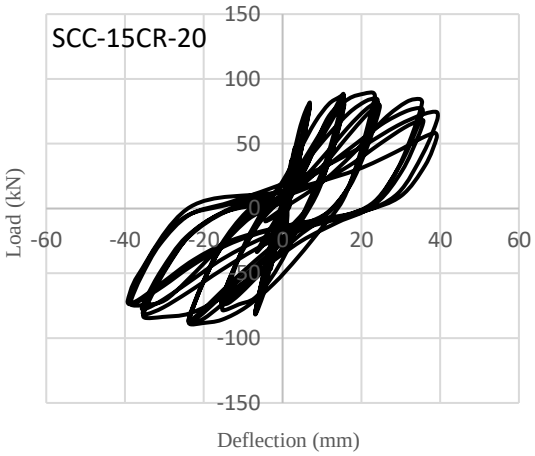
SCC-15CR-20
Load (kN)
Deflection (mm)

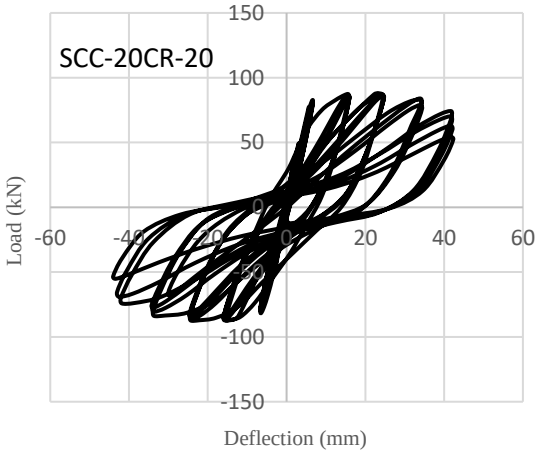
SCC-20CR-20
Load (kN)
Deflection (mm)

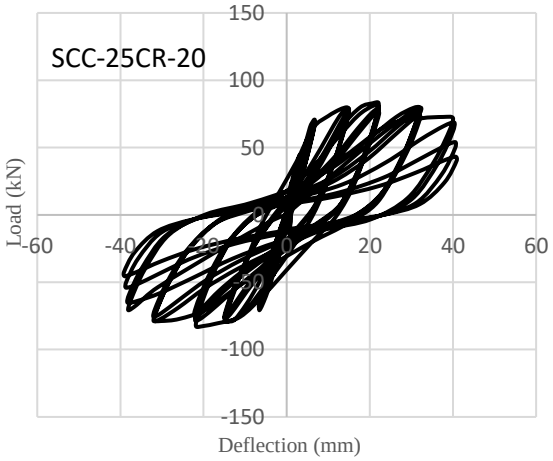
SCC-25CR-20
Load (kN)
Deflection (mm)

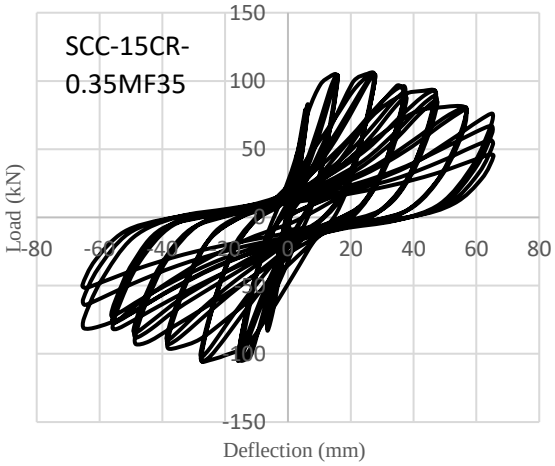
SCC-15CR-
0.35MF35
Load (kN)
Deflection (mm)

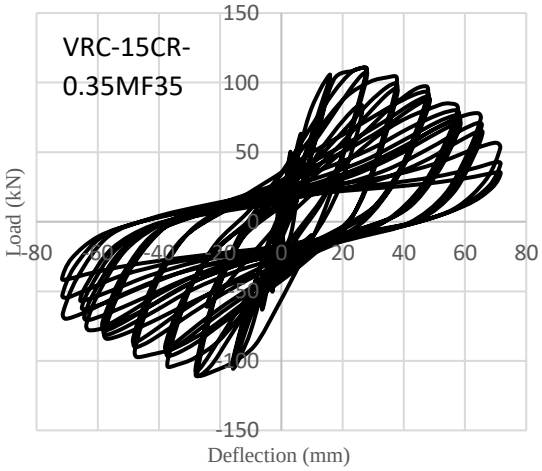
VRC-15CR-
0.35MF35
Load (kN)
Deflection (mm)

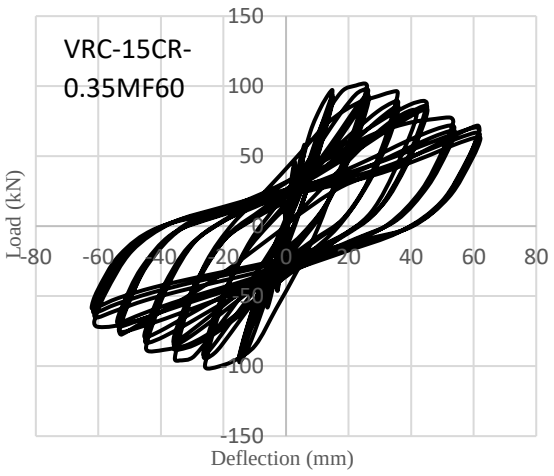
VRC-15CR-
0.35MF60
Load (kN)
Deflection (mm)

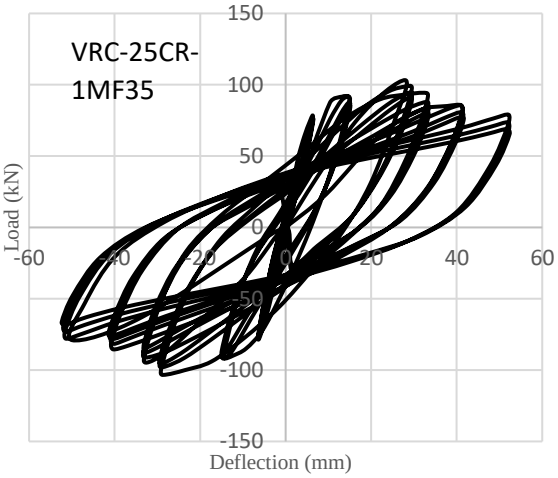
VRC-25CR-
1MF35
Load (kN)
Deflection (mm)

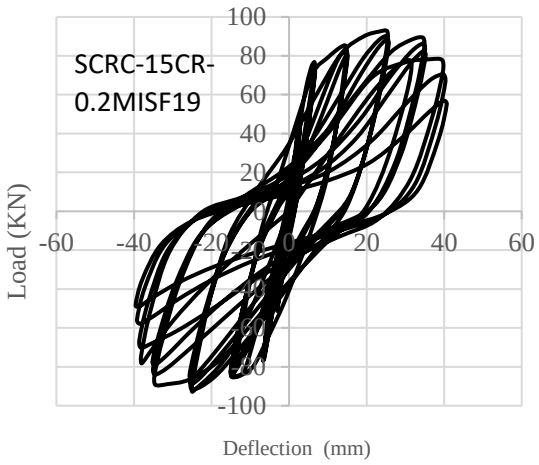
SCRC-15CR-
0.2MISF19
Load (KN)
Deflection (mm)

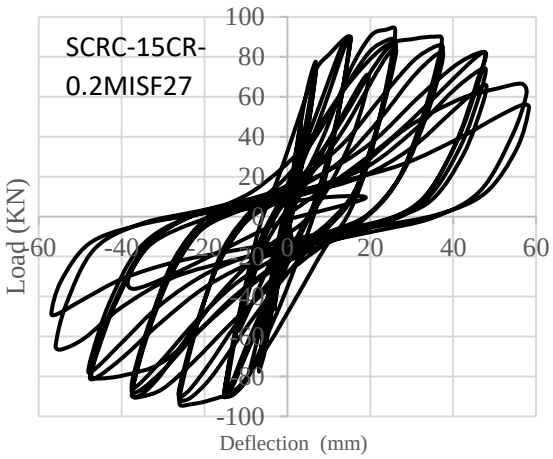
SCRC-15CR-
0.2MISF27
Load (KN)
Deflection (mm)

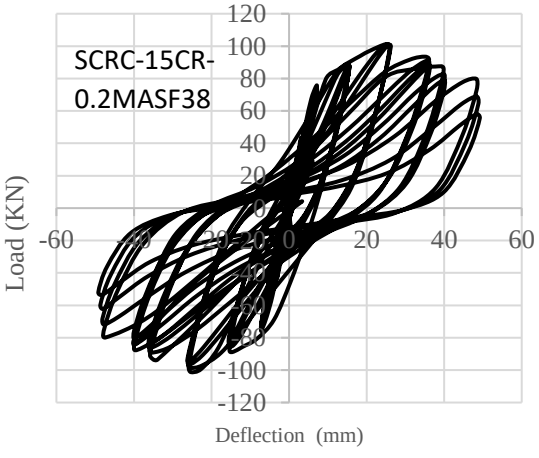
SCRC-15CR-
0.2MASF38
Load (KN)
Deflection (mm)

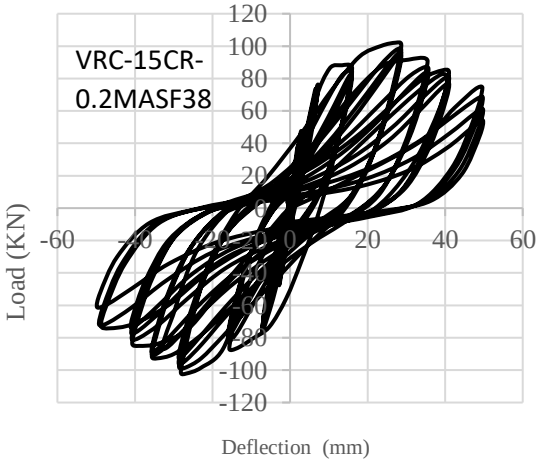
VRC-15CR-
0.2MASF38
Load (KN)
Deflection (mm)

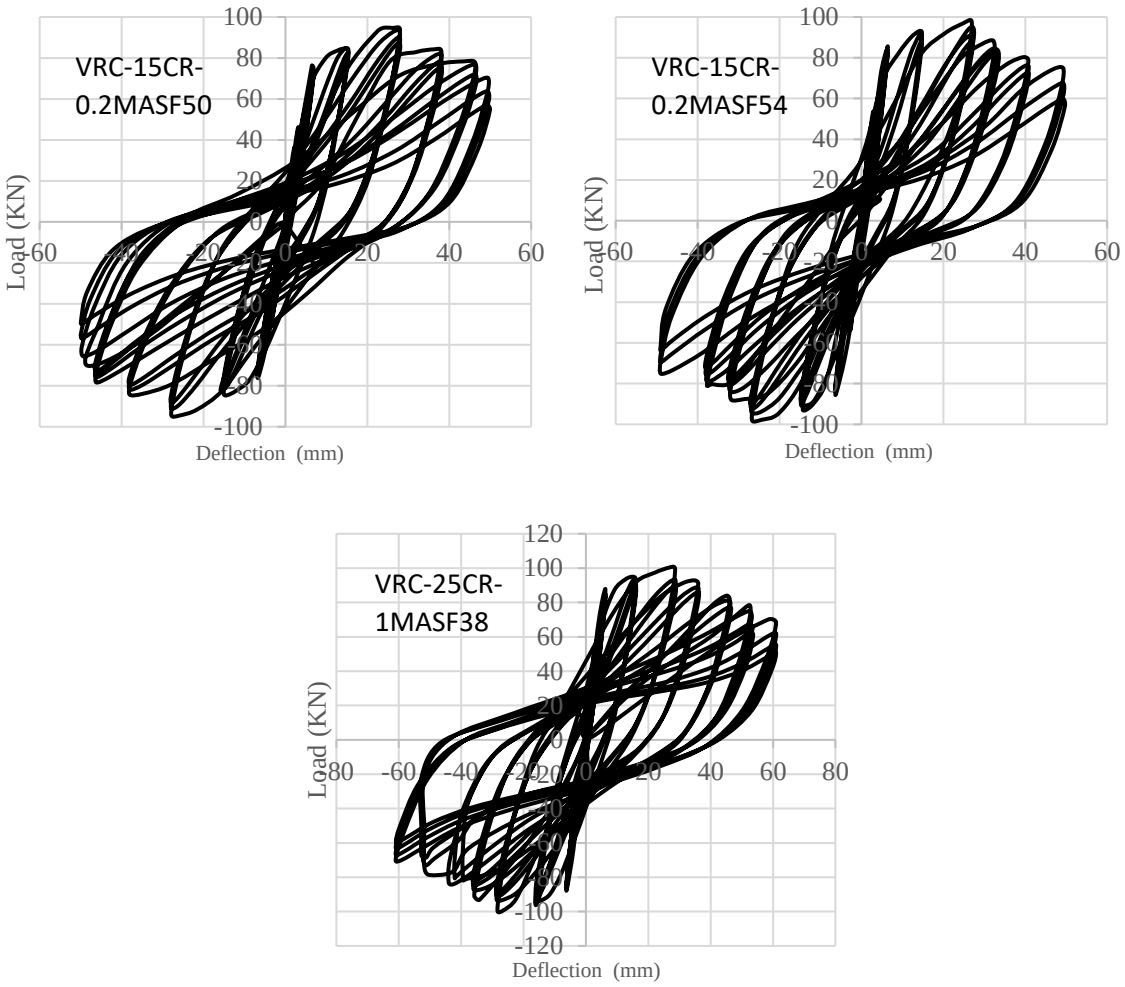

Figure 7-14 Load deflection curve for reverse cyclic loading (hysteresis cycles) for tested joints

8 Discussion of results from experimental study 5: structural behavior of rubberized ECC beam-column joints under cyclic loading

8.1 Introduction

This chapter presents the structural behavior of rubberized engineered cementitious composite (ECC) beam-column joints under cyclic loading. The effect of using different cementitious materials (SCMs) and different sand types on the cyclic behavior of ECC joints were also investigated. The main parameters were the percentage of CR (0%, 5%, 10%, and 15% by volume of sand), type of SCMs (MK, SLF, and FA), and type of sand used (silica sand and natural sand). The investigation also tested a conventional normal concrete with 10mm coarse aggregate size for comparison. The beam-column joint in this study was designed according to strong-column weak beam concept to put more focus on the ductile failure rather than brittle failure. The structural performance of tested beam-column joints was evaluated based on the load-deflection envelop response, hysteresis behavior, initial stiffness, deformability, cracking behavior, displacement ductility, brittleness index, energy dissipation, first cracking load , and ultimate load. **Table 8-1**, **Table 8-2** and **Table 8-3** present the results obtained from the cyclic load tests of tested joints. The results and discussions presented in this chapter have been published in the paper number eight mentioned earlier at the beginning of this thesis.

Table 8-1 Yield deflection, ultimate deflection, ductility, brittleness index, compressive strength, and STS

Joint #	Mixture ID	Deflection at yield Δy (mm)	Deflection at ultimate load (mm)	Ultimate deflection Δu (mm)	Ductility (Δu / Δy)	Brittleness index	*f'c* (MPa)	STS (MPa)
S1	ECC-FA	4.58	18.82	27.5	6	0.2	49	6.4
S2	ECC-FA-5CR	5.08	19.86	33	6.49	0.18	45.6	6.1
S3	ECC-FA-10CR	5.22	20.41	35.8	6.86	0.16	39.7	5.8
S4	ECC-FA-15CR	5.6	21.2	39.8	7.1	0.15	35.2	5.6
S5	ECC-MK	4.25	16.6	24	5.65	0.22	63.3	7.2
S6	ECC-SLF	4.32	17.63	25	5.79	0.21	54.8	6.7
S7	ECC-FA-NS	4.8	16.87	25.5	5.31	0.23	48.5	6.3
S8	NC	5.67	13.6	22.1	3.9	0.33	51	3.5

Table 8-2 Results of reverse cyclic loading

Joint #	Mixture ID	First crack load (KN)	Ultimate load (KN)	Failure mode	Initial stiffness (KN/mm)	Crack width	
						At beam-column interface (mm)	Within joint panel (mm)
S1	ECC-FA	36.05	110.71	B-mode	23.45	4.8	--
S2	ECC-FA-5CR	33.1	105.24	B-mode	21.36	4.5	--
S3	ECC-FA-10CR	29.6	101.46	B-mode	19.98	4	--
S4	ECC-FA-15CR	26.7	97.63	B-mode	18.5	3.5	--
S5	ECC-MK	40.15	121.46	B-mode	26.71	3.8	--
S6	ECC-SLF	38.91	118.06	B-mode	25	4	--
S7	ECC-FA-NS	33.04	102.79	B-mode	19.73	5	--
S8	NC	28.5	92.5	B-mode	15.9	5.7	--

Table 8-3 Cumulative energy dissipation

Step #	S1	S2	S3	S4	S5	S6	S7	S8
	E_d (KN.mm)	E_d (KN.mm)	E_d (KN.mm)	E_d (KN.mm)	E_d (KN.mm)	E_d (KN.mm)	E_d (KN.mm)	Ed (kN.mm)
1	1.0	1.4	1.6	1.7	1.0	1.0	0.9	0.2
2	4.6	5.1	5.2	6.1	4.4	4.5	4.2	1.0
3	14.2	26.9	28.3	31.0	14.1	14.1	11.6	4.5
4	40.7	69.3	76.4	89.4	38.1	39.1	37.5	20.2
5	105.1	133.0	159.2	177.0	93.4	97.2	91.1	39.7
6	379.9	506.1	628.7	768.2	351.0	361.2	319.4	169.5
7	2268.8	2402.7	2645.4	3173.0	2116.1	2188.9	2091.6	1269.5
8	6130.2	6380.8	6815.1	7455.8	5968.0	6087.7	5776.5	3329.1
9	10163.8	10420.8	11019.4	12649.9	9847.1	10056.1	9666.3	5940.6
10	14918.5	15326.3	16614.8	19416.7	13144.6	14199.0	13098.4	9236.6
11	21251.2	22488.4	23677.8	26170.8	19642.7	20194.0	18874.7	13610.9

8.2 Mechanical properties results

Table 8-1 shows the 28-day compressive strength and STS of all tested mixtures. From the table, it can be seen that the NC mixture exhibited a compressive strength and STS of 51 MPa and 3.5 MPa, respectively. For ECC mixtures, the inclusion of CR as a partial replacement of silica sand generally reduced the compressive strength and STS of developed mixtures. For example, adding 5% CR to ECC mixture (S2) reduced the compressive strength and STS by 7% and 4.7%, respectively, compared to reference ECC mixture without CR (S1). Farther increase in the percentage of CR (above 5%), resulted in a further decrease in the compressive strength and STS. For instance, a significant reduction in the compressive strength and STS reached up to 28.2% and 12.5%, respectively, was observed when the percentage of CR increased to 15%. This behavior may be attributed to

- The elastic nature of CR compared to the hardening cement mortar, which allows the CR to experience higher strain compared to hardening mortar and in turn developing and propagating numerous micro-cracks which weaken mixture (Ismail and Hassan, 2016; Najim and Hall, 2010).
- The significant low stiffness of CR particles compared to hardened cement paste which contributes to neglect the area of CR particles in resisting the applied load and in turn reducing the effective area that resisting applied stress (Khaloo et al., 2008).

The results also showed that partial replacement of FA with other SCMs such as MK and SLF increased the compressive strength and STS of ECC mixtures. For example, partial

replacement of FA with MK immensely increased the compressive strength and STS by 29.2% and 12.5%, respectively (S5 compared to S1). These increases reached up to 11.8% and 4.7%, respectively (S6 compared to S1), when SLF was used. The increase in the compressive strength and STS with the addition of MK or SLF may be attributed to the high pozzolanic reactivity of MK and SLF compared to FA which helped to significantly density the mixture and increase the overall mechanical properties of tested mixtures. From Table 8-1, it can be also noted that replacing the silica sand with natural sand with larger aggregate size showed a negligible effect on the compressive strength and STS of ECC mixtures. For example, the difference in compressive strength and STS did not exceed 1% when silica sand was fully replaced with natural sand (S7 compared to S1).

8.3 Load-deflection envelop curves

Figure 8-1a shows the envelop load-deflection curves for ECC joints with different CR percentages. The envelop curves were drawn based on the points of maximum load from the first cycle of each load step and their corresponding deflections from the hysteresis loop. From the figure, it can be seen that there is a slight difference between the maximum load in the push and pull directions. This may be related to the geometrical imperfections and steel bars disposition. Table 8-1 shows the results of ultimate deflections and deflections corresponding to ultimate load, in which ultimate deflection represents the deflection corresponding to 90% of ultimate load in the descending branch of load-deflection envelop curve. This percentage was chosen based on previous studies conducted in this area (Faleschini et al., 2017; Paulay, 1989). From Figure 8-1a and Table

8-1, it can be observed that increasing the CR percentage generally increased the ultimate deflection and deflection corresponding to ultimate load. For example, increasing the CR percentage from 0% to 15 % significantly increased the ultimate deflection and deflection corresponding to ultimate load by 44.7% and 12.6%, respectively, (S4 compared to S1). This may be attributed to the high elasticity of CR particles which exhibit a large elastic deformation before failure (Ganesan et al., 2013). Figure 8-1a also showed that adding CR generally reduced the rate of strength degradation after reaching the ultimate load. By comparing joint S4 with 15% CR to joint S1 with 0% CR, it can be seen that the slope of the descending branch of load-deflection curve for S4 is more flattened compared to that of joint S1, indicating a more ductile failure. It can be also noted that increasing the percentage of CR appeared to decrease the initial stiffness of beam-column joints. This can be related to the reduction in the compressive strength resulted from adding CR.

Figure 8-1b shows the load-deflection envelop curve for NC joint and ECC joints with partial replacement of FA with MK and SLF and fully replacement of silica sand with natural sand (S5-S8). Table 8-1 presents the deflections at ultimate load and ultimate deflections for joints (S5-S8). Partial replacement of FA with MK or SLF appeared to have a negative effect on the ultimate deflection and deflection at ultimate load. For example, partial replacement of FA with MK reduced the ultimate deflection and deflection at ultimate load by 12.7% and 11.8%, respectively, while these reductions reached up to 9% and 6.3%, respectively, when SLF was used. The results also revealed that using MK or SLF increased the initial stiffness of beam-column joints by 13.9% and 6.6%, respectively compared to joint with FA only (S5 and S6 compared to S1). This may be related to the enhancement of the fiber-matrix chemical bond and the increase in the

matrix toughness when using MK or SLF compared to FA only (Wang and Li, 2006; Şahmaran st al., 2009). By looking at Figure 8-1b, it can be also seen that the rate of strength degradation in joint with MK is slightly higher than that of joint with SLF and reference joint (S5 compared to S1 and S6), indicating a slight brittle failure. The results also indicated that the full replacement of silica sand with natural sand resulted in a reduction in the initial stiffness (15.9%), ultimate deflection and deflection at ultimate load. This may be attributed to that larger aggregate size in natural sand increases the possibility of aggregate interlock which provide higher matrix toughness (Li, 1997; Li et al., 1995) and therefore, leads to a lower deformation capacity. It should be noted that NC joint showed the lowest deformation capacity compared to all tested ECC joints. By comparing reference joint S1 to NC joint S8, it can be seen that the slope of the descending branch of load-deflection envelop curve for S1 is more flattened compared to that of joint S8, indicating a more ductile failure. Moreover, the slope of the linear portion of load-deflection envelop curve for NC joint (S8) appeared to be lower than that of reference joint S1, indicating lower initial stiffness of joint S8 compared to S1.

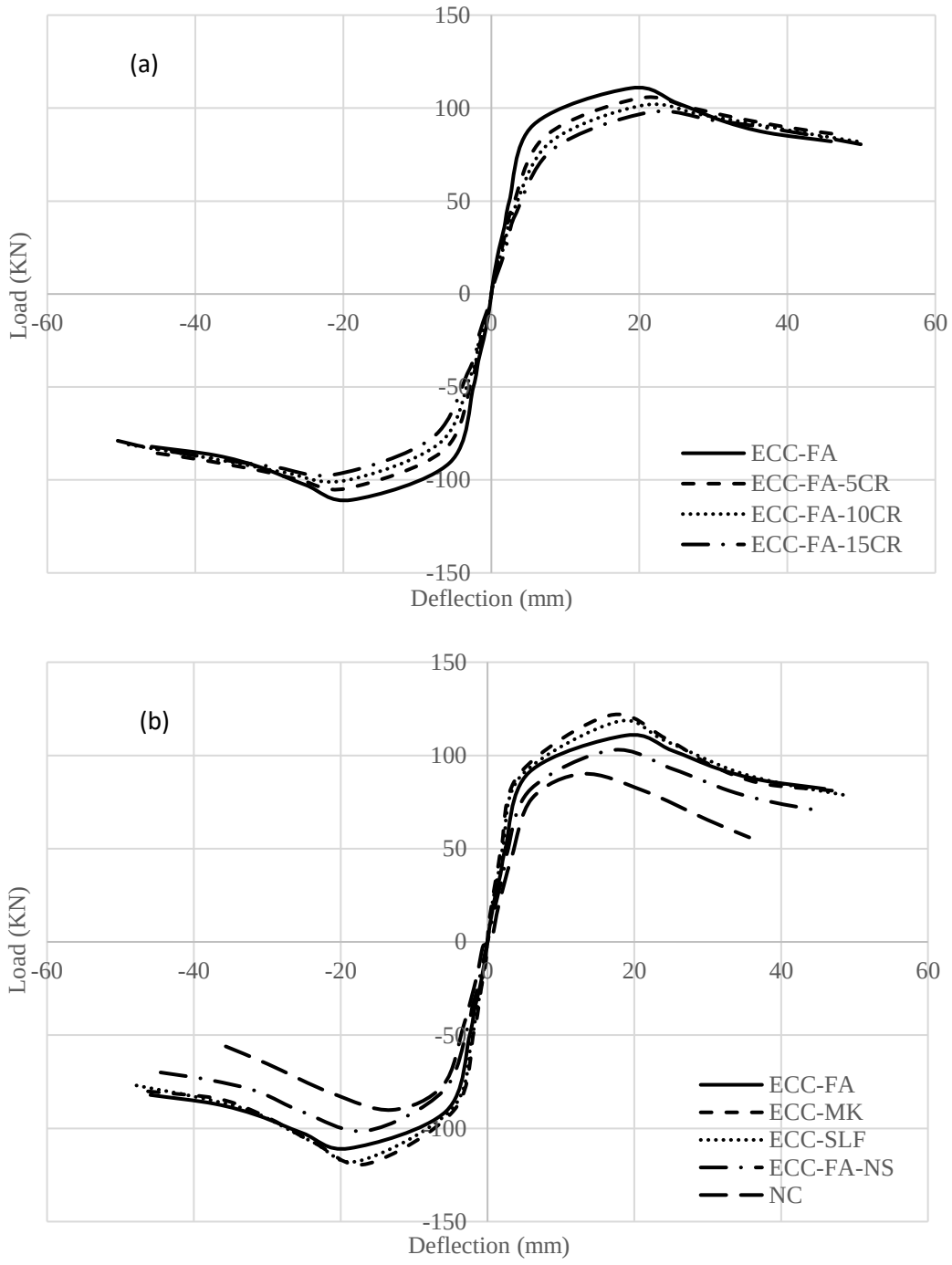

Figure 8-1 Load-deflection envelop curves a) ECC joints with different percentage of CR, b) NC joint and ECC joints with different SCMs and different aggregate type.

8.4 Failure modes and cracking pattern

Figure 8-2 shows the cracking pattern for tested ECC joints with different percentage of CR, different SCMs, and different sand type. All crack widths in Figure 8-2 are in mm and their values are corresponding to the failure load at cycle 21 (load step 7). Table 8-2 presents the maximum crack width at failure stage and failure mode for the tested joints. It can be observed that all tested joints showed beam yielding failure (B-mode), in which the beam longitudinal reinforcement reached yield (as indicated by the strain gauges attached to the steel reinforcement) without any visual sign of shear failure within the beam-column joint (see Figure 8-2). Figure 8-2 also showed that increasing the percentage of CR generally increased the number of cracks but with smaller crack widths. For example, increasing the percentage of CR from 0% to 15 % increased the number of cracks from 11 to 16 cracks and decreased the maximum crack width from 4.8mm to 3.5mm (joint S1 compared to S4). This may be attributed to the reduction in the concrete tensile strength that resulted from adding CR, as confirmed by STS results (See Table 8-1). This reduction in the tensile strength allowed to initiate more cracks compared to joint without CR. In addition, the low modulus of elasticity of CR particles resulted in a differential strain rate between soft rubber particle and hardened cement matrix. This difference in strain rate contributed to generate a stress concentration at rubber-mortar interface and in turn helped to develop large number of cracks (Ismail and Hassan, 2016; Najim and Hall, 2010). The results also indicated that partially replacing the FA with MK or SLF reduced the number of cracks and maximum crack width compared to the reference joint (S5 and S6 compared to S1). For example, using MK and SLF reduced the

maximum crack width from 4.8mm in joint S1 to 4mm and 3.8mm in joints S5 and S6, respectively. This can be explained such that the joint with FA has a higher deformability which allows higher number of cracks and wider crack widths compared to joints with MK or SLF that have lower deformability. From the results, it can be also seen that using natural sand with larger aggregate size compared to silica sand exhibited a significant lower number of cracks and a slightly higher crack widths. This behavior may be attributed to that the higher matrix toughness of ECC with natural sand (as mentioned earlier) which reduces the chance to develop multiple cracking compared to joint with silica sand (Li, 1997; Li et al., 1995). Furthermore, using smaller aggregate size can help to obtain better dispersion of fiber in the matrix (compared to larger aggregate size). The better dispersion of fibers improves the fibers stitching mechanism and hence, helps to reduce the crack width. Therefore, using silica sand showed slightly less crack width compared to using natural sand. By looking at joint with NC mixture (S8), it can be observed that although NC joint did not show shear failure (no shear cracks was observed in the joint zone), the cracking pattern exhibited a significant merged shear cracks in the beam portion. On the other hand, unlike NC joint, all tested ECC joints showed flexural cracks distributed in the beam portion with finer crack widths ranged from 0.02mm to 0.25mm. The cracking pattern clearly highlighted the enhanced shear strength of ECC compared to NC, in which no significant shear cracks were observed in the beam portion of ECC specimens.

Failure Load = 110.7 KN
ECC-FA

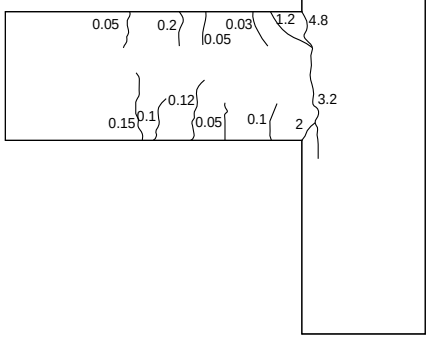

Failure Load = 105.2 KN
ECC-FA-5CR

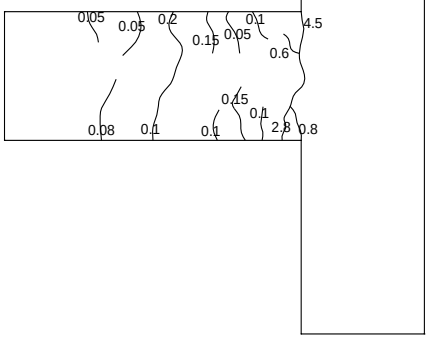

Failure Load = 101.5 KN
ECC-FA-10CR

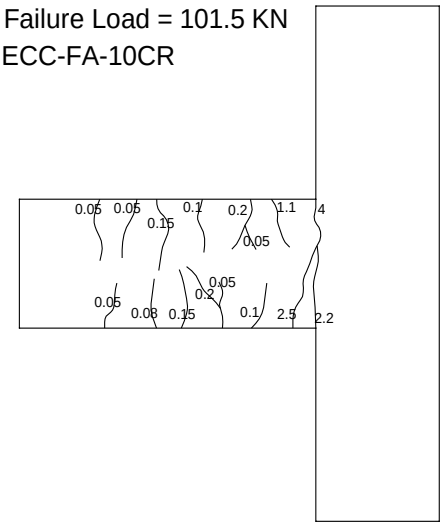

Failure Load = 97.6 KN
ECC-FA-15CR

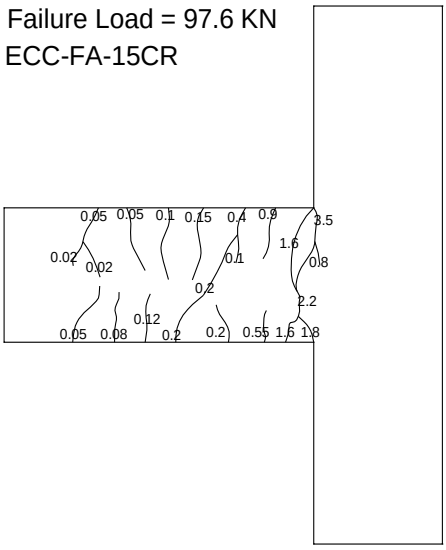

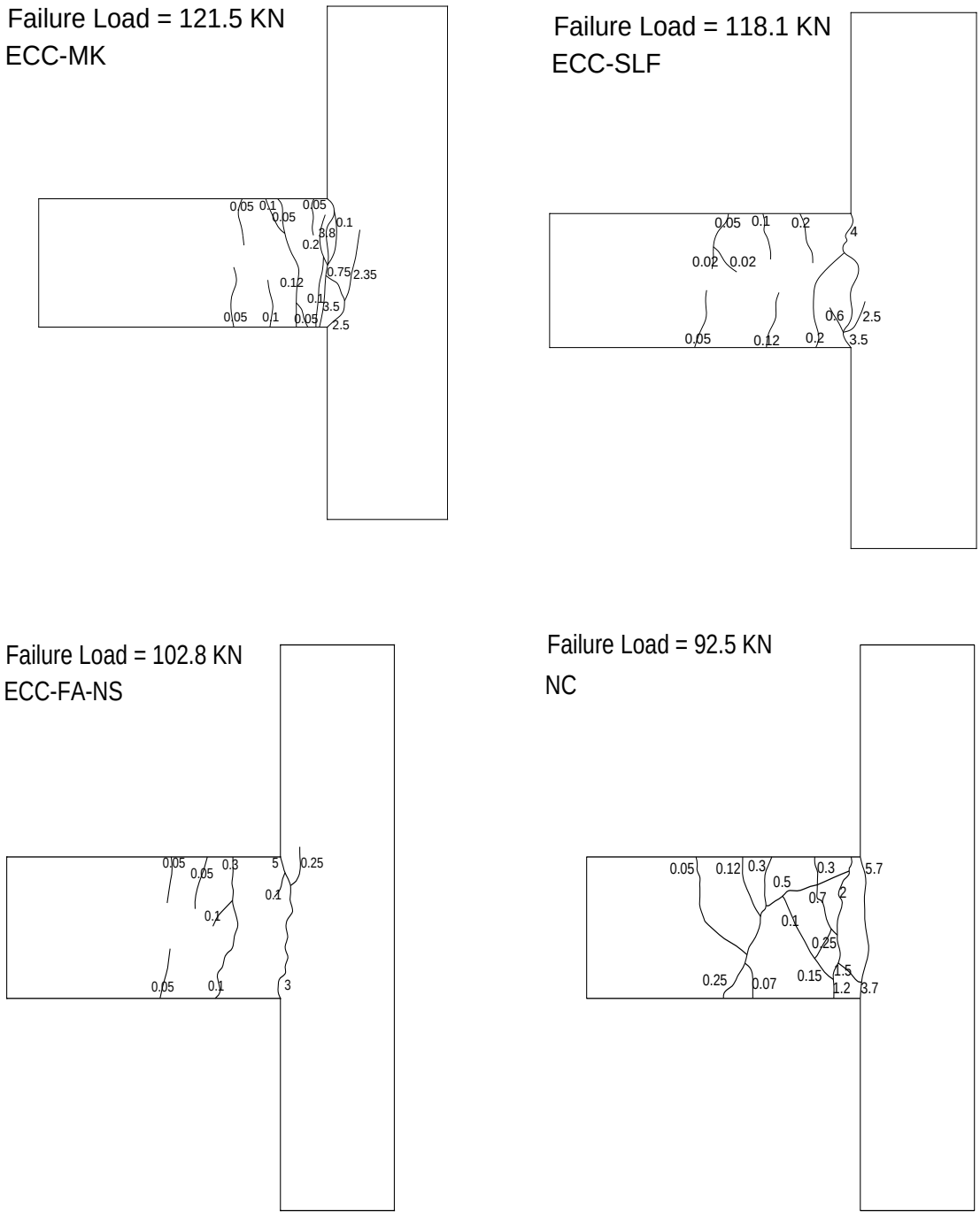

Figure 8-2 Failure cracking pattern for tested joints

8.5 Displacement ductility and brittleness index

The displacement ductility in this study is defined as the ratio between the ultimate displacement and the yield displacement. The displacement ductility proved to have a direct relation with the bonding capacity and reinforcement anchorage (Rajagopal and Prabavathy, 2014; Shiohara, 2004). Furthermore, the bonding capacity has a direct proportion with the square root of the compressive strength (Shannag et al., 2002). Therefore, as the compressive strength increases the bonding strength increases and in turn the displacement ductility improves. The yield displacement can be defined as the intersection between the horizontal line at 90% of ultimate load and the extension of the line that passes through origin and 50% of ultimate load. Meanwhile, the displacement that corresponding to the intersection between the horizontal line at 90% of the ultimate load and the descending branch of load-deflection envelop curve can be defined as the ultimate load (Shannag et al., 2002), see Figure 8-3a. Table 8-1 and Figure 8-4a show the displacement ductility for ECC joints with CR percentage varied from 0% to 15%. From the table and the figure, it can be observed that the inclusion of CR generally enhanced the displacement ductility of tested joints. For example, increasing the CR percentage up to 15% significantly increased the displacement ductility by 18.3% compared to reference joint without CR (S4 compared to S1). This behavior may be attributed to the low stiffness of CR, which contributed to enhance the deformability and strain capacity and in turn enhanced the ductility.

Table 8-1 and Figure 8-4b show the displacement ductility for NC joint and ECC joints with MK, SLF, and natural sand. It can be seen that, partial replacement of FA with MK

or SLF resulted in a slight reduction in the displacement ductility. The reduction in the displacement ductility in joints with MK and SLF (S5 and S6) reached up to 5.8% and 3.5%, respectively compared to the reference joint (S1). This may be related to the higher toughness of concrete matrix resulted from adding MK/SLF, which contributed to limit the deformation capacity and in turn negatively affected the displacement ductility. The results also revealed that the full replacement of silica sand with natural sand considerably reduced the displacement ductility by 11.5% compared to reference joint (S7 compared to S1). This reduction may be attributed to the increase of the mixture toughness with larger aggregate size (as explained earlier). The increase of the mixture toughness reduces the deformation capacity which has a direct effect of reducing the displacement ductility. It should be noted that the reference ECC joint showed a higher displacement ductility of 53.8% compared to NC joint counterpart with comparable strength (S1 compared to S8). However, the displacement ductility of NC joint falls within the range of 3 to 5, which is considered suitable for structural members in areas of seismic activities, as reported by previous researchers (Ashour, 2000; Teo et al., 2006; Gunasekaran et al., 2013). It is worth noting that the design base shear, which is considered an important factor in designing structures in seismic areas, has an adverse relationship with the displacement ductility. Therefore, the enhanced ductility of ECC joints, especially in joints with CR, compared to NC joint can contribute to decrease the design base shear, which in turn helps to obtain an economical design for the structural members subjected to seismic actions.

Since the concrete is a brittle material, its brittleness index should be higher than other ductile materials. The brittleness index of joints subjected to cyclic loading can be defined

as the ratio between the elastic energy capacity and the plastic energy capacity (A2/A1 in Figure 8-3b). Table 8-1 and Figure 8-4a show the brittleness index for ECC joints with different percentage of CR. Increasing the percentage of CR significantly decreased the brittleness index value, in which increasing the CR percentage from 0% to 15% significantly reduced the brittleness index by 25%. The significant reduction in the brittleness index value resulted from increasing the CR percentage clearly highlight the enhanced ductility of tested joints. This may be attributed to the same reasons discussed before in ductility section. Table 8-1 and Figure 8-4b show the brittleness index of NC joint and ECC joints with MK, SLF, and natural sand. From the table and the figure, it can be observed that NC joint showed a higher brittleness index of 43.5% compared to reference ECC joint with comparable compressive strength, which clearly highlight the enhanced ductility of ECC joint compared to NC joint. The results also revealed that partial replacement of FA with MK or SLF increased the brittleness index by 10% and 5%, respectively, compared to reference joint (S5 and S6 compared to S1). It can be also noted that using natural sand instead of silica sand (joint S7) resulted in a considerable increase in the brittleness index value reached up to 15% compared to reference joint (S1). This increase in the brittleness index value obviously emphasize the negative effect of using natural sand on the joints ductility.

8.6 Energy dissipation

The non-linear behavior of beam-column joints under cyclic loading has been evaluated by calculating the hysteretic energy dissipation which represents the energy dissipation in

post-elastic zone. The hysteretic energy dissipation capacity can be calculated by summing up the energy dissipation of each load step until failure. The energy dissipation of each load step can be defined as the area enclosed by the hysteretic loops of the load step in the load-deflection curve (Topçu, 1997). Figure 8-5 shows the hysteresis cycles of the load-deflection curves for all tested joints (S1-S8). Table 8-3 and Figure 8-4c present the energy dissipation capacity of ECC joints with different percentage of CR. From the figure and the table, it can be noted that increasing the percentage of CR significantly enhanced the energy dissipation capacity of tested joints. For instance, by comparing joint S4 to joint S1, it can be observed that the energy dissipation capacity increased significantly by 23.2% when the percentage of CR increased from 0% to 15%. This may be attributed to the higher flexibility of CR particles which contributed to enhance the deformability of the tested joints and in turn dissipated large amount of energy. Table 8-3 and Figure 8-4d show the energy dissipation capacity of NC joint, ECC joints with MK and SLF, and ECC joint with natural sand. From the results, it can be revealed that developing high strength ECC with high pozzolanic reactivity materials such as MK and SLF as a partial replacement of FA in ECC mixtures slightly reduced the energy dissipation capacity. For example, partially replace the FA with MK and SLF slightly reduced the energy dissipation capacity by 7.6% and 4.9%, respectively, compared to reference joint (S5 and S6 compared to S1). This behavior can be explained by the fact that using MK or SLF helped to increase the cement matrix toughness and decreased the deformation capacity and in turn reduces the energy dissipation. The results also indicated that using natural sand with larger aggregate size (compared to silica sand) led to a significant reduction in the energy dissipation capacity reached up to 11.2% compared to

reference joint (S7 compared to S1). This can be related to the lower ultimate load and deformation capacity of joint with natural sand (compared to joint with natural sand) which negatively affected the energy dissipation capacity of the tested joint. From the results, it can be also observed that energy dissipation capacity of reference ECC joint significantly increased by 56.1% compared to that of NC joint with comparable strength (S1 compared to S8). This can be attributed to the enhanced ultimate load and deformation capacity of ECC joint compared to NC one.

8.7 First crack load and ultimate load

The first crack load was noticed by visual inspection and confirmed with the load value corresponding to the change in slope of the load-deflection envelop curve. Table 8-2 and Figure 8-4e show the first crack load and ultimate load for ECC joints with different percentage of CR. Increasing the percentage of CR, in general, reduced the first crack load and ultimate load. For example, increasing the percentage of CR from 0% to 15% showed a noticeable decrease in the first crack load and ultimate load reached up to 25.9% and 11.8%, respectively, (S4 compared to S1). This may be attributed to the reduction in the compressive strength and STS resulted from adding CR. It should be noted that the first crack load is more affected by the tensile strength of concrete more than the ultimate load. Therefore, the reduction in the first crack load resulted from increasing the percentage of CR was more pronounced than the reduction in the ultimate load. Table 8-2 and Figure 8-4f show the first crack load and ultimate load for ECC joints with MK, SLF, and natural sand. The results in the figure and the table indicated that using MK or SLF as a partial replacement of FA in ECC joints generally increased the

first crack load and ultimate load compared to reference joint (S5 and S6 compared to S1). For example, in comparison with reference joint (S1), using MK increased the first crack load and ultimate by 11.4% and 9.7%, respectively, while using SLF increased the first crack load and ultimate load by 7.9% and 6.6%, respectively. This behavior may be attributed to the higher pozzolanic reactivity and the filler effect of SLF and MK which helped to develop a denser concrete matrix and in turn enhance the ultimate load. The results also showed that using natural sand with larger aggregate size (compared to silica sand) slightly reduced the first crack load and ultimate load compared to the reference joint (S7 compared to S1). It should be noted that although NC joint has a comparable compressive strength with ECC reference joint, ECC joint showed a first crack load and ultimate load of 26.5% and 19.7%, respectively, higher than NC joint (S1 compared to S8).

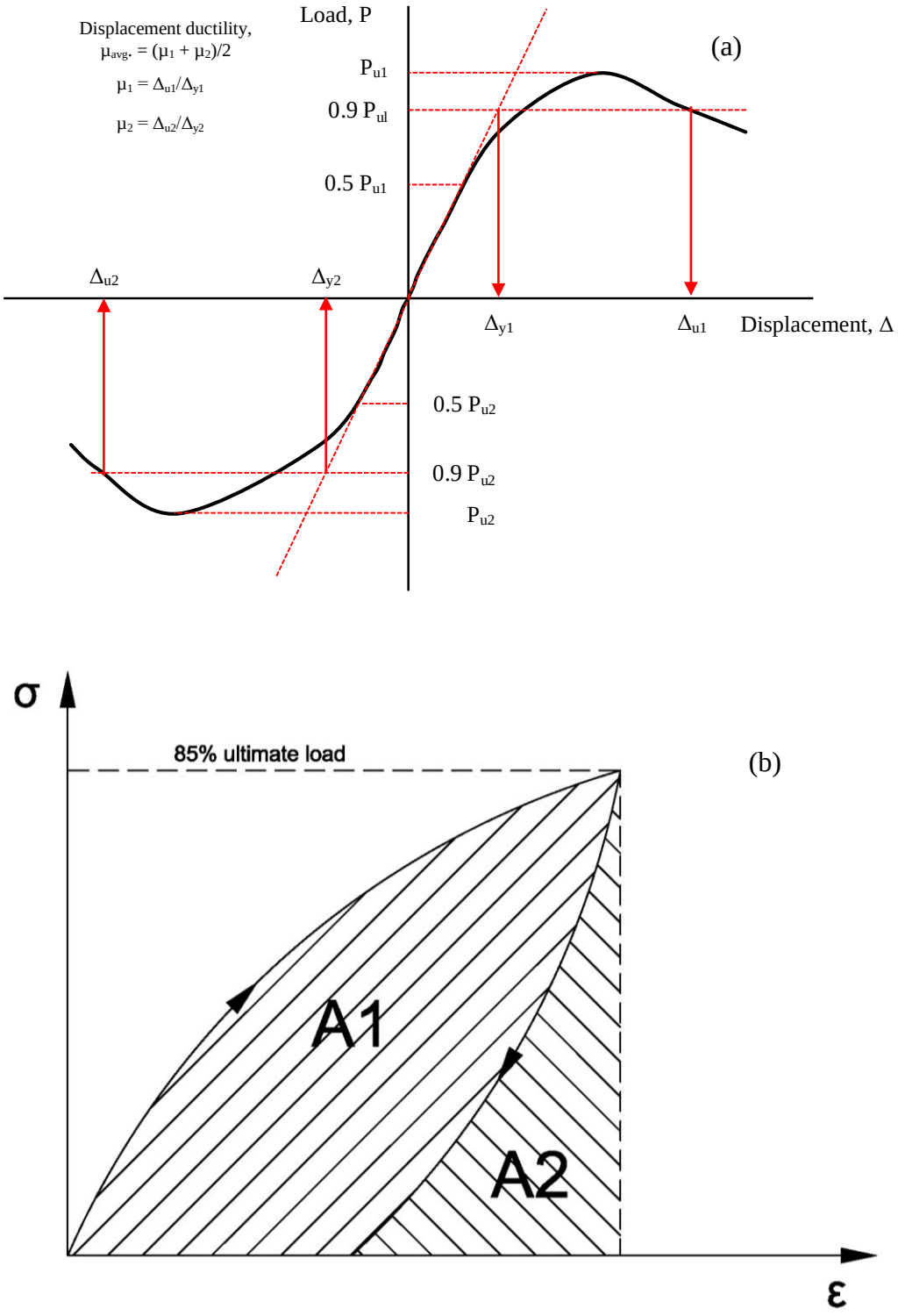

Figure 8-3 (a) Definition of ductility; (b) Definition of brittleness index

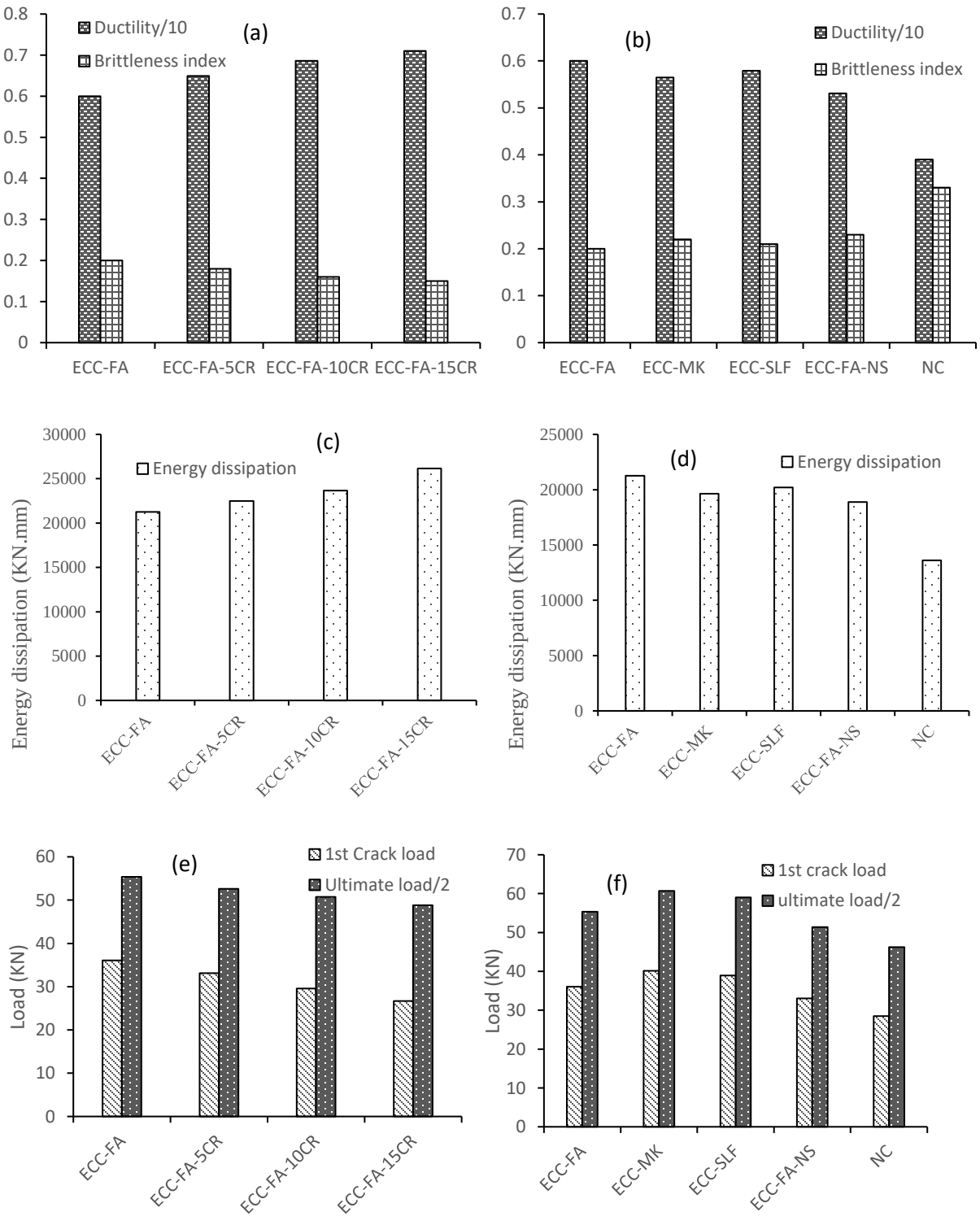

Figure 8-4 Influence of CR %, SCMs Type, and aggregate type on ductility, brittleness, energy dissipation, first crack load, and ultimate load.

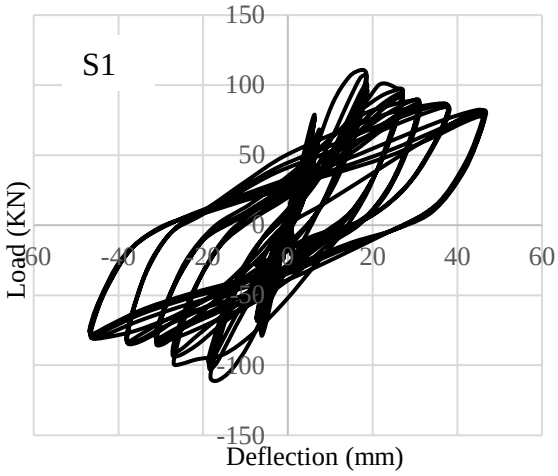
S1
Load (KN)
Deflection (mm)
150
100
50
0
-50
-100
-150
-60
-40
-20
0
20
40
60

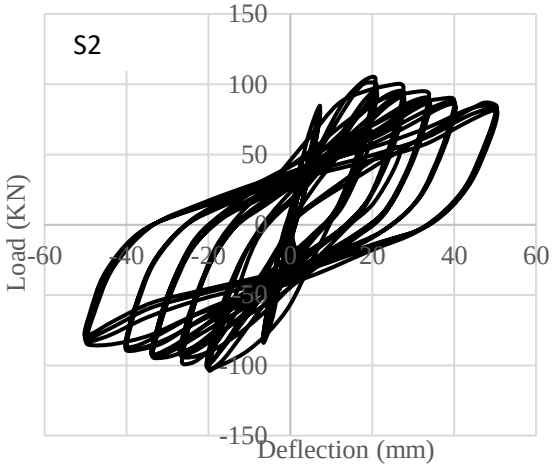
S2
Load (KN)
Deflection (mm)
150
100
50
0
-50
-100
-150
-60
-40
-20
0
20
40
60

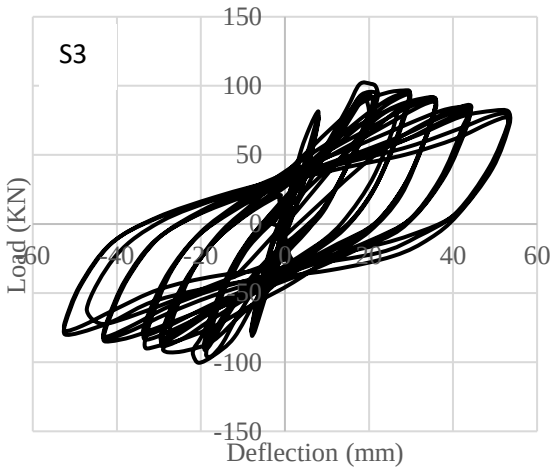
S3
Load (KN)
Deflection (mm)
150
100
50
0
-50
-100
-150
-60
-40
-20
0
20
40
60

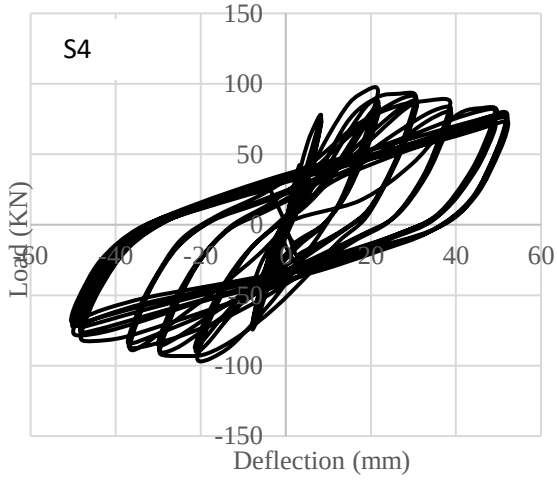
S4
Load (KN)
Deflection (mm)
150
100
50
0
-50
-100
-150
-60
-40
-20
0
20
40
60

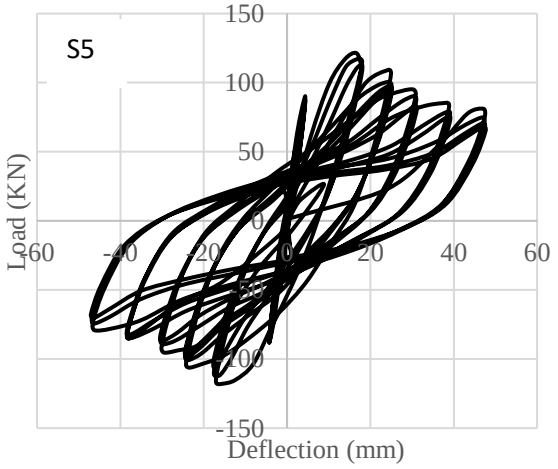
S5
Load (KN)
Deflection (mm)
150
100
50
0
-50
-100
-150
-60
-40
-20
0
20
40
60

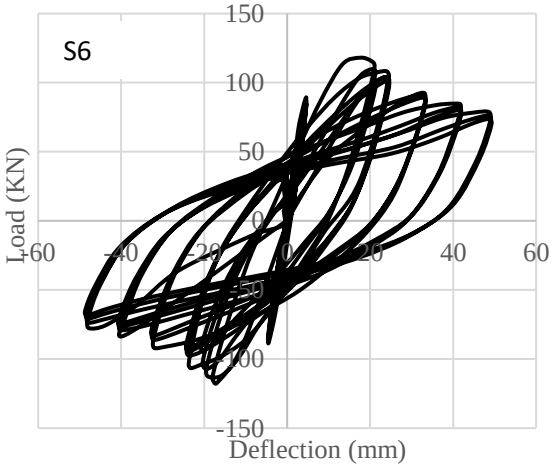
S6
Load (KN)
Deflection (mm)
150
100
50
0
-50
-100
-150
-60
-40
-20
0
20
40
60

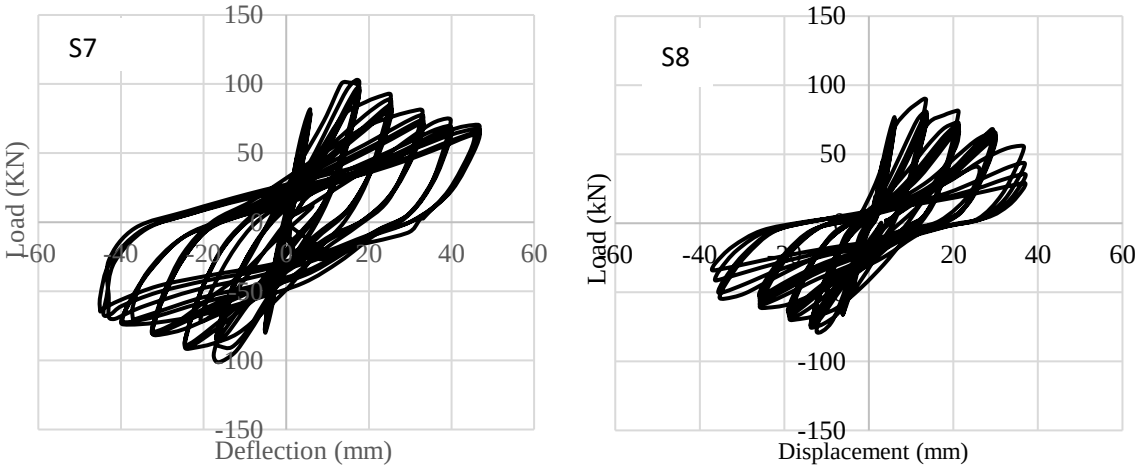

Figure 8-5 Load-deflection curve for reverse cyclic loading (hysteresis cycles) for tested joints

Conclusions and recommendations

9.1 Conclusions

The research conducted in this thesis included five consecutive experimental studies, which investigated the combined effect of CR with SFs/MFs on the development of new types of concrete with promising potentials for multiple structural applications. These studies aimed to promote the use of waste rubber in concrete industry, especially when different types of fibers are used. Different SCMs, aggregate sizes, MFs lengths and volumes, and SFs lengths, types, and volume were used to optimize the fresh and mechanical properties of the developed mixtures. The combined effect of the CR and SFs/MFs on the flexural and shear behavior of large-scale concrete beams was investigated in this thesis. Moreover, the cyclic performance of rubberized SCC/VC/ECC beam-column joints reinforced with different types, length, and volumes of fibers was also evaluated.

The following conclusions can be drawn based on the analysis of the experimental results induced from the completed studies in this research work:

9.1.1 Use of SFs/MFs to optimize the fresh properties, stability, and strength of SCRC mixtures with different binder content and SCMs (Experimental study 1)

- The use of SLF helped to develop successful SLFSCRC mixtures having acceptable SCC fresh properties, reduced self-weight, and enhanced compressive strength, STS, and FS. In this investigation, it was possible to develop SCRC mixture using SLF only with up to 25% CR.

- Increasing the percentage of CR in SLFSCRC mixtures showed a negative impact on the flowability, passing ability, stability, and HRWRA demand. In addition, the mechanical properties of SLFSCRC mixtures were negatively affected by the inclusion of CR, in which varying the percentage of CR from 0% to 20% decreased the compressive strength, STS, and FS by 58.2%, 41.1%, and 45.9%, respectively.
- Increasing the binder content generally enhanced the flowability, passing ability, and stability of SLFSCRC mixtures. This enhancement helped to maximize the percentage of CR that could be used in SLFSCRC mixtures. It was possible to use up to 25% CR with 600 kg/m^3 binder content mixture while only 20% and 5% CR was possible to be used with 550 kg/m^3 and 500 kg/m^3 binder contents mixtures, respectively.
- Compared to FA and GGBS, the use of SLF and/or MK in SCRC mixture showed improve passing ability and stability but with reduced mixture flowability. In addition, the incorporation of either SLF or MK in SCRC greatly enhanced the compressive strength, STS, and FS compared to FA and GGBS. On the other hand, the use of SLF in SCRC showed more improvement in the flowability with less HRWRA demand compared to MK.
- The addition of MK to SLFSCRC improved the mixture viscosity and particle suspension and helped to maximize the percentage of CR that could be used in SLFSCRC mixtures. The mechanical properties were also enhanced with the addition of MK to SLFSCRC. The compressive strength, STS, and FS increased by 3.39%, 3.59%, 4.07%, respectively when MK was added to SLFSCRC mixture.

- Increasing the percentage of CR in SCRC mixtures with MK and FA appeared to have a negative impact on their flowability, passing ability, stability, and HRWRA demand, which in turn limited the safe percentage of CR that can be used to develop successful SCRC mixtures to a maximum of 30%.
- Combining SFs and CR in SCC mixtures seemed to heighten the inter-particle friction and blockage, which reduced the fresh properties of the mixtures, especially the passing ability. Such negative impacts significantly limited the possible combination of high percentages of CR and larger volumes of fibers. With 550 kg/m^3 binder content it was possible to develop successful SCRC with SFs having up to 20% CR and 0.2% SFs.
- Using 19mm or 27mm SFs (SF19 or SF27) in SCRC mixtures restricted the maximum amounts of CR to 20%. Increasing the length of SFs to 38mm or 50mm further reduced the flowability, stability, and passing ability, which limited the safe amount of CR that can be used in FRSCRC mixtures to 15% and 10% for SF38 and SF50, respectively.
- Increasing the percentage of CR in SCRC mixtures negatively affected the compressive strength, STS, FS, and ME. On the other hand, the results of impact resistance in both the drop-weight and flexural impact resistance tests greatly improved with higher percentages of CR.
- In the drop-weight test (recommended by ACI-544), increasing the percentage of CR up to 30% in SCRC mixtures exhibited a continuous energy absorption enhancement that reached up to 91% compared to mixtures with no CR. On the other hand, beams

subjected to flexural impact loading showed the highest improvement in impact resistance at 25% CR, which reached up to 2.42 times compared to the results of mixtures with no CR.

- Using SFs in SCRC mixtures showed an insignificant effect on the 7- and 28-day compressive strengths and ME, while the 7- and 28- day STS and FS were greatly enhanced. The highest improvements in the STS and FS were achieved when SF38 was used.
- Increasing the length of SFs from 19mm to 38mm did not significantly affect the compressive strength while the 28-day STS and FS were enhanced due to the improved bond between the fibers and mortar. However, when adequate fiber-mortar bonding is achieved, fibers with higher tensile strength (SF38 compared to SF50) exhibited better STS and FS.
- Adding SFs to SCRC mixtures greatly improved the results of both the drop-weight impact resistance and flexural impact resistance tests. Using longer fibers also appeared to have a significant effect on improving the impact resistance, in which the use of SF38 increased N_1 and N_2 by an average of 36.2% and 44.4%, respectively, compared to mixtures with 19mm SFs.
- Although the compressive strength of VRC was negatively affected by the inclusion of high percentages of CR and SFs, the STS, FS, and impact resistance of the mixtures appeared to remarkably improve. Using 1% SFs generally appeared to mostly compensate for the reduction in STS and FS that resulted from adding 30% CR.

- Using SF54 seemed to be the most effective type of SFs at improving STS, FS, and impact resistance. On the other hand, MFs appeared to be the most effective type of all fibers at improving the mechanical properties and impact resistance of concrete. However, SFs had an advantage over MFs by providing further reduction in the self-weight of mixtures.

9.1.2 Influence of SFs' type, length, and volume on enhancing the structural performance of rubberized concrete (Experimental study 2)

- Increasing the percentage of CR up to 15% slightly decreased the flexural stiffness, maximum crack width, first cracking moment, and bending moment capacity, while significantly increased the deformability, number of randomly distributed cracks, displacement ductility, and energy absorption.
- Using MISFs in SCRC beams exhibited a slight enhancement in the deformability, flexural stiffness, displacement ductility, energy absorption, first cracking moment, and bending moment capacity. For example, adding MISF19 to the SCRC beam increased the ultimate deflection, ductility, energy absorption, first cracking moment, and bending moment capacity by 3.6%, 2.1%, 3.85%, 2.2%, and 1.8%, respectively, compared to its SCRC counterpart without fibers.
- Unlike MISFs, using MASFs in SCRC beams showed a significant increase in the deformability, displacement ductility, energy absorption, first cracking moment, and bending moment capacity, in which the increases reached up to 7.8%, 6.3%, 13.3%, 10.2%, and 4.2%, respectively compared to SCRC counterparts without fiber.

- The results of this investigation revealed that using SFs in SCRC beams generally increased the number of cracks and maximum crack width compared to their SCRC counterparts without fibers. Meanwhile, using MASFs showed a higher increase in the number of cracks and maximum crack width compared to using MISFs.
- All design codes exhibited an overestimation of the $\boldsymbol{M_{cr}^{theo}}$ for SCRC, SFSCRC, VRC, and SFVRC beams. However, the inclusion of SFs in SCRC and VRC beams appeared to decrease the error in the prediction of $\boldsymbol{M_{cr}^{theo}}$ compared to beams with CR only.
- Increasing the MASF length from 38mm to 50mm showed less improvement in the deformability, flexural stiffness, ductility, energy absorption, first cracking moment, and bending moment capacity of tested beams. However, using MASF54, which has longer fibers, appeared to yield better enhancement in the deformability, flexural stiffness, ductility, energy absorption, first cracking moment, and bending moment capacity compared to MASF50 (but still less than MASF38). This may be attributed to the higher tensile strength and rigidity of MASF54 compared to MASF50, which boosted the fiber role in transferring the stress across the cracked section, thus allowing the beam to sustain higher loads and experience larger deformations.
- Despite the considerable reduction in the bending moment capacity when using high percentage of CR (30%), combining high percentage of MASF38 (1%) with high percentage of CR (30%) compensated for this reduction, achieving around

91% bending moment capacity compared to the control beam. This combination of high percentage of CR and SFs also helped to develop a semi-lightweight concrete mixture with a density of 2094kg/m^3.

9.1.3 Effect of SFs on shear capacity of reinforced rubberized concrete beams (Experimental study 3)

- Compared to the control beam (beam with no CR), using 30% CR reduced the ultimate shear load, post-diagonal cracking resistance, energy absorption capacity, and cracking moment by up to 35.5%, 15.7%, 19.3%, and 44.1%, respectively, while the ultimate deformation capacity increased by 30%.
- Beams with CR exhibited failure behavior similar to that of the control beam (beam with no CR), in which the failure occurred by the formation of a major single diagonal crack. However, the addition of CR appeared to change the cracking behavior of tested beams, which was characterized by a higher number of cracks with smaller widths compared to the control beam.
- In both FRSCRC and FRVRC, the addition of SFs generally improved the shear and cracking behavior of the tested beams. For example, adding short 19mm SFs (MISF19) exhibited improvements in terms of ultimate shear load, post-diagonal cracking resistance, energy absorption capacity, cracking moment, and deformation capacity, which reached up to 5.8%, 4.3%, 19.6%, 3.3%, and 5%, respectively, at volume fraction of 0.2%, and reached up to 14.6%, 13.1%, 45.1%, 8%, and 14.9%, respectively, at volume fraction of 1%.

- Increasing the length of fibers led to further improvements in the shear performance of the tested beams. However, the ultimate shear load, post-diagonal cracking resistance, energy absorption capacity, cracking behavior, and deformation capacity of beams reached their maximum values when 38mm fibers were used (MASF38), achieving increases of 70.9%, 41.3%, 125.6%, 15%, and 26.9%, respectively, compared to beam with no fibers. Additional increases in length of the MASFs (MASF50 and MASF54) showed less improvement.
- At a given fiber volume fraction, and by providing enough developmental length for the fiber to prevent pull-out failure, increasing the tensile strength and rigidity of SFs can be a key factor to improve the fibres' contribution to shear strength, post-diagonal cracking resistance, energy absorption capacity, cracking behavior, and deformation capacity of reinforced concrete beams.
- Adding MISFs and MASFs to rubberized concrete beams improved the cracking pattern at the failure stage, in which more flexural and flexural-shear cracks with narrower widths were developed prior to failure compared to beams with no fibers, especially when 1% volume fraction was used, which indicates the effectiveness of the fibres' bridging mechanism.
- Combining 30% CR with 1% MISFs and/or MASFs greatly contributed to the development of sustainable semi-lightweight concrete beams with promising structural capacity, especially in the case of MASF38 and MASF54. Using 1% of MASF38 or MASF54 completely compensated for the reduction in the shear strength of reinforced concrete beams due to the inclusion of 30% CR, while it

achieved much higher deformation capacity, post-diagonal cracking resistance, and energy absorption compared to the control beam.

9.1.4 Cyclic loading of large-scale rubberized concrete beam-column joints with/without SFs (Experimental study 4)

- Increasing the percentage of CR up to 15% in beam-column joints improved the deformability, ductility, energy dissipation, brittleness index, rate of stiffness degradation, and cracking behavior, while the initial stiffness, first crack load, and ultimate load decreased.
- All tested beam-column joints showed a significant reduction in the load carrying capacity and reduced deformability when using high percentages of CR (up to 25%) in the mixture. These decreases in the load carrying capacity and deformability negatively affected the ductility, brittleness index, and energy dissipation of the tested specimens.
- The failure mode of the tested beam-column specimens was greatly affected by the percentage of CR in the mixture. Using more than 15% CR changed the failure mode of the tested specimens from B-mode to BJ-mode, which limited the deformation capacity due to the strength reduction resulting from panel joint cracking.
- The first crack load of beam-column joints was significantly affected by increasing the percentage of CR compared to the ultimate load. Increasing the percentage of CR from 0% to 25% reduced the first crack load by 39% while the ultimate load was reduced by 19%.

- The results also revealed that for 2% flexural reinforcement and 0.6% shear reinforcement, the optimum percentage of CR to be used in beam-column joints is 15%. Although using 15% CR appeared to slightly reduce the load carrying capacity (not more than 10%), the ductility, brittleness index, deformability, and energy dissipation were greatly enhanced. For example, increasing the CR percentage up to 15% resulted in an increase in ductility and energy dissipation reached up to 18.7% and 20.9%, respectively.
- The results of this investigation revealed that for beam-column joints with 10mm coarse aggregate, the optimum percentage of CR to be used was 15%. Up to this limit, the load carrying capacity was slightly reduced, while the ductility, brittleness index, deformability, and energy dissipation were greatly enhanced. Similar behavior in terms of load carrying capacity, brittleness index, deformability, and energy dissipation was also noted in mixtures with 20mm coarse aggregate but with a 20% optimum percentage of CR.
- At low percentage of CR (up to 15%), where all joints exhibited B-mode failure, smaller aggregate (10mm) joints showed slight improvements in the ultimate deflection, initial stiffness, ductility, energy dissipation, first crack load, and load carrying capacity compared with the larger aggregate (20mm) joints. However, at higher percentage of CR (20%), the increased shear strength resulting from the improved aggregate interlock of the larger aggregate size helped to change the failure mode from BJ-mode (in 10mm coarse aggregate joints) to B-mode (in

20mm coarse aggregate joints). This contributed to enhancing the overall beam-column joint behavior.

- Adding MFs to SCRC and VRC beam-column joints helped to improve the deformability, ductility, energy dissipation, initial stiffness, cracking behavior, first crack load, and load carrying capacity. For example, adding 0.35% MFs (35mm) to SCRC mixture with 15% CR increased the initial stiffness, first crack load, load carrying capacity, ductility, and energy dissipation by 11.1%, 42.2%, 15.6%, 22.4%, and 50.5%, respectively, compared with joint without MFs.
- VRC mixtures with MFs showed insignificant difference in results compared with their SCRC counterparts. Furthermore, joints with longer MFs (60mm) showed a slight reduction in the load carrying capacity, deformability, ductility, and energy dissipation compared with joints with shorter MFs (35mm).
- It was not possible to develop SCC mixtures with high percentage of CR and high percentage of MFs due to the significant reduction in the fresh properties of the mixture. However, combining 1% MFs with 25% CR in VRC mixture enhanced the overall behavior of beam-column joints and changed the failure mode from BJ-mode to B-mode. This enhancement helped to compensate for the reduction in the load carrying capacity that occurred in joint with high percentage of CR and no MFs.
- The results of this investigation revealed that using MISFs in SCRC beam-column joints showed a slight enhancement in the deformability, ductility, energy dissipation, initial stiffness, cracking behavior, first crack load, and load carrying

capacity. For example, adding 0.2% MISF27 (27mm) to SCRC mixture with 15% CR increased the initial stiffness, first crack load, load carrying capacity, ductility, and energy dissipation by 4.6%, 13.6%, 3.1%, 7.8%, and 8.8%, respectively, compared to joint without MISFs.

- Unlike MISFs, using MASFs in SCRC joints exhibited a significant improvement in the structural behavior of beam-column joints under cyclic load. For instance, in the joint with MASF38 (38mm) the improvement reached up to 9.3%, 38%, 10.5%, 20.8%, and 36.8% in the initial stiffness, first crack load, load carrying capacity, ductility, and energy absorption, respectively, compared to joints without MASFs.
- By comparing all types/lengths of SFs used in this study, it can be revealed that the highest improvements in the performance of cyclic behavior of beam-column joints in terms of first crack load, load carrying capacity, initial stiffness, ductility, cracking behavior, and energy dissipation was noticed when MASF38 was used.
- Increasing the fiber length resulted in less improvement in the structural performance of beam-column joints including initial stiffness, first crack load, cracking behavior, load carrying capacity, ductility, brittleness index, and energy dissipation. This can be attributed to the fact that for a similar percentage of fibers in the mixture, using shorter fibers increases the probability that a single fiber will be oriented perpendicularly to the crack width, thus achieving higher load carrying capacity.

- Comparing MISF27 to MISF19, which both failed under fiber pullout failure, it can be seen that using rough texture fibers (MISF27) helped to enhance the bonding between fibers and concrete matrix, improving the structural performance of beam-column joints. Meanwhile, comparing MASF54 to MASF50, which both failed under fiber tension failure, we can see that increasing the tensile strength of the fiber contributed to boosting the effect of fibers in transferring the stresses across the cracked section, which in turn enhanced the structural performance of the joint.
- Using high percentage of SFs (1%) in mixture with high percentage of CR (25%) contributed to compensate for the reduction in the load carrying capacity that resulted from using high percentage of CR and helped to enhance the overall behavior of beam-column joints under cyclic loading. This enhancement allowed to develop joint with significant improvements in ductility, cracking behavior, brittleness index, first crack load, and energy dissipation.

9.1.5 Structural behavior of rubberized ECC beam-column joints under cyclic loading (Experimental study 5)

- Partial replacement of silica sand with up to 15 % CR in ECC showed a significant reduction in the compressive strength and STS reached up to 28.2% and 12.5%, respectively, compared to reference mixture without CR. Meanwhile, the full replacement of silica sand with natural sand exhibited an insignificant effect on the compressive strength and STS of ECC joints.

- Using MK or SLF as a partial replacement of FA in ECC joints appeared to significantly increase the mechanical properties of ECC joints. For example, using 10% SLF as a partial replacement of FA increased the compressive strength and STS by 11.8% and 4.7%, respectively, while these increases reached up to 29.2% and 12.5% (compared to reference joint, S1) when 20% MK was used.
- Increasing the percentage of CR from 0% to 15% considerably increased the ultimate deflection, deflection at ultimate load, ductility, and energy dissipation by 44.7%, 12.6%, 18.3%, and 23.2%, respectively, while the initial stiffness, first crack load, and ultimate load decreased by 21.1%, 25.9%, and 11.8%, respectively.
- Using MK or SLF as a partial replacement of FA in ECC beam-column joints slightly reduced the deformability, ductility, and energy dissipation while the first crack load, initial stiffness, and ultimate load significantly improved.
- Although using natural sand (locally available aggregate) showed comparable compressive strength and STS to ECC made with silica sand, ECC beam-column joint made with natural sand yielded lower ultimate deflection, initial stiffness, ductility, energy dissipation, first crack load, and ultimate load by 7.3%, 15.9%, 11.5%, 11.1%, 8.3%, and 7.2%, respectively, compared to that made with standard ECC joint (S1).
- Increasing the percentage of CR (as a partial replacement of silica sand) generally increased the number of cracks but with lower cracks widths. On the other hand, the full replacement of silica sand with natural sand exhibited significant lower

number of cracks and slightly higher cracks widths. Compared to standard ECC joint, joints with MK or SLF showed a lower number of cracks and finer crack widths.

- Although NC joint has a comparable strength with reference ECC joint (S1), ECC joint showed a significant enhancement in the structural performance under cyclic loads compared to NC joint. This improvement reached up to 53.8%, 43.5%, 56.1%, 26.5%, and 19.7% in the ductility, brittleness index, energy dissipation, first crack load, and ultimate load, respectively. However, NC joint exhibited an adequate ductility for structural members in areas of seismic activities.

9.2 Research contribution

The main contributions of this research can be concluded as follows:

- Combining the beneficial effects of using waste CR with the desired properties of different types of fibers to develop a number of successful SCRC, FRSCRC mixtures with promising potential usage in structural applications that require high-impact resistance, ductility, and energy dissipation.
- Using SFs with low-density in addition to low-density CR contributed to develop semi-light weight concrete that can helps to achieve more economical design of building.
- Utilizing different SCMs, and different fibers types (MFs/SFs) in rubberized concrete mixtures helped to alleviate the reduction in the mechanical properties that resulted from using high percentage of CR, allowing to

maximize the beneficial effect of using CR with a minimum reduction in the mechanical properties.

- Alleviating the lack of sufficient data regarding the combined effect of CR and SFs on the flexural and shear behavior of concrete beams including cracking behavior, ductility, energy absorption, and stiffness.
- Determining the optimum percentage of CR that can be used to enhance the cyclic behavior of beam-column joints including the ductility, brittleness index, energy dissipation, cracking behavior, failure mode, and strength degradation with a minimum reduction in the load carrying capacity.
- Using SFs/MFs to alleviate the reduction in the load carrying capacity of the beam-column joint that resulted from using high percentage of CR. In addition to further enhancing the structural behavior of beam-column joints under cyclic loading.
- The results of cyclic load testing can also provide a novel database that may help to validate and/or calibrate further analytical and numerical studies (for future studies).

9.3 Recommendations for future research

- Further investigations are needed to evaluate the durability of rubberized concrete mixtures and SFs rubberized concrete mixtures against abrasion, salt scaling resistance, chloride diffusion, and sulfate attacks.

- Studying the influence of CR with/without SFs on creep and shrinkage of SCC and VC.
- Evaluating the effect of fire on the mechanical properties and structural performance of SCRC, SFSCRC, VRC, and SFVRC.
- Evaluating the effect of changing in the beam' size, longitudinal reinforcement ratio, and shear span-to-effective depth ratio on the shear and flexural performance of large-scale reinforced rubberized concrete beams.

References

Ababneh A, Al-Rousan R, Alhassan M, Alqadami M (2017) Influence of synthetic fibers on the shear behavior of lightweight concrete beams. Adv Struct Engr 20(11): 1671-1683.

Abadel A, Abbas H, Almusallam T, Al-Salloum Y and Siddiqui N (2015) Mechanical properties of hybrid fibre-reinforced concrete–analytical modelling and experimental behaviour. Magazine of Concrete Research:1-21.

Abouhussien AA., Hassan AAA and Ismail MK (2015) Properties of Semi-Lightweight Self-Consolidating Concrete Containing Lightweight Slag Aggregate. *Construction and Building Materials* 75: 63-73.

ACI (American Concrete Institute) (2008) Building code requirements for structural concrete (ACI 318-08) and commentary (ACI 318R-08). American Concrete Institute, Farmington Hills, MI, 465.

ACI 352R-02 (2002) Recommendations for Design of Beam-Column Connections in Monolithic Reinforced Concrete Structures.

ACI 544.2R-89 (1999) Measurement of properties of fiber reinforced concrete. West 481 Conshohocken, PA, USA.

Aiello MA and Leuzzi F (2010) Waste tyre rubberized concrete: properties at fresh and hardened state. *Waste Management* 30(8-9): 1696-1704.

Albano C, Camacho N, Reyes J, Feliu JL, Hernández M (2005) Influence of scrap rubber addition to Portland I concrete composites: destructive and non-destructive testing. Comp Struct 71(3-4): 439-446.

Al-Tayeb MM, Bakar BHA, Ismail H and Akil HM (2013) Effect of partial replacement of sand by recycled fine crumb rubber on the performance of hybrid rubberized-normal concrete under impact load: experiment and simulation. *Journal of Cleaner Production* 59: 284–289.

Al-Tayeb MM, Bakar BHA, Ismail H and Akil HM (2012) Impact resistance of concrete with partial replacements of sand and cement by waste rubber. *Polymer-Plastics Technology and Engineering* 51(12): 1230–1236.

Altoubat S, Yazdanbakhsh A and Rieder KA (2009) Shear behavior of macro-syntheticfiber-reinforced concrete beams without stirrups. ACI Materials Journal, 106(4):381-389.

Ashour SA (2000) Effect of compressive strength and tensile reinforcement ratio on flexural behavior of high-strength concrete beams. *Engineering Structures* 22: 413–423.

ASTM C143/C143M (2015) Standard test method for slump of hydraulic-cement concrete. ASTM International, West Conshohocken, PA, USA.

ASTM C989/C989M (2014) Standard specification for slag cement for use in concrete and mortars. ASTM International, West Conshohocken, PA, USA.

ASTM C1240 Standard specification for use of silica fume as a mineral admixture in hydraulic-cement concrete, mortar, and grout. West Conshohocken, PA.

ASTM C494 (2013) Standard specification for chemical admixtures for concrete. ASTM International, West Conshohocken, PA.

ASTM C150/C150M (2012) Standard specification for Portland cement. ASTM International, West Conshohocken, PA, USA.

ASTM C618 (2012) Standard specification for coal fly ash and raw or calcined natural pozzolan for use in concrete. ASTM International, West Conshohocken, PA, USA.

ASTM C39 (2011) Standard test method for compressive strength of cylindrical concrete specimens. ASTM International, West Conshohocken, PA, USA.

ASTM C496 (2011) Standard test method for splitting tensile strength of cylindrical concrete specimens. ASTM International, West Conshohocken, PA.

ASTM C78 (2010) Standard test method for flexural strength of concrete (using simple beam with third-point loading). ASTM International, West Conshohocken, PA.

Australian Standard (1988) Concrete structures. AS 3600, Standards Association of Australia, Sydney, Australia.

Barluenga G, Palomar I and Puentes J (2013) Early age and hardened performance of cement pastes combining mineral additions. *Materials and structures 46*(6): 921-941.

Batayneh MK, Marie I and Asi I (2008) Promoting the use of crumb rubber concrete in developing countries. *Waste Management* 28(11): 2171-2176.

Banthia N, Bindiganavile V, Mindess S, In: Naaman AE, Reinhardt HW (2003) editors. Proceedings of an international conference. USA: Ann Arbour : 117–31.

Banthia NA (1990) Study of Some Factors Affecting the Fiber-Matrix Bond in Steel Fiber Reinforced Concrete. *Canadian Journal of Civil Engineering* 17(4): 610-620.

Bentur A, (2007) Mindess, S., (Ed.), *Fibre reinforced cementitious composites* (2nd Edition). New York: Taylor & Francis.

Bignozzi MC and Sandrolini F (2006) Tyre rubber waste recycling in selfcompacting concrete. Cement and Concrete Research 36(4): 735-739.

Bindhu KR and Jaya KP (2010) Strength and behaviour of exterior beam column joints with diagonal cross bracing bars. Journal of Civil Eng. 11: 397–410.

BIS, IS. 13920 (1993) Ductile detailing of reinforced concrete structures subjected to seismic forces—Code of practice. Bureau of Indian Standards, Second revision.

Buratti N, Mazzotti C and Savoia M (2011) Post-cracking behaviour of steel and macro-synthetic fibre-reinforced concretes. *Construction and Building Materials 25*(5): 2713-2722.

Canadian Standards Association (CSA) Committee A23.3 (2004) Design of concrete structures. CSA A23.3-04, Canadian Standards Association, Rexdale, Ontario, Canada.

Carnovale, DJ (2013) Behaviour and analysis of steel and macro-synthetic fibre reinforced concrete subjected to reversed cyclic loading: a pilot investigation. (Doctoral dissertation).

Choi SY, Park YH and Jung WT (2012) A study on the bond performance improvement of polypropylene macro fibers according to the change of surface area.Advanced Materials Research, :1440-1446.

Choi Y and Yuan RL (2005) Experimental relationship between splitting tensile strength and compressive strength of GFRC and PFRC. Cement and Concrete Research 35(8):1587-91.

Corinaldesi V and Moriconi G (2015) Use of synthetic fibers in self-compacting lightweight aggregate concretes. Journal of Building Engineering 4: 247–254.

Cyr M and Mouret M (2003) Rheological characterization of superplasticized cement pastes containing mineral admixtures: consequences on self-compacting concrete design. *In ACI Special Publication*. *ACI, Farmington Hills, MI, USA,* 217: 241–256.

EFNARC (2005) The European guidelines for self-compacting concrete specification, production and use. European Federation for Specialist Construction Chemicals and Concrete Systems, English ed. Norfolk, UK.

Elchalakani, M. (2015, February). High strength rubberized concrete containing silica fume for the construction of sustainable road side barriers. In Structures 1:20-38

Eldin NN and Senouci AB (1994) Measurement and prediction of the strength of rubberized concrete. *Cement and Concrete Composites* 16(4): 287–298.

Eldin NN and Senouci AB (1993) Rubber tyre particles as concrete aggregate. Journal of Materials in Civil Engineering 5: 478-496.

Emiroglu M, Halidun M and Yildiz S (2007) An investigation on ITZ microstructure of the convcrete containng waste viehicle tire" in 8th International Fracture Conferenc, 7-9 November, Istanbul/TURKEY.

EN 1992-1-1 (2005) Eurocode 2 – Design of Concrete Structures – Part 1–1: General Rules and Rules for Buildings, Thomas Telford, London, UK.

Faleschini F, Hofer L, Zanini MA, dalla Benetta M and Pellegrino, C (2017) Experimental behavior of beam-column joints made with EAF concrete under cyclic loading. *Engineering Structures* 139:81-95.

Fattuhi NI and Clark LA (1996) Cement-based materials containing shredded scrap truck tyre rubber. Construction and Building Materials 10(4): 229-236.

Ganesan N, Raj B and Shashikala AP (2013) Behavior of self-consolidating rubberized concrete beam-column joints. *ACI Materials Journal* 110(6): 697-704.

Ganesan N, Indira PV, Abraham R. (2007) Steel fibre reinforced high performance concrete beam-column joints subjected to cyclic loading. ISET J Earthq Tech 44.3-4: 445–456.

Ganjian E, Khorami M and Maghsoudi AA (2009) Scrap-tyre-rubber replacement for aggregate and filler in concrete. Construction and Building Materials 23(5):1828-1836.

Garrick G (2005) Analysis and testing of waste tire fiber modified concrete. Master thesis. The Department of Mechanical Engineering, the Graduate Faculty of the Louisiana State University and Agricultural and Mechanical College.

Gencel O, Ozel C, Brostow W and Martinez-Barrera G (2011) Mechanical properties of self-compacting concrete reinforced with polypropylene fibres. Materials Research Innovations 15(3): 216-225.

Gesoğlua M, Güneyisi E, Khoshnaw G and Ipek S (2014) Abrasion and freezing–thawing resistance of pervious concretes containing waste rubbers. *Construction and Building Materials* 73: 19–24.

Ghernouti Y, Rabehi B, Bouziani T, Ghezraoui H and Makhloufi A (2015) Fresh and hardened properties of self-compacting concrete containing plastic bag waste fibers (WFSCC). Construction and Building Materials 82:89-100.

Grabois TM, Cordeiro GC and Toledo Filho RD (2016) Fresh and hardened-state properties of self-compacting lightweight concrete reinforced with steel fibers. Constr Build Mater 104: 284–292.

Gunasekaran K, Annadurai R and Kumar PS (2013) Study on reinforced lightweight coconut shell concrete beam behavior under flexure. *Materials & Design* 46:157-167.

Güneyisi E (2010) Fresh properties of self-compacting rubberized concrete incorporated with fly ash. *Materials and Structures* 43: 1037-1048.

Güneyisi E, Gesoğlu M and Özturan T (2004) Properties of rubberized concretes containing silica fume. *Cement and Concrete Research* 34(12): 2309–2317.

Gupta T, Sharma RK and Chaudhary S (2015) Impact resistance of concrete containing waste rubber fiber and silica fume. *International Journal of Impact Engineering* 83: 76–87.

Hall MR, Najim KB (2014) Structural behaviour and durability of steel-reinforced structural Plain/Self-Compacting Rubberised Concrete (PRC/SCRC). Constr Build Mater 73: 490–497.

Hamoush S, Abu-Lebdeh T and Cummins T (2010) Deflection behavior of concrete beams reinforced with PVA micro-fibers. Constr Build Mater 24(11): 2285–2293.

Hasan MJ, Afroz M and Mahmud HMI (2011) an experimental investigation on mechanical behavior of macro synthetic fiber reinforced concrete. *International Journal of Civil and Environmental Engineering* 11(3):18-23.

Hassan AAA, Ismail MK, Mayo JR (2015) Mechanical properties of self-consolidating concrete containing lightweight recycled aggregate in different mixture compositions. J Build Eng. 4: 113-126.

Hassan AAA, Lachemi M, Hossain KMA (2010) Effect of metakaolin and silica fume on rheology of self-consolidating concrete ACI Mater J 109 (6): 657–664.

Hassan AAA, Hossain KMA and Lachemi M (2008) Behavior of Full-Scale Self-Consolidating Concrete Beams in Shear. *Cement and Concrete Composites* 30:588–596.

Hernández-Olivares F, Barluenga G, Bollati M and Witoszek B (2002) Static and dynamic behaviour of recycled tyre rubber-filled concrete. Cement and Concrete Research 32(10):1587-1596.

Huang X, Ranade R, Ni W and Li VC (2013) Development of Green Engineered Cementitious Composites Using Iron Ore Tailings as Aggregates. *Construction and Building Materials* 44: 757–764.

Imran I, Sugiri S, Pane I (2015) Behaviour of macro synthetic fiber reinforced concrete columns under concentric axial compression. Procedia Engineering 125: 987-994.

Ismail MK, Hassan AA (2017) Shear behaviour of large-scale rubberized concrete beams reinforced with steel fibres. Constr Build Mater 140: 43–57.

Ismail MK, Hassan AA (2016) Performance of full-scale self-consolidating rubberized concrete beams in flexure. ACI Mater. J. 113: 207–218.

Ismail MK, Hassan AAA (2016b) Impact Resistance and Acoustic Absorption Capacity of Self-Consolidating Rubberized Concrete. ACI Mater J 113(6).

Ismail MK, and Hassan AAA (2015) Influence of mixture com- position and type of cementitious materials on enhancing the fresh properties and stability of self-consolidating rubberized concrete. J. Mater. Civ. Eng., 10.1061/(ASCE)MT.1943-5533.0001338, 04015075.

Jun LJ, gang NJ, jun WC, Jin B and liu YY (2016) Investigation on mechanical properties and microstructure of high performance polypropylene fiber reinforced lightweight aggregate concrete. Constr Build Mater 118: 27–35.

Jun P and Mechtcherine V (2010) Behaviour of Strain-Hardening Cement-Based Composites (SHCC) under monotonic and cyclic tensile loading: part 1–experimental investigations. *Cement and concrete composites* 32:801–809.

Kani GNJ, Huggins MW and Wittkopp RR (1979) Shear in reinforced concrete. Toronto: University of Toronto Press: 1–225.

Karahan O, Özbay E, Hossain KMA, Lachemi M and Atis CD (2012) Fresh, mechanical, transport, and durability properties of self-consolidating rubberized concrete. *ACI Materials Journal* 109(4): 413-420.

Khaloo A, Raisi EM, Hosseini P and Tahsiri H (2014) Mechanical performance of self-compacting concrete reinforced with steel fibers. *Construction and Building Materials* 51: 179–186.

Khaloo AR, Dehestani M and Rahmatabadi P (2008) Mechanical properties of concrete containing a high volume of tire-rubber particles. *Waste Manage*ment 28(12): 2472–2482.

Khatib ZR and Bayomy FM (1999) Rubberized Portland cement concrete. *ASCE Journal of Materials in Civil Engineering* 11(3): 206–213.

Khayat KH, Kassimi F and Ghoddousi P (2014) Mixture design and testing of fiber-reinforced self-consolidating concrete. ACI Materials Journal 111(2): 143–151.

Kim JK, Kim JS, Ha GJ and Kim Y (2007) Tensile and fiber dispersion performance of ECC (engineered cementitious composites) produced with ground granulated blast furnace slag. Cem. Concr. Res. 37(7): 1096–1105.

Koehler EP, Fowler DW (2007) Aggregates in Self-Consolidating Concrete (Research report ICAR 108-2F). Aggregates Foundation for Technology, Research and Education.

Kong, HJ, Bike SG and Li VC (2003) Development of a selfconsolidating engineered cementitious composite employing electrosteric dispersion/stabilization. Cem. Concr. Compos 25(3): 301–309.

Lee JH, Yoo DY and Yoon YS (2016) Mechanical behaviour of concrete with amorphous metallic and steel fibres. Magazine of Concrete Research 68(24):1253-64.

Leyden J (1991) Cryogenic Processing and Recycling. Rubber World 203(6): 28- 29.

Lijuan L, Shenghua R and Lan Z (2014) Mechanical properties and constitutive equations of concrete containing a low volume of tire rubber particles. *Construction and Building Materials* 70: 291–308.

Li VC and Tailoring ECC (2012) for special attributes: a review. *International Journal of Concrete Structures and Materials* 6(3):135–44.

Li VC (2003) On Engineered Cementitious Composites (ECC) a review of the material and its applications. *Journal of Advanced Concrete Technology* 1(3):215-230.

Li VC, Wang S and Wu C (2001) Tensile strain-hardening behavior of polyvinyl alcohol engineered cementitious composite (PVA-ECC). *ACI Mater Journal* 98(6):483-492.

Li VC (1998) Engineered cementitious composites (ECC)—Tailored composites through micromechanical modeling. Fiber reinforced concrete: Present and the future, N. Banthia, A. Bentur, and A. Mufti, eds., Canadian Society of Civil Engineers, Montreal, 64–97.

Li VC (1997) Engineered Cementitious Composites Tailored Composites through Micromechanical Modeling. *Fiber Reinforced Concrete: Present and the Future, N. Banthia, A. Bentur, and A. Mufti, eds., Canadian Society of Civil Engineering* 64-97.

Li VC (1995) Mishra DK and Wu HC (1995) Matrix Design for Pseudo Strain-Hardening Fiber Reinforced Cementitious Composites. *Materials and Structures* 28(183): 586-595

Li VC (1993) From micromechanics to structural engineering—The design of cementitious composites for civil engineering applications. Proc. J. Soc. Civ. Eng 471:1–24, 1–12.

Li VC, Ward R and Hamza AM (1992) Steel and synthetic fibers as shear reinforcement. ACI Materials Journal, 89(5):499-508.

Ma H, Wang HH, Li ZB, Sun XY and Zhang XW (2012) Experimental study on the seismic performance of macro-synthetic fiber-reinforced concrete ductile columns. Advanced Materials Research, 446: 2345-2350.

Madandoust R and Mousavi SY (2012) Fresh and hardened properties of self-compacting concrete containing metakaolin. *Construction and Building Materials* 35: 752-760.

Majdzadeh F, Soleimani SM and Banthia N (2006) Shear strength of reinforced concrete beams with a fiber concrete matrix. Canadian Journal of Civil Engineering 33(6): 726-734.

Massoud MT, Abou-Zeid MN and Fahmy EH (2003) Polypropylene fibers and silica fume concrete for bridge overlays. In Submitted for Presentation and Publication In the 82nd Annual Meeting of the Transportation Research Board.

Mohammed BS, Khandaker M, Anwar H, Jackson TES, Grace W and Abdullahi M (2012) Properties of crumb rubber hollow concrete block. J. Clean. Prod. 23: 57-67.

Monteiro I, Branco FA, De Brito J and Neves R (2012) Statistical analysis of the carbonation coefficient in open air concrete structures. Construction and Building Materials 29:263-269.

Nagdi K (1993) Rubber as an Engineering materials: Guidelines for Users. Hanser Publication, Munch, Germany.

Naito C, States J, Jackson C and Bewick B (2014) Assessment of crumb rubber concrete for flexural structural members. *ASCE Journal of Materials in Civil Engineering* 26(10): 751-758.

Najim KB and Hall M (2013) Crumb rubber aggregate coatings/pre-treatments and their effects on interfacial bonding, air entrapment and fracture toughness in self-compacting rubberised concrete (SCRC). *Materials and Structures* 46: 2029–2043.

Najim KB and Hall M (2012) Mechanical and dynamic properties of self-compacting crumb rubber modified concrete. *Construction and Building Materials* 27: 521–530.

Najim KB and Hall MR (2010) A review of the fresh/hardened properties and applications for plain- (PRC) and self-compacting rubberised concrete (SCRC). *Construction and Building Materials* 24: 2043–2051.

Nehdi A and Khan M (2001) Cementitious composites containing recycled tire rubber: An overview of engineering properties and potential applications. *Cement, Concrete, and Aggregates* 23(1): 3–10.

Nili M and Afroughsabet V (2010) Combined effect of silica fume and steel fibers on the impact resistance and mechanical properties of concrete. International Journal of Impact Engineering 37(8): 879-886.

Oh BH, Park DG, Kim JC and Won JP (2002) Realistic prediction of post-cracking behavior in synthetic fiber reinforced concrete beam. Korea Concrete Institute Journal 14(6): 900-909.

Onuaguluchi O (2015) Effects of surface pre-coating and silica fume on crumb rubber-cement matrix interface and cement mortar properties. *Journal of Cleaner Production* 104: 339-345.

Onuaguluchi O and Panesar DK (2014) Hardened properties of concrete mixtures containing pre-coated crumb rubber and silica fume. *Journal of Cleaner Production* 82: 125-131.

Özbay E, Karahan O, Lachemi M, Hossain KMA and Duran Atiş C (2012) Investigation of Properties of Engineered Cementitious Composites Incorporating High Volumes of Fly Ash and Metakaolin. *ACI Materials Journal* 109(5).

Paulay T (1989) Equilibrium criteria for reinforced concrete beam-column joints. Structural Journal 86(6): 635-643.

Pelisser F, Zavarise N, Longo TA and Bernardin AM (2011) Concrete made with recycled tire rubber: Effect of alkaline activation and silica fume addition. *Journal of Cleaner Production* 19: 757-763.

Rahman M, Al-Ghalib A, Mohammad F (2014) Anti-vibration characteristics of rubberized reinforced concrete beams. Mater struct 47(11): 1807-1815.

Rajagopal S, Prabavathy S (2014) Exterior beam-column joint study with non-conventional reinforcement detailing using mechanical anchorage under reversal loading. Sadhana 39: 1185–1200.

Reda Taha MM, El-Dieb AS, Abd El-Wahab MA and Abdel-Hameed ME (2008) Mechanical, fracture, and microstructural investigations of rubber concrete. *ASCE Journal of Materials in Civil Engineering* 20(10): 640–649.

Richardson AE (2005) Bond characteristics of structural polypropylene fibres in concrete with regard to post-crack strength and durable design. Structural Survey 23(3): 210-230.

Roesler JR, Altoubat SA, Lange DA, Rieder K and Ulreich GR (2006) Effect of synthetic fibers on structural behavior of concrete slabs-on-ground. ACI Materials Journal-American Concrete Institute 103(1):3-10.

Sadek DM and El-Attar MM (2014) Structural behavior of rubberized masonry walls. *Journal of Cleaner Production* 89: 174–186.

Sahmaran M and Li VC (2010) Engineered cementitious composites: Can composites be accepted as crack-free concrete?. Transp. Res. Rec. 2164: 1–8.

Şahmaran M, Lachemi M, Hossain KMA, Ranade R and Li VC (2009) Influence of Aggregate Type and Size on Ductility and Mechanical Properties of Engineered Cementitious Composites. *ACI Materials Journal* 106(3):308-316.

Segre N, Joekes I (2000) Use of tire rubber particles as addition to cement paste. Cem Concr Res 30(9): 1421-1425.

Shannag M, Barakat S and Abdul-Kareem M. (2002) Cyclic behavior of HPFRC-repaired reinforced concrete interior beam-column joints. Materials and Structures 35: 348–356.

Sherwood PT (1995) The use of waste and recycled materials in roads. Proceedings of Institution of Civil Engineers, Transportations, 111:116-124.

Shiohara H (2004) Quadruple flexural resistance in R/C beam-column joints. In 13th World Conference on Earthquake Engineering.

Siddique R and Naik TR (2004) Properties of concrete containing scrap-tire rubber - an overview. Waste Management 24(6): 563-569.

Singha S, Shuklaa A and Brownb R (2004) Pullout Behavior of Polypropylene Fibers from Cementitious Matrix *Cement and Concrete Research* 34: 1919–1925.

Sohrabi MR and Karbalaie M (2011) An experimental study on compressive strength of concrete containing crumb rubber. International Journal of Civil & Environmental IJCEE 11(3): 24-28.

Soroushian P, Khan A and Hsu J (1992) Mechanical properties of concrete materials reinforced with polypropylene or polyethylene fibers. ACI Materials Journal 89(6): 535-540.

Su H, Yang J, Ling T, Ghataora GS and Dirar S (2015) Properties of concrete prepared with waste tyre rubber particles of uniform and varying sizes. *Journal of Cleaner Production* 91: 288-296.

Suthiwarapirak P, Matsumoto T and Kanda T (2004) Multiple cracking and fiber bridging characteristics of engineered cementitious composites under fatigue flexure. *Journal of Material in Civil Engineering* 16:433–443.

Taylor HPJ (1974) The Fundamental Behavior of Reinforced Concrete Beams in Bending and Shear. ACI SP-42: 43–77.

Teo DC, Mannan MA and Kurian JV (2006) Flexural behaviour of reinforced lightweight concrete beams made with oil palm shell (OPS). *Journal of advanced concrete technology* 4(3):459-468.

Thomas BS, Kumar S, Mehra P, Gupta RC, Kalla P, Joseph M and Cseteney L (2016) Abrasion resistance of sustainable green concrete containing waste tire rubber particles. *Construction and Building Materials* 124: 906-909.

Thomas BS, Gupta RC, Mehra P and Kumar S (2015) Performance of high strength rubberized concrete in aggressive environment. *Construction and Building Materials* 83: 320-326.

Thomas BS, Gupta RC, Kalla P and Cseteney L (2014) Strength, abrasion and permeation characteristics of cement concrete containing discarded rubber fine aggregates. *Construction and Building Materials* 59: 204-212.

Topçu IB and Bilir T (2009) Experimental investigation of some fresh and hardened properties of rubberized self-compacting concrete. *Materials and Design* 30(8): 3056–3065.

Topcu IB (1995) The properties of rubberized concretes. Cement and Concrete Research 25(2):304-10.

Turer A (2012) Recycling of scrap tires, Material Recycling-Trends and Perspectives, http://cdn.intechopen.com/pdfs/32586/InTech-Recycling_of_scrap_tires.pdf, (Accessed on February 2017).

Wang HY, Yung LC and Hua LH (2013) A study of the durability properties of waste tire rubber applied to self-compacting concrete. *Construction and Building Materials* 41: 665-672.

Wang S and Li VC (2006) High Early Strength Engineered Cementitious Composites. *ACI Materials Journal*, 103(2): 97–105.

Wang Y, Wu HC, Victor CL (2000) Concrete reinforcement with recycled fibers. J mater in civ eng. 12 (4): 314-319.

Wang Y, Backer S and Li VC (1987) An experimental study of synthetic fibre reinforced cementitious composites. Journal of Materials Science, 22(12): 4281 -4291.

Won JP, Lim DH and Park CG (2006) Bond behaviour and flexural performance of structural synthetic fibre-reinforced concrete. Magazine of Concrete Research 58(6): 401-410.

Yang E, Garcez E and Li VC (2012) Development of Pigmentable Engineered Cementitious Composites for Architectural Elements Through Integrated Structures and Materials Design. *Materials and Structures* 45(3): 425–32.

Yang EH, Yang Y and Li VC (2007) Use of High Volumes of Fly Ash to Improve ECC Mechanical Properties and Material Greenness. *ACI Materials Journal* 104(6): 620-628.

Yap SP, Bu CH, Alengaram UJ, Mo KH and Jumaat MZ (2014) Flexural toughness characteristics of steel–polypropylene hybrid fibre-reinforced oil palm shell concrete. Mater Des 57: 652–659.

Youssf O, ElGawady MA, Mills JE (2015) Experimental investigation of crumb rubber concrete columns under seismic loading. Struct 3: 13-27.

Youssf O, ElGawady MA, Mills JE and Ma X (2014) An experimental investigation of crumb rubber concrete confined by fibre reinforced polymer tubes. *Construction and Building Materials* 53: 522–532.

Zheng L, Sharon HX, Yuan Y (2008) Experimental investigation on dynamic properties of rubberized concrete. Constr Build Mater 22: 939–947.

Zhang J and Li VC (2002) Monotonic and fatigue Performance in Bending of Fiber-Reinforced Engineered Cementitious Composite in Overlay System. *Cement and Concrete Research* 32:415–423.

Zhang C, Gopalaratnam VS and Yasuda HK (2000) Plasma treatment of polymeric fibers for improved performance in cement matrices. Journal of Applied Polymer Science 76(14): 1985-1996.

Zheng Z and Feldman D (1995) Synthetic fibre-reinforced concrete. Progress in Polymer Science 20(2):185-210.

Zhou J, Qian S, Guadalupe Sierra Beltran M, Ye G, Breugel KV and Li VC (2010) Development of Engineered Cementitious Composites with Limestone Powder and Blast Furnace Slag. Materials and Structures 43(6): 803–14.

Zhu Y, Zhang Z, Yang Y and Yao Y (2014) Measurement and correlation of ductility and compressive strength for engineered cementitious composites (ECC) produced by binary and ternary systems of binder materials: Fly ash, slag, silica fume and cement. *Construction and Building Materials* 68:192–198.